Raja R. Huilgol

Fluid Mechanics of Viscoplasticity

Springer

Fluid Mechanics of Viscoplasticity

Raja R. Huilgol

Fluid Mechanics of Viscoplasticity

Springer

Raja R. Huilgol
Flinders Mathematical Sciences Laboratory
School of Computer Science, Engineering
and Mathematics
Flinders University of South Australia
Adelaide
Australia

ISBN 978-3-662-45616-3 ISBN 978-3-662-45617-0 (eBook)
DOI 10.1007/978-3-662-45617-0

Library of Congress Control Number: 2014956372

Springer Heidelberg New York Dordrecht London

Printed on acid-free paper

Springer-Verlag GmbH Berlin Heidelberg is part of Springer Science+Business Media
(www.springer.com)

Dedicated to Lord Ganesha

Preface

It seems to be an opportune moment to produce a book on viscoplastic fluid mechanics. There is a vast amount of material covering the theoretical aspects of the subject, as well as numerical modelling. When I began this monograph, I was very surprised to find the treasure that was lying in front of me and this is an account of the voyage of discovery.

The first chapter lays out the essential features of viscoplasticity through a detailed study of the flow of a Bingham fluid in a channel. The influence of the yield stress on the critical pressure drop to sustain the flow, the velocity field, the flow rate and the inherent nonlinearity of the constitutive model are explored in-depth. Non-dimensionalisation, and its use in defining the Bingham number and deriving the Buckingham equation is demonstrated, and the solution to the latter is found. The next section deals with the nature of free boundary problems, such as the Stefan problem. The location of the yield surface in the channel flow of the Bingham fluid is also a free boundary problem, and the corresponding velocity field can be obtained through the minimum of a suitably chosen functional or the solution of its equivalent variational inequality. The chapter closes with a brief review of the experiments which challenge and support the assumption that viscoplastic fluids exist, and a summary of the aim of the rest of the book.

The next two chapters are concerned with the basic kinematics of the flows of fluids and the balance equations of continuum mechanics so that this monograph is self-contained. Chapter 4 examines in-depth the role of pressure in incompressible media and the formulation of constitutive equations to respond to the incompressibility of a material, treating it as a constraint on a given motion. The extension to incompressible viscoplastic fluids is made and the consequence of treating the yield stress effect as a response to a second constraint is explored, leading to the concept of the viscoplasticity constraint tensor. Next, the constitutive equations for compressible viscoplastic fluids are derived. Finally, the correspondence between one-dimensional Bingham, Herschel-Bulkley and Casson models and their three-dimensional versions is exhibited.

Chapter 5 is concerned mostly with the steady shearing flows of Bingham fluids with a brief mention of modelling the effects of heat transfer. Chapter 6 deals with the unsteady shearing flow in a channel. The lateral movement of the yield surface in the initiation of this flow is described, and the broad question regarding the kinematics and dynamics of this lateral motion is answered through an application of Hadamard's theory of propagating singular surfaces.

Chapter 7 is a sample of analytical approximation techniques to understand the flows of viscoplastic fluids. The lubrication paradox and its resolution through an examination of the flow of a Bingham fluid in a wavy channel are discussed. Next, the equations governing the axisymmetric and asymmetric Hele-Shaw flows of viscous and viscoplastic fluids are derived. Finally, a summary of the results obtained in the study of the linearised stability of the channel and helical flows of a Bingham fluid is given.

In Chap. 8, variational principles and variational inequalities associated to the flows of incompressible viscoplastic fluids are derived through the principle of virtual power. A summary of the results from convex analysis needed to understand this material is included and the equivalences, when they exist, between the minimiser of a functional, the solution of the corresponding variational inequality and that of the equations of motion are explored. Simplifications of the variational inequality occur in several flows and these are listed. Finally, a basic inequality is derived to model the flows of compressible viscoplastic fluids. In Chap. 9, the variational principle is applied to obtain the minimum pressure drop per unit length to sustain the steady flow of a Bingham fluid in a pipe of arbitrary cross-section. Next, the roles of the variational principle and the associated variational inequality are examined to understand when bubbles remain static in viscoplastic fluids, and when rigid bodies move in such materials. Proofs are also provided to show that steady shearing flows in a Bingham fluid come to rest in a finite time when the driving mechanism falls below a critical value, emphasising the role of variational inequalities. Finally, the energy principles are employed in the nonlinear stability analysis of the flow of a Bingham fluid in a channel and a pipe of circular cross-section.

The final chapter is concerned with numerical modelling through the applications of the augmented Lagrangian and the operator-splitting methods. Since the solution of the minimisation problems in finite dimensions through the augmented Lagrangian method leads naturally to its extension to the flow problems in Bingham fluids, this method is described in detail in the first two sections. Next, the operator-splitting method is introduced and employed to study the thermally driven cavity flow of a Bingham fluid. The chapter closes with a section on numerical modelling of flows of compressible viscoplastic fluids with a study of the lid-driven cavity flow of a weakly compressible viscoplastic fluid. Some comments on the use of regularised models in numerical modelling are also offered.

And, the last word. Viscoplastic fluid mechanics means yield stress and the location(s) of yield surface(s). That is, free boundary problems, variational

principles, variational inequalities and convex analysis with augmented Lagrangian and operator-splitting methods following from them. In writing this book, apart from including solutions to problems obtained through traditional approaches to fluid mechanics, my aim has been to emphasise the pre-eminence of the modern approach to this subject.

Adelaide, December 2014 Raja R. Huilgol

Acknowledgments

Much of the material in Chaps. 7–10 of this monograph is derived from the research funded by the Australian Research Council and Moldflow Pty. Ltd. under Linkage Grants during 2005–2009. The final editing has been completed during a period of Outside Studies Programme Leave from Flinders University.

Turning to the figures in the book, I am deeply indebted to Professor G. Georgiou, University of Cyprus, for producing Figs. 1.1–1.4, 4.1, 4.2, 5.1, 5.2 and 9.1. And, to Mr. G.H.R. Kefayati for Figs. 7.3 and 8.1.

I would also like to thank Professor I.A. Frigaard, University of British Columbia, for sending me Figs. 7.1 and 7.2 used in Sect. 7.2, and to Elsevier for the permission to use these figures. In addition, I wish to thank Elsevier for the permission to reproduce the table on p. 190 and Figs. 9.2–9.6, as well as Figs. 10.1–10.18 from my articles in the Journal of Non-Newtonian Fluid Mechanics.

Finally, I would like to thank Dr. Christoph Baumann, Senior Engineering Editor, Springer, for his enormous help in producing this monograph.

Contents

1 The Basic Features of Viscoplasticity 1
1.1 Bingham Fluid at Rest in a Channel 1
1.2 Sign of the Shear Stress. 2
1.3 Critical Pressure Drop and the Constitutive Relation 3
1.4 The Solution 5
1.5 Flow Rate 6
1.6 Inherent Nonlinearity. 6
1.7 Non-dimensionalisation 7
1.8 The Buckingham Equation. 9
1.9 Free Boundary Problems 10
1.10 The Minimiser and the Variational Inequality 14
1.11 Effects of Wall Slip 16
1.12 Experimental Support 18
1.13 Summary 20
References. 20

2 Kinematics of Fluid Flow 23
2.1 Kinematical Preliminaries. 24
2.2 Relation Between the Velocity and Deformation Gradients. . . . 26
2.3 Rigid Motion 27
2.4 Polar Decomposition, Spin and Stretching 28
2.5 Steady Velocity Fields and Their Rivlin-Ericksen Tensors 30
Appendix 32
References. 34

3 Fundamental Equations 35
3.1 Conservation of Mass 36
3.2 Cauchy's First Law. 37
3.3 Cauchy's Second Law 39

3.4 Conservation of Energy 41
3.5 Control Volume and Control Surface. 43
Appendix 45
Reference 46

4 Constitutive Equations 47
4.1 Pressure and Incompressibility 48
4.1.1 The Meaning of Pressure 48
4.2 Incompressible Viscoplastic Fluids 51
4.2.1 Equations of Motion for Incompressible Materials. . . . 54
4.3 Viscoplasticity Constraint Tensor 54
4.4 Regularisation 56
4.5 Compressible Viscoplastic Fluids 58
4.6 Analogues for Incompressible Viscoplastic Fluids 59
4.6.1 One Dimensional Models. 60
4.6.2 Some Results from Tensor Analysis 62
4.6.3 Three Dimensional Models 63
References. 64

5 Analytic Solutions: Steady Flows 65
5.1 Simple Shearing Flow 66
5.2 Flow in a Channel 66
5.3 Flow Down an Inclined Plane 66
5.4 Flow in a Pipe of Circular Cross-Section 68
5.4.1 The Buckingham Equation 71
5.5 Axial Flow in a Concentric Annulus 72
5.6 Couette Flow 76
5.7 Helical Flow 79
5.8 Steady Flows of General Viscoplastic Fluids 83
5.9 Heat Transfer Problems 83
5.9.1 Heat Transfer Between Two Parallel Plates 83
5.9.2 More General Problems 85
References. 86

6 Analytic Solutions: Unsteady Shearing Flows 87
6.1 Unsteady Flow in a Channel 87
6.1.1 The Solution 90
6.1.2 Approximate Solution 96
6.1.3 Laplace Transform 98
6.1.4 Application of Maximum Principles 98
6.2 Unsteady Couette and Poiseuille Flows 99
6.3 Unsteady Flow in a Half-Space 100
6.3.1 An Initial Value Problem. 100
6.3.2 Singular Surfaces in Motion 103

6.3.3 Hadamard Lemma and Unsteady Shearing Flows in Viscoplastic Fluids. 104
6.3.4 Implications of the Continuity of $\partial\sigma/\partial y$ at the Yield Surface 107
6.3.5 Extensions to Other Shearing Flows 107
6.3.6 Open Ended Problems 109
References. 110

7 Analytical Approximation Techniques 113
7.1 The Lubrication Paradox 114
7.2 Steady Flow in a Wavy Channel—The Periodic Case 116
7.2.1 Zeroth Order Solution 118
7.2.2 First Order Corrections 119
7.2.3 Breaking the Unyielded Plug 121
7.3 Hele-Shaw Flow Problems 121
7.3.1 The Viscometric Fluidity Function 123
7.3.2 Papanastasiou Model 124
7.3.3 The Symmetric Case 126
7.3.4 The Average Velocity Field in the Symmetric Case. 126
7.3.5 Hele-Shaw Flow Equations 128
7.3.6 The Asymmetric Case 129
7.4 Linearised Stability Analysis 132
7.5 Summary 137
References. 137

8 Variational Principles and Variational Inequalities 139
8.1 Minimum and Maximum Principles for Incompressible Viscoplastic Fluids 140
8.1.1 Basic Definitions and Principle of Virtual Power 140
8.1.2 The Velocity and Stress Functionals 142
8.1.3 Proofs of the Theorems 145
8.1.4 Equality of $\Phi(\mathbf{u})$ and $\Psi(\mathbf{T})$ 148
8.1.5 Shear Rate Dependent Yield Stress 149
8.1.6 Steady Flow in a Pipe of Uniform Cross-Section 149
8.2 Virtual Power and the Basic Inequality for Incompressible Viscoplastic Fluids 150
8.2.1 A Point-Wise Inequality: Isochoric Velocity Fields . . . 150
8.2.2 The Integral Inequality 152
8.3 A General Energy Balance Equation for Viscoplastic Fluids. . . 154
8.4 Fundamental Inequality: Non-isochoric Trial Velocity Fields 155

8.5 Variational Principles and Fundamental Inequality in the Presence of Wall Slip . . . 156
8.6 Convex Analysis and Its Applications . . . 158
8.6.1 The Direct Method . . . 159
8.6.2 Convex Set and Convex Functionals . . . 161
8.6.3 Existence and Uniqueness . . . 164
8.6.4 Variational Inequality . . . 165
8.6.5 Equivalence of the Minimiser and the Solution of the Variational Inequality . . . 166
8.7 Equivalence of the Solution of the Variational Inequality and the Equations of Motion . . . 168
8.8 Special Cases of the Variational Inequality . . . 170
8.8.1 Flows with Zero Stress Power Difference . . . 170
8.8.2 Flows with Non-zero Stress Power Difference . . . 171
8.8.3 The Trilinear Functional Involving Acceleration Terms . . . 173
8.9 Viscoplasticity Constraint Tensor: The Final Equivalence . . . 175
8.10 The Basic Inequality for Compressible Viscoplastic Fluids . . . 176
References . . . 180

9 Energy Methods in Action: Equality, Inequality and Stability . . . 181
9.1 Axial Flow in a Pipe of Arbitrary Cross-Section . . . 181
9.1.1 The Minimum Pressure Drop per Unit Length to Initiate a Steady Flow . . . 182
9.1.2 Existence of Stagnant Zones . . . 189
9.1.3 Bounds on the Magnitude of the Core and Its Maximum Velocity . . . 192
9.2 Static Bubbles in Viscoplastic Fluids . . . 193
9.2.1 Critical Value of the Bingham Number to Prevent Bubble Motion . . . 196
9.2.2 Critical Value from Stress Maximisation . . . 197
9.2.3 A Condition for a Bubble to Move: An Upper Bound for the Bingham Number . . . 199
9.3 Motions of Rigid Bodies in Viscoplastic Fluids . . . 201
9.4 Initiation and Cessation of Unsteady Shearing Flows . . . 207
9.4.1 The Approach to the Steady State . . . 207
9.4.2 The Proof of the Energy Inequality . . . 208
9.4.3 Cessation of the Steady Flow in a Channel . . . 209
9.4.4 Cessation of Steady Simple Shear Flow . . . 211
9.4.5 Cessation of Steady Flow in a Pipe . . . 212
9.4.6 Cessation of Steady Couette Flow . . . 213
9.4.7 Effects of Wall Slip . . . 216

9.5 Nonlinear Stability Analysis . . . 217
9.5.1 Dissipation Terms . . . 219
9.5.2 Global Stability Bounds . . . 220
9.5.3 Conditional Stability . . . 221
References . . . 223

10 Numerical Modelling . . . 225
10.1 Augmented Lagrangian Methods: Finite Dimensional Case . . . 226
10.2 Augmented Lagrangian Methods for Bingham Fluids . . . 230
10.2.1 Optimality Conditions of the Augmented Lagrangian Functional . . . 232
10.2.2 More General Problems . . . 234
10.3 Operator-Splitting Method for Thermally Driven Flows . . . 235
10.3.1 The Flow Problem and Mathematical Formulation . . . 236
10.3.2 Non-dimensionalisation . . . 237
10.3.3 Numerical Procedure . . . 240
10.3.4 Discussion of the Results . . . 242
10.4 Compressibility Effects: Numerical Experiments . . . 250
10.4.1 Operator-Splitting Methods: Compressible Viscous Fluids . . . 250
10.4.2 Compressible Viscoplastic Fluids: Isothermal Case . . . 255
10.4.3 Operator-Splitting Method . . . 258
10.5 Flow in a Cavity: Weakly Compressible Fluid . . . 260
10.6 Regularised Models . . . 267
References . . . 269

Index . . . 271

Chapter 1
The Basic Features of Viscoplasticity

1.1 Bingham Fluid at Rest in a Channel

Consider an incompressible Bingham fluid at rest between two parallel walls. Assume that the domain Ω of the fluid can be described through a region symmetrical about the x-axis as follows:

$$\Omega = \{(x, y) : -\infty < x < \infty,\ -H \leq y \leq H\}. \tag{1.1.1}$$

See Fig. 1.1. Let a constant pressure gradient be applied to the fluid in the x-direction so that we can describe the pressure field in the fluid through $p(x, y) = -Gx + f(y)$, where $G > 0$ is the constant pressure drop per unit length and $f(y)$ is a function of y, which is irrelevant here. Ignoring any body force, the equations of equilibrium lead to

$$-\frac{\partial p}{\partial x} + \frac{\partial \sigma}{\partial y} = 0, \tag{1.1.2}$$

where σ is the shear stress in the fluid. This equation can be integrated for the shear stress and one obtains

$$\sigma = -Gy + b, \tag{1.1.3}$$

where b is the constant of integration. Since the domain is symmetrical about the x-axis, one can assume that $b = 0$. Thus, $\sigma = -Gy$.

The ability of a Bingham fluid to remain at rest under a constant pressure drop per unit length G, albeit for a limited range, requires further investigation, especially since the shear stress distribution in the channel is given by $\sigma = -Gy$ for both purely viscous and viscoplastic fluids. The former class of fluids will flow regardless of how small G is, whereas the latter will not move unless the pressure drop per unit length G exceeds a critical value G_c, which depends on the yield stress of the fluid. To determine G_c, an explanation regarding the change in sign of the shear stress across the channel is given, paving the way for a formula relating G_c to the yield stress τ_y of the fluid.

R.R. Huilgol, *Fluid Mechanics of Viscoplasticity*, DOI 10.1007/978-3-662-45617-0_1

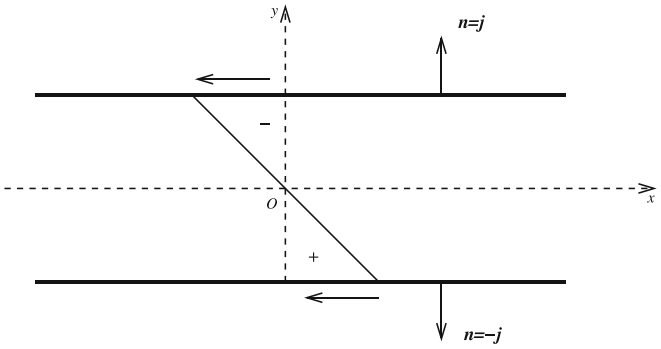

Fig. 1.1 Shear stress distribution across a channel due to a constant applied pressure gradient, with external shear stress vectors and external unit normals

1.2 Sign of the Shear Stress

One can see that the shear stress is *negative* above the x-axis and is *positive* below it. This needs some explanation. First of all, as the pressure drop tries to move the fluid in the positive x-direction, the shear stresses on the two walls oppose it. See Fig. 1.1. While a more detailed description of Cauchy's stress principle is provided in Chap. 3, at present it is sufficient to assume that the stress tensor $\mathbf{T}$ in the fluid is symmetric and two-dimensional, given in matrix form through:

$$\mathbf{T} = \begin{bmatrix} T_{11} & T_{12} \\ T_{21} & T_{22} \end{bmatrix}, \quad T_{12} = T_{21}. \tag{1.2.1}$$

On the plane $y = H$, the external unit normal $\mathbf{n} = \mathbf{j}$ is oriented towards the positive y-direction. Cauchy's stress principle says that the external stress vector $\mathbf{t}$ on this plane is given by $\mathbf{t} = \mathbf{Tn}$. So,

$$\mathbf{t} = \begin{bmatrix} T_{11} & T_{12} \\ T_{21} & T_{22} \end{bmatrix} \begin{bmatrix} 0 \\ 1 \end{bmatrix} = \begin{bmatrix} T_{12} \\ T_{22} \end{bmatrix} = \begin{bmatrix} -\sigma_w \\ T_{22} \end{bmatrix}, \tag{1.2.2}$$

where σ_w is the magnitude of the shear stress at the wall. Since this external stress points in the negative x-direction, the shear stress $T_{12} < 0$ in the fluid. This negative value persists till it changes from a negative to a positive value, as one moves from the plane $y = H$ to the plane $y = -H$. Now, why is the shear stress on the plane $y = -H$ positive? This is because on this plane, the external unit normal is given by $\mathbf{n} = -\mathbf{j}$. So, the external stress vector is given by

$$\mathbf{t} = \begin{bmatrix} T_{11} & T_{12} \\ T_{21} & T_{22} \end{bmatrix} \begin{bmatrix} 0 \\ -1 \end{bmatrix} = \begin{bmatrix} -T_{12} \\ T_{22} \end{bmatrix} = \begin{bmatrix} -\sigma_w \\ T_{22} \end{bmatrix}. \tag{1.2.3}$$

Obviously, the shear stress $T_{12} > 0$ here.

Once again, note that the sign of the shear stress is independent of the constitutive equation and applies to all continuous media.

1.3 Critical Pressure Drop and the Constitutive Relation

Now, let the pressure drop G be increased slowly. The shear stress will grow in magnitude till the magnitude of the wall shear stress, σ_w, equals the yield stress, τ_y, of the fluid. That is $\sigma_w = \tau_y$. Consider the axial force acting on the fluid over a cube of height $2H$ in the y-direction, unit width in the z-direction and unit length in the x-direction. This force is given by $2GH$. Opposing it are the forces on the boundaries of the channel at the top and bottom. Per unit length in the x-direction and unit width in the z-direction, these forces are given by $2\tau_y$. Thus, the flow is incipient when the critical pressure drop per unit length is given by

$$G_c = \frac{\tau_y}{H}. \tag{1.3.1}$$

Note that the fluid does not flow till this critical value has been exceeded. If the pressure drop per unit length G is increased beyond G_c, the fluid will flow with the yielding occurring at the wall at first. Assuming that the transient effects have died away and that the flow is steady, there will be a boundary layer of the Bingham fluid moving as a liquid, while away from the wall, the Bingham material will flow as a solid plug; these phenomena require some explanation.

The yield stress and the adherence condition at the wall together prevent the Bingham fluid from undergoing a deformation, i.e., shearing, till the magnitude of the shear stress at the wall, due to the applied pressure gradient, exceeds the yield stress. Elsewhere in the flow domain, the yield stress prevents the fluid from undergoing a deformation, i.e., shearing, where the magnitude of the shear stress is less than or equal to the yield stress. From Figs. 1.1 and 1.2, one sees that this situation arises in a symmetrical region around the centre of the channel. Since there is no fixed boundary at the centre, the only way the fluid can undergo zero deformation is to move as a solid plug.

To understand these matters in detail, let the flow occur in the x-direction with a velocity field given by $u = u(y)$. Since a plug flow exists around the x-axis, we see that

$$u(y) = u(0), \quad 0 \le y \le h, \tag{1.3.2}$$

where h is the semi-width of the plug. Note that in the rigid core, $du/dy = 0$. In $h \le y \le H$, the fluid moves like a viscous liquid. Obviously, one does not know the exact nature of the velocity distribution in this boundary layer. Clearly, one needs a constitutive equation to proceed.

The commonly used constitutive assumption is that the magnitude of the shear stress in the plug is less than or equal to the yield stress τ_y, while in the yielded

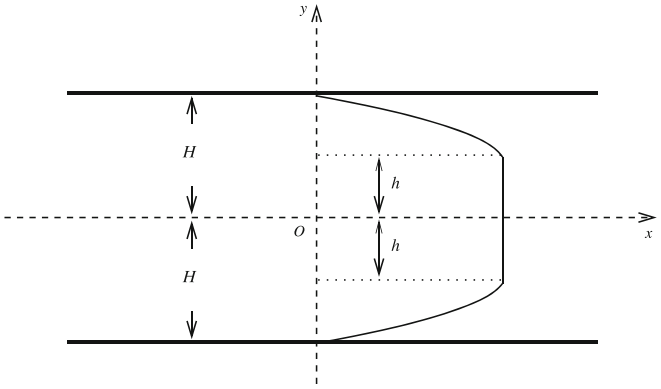

Fig. 1.2 Steady flow in a channel due to a constant applied pressure drop per unit length, with a moving rigid core and yielded zones next to the walls

domain, the magnitude of the shear stress exceeds the yield stress, augmented by a shear rate dependent stress. So, we have

$$du/dy = 0, \quad |\sigma| \leq \tau_y, \tag{1.3.3}$$

And,

$$\sigma = \eta \frac{du}{dy} + \frac{\tau_y}{|du/dy|} \frac{du}{dy}, \tag{1.3.4}$$

where η is the viscosity of the fluid. Since the velocity in the fluid increases from zero at the boundary to the plug velocity at $y = h$, it is clear that $du/dy \leq 0$ in the yielded region, $h \leq y \leq H$. So, we can write the constitutive equation as

$$-\tau_y \leq \sigma \leq 0, \quad 0 \leq y \leq h, \tag{1.3.5}$$

$$-\tau_y + \eta \frac{du}{dy} = \sigma, \quad h \leq y \leq H. \tag{1.3.6}$$

Keeping in mind that the pressure drop per unit length $G > G_c > 0$ is a constant, one is faced with the following questions:

1. How wide is the plug, or how can one find h?
2. What is the constant speed $u(0)$ of the plug?
3. What is the velocity distribution $u = u(y)$ in $h \leq y \leq H$?
4. What are the boundary conditions on $u = u(y)$ at the interface between the plug flow and the boundary layer?

The answers to these questions can be found easily in the problem at hand as can be seen next.

1.4 The Solution

Once again, ignoring the body force and realising that the acceleration field is zero when $u = u(y)$, the equation of motion is the same as (1.1.2). Thus, the shear stress is given by $\sigma = -Gy$ again. Since this is a continuous function of y, it follows that at the interface between the rigid core and the yielded region

$$\sigma(h^-) = \sigma(h^+) = -\tau_y = -Gh, \tag{1.4.1}$$

which means that the semi-width of the plug is given by $h = \tau_y/G$. The constitutive Eqs. (1.3.5) and (1.3.6) lead to the condition that $du/dy = 0$ at $y = h$. This is one of the boundary conditions at the yield surface located at $y = h$.

In $h < y < H$, the constitutive relation (1.3.6) can be replaced by

$$\eta \frac{du}{dy} = -Gy + \tau_y, \tag{1.4.2}$$

since $\sigma = -Gy$. It is easy to integrate Eq. (1.4.2) and one obtains:

$$u(y) = -\frac{G}{2\eta} y^2 + \tau_y y + b, \tag{1.4.3}$$

where the constant b has to be determined. Since the fluid adheres to the boundary $y = H$ which is at rest, one has $u(H) = 0$. Thus,

$$b = \frac{G}{2\eta} H^2 - \tau_y H. \tag{1.4.4}$$

The velocity field in the yielded region now has the form

$$u(y) = \frac{G}{2\eta}(H^2 - y^2) - \frac{\tau_y}{\eta}(H - y), \quad h \le y \le H. \tag{1.4.5}$$

Note that the first part of the velocity field is the same as that in a Newtonian fluid; the second part is that due to the yield stress. The influence of the yield stress is to cause the parabolic velocity field of the Newtonian fluid to become flatter.

Next, the second boundary condition on the velocity field $u(y)$, located at $y = h$, is that it be continuous. Thus, one obtains the velocity of the plug through $u(y) = u(h)$, $0 \le y \le h$, where the latter can be found from (1.4.5). Thus,

$$u(y) = \frac{G}{2\eta}(H - h)^2, \quad 0 \le y \le h. \tag{1.4.6}$$

Now that $u = u(y)$ has been found, it can be seen that $u'(H) < 0$ and that $u'(-H) > 0$. These results are in accord with the earlier assertion that the shear stress $\sigma(H) < 0$, $\sigma(-H) > 0$. Finally, the symmetry of the velocity field about the x-axis means that the velocity field is known throughout $-H \le y \le H$.

1.5 Flow Rate

The flow rate Q in the channel can be calculated quite readily through integration by parts as follows. Since the flow is symmetric about the x-axis, and $u(y)y = 0$ at both $y = 0$ and $y = H$,

$$Q = 2\int_0^H u\,dy = -2\int_0^H yu'\,dy. \tag{1.5.1}$$

Thus, using (1.4.5) with $\tau_y = Gh$, one obtains

$$Q = -2\int_0^H yu'\,dy = \frac{2G}{\eta}\int_h^H y(y-h)\,dy, \tag{1.5.2}$$

because $u' = 0$ in $0 \le y \le h$. Hence,

$$Q = \frac{2GH^3}{3\eta}\left[1 - \frac{3}{2}\left(\frac{h}{H}\right) + \frac{1}{2}\left(\frac{h}{H}\right)^3\right]. \tag{1.5.3}$$

Now, the fact that $\sigma = -Gy$ in Ω means that $\tau_y = Gh$, and the magnitude of the wall shear stress $\sigma_w = GH$. Thus, $h/H = \tau_y/\sigma_w$. Hence, (1.5.3) becomes

$$Q = \frac{2H^2\sigma_w}{3\eta}\left[1 - \frac{3}{2}\left(\frac{\tau_y}{\sigma_w}\right) + \frac{1}{2}\left(\frac{\tau_y}{\sigma_w}\right)^3\right]. \tag{1.5.4}$$

1.6 Inherent Nonlinearity

Since the velocity field satisfies a linear differential equation, it would appear that linearity would prevail and the principle of superposition should apply. That is, if $u_1 = u_1(y, G_1), u_2 = u_2(y, G_2)$ are two velocity fields under the constant pressure drops per unit length G_1, G_2 respectively, superposition would mean that $u(y, G_1 + G_2) = u_1(y, G_1) + u_2(y, G_2)$. However, this is false because the location of the yield surface is not a linear function of the pressure drop, and the vanishing of the shear rate at the yield surface is crucial in determining the velocity field. To be precise, let the location of the yield surfaces under the pressure drops G_1, and G_2 be h_1 and h_2 respectively. Thus,

$$h_1 = \frac{\tau_y}{G_1}, \quad h_2 = \frac{\tau_y}{G_2}. \tag{1.6.1}$$

However, the yield surface due to the pressure drop (G_1+G_2) is located at h, given by

$$h = \frac{\tau_y}{G_1 + G_2} \neq h_1 + h_2. \tag{1.6.2}$$

A different way of understanding the nonlinearity is to look at (1.4.5). Without loss of generality, let $G_1 \geq G_2$, and consider y such that this point lies within the yielded zone whether the pressure drop per unit length is G_2, G_1, or $G_1 + G_2$. That is

$$\frac{\tau_y}{G_1 + G_2} < \frac{\tau_y}{G_1} \leq \frac{\tau_y}{G_2} < y < H. \tag{1.6.3}$$

Given this,

$$\begin{aligned} u_1(y, G_1) + u_2(y, G_2) &= \frac{G_1 + G_2}{2\eta}(H^2 - y^2) - 2\frac{\tau_y}{\eta}(H - y), \\ u(y, G_1 + G_2) &= \frac{G_1 + G_2}{2\eta}(H^2 - y^2) - \frac{\tau_y}{\eta}(H - y), \\ &\neq u_1(y, G_1) + u_2(y, G_2). \end{aligned} \tag{1.6.4}$$

In fact, $u(y, 2G) \neq 2u(y, G)$. This loss of linearity rules out the application of Laplace transform methods to solve initial-boundary value problems in the flows of Bingham fluids; for additional reasons, see Sect. 6.1.3.

1.7 Non-dimensionalisation

There are two distinct length, time and velocity scales associated with a Bingham fluid. One is the intrinsic set arising from the material properties, viz. the density ρ, the viscosity η and the yield stress τ_y. The second is induced by a given flow and we shall return to this later.

It is simple to note that an intrinsic mass M, length L and time scales T are given by

$$M \sim \eta^3/\sqrt{\rho\tau_y^3}, \quad L \sim \sqrt{\eta^2/\rho\tau_y}, \quad T \sim \eta/\tau_y. \tag{1.7.1}$$

The characteristic velocity U derived from the above length and time scales is:

$$U \sim \sqrt{\tau_y/\rho}. \tag{1.7.2}$$

The scales recorded here are not used, if at all, for the flow induced entities are to be preferred.

That is, when solving initial-boundary value problems, it is preferable to replace the length, velocity, the pressure and stresses and time through non-dimensional quantities, which are induced by the flow under consideration. As an example, consider the flow in a channel. Using the width H of the channel and a characteristic velocity U related to the flow rate, say, one can render the (x, y) coordinates, the velocity u, and time t in a non-dimensional form as follows:

$$\tilde{x} = x/H, \quad \tilde{y} = y/H, \quad \tilde{u} = u/U, \quad \tilde{t} = Ut/H. \tag{1.7.3}$$

As far as the pressure p, and the wall shear stress σ_w are concerned, we need a characteristic stress. This is provided by $\eta U/H$, for U/H has the dimension of shear rate. Thus, one obtains

$$\tilde{p} = pH/\eta U, \quad \tilde{\sigma}_w = \sigma_w H/\eta U. \tag{1.7.4}$$

Since the Bingham number Bn plays a significant role in viscoplastic fluid mechanics, its definition follows next:

$$\mathrm{Bn} = \tau_y H/\eta U. \tag{1.7.5}$$

The Bingham number is a measure of the importance of the yield stress relative to the viscous stress.

To demonstrate how non-dimensionalisation works, consider the following where the relationship between $\partial p/\partial x$ and $\partial \tilde{p}/\partial \tilde{x}$ is made explicit, i.e.,

$$\frac{\partial p}{\partial x} = \frac{\eta U}{H}\frac{\partial \tilde{p}}{\partial \tilde{x}}\frac{\partial \tilde{x}}{\partial x} = \frac{\eta U}{H^2}\frac{\partial \tilde{p}}{\partial \tilde{x}}. \tag{1.7.6}$$

As a second example, we can express the flow rate Q in (1.5.4) as $Q = H^2 U\tilde{Q}$. Thus,

$$\tilde{Q} = \frac{2\tilde{\sigma}_w}{3}\left[1 - \frac{3}{2}\left(\frac{\mathrm{Bn}}{\tilde{\sigma}_w}\right) + \frac{1}{2}\left(\frac{\mathrm{Bn}}{\tilde{\sigma}_w}\right)^3\right]. \tag{1.7.7}$$

Finally, consider a typical equation of motion:

$$-\frac{\partial p}{\partial x} + \frac{\partial \sigma}{\partial y} = \rho\frac{\partial u}{\partial t}. \tag{1.7.8}$$

We obtain

$$\frac{\eta U}{H^2}\left[-\frac{\partial \tilde{p}}{\partial \tilde{x}} + \frac{\partial \tilde{\sigma}}{\partial \tilde{y}}\right] = \frac{\rho U^2}{H}\cdot\frac{\partial \tilde{u}}{\partial \tilde{t}}. \tag{1.7.9}$$

Dividing through by $\eta U/H^2$, the right side becomes the Reynolds number $\mathrm{Re} = \rho UH/\eta$. Thus, the equation of motion can be put into the non-dimensional form:

$$-\frac{\partial \tilde{p}}{\partial \tilde{x}} + \frac{\partial \tilde{\sigma}}{\partial \tilde{y}} = \mathrm{Re}\frac{\partial \tilde{u}}{\partial \tilde{t}}. \tag{1.7.10}$$

After this non-dimensionalisation, the usual procedure is to drop the tildes with the understanding that every entity in the equation has zero dimension. This results in the following:

$$-\frac{\partial p}{\partial x} + \frac{\partial \sigma}{\partial y} = \mathrm{Re}\frac{\partial u}{\partial t}. \tag{1.7.11}$$

In viscoplastic fluid mechanics, quite often one is not interested in the effect of the Reynolds number on the velocity field. In this case, one can eliminate the Reynolds

number from the above equation by choosing a different form for $\tilde{t}$ in (1.7.3). That is, let

$$\tilde{t} = \frac{\eta}{\rho H^2} t. \tag{1.7.12}$$

Then, (1.7.9) has the form

$$\frac{\eta U}{H^2}\left[-\frac{\partial \tilde{p}}{\partial \tilde{x}} + \frac{\partial \tilde{\sigma}}{\partial \tilde{y}}\right] = \frac{\eta U}{H^2}\frac{\partial \tilde{u}}{\partial \tilde{t}}. \tag{1.7.13}$$

Dropping the tildes, one obtains a different version of the equation of motion:

$$-\frac{\partial p}{\partial x} + \frac{\partial \sigma}{\partial y} = \frac{\partial u}{\partial t}. \tag{1.7.14}$$

1.8 The Buckingham Equation

The flow rate Q in (1.5.4) can be written in a different form by substituting $y_0 = h/H$, and introducing the average velocity U so that $Q = 2UH$. Since $GH = \tau_y/y_0$, a partial transformation of (1.5.4) leads to the following:

$$U = \frac{\tau_y H}{3\eta y_0}\left[1 - \frac{3}{2}y_0 + \frac{1}{2}y_0^3\right]. \tag{1.8.1}$$

Using the Bingham number Bn, defined in (1.7.5), one finds that (1.8.1) becomes

$$\frac{3y_0}{\mathrm{Bn}} = \left[1 - \frac{3}{2}y_0 + \frac{1}{2}y_0^3\right]. \tag{1.8.2}$$

This leads to the Buckingham equation:

$$y_0^3 - 3\left(1 + \frac{2}{\mathrm{Bn}}\right)y_0 + 2 = 0. \tag{1.8.3}$$

We know that $0 < y_0 < 1$. However, when $\mathrm{Bn} = 3$ in (1.8.3), the resulting equation

$$x^3 - 5x + 2 = 0, \tag{1.8.4}$$

has a root $x = 2$. The other two roots are: $-(\sqrt{2}+1)$, $(\sqrt{2}-1)$. Clearly, the last root is the desired one.

Thus, it is essential to prove that the Buckingham equation (1.8.3) has only one positive, real root less than 1. To establish this, consider the general cubic equation

$$ax^3 + bx^2 + cx + d = 0, \tag{1.8.5}$$

where a, b, c, d are all real. The roots of the equation depend on the discriminant $\triangle$:

$$\triangle = 18abcd - 4b^3d + b^2c^2 - 4ac^3 - 27a^2d^2. \tag{1.8.6}$$

In particular, if $\triangle > 0$, the roots of (1.8.5) are all real and distinct. Determining the value of $\triangle$ for the Buckingham equation (1.8.3), we find that

$$\triangle = -4c^3 - 108 = 108\left(1 + \frac{2}{\mathrm{Bn}}\right)^3 - 108 > 0. \tag{1.8.7}$$

Hence, the roots of the Buckingham equation are all real and distinct. If these roots are α, β, γ, it is obvious that

$$\alpha + \beta + \gamma = 0, \quad -\alpha\beta\gamma = 2. \tag{1.8.8}$$

Thus, only one root must be negative while the other two are positive; suppose that $\gamma < 0,\ \alpha > 0, \beta > 0$. From $(1.8.8)_2$ it follows that

$$\alpha\beta(\alpha + \beta) = 2. \tag{1.8.9}$$

Hence, it is easy to see that $0 < \alpha < 1,\ \beta > 1$. Obviously, out of the two positive roots, one chooses $y_0 = \alpha$ as the desired solution. These derivations are clearly in accord with the roots of the equation $x^3 - 5x + 2 = 0$ in (1.8.4).

Finally, the width of the plug disappears as the Bingham number $\mathrm{Bn} \to 0$, for the Bingham fluid turns into a Newtonian fluid; and (1.8.3) implies that the width of the plug approaches 1 as $\mathrm{Bn} \to \infty$. These two observations can be employed to perform a regular perturbation analysis of y_0 in (1.8.3), and it will be found that [1]:

$$y_0 \sim \frac{1}{3}\mathrm{Bn} - \frac{1}{6}\mathrm{Bn}^2 \quad \text{as } \mathrm{Bn} \to 0. \tag{1.8.10}$$

Assuming that as $\mathrm{Bn} \to \infty$,

$$y_0 \sim 1 + a_1\mathrm{Bn}^{-p} + a_2\mathrm{Bn}^{-q} + \cdots, \quad q > p, \tag{1.8.11}$$

one can prove that $p = 1/2,\ q = 1,\ a_1 = -\sqrt{2},\ a_2 = 2/3$. That is, the following asymptotic expansion [1] holds for large Bn :

$$y_0 \sim 1 - \frac{\sqrt{2}}{\mathrm{Bn}^{1/2}} + \frac{2}{3\ \mathrm{Bn}} + O(\mathrm{Bn}^{-3/2}). \tag{1.8.12}$$

1.9 Free Boundary Problems

The problem discussed above in Sect. 1.3 and its solution in Sect. 1.4 are typical of the behaviour of the flow of Bingham and other viscoplastic fluids. That is, one has to find the width of the plug or its exact shape; it may well be that there are regions,

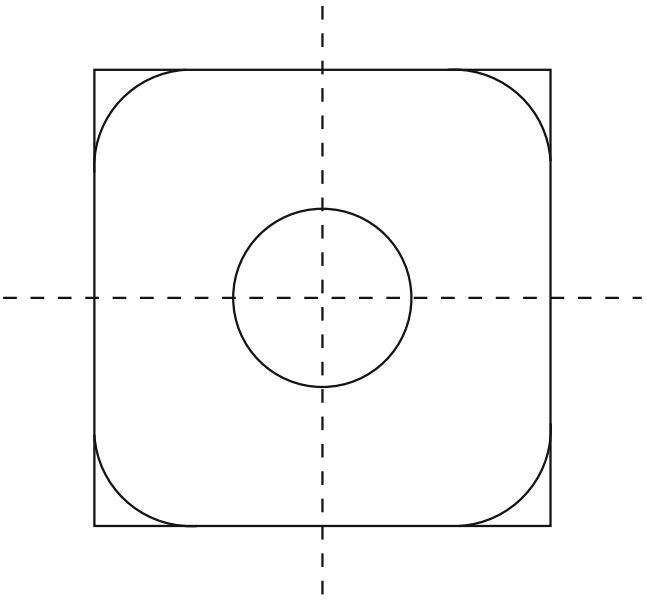

Fig. 1.3 Steady flow in a pipe of square cross-section due to a constant pressure drop per unit length, with a moving rigid core in the centre, and symmetric, stagnant regions at the corners

especially in corners, where the fluid is at rest. For example, see Fig. 1.3, where the flow in a pipe of square cross-section is shown with a plug flow in the middle and regions of rest in the corners. Thus, the velocity field has to be found and the interface(s) between the yielded and unyielded regions have to be determined as a part of the solution. This is an example of a free boundary problem; this expression is used to describe the following:

- determination of a stationary boundary or boundaries as part of a steady state problem,
- unsteady problems where the position and shape of the *moving boundary* has to be determined as a function of space and time.

Such problems are not easy to solve, especially when the flow is unsteady. There are numerous examples of these in engineering and mathematical physics. Here, we shall mention two only.

One of the first example of a free boundary problem involves the change of phase and is called the Stefan problem. In simple terms, let the half-space $y > 0$ be filled with ice at a temperature of zero degree centigrade. At $t = 0$, the wall at $y = 0$ is placed and kept thereafter at a constant temperature $T_0 > 0$. It is clear that the ice near the wall will start melting and the melting front, a free boundary, will start propagating into the frozen ice. Suppose that the melting front is located at $y = \delta(t)$ at time $t \geq 0$, with $\delta(0) = 0$. The problem now is to find the temperature distribution $T = T(y, t)$ in $0 \leq y \leq \delta(t)$, as well as the location of the moving front at $y = \delta(t)$.

Since the temperature distribution satisfies the heat equation in the molten liquid, viz., water, one has the following problem to solve:

$$\frac{\partial T}{\partial t} - a\frac{\partial^2 T}{\partial y^2} = 0, \quad 0 < y < \delta(t), \ t > 0, \tag{1.9.1}$$

where a is the diffusivity. Turning to the boundary conditions, the first boundary condition is obtained from that at $y = 0$; the second from the fact that at the molten front, the water and the ice ahead of it are both at zero degree centigrade. Thus,

$$T(0, t) = T_0, \quad T(\delta(t), t) = 0, \quad t \geq 0. \tag{1.9.2}$$

This is not all, for the molten front will not move unless it melts the ice with which it comes into contact. From Fourier's law of heat conduction, this process requires that the temperature gradient at $y = \delta(t)^-$ be non-zero; in fact it is negative because of the fall in the temperature from the wall to the molten front. Assuming that the mass density of ice is ρ, the latent heat of melting is ν, and k is the heat conductivity coefficient, the heat balance equation shows that

$$-k\frac{\partial T}{\partial y}(\delta(t)^-, t) = \nu\rho\frac{d\delta(t)}{dt}. \tag{1.9.3}$$

The crucial point to note is that at the free boundary, i.e., at the molten front, two boundary conditions have to be imposed.

The solution of the Stefan problem is well known and can be found in several places; for example, see Stakgold [2], from which one finds that

$$T(y, t) = T_0 - \frac{T_0}{\operatorname{erf}\alpha}\operatorname{erf}\left(\frac{y}{2\sqrt{at}}\right), \tag{1.9.4}$$

where α is the solution of the equation:

$$\frac{e^{-\alpha^2}}{\operatorname{erf}\alpha} = \left(\frac{\nu\rho a}{kT_0}\pi^{1/2}\right)\alpha. \tag{1.9.5}$$

Finally,

$$\delta(t) = 2\alpha\sqrt{at}. \tag{1.9.6}$$

In sum, the temperature distribution in water along with the location of the molten front have now been found.

While it took several decades to recast the Stefan problem as a variational inequality [3], the theoretical development of this method began with the solution of the *obstacle problem*: a brief description follows next. Suppose that a membrane is stretched over a circular ring, lying in the (x, y) plane with its centre at $(0, 0)$. Let

this membrane be pushed up by a rod with a hemispherical top. Assuming that the diameter of the hemisphere is less than that of the ring, it is clear that as more force is applied, the membrane will stretch further. And, the curve of mutual contact between the membrane and the obstacle pushing it will increase in size. This boundary of mutual contact is another example of a *free boundary*. Thus, the solution of the deflection problem requires finding both the shape of the deformed membrane as well as the free boundary. Once again, on this boundary, one imposes two conditions: the first says that the deflection of the membrane is the same as the height of the obstacle above the (x, y) plane, and the second says that the gradients of the two surfaces are equal along this curve.

In the obstacle problem, spurious and unphysical solutions may exist. To understand this, consider the equivalent, one-dimensional version. Here, an elastic string lying between $0 \leq x \leq L$ is pushed up by an obstacle. See Fig. 1.4. In this case, the correct solution can be obtained by inspection, as shown by the dotted line. However, a spurious solution may exist. To demonstrate this, let the obstacle function $\psi = \psi(x)$ cross the x-axis at two points $x = \alpha,\ \beta$. An unphysical solution $u = u(x)$, describing the deflection of the string, would take the form:

$$u(x) = \begin{cases} 0, & 0 \leq x \leq \alpha, \\ \psi(x), & \alpha \leq x \leq \beta, \\ 0, & \beta \leq x \leq L. \end{cases} \tag{1.9.7}$$

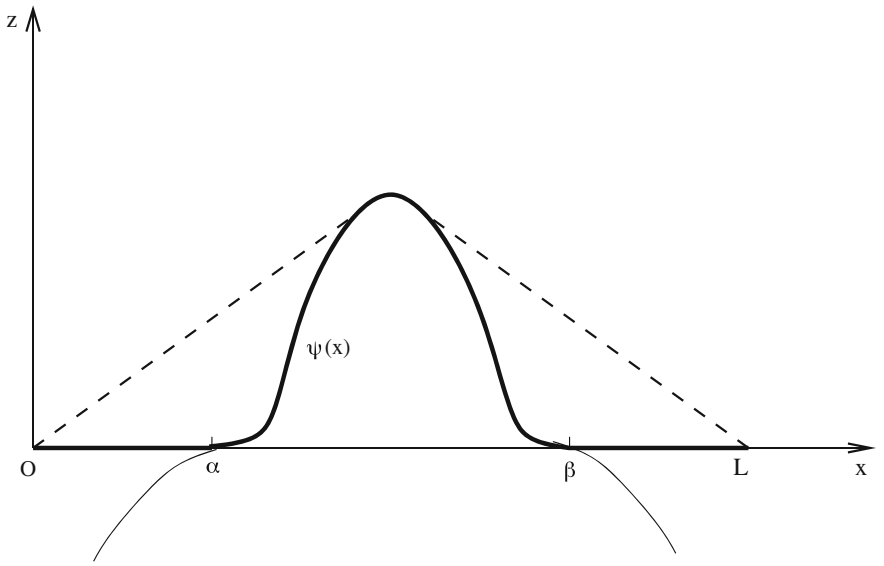

Fig. 1.4 Deflection of an elastic string by an obstacle. True solution: - - - - . Spurious solution: *Thick line*

In order to rule out such unacceptable solutions, the theory of variational inequalities, based on using either the principle of virtual work or virtual power, was developed [4]. Typically, in steady flow problems of viscoplastic fluids, elliptic variational inequalities arise; in unsteady flows, parabolic inequalities appear. For a detailed exposition, see Baiocchi [4], Kinderlehrer [5], Baiocchi and Capelo [6] and Duvaut and Lions [7, 8].

Obviously, there is a great deal of similarity between the obstacle problem and the flow of a Bingham fluid in a channel, say. Just as in the case of the obstacle problem, the solution of this flow problem in a Bingham fluid requires two boundary conditions at the yield surface: the continuity of the velocity field and the vanishing of the velocity gradient. Whereas in the former, the coincidence set describing the contact between the obstacle and the membrane is enlarged as the force is increased, in the latter the size of the plug flow decreases with an increase in the pressure drop per unit length. Following upon the publication of the treatise by Duvaut and Lions [7, 8] demonstrating the application of the variational inequality approach to the solution of flow problems in Bingham fluids, a great amount of research was done. Several of these investigations will be examined in depth from Chap. 8 onwards, although a short version applicable to the channel flow will be discussed next.

1.10 The Minimiser and the Variational Inequality

In order to introduce the concept of a variational inequality, consider the problem of finding the minimum of $y = f(x),\ x \in [a, b]$, where $f(x)$ is continuously differentiable over its domain, with one sided derivatives at the end points. For the sake of argument, let $f(x_0)$ be the unique minimum, where $x_0 \in [a, b]$. In this case, it is clear that derivative $f'(x_0)$ satisfies one of the following conditions:

$$f'(x_0) = \begin{cases} \geq 0, & x_0 = a, \\ 0, & a < x_0 < b, \\ \leq 0, & x_0 = b. \end{cases} \tag{1.10.1}$$

Hence, it follows that

$$f'(x_0) \cdot (x - x_0) \geq 0, \quad x \in [a, b]. \tag{1.10.2}$$

Thus, one can seek the minimum of $y = f(x)$ as: find x_0 such that it is the solution of the inequality (1.10.2).

Similarly, it will be shown in Chap. 8 that that flow of the Bingham fluid in a channel is the minimiser of the following functional:

$$\Phi(v) = \frac{1}{2}\eta a(v, v) + \tau_y j(v) - (G, v), \tag{1.10.3}$$

where $v = v(y)$ is sufficiently smooth and vanishes on the boundary of the channel, i.e., $v(\pm H) = 0$. Here, the three functionals appearing in (1.10.3) are given by

$$a(v, v) = \int_{-H}^{H} v'^2 \, dy, \tag{1.10.4}$$

$$j(v) = \int_{-H}^{H} |v'| \, dy, \tag{1.10.5}$$

$$(G, v) = \int_{-H}^{H} Gv \, dy. \tag{1.10.6}$$

Again, in Chap. 8, it will be shown that the minimiser satisfies the variational inequality (cf. (1.10.2)):

$$\eta a(u, v - u) + \tau_y[j(v) - j(u)] \geq (G, v - u), \tag{1.10.7}$$

where $u = u(y)$ is the solution velocity field, and $v = v(y)$ is any sufficiently smooth velocity field such that $v(\pm H) = 0$.

From this inequality, one can obtain the energy equation satisfied by the solution $u = u(y)$ as follows. If one chooses $v = 2u$, it can be seen that (1.10.7) becomes

$$\eta a(u, u) + \tau_y j(u) - (G, u) \geq 0, \tag{1.10.8}$$

while choosing $v = 0$ results in

$$-\eta a(u, u) - \tau_y j(u) + (G, u) \geq 0. \tag{1.10.9}$$

Now, a real number α cannot satisfy both of the inequalities $\alpha \geq 0$ and $-\alpha \geq 0$, unless $\alpha = 0$. So, the solution velocity field $u = u(y)$ satisfies the equation of energy balance:

$$\eta a(u, u) + \tau_y j(u) = (G, u). \tag{1.10.10}$$

This energy equation is important for it serves as a check on the numerical scheme employed to minimise either $\Phi(v)$, or to solve the variational inequality in (1.10.7). Note that the integrals in (1.10.4)–(1.10.7) are all defined over $-H \leq y \leq H$, and not over a sub-interval. So, even if $u' = 0$ in the rigid core, the integrals are always non-negative. Obviously, they are all zero if the pressure drop $G < G_c$.

The energy equation shows that the minimum of the functional $\Phi(v)$ is not zero. Rather, it is given by

$$\min_{v \neq 0} \Phi(v) = -\frac{1}{2} \eta a(u, u) < 0. \tag{1.10.11}$$

If the flow is unsteady, that is $u = u(y, t)$, the energy equation can be derived from the corresponding variational inequality, which is

$$\rho\left(\frac{\partial u}{\partial t}, v - u\right) + \eta a(u, v - u) + \tau_y[j(v) - j(u)] \geq (G, v - u). \tag{1.10.12}$$

Following the procedure used when the flow is steady, one obtains the energy equation:

$$\rho\left(\frac{\partial u}{\partial t}, u\right) + \eta a(u, u) + \tau_y j(u) = (G, u). \tag{1.10.13}$$

Given this equation, one can consider the following problem: suppose that a Bingham fluid is undergoing a steady flow in a channel. At time $t = 0^+$, let us say that the pressure drop per unit length G is reduced to zero, forcing the Bingham fluid to come to rest eventually due to the effects of viscous and yield stress dissipation. In a Newtonian fluid, the corresponding problem can be solved analytically and it can be shown that the extinction time is *infinite*. Surprisingly, this extinction time is *finite* in Bingham and other viscoplastic fluids. This is another *major distinction* between purely viscous and viscoplastic fluids, a discovery made by Glowinski [9] in connection with the cessation of flows in a pipe of arbitrary cross-section. In these cessation problems, the dynamics behind the lateral movement of the yield surface, while the velocity field goes to zero, needs a detailed explanation. These matters will be explored in depth in Chaps. 6 and 9.

In sum, this book presents a collection of solutions to problems for the flows of Bingham fluids which can be solved analytically. And, when that is not possible, it shows how to tackle these problems through numerical simulation of the relevant variational principles and inequalities.

1.11 Effects of Wall Slip

Navier (c. 1827) seems to have been the first to recognise that a fluid may not adhere to the bounding wall in a motion; instead, it may slip along it with a wall slip velocity u_w proportional to the wall shear stress σ_w. However, common experience with moving a heavy object along a floor suggests that a stick-slip mechanism is to be preferred. That is, the fluid does not slip until the wall shear stress exceeds a critical value, τ_c. When σ_w increases beyond this critical value, there is a nonlinear relationship between the new wall shear stress and the slip velocity u_w. Thus, consider the following stick-slip model:

$$u_w = 0, \ \sigma_w \leq \tau_c; \qquad \sigma_w = \tau_c + f(u_w)u_w, \ \sigma_w > \tau_c. \tag{1.11.1}$$

This boundary condition is very similar to that of the constitutive relation of the Bingham fluid and is due to Fortin et al. [10], who based their assumptions on the

critical wall shear stress observed by Ramamurthy [11] in a capillary rheometer. These experiments, performed on non-viscoplastic fluids, showed that the critical wall shear stress τ_c is relatively insensitive to molecular characteristics, such as molecular weight, MWD and chain branching, as well as the melt temperature and the detailed design of the capillary. However, in blown film fabrication, materials of construction for the die land region have a significant influence on melt fracture. Hence, in general, the critical wall shear stress τ_c is not an intrinsic *material property*; rather, it is allied to the process under consideration.

Nevertheless, in the sequel, τ_c will be regarded as a material property; without such an assumption, it is not possible to study the influence of wall slip in the flows of viscoplastic fluids. Turning to (1.11.1), one notes that the usual separation of the boundary of the flow domain into a part on which the velocity is prescribed and another on which the stress vector is given is no longer valid. The former disappears and is replaced by that part on which the wall shear stress is defined, as in (1.11.1). Secondly, the critical value τ_c may be quite different from the yield stress τ_y in a Bingham fluid; hence, whether a flow exists with or without wall slip depends on the relative strengths of these two properties.

Turning to the flow of a Bingham fluid in a channel, we shall assume that in (1.11.1), the velocity dependent wall shear stress is given by $f(u_w)u_w = Du_w^s$, where D is a constant and the exponent $s > 0$. Introduce the non-dimensional variables

$$\tilde{h} = \frac{h}{H}, \quad \tilde{u}_w = \frac{u_w}{U}, \quad \tilde{G} = \frac{GH}{\tau_y}, \quad S_c = \frac{\tau_c}{\tau_y}, \quad S_n = \frac{DU^s}{\tau_y}, \tag{1.11.2}$$

and denote by $\tilde{G}$, the non-dimensional pressure drop per unit length; next S_c is the critical yield stress number and, finally, S_n is called the slip number. Of course, U is the characteristic velocity and H is the length scale. Dropping the tildes and assuming that $f(u_w)u_w = Du_w^s$, the non-dimensional form of (1.11.1) is given by

$$u_w = 0, \ \sigma_w \le S_c; \qquad \sigma_w = S_c + S_n u_w^s, \ \sigma_w > S_c. \tag{1.11.3}$$

In practice, it is better to recast the above as follows:

$$u_w = \begin{cases} 0, & \sigma_w \le S_c, \\ \left((\sigma_w - S_c)/S_n\right)^{1/s}, & \sigma_w > S_c. \end{cases} \tag{1.11.4}$$

One is faced with four distinct possibilities, as far as the steady flow in a channel is concerned.[1] Noting that the non-dimensional critical pressure drop per unit length

[1] In [12], the stick-slip model has been used to examine the initiation and cessation of the flows of viscoplastic fluids in a pipe of circular cross-section. The treatment given above is influenced by that work.

is given by $\tilde{G}_c = G_c H/\tau_y = 1$, where (1.3.1) has been employed, the following may occur:

- Suppose that $G < \min(S_c, 1)$. In this case, no flow can occur.
- Let $G > \max(S_c, 1)$. In this situation, there is the usual channel flow with wall slip; this is similar to the flow in a pipe of circular cross-section, considered in [10]. That is, the wall shear stress $\sigma_w = G$, and the velocity field is given by

$$u(y) = u_w + \frac{G}{2}\begin{cases} (1-h)^2, & 0 \le y \le h, \\ (1-y^2) - 2h(1-y), & h \le y \le 1, \end{cases} \tag{1.11.5}$$

  where the slip velocity

$$u_w = \left(\frac{G - S_c}{S_n}\right)^{1/s}, \tag{1.11.6}$$

  and the yield surface is located at

$$h = \frac{\tau_y}{\sigma_w} < 1. \tag{1.11.7}$$

- Next, let $1 < G < S_c$. The Bingham fluid will flow without slip, i.e., $u_w = 0$ in (1.11.5).
- Finally, let $S_c < G < 1$. The fluid will slip along the wall and flow as a rigid body with a constant velocity u_w, given by (1.11.6).

The stick-slip model can be used to derive a new variational principle and a variational inequality; this matter is covered in Sect. 8.5. Finally, one can use it to examine the cessation of the steady flow of a Bingham fluid in a channel or in a pipe of circular cross-section; see Sect. 9.4.7.

1.12 Experimental Support

While the theory behind the fluid mechanics of viscoplastic fluids is elegant and worth studying it in its own right, it would be desirable to find experimental evidence to justify the pursuit of this knowledge. Here, we shall summarise some of the evidence based on various review articles available in the literature.

The very first evidence of viscoplasticity was found by Schwedoff in the 1890s, when he performed experiments on colloidal gelatin solutions using a Couette device. Interestingly, his experiments seem to be the first set of measurements of non-Newtonian behaviour, for his data indicated a nonlinear relationship between the torque and angular velocity in this instrument. In particular, he had to incorporate a yield value to describe his results [13]. Subsequently, the work of Bingham and Green in the 1920s led to widespread acceptance that some fluids exhibit yield stress behaviour [14]. In particular, many materials of industrial importance, such as concentrated

suspensions, red mud residues, pastes, foodstuffs, emulsions, foams, waxy crude oils, fibre reinforced plastics and other composites are viscoplastic. However, doubts have been raised that fluids regarded as yield stress materials do not possess a *true yield stress*. For example, Barnes [15] is of the opinion that these materials should be regarded as fluids which creep with a constant value of viscosity, of the order of 10^6 Pa. s, when the applied shear stress is exceedingly small; that they flow like liquids with a much lower viscosity when the shear stress is quite large; and that the transition from one regime to another occurs quite often across a very narrow range of the applied stress. Thus, these materials should not be considered as viscoplastic although they are routinely regarded as such. Here, we shall offer some comments regarding the experimental evidence both in support of and in opposition to the view that some materials are viscoplastic.

As remarked by Nguyen and Boger [16], the controversy over the existence of a true yield stress is not new; it appeared very soon after Bingham and Green discovered that paint was not a truly viscous liquid. More recently, it has resurfaced with the experiments performed by Barnes and Walters [17] which show that several fluids deemed to be viscoplastic do not possess a true yield stress. Essentially, in their experiments, Barnes and Walters found that when a conventional rheometer, such as the Weissenberg Rheogoniometer, was used to measure the dependence of the shear stress on the shear rate, they could not obtain accurate results at shear rates below about $10^{-2}\,\mathrm{s}^{-1}$, and certainly not below $10^{-3}\,\mathrm{s}^{-1}$. In this rheometer, the plot of shear stress versus the shear rate produces a graph which seems to intersect with the shear stress axis at a *yield stress* value of $\tau_y = 9.5\,\mathrm{Pa}$. See Fig. 3a in [17].

On the other hand, when the same fluid was subjected to shearing in a constant stress rheometer, such as the Deer Rheometer Mk II capable of producing shear rates as low as $10^{-6}\,\mathrm{s}^{-1}$, it was found by Barnes and Walters [17] that the viscosity of the liquid attained a Newtonian plateau. See Fig. 4 in [17]. That is, while the fluid exhibited non-Newtonian behaviour, it did not possess a true yield stress. In the last few years, devices capable of completing a revolution every few days or few years have appeared on the market. It has been found that even at these slow speeds of rotation, many fluids suspected of being viscoplastic do not seem to possess a true yield stress. The obvious question to ask is this: if an instrument is capable of completing a revolution every 20 years, is the fluid in the rheometer being sheared in this infinitesimally slow process? Granting this occurs, a fluid which exhibits creep has to be modelled as a non-Newtonian, viscous fluid, especially if an industrial process exists in which such time scales are important.

Thus, one is faced with the following contentious issue: do there exist any fluids which are truly viscoplastic? The answer to this question depends on the time scale of the industrial process which one wishes to study either through theory or experiments. One simple example of the importance of the time scale comes from rubber. The experiments done by Rivlin during 1948–1952 showed that a theoretical basis for describing the data exists if one models rubber as an incompressible, elastic solid undergoing finite deformations; for a review, see [18]. While this is true for reasonably slow deformations, it is also known that under fast processes, rubber crystallises and, in this process, it cannot be described as a finitely elastic material [19]. So, the

theory of finite deformations of rubber applies under some conditions only. That is, depending on the circumstances, one has to choose different constitutive equations to characterise rubber.

In a similar vein, Astarita [20] argued that yield stress was an *engineering reality*. That is, the flow behaviour of many materials used in several industrial processes could be best described and understood if they were regarded as viscoplastic fluids. While this view is shared by many, it is obvious that it would be desirable to find a material and perform experiments on it in the laboratory to show that it exhibits a true yield stress behaviour. Such a task has been accomplished by Tabuteau et al. [21], who studied the motion of falling spheres in Carbopol gels. They observed three regimes of motion in these experiments. Spheres of high density reached a constant terminal velocity, as in Newtonian fluids. Below a critical density, a sphere would come to a complete stop, indicating the existence of a yield stress. In the intermediate regime, the sphere continued to move with a velocity decreasing steadily with time.The yielding criterion and the drag force on the sphere were found to be in excellent agreement with the theoretical predictions of Beris et al. [22], and those of Beaulne and Mitsoulis [23]; see Figs. 3–7 in [21]. For a further discussion of this matter, see Chap. 9 where applications of variational principles are examined.

1.13 Summary

To summarise the argument so far: if the flow of a material occurs under a set of infinitesimally slow conditions, it may well be that the fluid is not viscoplastic; on the other hand, under many industrial processing conditions, the very same materials would be seen to possess a yield stress. To model the latter processes, there are mathematically exact constitutive equations to characterise viscoplastic fluids. The analysis of the flows of such materials, in particular that of the Bingham fluid, forms the basis of this monograph. In this connection, it is relevant to note that regularised models, such as the Papanastasiou model [24], do not deliver analytical solutions in a straight forward manner even in the case of simple steady flow problems. While their use has been widespread in order to overcome the problem of locating the yield surface in numerical simulations, it would be preferable to avoid such models, for they mask the true effects of yield stress. Instead, the use of precise numerical schemes, such as the augmented Lagrangian method and the operator-splitting method expounded in Chap. 10, to model the flows of viscoplastic fluids must be preferred to understand the real influence of the yield stress.

References

1. Nouar C, Frigaard IA (2001) Nonlinear stability of Poiseuille flow of a Bingham fluid: theoretical results and comparison with phenomenological criteria. J Non-Newt Fluid Mech 100: 127–149

2. Stakgold I (1968) Boundary value problems of mathematical physics, vol II. Macmillan, New York
3. Duvaut G (1973) Résolution d'un problème de Stéfan (Fusion d'un bloc de glace à zéro degré). C R Acad Sci Paris 276:1461–1463
4. Baiocchi C (1978) Free boundary problems and variational inequalities. Technical Summary Report 1883, Mathematics Research Center, University of Wisconsin-Madison
5. Kinderlehrer D (1978) Variational principles and free boundary problems. Bull Am Math Soc 84:7–26
6. Baiocchi C, Capelo A (1984) Variational and quasivariational inequalities: applications to free-boundary problems. Wiley, New York
7. Duvaut G, Lions JL (1972) Les inéquations on mécanique et en physique. Dunod, Paris
8. Duvaut G, Lions JL (1976) Inequalities in mechanics and physics. Springer, New York
9. Glowinski R (1974) Sur l'ecoulement d'un fluide de Bingham dans une conduite cylindrique. J de Méc. 13:601–621
10. Fortin A, Côté D, Tanguy PA (1991) On the imposition of friction boundary conditions for the numerical simulation of Bingham fluid flows. Comput Methods Appl Mech Eng 88:97–109
11. Ramamurthy AV (1986) Wall slip in viscous fluids and influence of materials of construction. J Rheol 30:337–357
12. Damianou Y, Philippou M, Kaoullas G, Georgiou GC (2014) Cessation of viscoplastic Poiseuille flow with wall slip. J Non-Newt Fluid Mech 203:24–37
13. Doraiswamy D (2002) The origins of Rheology: a short historical excursion. Rheol Bull 71(1):7–9, 11, 13–17
14. Bingham EC (1922) Fluidity and plasticity. McGraw-Hill, New York
15. Barnes HA (2007) The 'The yield stress myth?' paper - 21 years on. Appl Rheol 17:43110-1–43110-5
16. Nguyen QD, Boger DV (1992) Measuring the flow properties of yield stress fluids. Ann Rev Fluid Mech 24:47–88
17. Barnes HA, Walters K (1985) The yield stress myth? Rheol Acta 24:323–326
18. Rivlin RS (1960) Some topics in finite elasticity. In: Goodier JN, Hoff NJ (eds) Structural mechanics: proceedings of the first symposium on naval structural mechanics. Pergamon, Oxford, pp 169–198
19. Rajagopal KR (2011) Modeling a class of geological materials. Int J Adv Eng Sci Appl Math 3:2–13
20. Astarita G (1990) Letter to the editor: the engineering reality of the yield stress. J Rheol 34:275–277
21. Tabuteau H, Coussot P, de Bruyn JR (2007) Drag force on a sphere in steady motion through a yield-stress fluid. J Rheol 51:125–137
22. Beris AN, Tsamopoulos JA, Armstrong RC, Brown RA (1985) Creeping motion of a sphere through a Bingham plastic. J Fluid Mech 158:219–244
23. Beaulne M, Mitsoulis E (1997) Creeping motion of a sphere in tubes filled with Herschel-Bulkley fluids. J Non-Newt Fluid Mech 72:55–71
24. Papanastasiou TC (1987) Flow of materials with yield. J Rheol 31:385–404

Chapter 2
Kinematics of Fluid Flow

The study of kinematics has flourished as a subject where one may consider displacements and motions without imposing any restrictions on them; that is, there is no need to ask whether they are dynamically feasible in the physical world. Of course, the dynamical nature of a flow is impossible to ascertain a priori, because a flow which is possible in one fluid need not exist in another. However, in discussing viscoplastic fluid mechanics, memory effects are ignored, which means that the amount of material needed to understand the kinematics of the flows of such fluids is relatively modest.[1]

To begin, we introduce the concepts of the motion of a particle and relate it to the velocity and acceleration of the particle and extend these to a field description over the whole body. Defining the deformation and velocity gradients, a simple matrix differential equation is derived to relate them to one another. In turn, this equation solves the problem of determining when a velocity field in the Lagrangian description is steady in the Eulerian sense. Since this result may have applications in numerical modelling in the future, it has been mentioned in this chapter.

Next, the velocity gradient is introduced along with the first Rivlin-Ericksen tensor [2], denoted by $\mathbf{A}_1$. The latter is twice the symmetric part of the former, and it is shown that this symmetric tensor is a measure of the rate of stretching at a point in the flow. The skew-symmetric part of the velocity gradient is called the spin tensor $\mathbf{W}$, and it is closely related to the vorticity vector. The two tensors $\mathbf{A}_1$ and $\mathbf{W}$ determine when a fluid particle experiences a rigid motion, which is of importance in understanding the behaviour of a rigid core which may exist in a given flow domain.

Finally, the Appendix lists some basic results:

- The forms taken by the divergence and curl of a vector in Cartesian, cylindrical and spherical coordinates.
- The physical components of the first Rivlin-Ericksen tensor in Cartesian, cylindrical and spherical coordinates.

[1] Much of the material in this chapter, including the Appendix, follows the treatment in Huilgol and Phan-Thien [1].

R.R. Huilgol, *Fluid Mechanics of Viscoplasticity*, DOI 10.1007/978-3-662-45617-0_2

- The physical components of the spin tensor and their relation to the physical components of the curl of the velocity vector.

2.1 Kinematical Preliminaries

Let X be a particle of a body (a continuous medium) $\mathscr{B}$, and let X occupy a point in the three-dimensional Euclidean space $\mathbb{R}^3$, at a fixed instant $t = 0$. We shall call this configuration occupied by the body $\mathscr{B}$, the *reference configuration* $\mathscr{B}_R$. The coordinates X^α, of the point where X is at that fixed instant, are the *material coordinates* of the particle. The position vector of X at $t = 0$ will be denoted by $\mathbf{X}$.

Let X trace out a path in E^3. We shall denote this path by the curve

$$\mathbf{x} = \mathbf{M}(\mathbf{X}, t), \quad x^i = M^i\left(X^\alpha, t\right) \tag{2.1.1}$$

in the Euclidean space. Here t, the time coordinate, acts as a parameter and as t varies over a given time interval $\mathscr{I}$, the function $\mathbf{M}(\cdot, t)$ describes the path. Traditionally, the curve (2.1.1) is called the Lagrangian or material description of the motion of the particle. Note that $\mathbf{X} = \mathbf{M}(\mathbf{X}, 0)$, because $\mathbf{X}$ is the initial value for the motion.

Now, we are interested in the motion of the whole body $\mathscr{B}$ rather than a single particle. So, the domain of $\mathbf{M}$ is the Cartesian product $\mathscr{B}_R \times \mathscr{I}$, where the time interval $\mathscr{I}$ may or may not be finite. In other words, changing $\mathbf{X}$ in $\mathbf{M}(\mathbf{X}, \cdot)$ gives us the path of another particle of $\mathscr{B}$ so that, at time t, $\mathbf{M}(\mathbf{X}, t)$, $\mathbf{X} \in \mathscr{B}_R$, gives us the *spatial configuration* of $\mathscr{B}$.

We usually demand that $\mathbf{M}$ be continuously differentiable twice with respect to $\mathbf{X}$ and t, or $\mathbf{M} \in C^{2,2}$, though on the boundary $\mathbf{M}$ may be $C^{1,1}$. Hence the motion $\mathbf{M}$ is required to have a continuous gradient with respect to $\mathbf{X}$. We shall demand a stronger condition on this gradient: $\nabla_{\mathbf{X}}\mathbf{x}$ has a positive determinant everywhere. One notes that this guarantees that the inverse

$$\mathbf{X} = \mathbf{M}^{-1}(\mathbf{x}, t) \tag{2.1.2}$$

exists and is unique, locally at least. The stronger assumption of global inversion is made in continuum mechanics, on a piecewise basis if necessary; for without this assumption, many results of continuum mechanics which depend on the possibility of recasting a function, originally given in material coordinates, into spatial coordinates, become very difficult to establish. Indeed, this assumption of global invertibility is needed next in connection with the velocity field and later with the Reynolds transport theorem, for example.

The velocity $\mathbf{v}$ and the acceleration $\mathbf{a}$ of a particle are defined in the material or Lagrangian description through the functions:

$$\hat{\mathbf{v}} = \frac{\partial}{\partial t}\mathbf{M}(\mathbf{X}, t), \quad \hat{v}^i = \left.\frac{\partial M^i}{\partial t}\right|_{\mathbf{X}}, \tag{2.1.3}$$

$$\hat{\mathbf{a}} = \frac{\partial^2}{\partial t^2}\mathbf{M}(\mathbf{X}, t), \quad \hat{a}^i = \left.\frac{\partial^2 M^i}{\partial t^2}\right|_{\mathbf{X}}. \tag{2.1.4}$$

Hence, if the velocity $\mathbf{v}$ is defined over the body by the function $\hat{\mathbf{v}}(\mathbf{X}, t)$, the acceleration $\mathbf{a}$ is given by

$$\hat{\mathbf{a}} = \frac{\partial}{\partial t}\hat{\mathbf{v}}(\mathbf{X}, t). \tag{2.1.5}$$

However, we usually find it more convenient to express the velocity of $\mathbf{X}$ at time t in terms of the coordinates it occupies at time t. Such a description leads to an Eulerian or a spatial field $\mathbf{v}(\mathbf{x}, t)$.

Let us now give the velocity a Lagrangian description as well as an Eulerian representation:

$$\mathbf{v} = \hat{v}^\alpha\left(X^\beta, t\right)\mathbf{G}_\alpha = v^i\left(x^j, t\right)\mathbf{g}_i, \tag{2.1.6}$$

where $\mathbf{G}_\alpha$ and $\mathbf{g}_i$ are the base vectors at X^α and x^i, respectively, and the summation convention on repeated indices is employed. Then the spatial form of (2.1.5) becomes

$$a^i = \frac{\partial v^i}{\partial t} + v^i_{;j}\, v^j, \tag{2.1.7}$$

where the semi-colon (;) denotes the covariant derivative. In (2.1.7), we have come across the velocity gradient $v^i_{;j}$, identified by the symbol $\mathbf{L}$. Thus, the mixed and covariant components of $\nabla\mathbf{v} = \mathbf{L}$ are given by

$$L^i_j = v^i_{;j} \quad L_{ij} = v_{i;j}. \tag{2.1.8}$$

Hence the acceleration $\mathbf{a}$ has the following spatial representation:

$$\mathbf{a} = \frac{\partial \mathbf{v}}{\partial t} + \mathbf{L}\mathbf{v}. \tag{2.1.9}$$

Using the format of (2.1.7), we call the derivative

$$\frac{d}{dt}(\cdot) = \frac{\partial(\cdot)}{\partial t} + (\cdot)_{;j}\, v^j, \tag{2.1.10}$$

the *material derivative* of a spatial field $(\cdot)$.

A velocity field is said to be *steady* if $\mathbf{v} = \mathbf{v}(\mathbf{x})$, or it is independent of t when expressed according to $(2.1.6)_2$; it is *unsteady* if the velocity field depends explicitly on time, i.e., $\mathbf{v} = \mathbf{v}(\mathbf{x}, t)$. For unsteady flows, the term $\partial\mathbf{v}/\partial t$ represents the *local acceleration*, which is the acceleration measured at a fixed point in space; of course, it is zero in steady flows. For both steady and unsteady flows, $\mathbf{L}\mathbf{v}$ represents the *convected terms* which arise because the fluid particle is being convected from a point with one velocity vector to a second point where the velocity vector is different. Thus,

convected terms may arise either because the magnitude of the velocity is changing along the path of a particle or because the base vectors suffer a change of magnitude or direction, or both.

2.2 Relation Between the Velocity and Deformation Gradients

The gradient of $\mathbf{x}$ with respect to $\mathbf{X}$ is called the *deformation gradient*. We shall denote it by $\mathbf{F}$ and write:

$$\mathbf{F} = \nabla_{\mathbf{X}}\mathbf{x}, \quad F^i_{\ \alpha} = \frac{\partial x^i}{\partial X^\alpha} = x^i_{,\alpha}. \tag{2.2.1}$$

Note that the above definition means that

$$\mathbf{F}(\mathbf{X}, 0) \ = \ \mathbf{1}, \tag{2.2.2}$$

where $\mathbf{1}$ is the identity matrix. Next, due to the fact that det $\mathbf{F}$ (det denotes the determinant) is the Jacobian of the mapping and hence the measure of the ratio of the volumes in the $\mathbf{X}$ and $\mathbf{x}$ spaces, we demand that det $\mathbf{F} > 0$. This ensures that the mapping (2.1.1) is not degenerate, i.e., the conservation of mass is assured, and that the inversion in (2.1.2) is locally possible, as already remarked.

Now, there is a very simple relation between the two tensors $\mathbf{F}$ and $\mathbf{L}$. This arises from the equality of the mixed partial derivatives:

$$\frac{\partial}{\partial X^\alpha}\frac{\partial M^i}{\partial t} \ = \ \frac{\partial}{\partial t}\frac{\partial M^i}{\partial X^\alpha}. \tag{2.2.3}$$

Equivalently,

$$\frac{\partial \hat{v}^i}{\partial X^\alpha} \ = \ \frac{\partial}{\partial t}F^i_{\alpha}. \tag{2.2.4}$$

Expressing the velocity as a spatial field, we have

$$\frac{\partial \hat{v}^i}{\partial X^\alpha} \ = \ \frac{\partial v^i}{\partial x^j}\frac{\partial x^j}{\partial X^\alpha} \ = \ L^i_{\ j}F^j_{\alpha}. \tag{2.2.5}$$

Using the convention of the superposed dot as the material derivative, (2.2.4) and (2.2.5) may be combined and rewritten as

$$\dot{\mathbf{F}} \ = \ \mathbf{LF}. \tag{2.2.6}$$

This differential equation due to Noll [3] has numerous applications in nonlinear continuum mechanics.

In particular, the above identity solves the following problem: given a motion $\mathbf{x} = \mathbf{M}(\mathbf{X}, t)$, what is the necessary and sufficient condition that the velocity field be steady in an Eulerian description? To answer this, let $\hat{\mathbf{v}} = \hat{\mathbf{v}}(\mathbf{X}, t)$ be the Lagrangian form of the velocity field derived from the motion through (2.1.3). Suppose that the velocity of a particle at times t and 0 are related through

$$\hat{\mathbf{v}}(\mathbf{X}, t) = \mathbf{F}(\mathbf{X}, t)\hat{\mathbf{v}}(\mathbf{X}, 0). \tag{2.2.7}$$

Differentiating both sides with respect to t and using $\dot{\mathbf{F}} = \mathbf{LF}$, one finds that

$$\hat{\mathbf{a}}(\mathbf{X}, t) = \mathbf{L}(\mathbf{x}(\mathbf{X}, t), t)\hat{\mathbf{v}}(\mathbf{X}, t). \tag{2.2.8}$$

In turn, in the Eulerian description, this is nothing but the statement that $\mathbf{a} = \mathbf{Lv}$, or the flow is steady. Retracing the steps backwards, one finds that if the flow is steady in the Eulerian sense, then

$$\dot{\hat{\mathbf{v}}}(\mathbf{X}, t) = \dot{\mathbf{F}}(\mathbf{X}, t)\mathbf{F}^{-1}(\mathbf{X}, t)\hat{\mathbf{v}}(\mathbf{X}, t), \tag{2.2.9}$$

has the solution given by (2.2.7); see [4].

2.3 Rigid Motion

From analytical mechanics, it is well known that a rigid body moves in such a way that it translates and rotates about an axis as it does so. In continuum mechanics, one says that a material particle experiences a rigid motion if

$$\mathbf{x}(\mathbf{X}, t) = \mathbf{Q}(t)\mathbf{X} + \mathbf{c}(t), \tag{2.3.1}$$

where $\mathbf{Q}(t)$ is a time-dependent orthogonal tensor signifying the rotation and $\mathbf{c}(t)$ is the translation vector. The velocity vector is given by

$$\hat{\mathbf{v}}(\mathbf{X}, t) = \dot{\mathbf{Q}}(t)\mathbf{X} + \dot{\mathbf{c}}(t), \tag{2.3.2}$$

which has the following spatial representation:

$$\mathbf{v}(\mathbf{x}, t) = \dot{\mathbf{Q}}(t)\mathbf{Q}^T(t)\Big(\mathbf{x} - \mathbf{c}(t)\Big) + \dot{\mathbf{c}}(t), \tag{2.3.3}$$

from which it follows that the velocity gradient has the form $\mathbf{L}(t) = \dot{\mathbf{Q}}(t)\mathbf{Q}^T(t)$. Here, the superscript T denotes the transpose. Since the orthogonality of $\mathbf{Q}(t)$ implies that $\mathbf{Q}(t)\mathbf{Q}^T(t) = \mathbf{1}$, where $\mathbf{1}$ is the identity tensor, one obtains the following:

$$\frac{d}{dt}\Big(\mathbf{Q}(t)\mathbf{Q}^T(t)\Big) = \mathbf{0} \tag{2.3.4}$$

for all t. Clearly,

$$\frac{d}{dt}\left(\mathbf{Q}(t)\mathbf{Q}^T(t)\right) = \left(\frac{d}{dt}\mathbf{Q}(t)\right)\mathbf{Q}^T(t) + \mathbf{Q}(t)\frac{d}{dt}\left(\mathbf{Q}^T(t)\right) = \mathbf{0}. \tag{2.3.5}$$

However,

$$\frac{d}{dt}\left(\mathbf{Q}^T(t)\right) = \left(\frac{d}{dt}\mathbf{Q}(t)\right)^T. \tag{2.3.6}$$

Thus,

$$\left(\frac{d}{dt}\mathbf{Q}(t)\right)\mathbf{Q}^T(t) = \mathbf{W}(t), \tag{2.3.7}$$

where $\mathbf{W}(t)$ is skew-symmetric. That is, $\mathbf{W}(t) = -\mathbf{W}(t)^T$. Equivalently, the velocity gradient $\mathbf{L}(t)$ associated to the velocity field (2.3.3) is skew-symmetric.

2.4 Polar Decomposition, Spin and Stretching

Using the polar decomposition theorem [5], the deformation gradient $\mathbf{F}$ can be decomposed into the product:

$$\mathbf{F} = \mathbf{RU}, \tag{2.4.1}$$

where $\mathbf{R}$ is an orthogonal tensor, or it signifies a rotation, and $\mathbf{U}$ is positive definite and symmetric, or it denotes stretching. That is, the effect of $\mathbf{F}$ on an infinitesimal element is to stretch it and rotate it. Now, the relative deformation gradient $\mathbf{F}_t(\tau)$ is defined through

$$\mathbf{F}_t(\tau) = \mathbf{F}(\tau)\mathbf{F}(t)^{-1}. \tag{2.4.2}$$

It too has the polar decomposition:

$$\mathbf{F}_t(\tau) = \mathbf{R}_t(\tau)\mathbf{U}_t(\tau), \quad \mathbf{R}_t(t) = \mathbf{1}, \quad \mathbf{U}_t(t) = \mathbf{1}. \tag{2.4.3}$$

Now, employing (2.2.6) in (2.4.2), it follows that

$$\frac{d}{d\tau}\mathbf{F}_t(\tau) = \mathbf{L}(\tau)\mathbf{F}_t(\tau), \tag{2.4.4}$$

whence

$$\frac{d}{d\tau}\mathbf{F}_t(\tau)_{|\tau=t} = \mathbf{L}(t). \tag{2.4.5}$$

From (2.4.3), we can see that

$$\frac{d}{d\tau}\mathbf{F}_t(\tau) = \left(\frac{d}{d\tau}\mathbf{R}_t(\tau)\right)\mathbf{U}_t(\tau) + \mathbf{R}_t(\tau)\left(\frac{d}{d\tau}\mathbf{U}_t(\tau)\right)$$
$$= \left(\frac{d}{d\tau}\mathbf{R}_t(\tau)\right)\mathbf{R}_t(\tau)^T\mathbf{F}_t(\tau) + \mathbf{R}_t(\tau)\left(\frac{d}{d\tau}\mathbf{U}_t(\tau)\right). \tag{2.4.6}$$

Here, in the first term

$$\left(\frac{d}{d\tau}\mathbf{R}_t(\tau)\right)\mathbf{R}_t(\tau)^T \tag{2.4.7}$$

is skew-symmetric; see (2.3.7) above. Thus, from (2.4.5) it follows that

$$\mathbf{L}(t) = \left(\frac{d}{d\tau}\mathbf{R}_t(\tau)\right)_{|\tau=t} + \left(\frac{d}{d\tau}\mathbf{U}_t(\tau)\right)_{|\tau=t}$$
$$= \mathbf{W}(t) + \mathbf{D}(t), \tag{2.4.8}$$

where $\mathbf{W}(t)$ is skew-symmetric and $\mathbf{D}(t)$ is symmetric. Since $\mathbf{W}(t)$ is the derivative of a rotation tensor, it is called the *spin tensor*, while $\mathbf{D}(t)$ is called the *rate of deformation or rate of stretching tensor*. Note that

$$\mathbf{W}(t) = \frac{1}{2}\left(\mathbf{L}(t) - \mathbf{L}(t)^T\right), \quad \mathbf{D}(t) = \frac{1}{2}\left(\mathbf{L}(t) + \mathbf{L}(t)^T\right). \tag{2.4.9}$$

In viscoplastic fluid mechanics, it is preferable to use

$$\mathbf{A} = \mathbf{L} + \mathbf{L}^T, \tag{2.4.10}$$

which is called the first Rivlin-Ericksen tensor [2]. The first Rivlin-Ericksen tensor is usually denoted by $\mathbf{A}_1$. Since one does not need higher order Rivlin-Ericksen tensors in viscoplasticity, we shall use the notation $\mathbf{A}$ for the first order tensor in this book and simply refer to it as the Rivlin-Ericksen tensor. In indicial notation,

$$A_{ij} = v_{i;j} + v_{j;i}. \tag{2.4.11}$$

Clearly, one can see that the tensor $\mathbf{A}$, which is twice the symmetric part of the velocity gradient, is a measure of the rate of stretching in a given motion.

The vorticity vector $\boldsymbol{\omega}$ = curl $\mathbf{v}$ is defined through:

$$\omega^i = \varepsilon^{ijk}v_{k;j}, \tag{2.4.12}$$

where $\varepsilon^{ijk} = e^{ijk}/\sqrt{g}$, $g = \det g_{ij}$, where $g_{ij} = \mathbf{g}_i \cdot \mathbf{g}_j$. The tensor $e^{ijk} = e_{ijk}$ is the usual permutation tensor, which satisfies

$$e^{ijk} = e_{ijk} = \begin{cases} 1 & \text{if } \{\text{i, j, k}\} \text{ is an even permutation of 1, 2, 3,} \\ 0 & \text{if } \{\text{i, j, k}\} \text{ is not a permutation,} \\ -1 & \text{if } \{\text{i, j, k}\} \text{ is an odd permutation.} \end{cases} \tag{2.4.13}$$

There is a close relation between the vorticity vector and the spin tensor:

$$\omega^i = \varepsilon^{ijk} W_{kj}. \tag{2.4.14}$$

Finally, we can adduce the following equivalent conditions for a particle to undergo a rigid motion:

- The velocity gradient is skew-symmetric, i.e., $\mathbf{L}(t) = \mathbf{W}(t)$.
- The Rivlin-Ericksen tensor $\mathbf{A}(t) = \mathbf{0}$.
- The trace of $\mathbf{A}^2(t)$ is zero.

In viscoplastic fluid mechanics, one comes across several situations where the flow is rigid in one part of the domain or other. We have already seen such an example in Chap. 1 where the flow in a channel of a Bingham fluid has been studied. This example and others seem to suggest that a fluid particle once entrained in a rigid motion cannot escape from it; conversely, a fluid particle in a shearing flow cannot enter a zone where the flow is rigid. This is false because the necessary and sufficient conditions for a fluid particle to undergo a rigid motion are *local* conditions. That is, they apply to a particle at a point in space and at a particular time. Hence, there is no reason why a fluid particle cannot undergo both shearing and rigid motions along its trajectory. Such an example has been adduced by Frigaard and Ryan [6] in connection with the flow of a Bingham fluid in a wavy channel; see Sect. 7.2.

2.5 Steady Velocity Fields and Their Rivlin-Ericksen Tensors

Here, we list a number of steady velocity fields and the corresponding Rivlin-Ericksen tensors. These are obtained from the results in (A2.7)–(A2.9) in the Appendix. In each example,

$$\mathbf{A} : \mathbf{A} = \operatorname{tr} \mathbf{A}^2 = 2\dot{\gamma}^2, \tag{2.5.1}$$

where $\dot{\gamma} \geq 0$ is the rate of shear.

1. **Simple Shear Flow**: The velocity field in a simple shearing flow is given in Cartesian coordinates through

$$\dot{x} = \dot{\gamma} y, \quad \dot{y} = \dot{z} = 0, \quad \dot{\gamma} > 0, \tag{2.5.2}$$

and is supposed to occur between two parallel plates located at $y = 0$ and $y = H$ respectively. The bottom plate at $y = 0$ is at rest, while the top plate moves with

a speed $\dot{\gamma} H$ in the x-direction. From (A2.7), we obtain

$$\mathbf{A} = \begin{bmatrix} 0 & u_{,y} & 0 \\ \cdot & 0 & 0 \\ \cdot & \cdot & 0 \end{bmatrix} = \begin{bmatrix} 0 & \dot{\gamma} & 0 \\ \dot{\gamma} & 0 & 0 \\ 0 & 0 & 0 \end{bmatrix}, \quad \dot{\gamma} > 0. \tag{2.5.3}$$

2. **Channel Flow**: As discussed at length in Chap. 1, the velocity field in a channel flow is given by

$$\dot{x} = u(y), \quad \dot{y} = \dot{z} = 0, \tag{2.5.4}$$

and is supposed to occur between two parallel planes located at $y = -H$ and $y = H$ respectively, with $u(\pm H) = 0$. From (A2.7), we obtain

$$\mathbf{A} = \begin{bmatrix} 0 & \partial u/\partial y & 0 \\ \cdot & 0 & 0 \\ \cdot & \cdot & 0 \end{bmatrix} = \begin{bmatrix} 0 & u' & 0 \\ u' & 0 & 0 \\ 0 & 0 & 0 \end{bmatrix}, \quad \dot{\gamma} = |u'|. \tag{2.5.5}$$

3. **Flow in a Pipe of Circular Cross-section**: This flow, also known as a Poiseuille flow, occurs along the length of the pipe and the velocity distribution is axisymmetric. Using cylindrical coordinates, it is described through

$$\dot{r} = 0, \quad \dot{\theta} = 0, \quad \dot{z} = w(r), \quad 0 \le r \le R, \tag{2.5.6}$$

where R is the inner radius of the pipe. Because of the adherence condition, $w(R) = 0$. From (A2.8), we find that

$$\mathbf{A} = \begin{bmatrix} 0 & 0 & \partial w/\partial r \\ 0 & 0 & 0 \\ \partial w/\partial r & 0 & 0 \end{bmatrix} = \begin{bmatrix} 0 & 0 & w' \\ 0 & 0 & 0 \\ w' & 0 & 0 \end{bmatrix}, \quad \dot{\gamma} = |w'|. \tag{2.5.7}$$

4. **Flow in an Annulus**: The flow in a concentric annulus is similar to that in a pipe of circular cross-section, except that the axial flow occurs in the annulus defined through $R_1 \le r \le R_2$, where R_1 is the radius of the inner pipe, and R_2 is the radius of the outer pipe. Except that $w(R_1) = w(R_2) = 0$, the velocity field and the corresponding Rivlin-Ericksen tensor are given by (2.5.6) and (2.5.7) respectively.
5. **Flow in a Pipe of Arbitrary Cross-section**: This is again an axial flow along the length of a pipe, with the velocity field defined in terms of the coordinates (x, y) which lie in the plane of the cross-section of the pipe. That is,

$$\dot{x} = \dot{y} = 0, \quad \dot{z} = w(x, y). \tag{2.5.8}$$

Through (A2.7) we obtain

$$\mathbf{A} = \begin{bmatrix} 0 & 0 & \partial w/\partial x \\ 0 & 0 & \partial w/\partial y \\ \partial w/\partial x & \partial w/\partial y & 0 \end{bmatrix}. \tag{2.5.9}$$

This leads to

$$\dot{\gamma} = \left[\left(\frac{\partial w}{\partial x} \right)^2 + \left(\frac{\partial w}{\partial y} \right)^2 \right]^{1/2} \geq 0. \tag{2.5.10}$$

6. **Couette Flow**: The Couette flow arises from the azimuthal flow between two concentric rotating cylinders, of radii R_1 and R_2 respectively, with $R_2 > R_1$. We describe this through

$$\dot{r} = 0, \quad \dot{\theta} = \omega(r), \quad \dot{z} = 0, \quad \omega(R_1) = \Omega_1, \quad \omega(R_2) = \Omega_2. \tag{2.5.11}$$

The Rivlin-Ericksen tensor associated to this flow can be obtained from (A2.8) where $v = r\omega$, and

$$\mathbf{A} = \begin{bmatrix} 0 & r\omega' & 0 \\ r\omega' & 0 & 0 \\ 0 & 0 & 0 \end{bmatrix}, \quad \dot{\gamma} = r|\omega'|. \tag{2.5.12}$$

7. **Helical Flow**: Finally, helical flow of spiral flow, is a superposition of the Couette flow on the flow in an annulus. The velocity field is given by

$$u = 0, \quad v = r\omega(r), \quad w = w(r), \quad R_1 \leq r \leq R_2, \tag{2.5.13}$$

with $w(R_1) = w(R_2) = 0$, and the angular velocity $\omega(r)$ is prescribed on the cylindrical surfaces through $\omega(R_1) = \Omega_1$, $\omega(R_2) = \Omega_2$. The Rivlin-Ericksen tensor associated to this flow is given by

$$\mathbf{A} = \begin{bmatrix} 0 & r\omega' & w' \\ r\omega' & 0 & 0 \\ w' & 0 & 0 \end{bmatrix}, \quad \dot{\gamma} = (r^2\omega'^2 + w'^2)^{1/2}. \tag{2.5.14}$$

In Chap. 5, we shall exhibit analytical solutions to the above velocity fields for Bingham fluids.

Appendix

In this Appendix, we list some basic results which are used in this monograph as required.

1. *Divergence and curl of vectors*. We list below the divergence and curl of vectors in the three coordinate systems.
Divergence: div $\mathbf{v} = \nabla \cdot \mathbf{v}$.
Cartesian: Physical components: u, v, w.

$$\frac{\partial u}{\partial x} + \frac{\partial v}{\partial y} + \frac{\partial w}{\partial z}. \tag{A2.1}$$

Cylindrical: Physical components: u, v, w.

$$\frac{\partial u}{\partial r} + \frac{u}{r} + \frac{1}{r}\frac{\partial v}{\partial \theta} + \frac{\partial w}{\partial z}. \tag{A2.2}$$

Spherical: Physical components: u, v, w.

$$\frac{\partial u}{\partial r} + \frac{2u}{r} + \frac{1}{r}\frac{\partial v}{\partial \theta} + \frac{v}{r}\cot\theta + \frac{1}{r\sin\theta}\frac{\partial w}{\partial \phi}. \tag{A2.3}$$

curl: $\boldsymbol{\omega} = \text{curl}\,\mathbf{v} = \nabla \times \mathbf{v}$.
Cartesian:

$$\boldsymbol{\omega} = \begin{bmatrix} w_{,y} - v_{,z} \\ u_{,z} - w_{,x} \\ v_{,x} - u_{,y} \end{bmatrix}, \tag{A2.4}$$

where $w_{,y} = \partial w/\partial y$, etc.
Cylindrical:

$$\boldsymbol{\omega} = \begin{bmatrix} \frac{1}{r}w_{,\theta} - v_{,z} \\ u_{,z} - w_{,r} \\ (v/r) + v_{,r} - (1/r)u_{,\theta} \end{bmatrix}. \tag{A2.5}$$

Spherical:

$$\boldsymbol{\omega} = \begin{bmatrix} (1/r)w_{,\theta} + (w/r)\cot\theta - (1/r\sin\theta)v_{,\phi} \\ (1/r\sin\theta)u_{,\phi} - (w/r) - w_{,r} \\ (v/r) + v_{,r} - (1/r)u_{,\theta} \end{bmatrix}. \tag{A2.6}$$

2. *Components of the Rivlin-Ericksen Tensor*. The physical components of the Rivlin-Ericksen tensor $\mathbf{A}$ are listed in Cartesian, cylindrical and spherical coordinates below, in terms of the physical components of the velocity field $\mathbf{v}$.
Cartesian:

$$\mathbf{A} = \begin{bmatrix} 2u_{,x} & (u_{,y} + v_{,x}) & (u_{,z} + w_{,x}) \\ \cdot & 2v_{,y} & (v_{,z} + w_{,y}) \\ \cdot & \cdot & 2w_{,z} \end{bmatrix}. \tag{A2.7}$$

Cylindrical:

$$\mathbf{A} = \begin{bmatrix} 2u_{,r} & [(1/r)u_{,\theta} + v_{,r} - (v/r)] & (u_{,z} + w_{,r}) \\ \cdot & (2/r)(u + v_{,\theta}) & (v_{,z} + (1/r)w_{,\theta}) \\ \cdot & \cdot & 2w_{,z} \end{bmatrix}. \tag{A2.8}$$

Spherical:

$$\mathbf{A} = \begin{bmatrix} 2u_{,r} & [(1/r)u_{,\theta} + v_{,r} - (v/r)] & [(1/r\sin\theta)u_{,\phi} + w_{,r} - (w/r)] \\ \cdot & [(2/r)(u + v_{,\theta})] & [(1/\sin\theta)v_{,\phi} + w_{,\theta} - w\cot\theta]/r \\ \cdot & \cdot & 2/r\sin\theta\left(w_{,\phi} + u\sin\theta + v\cos\theta\right) \end{bmatrix}. \tag{A2.9}$$

In (A2.7)–(A2.9), the dots denote the symmetry of the tensor.

3. *Components of the Spin Tensor*. Finally, we note that the velocity field $\mathbf{v}$ gives rise to the vorticity $\boldsymbol{\omega}$ through curl $\mathbf{v} = \boldsymbol{\omega}$. Since we know the physical components of $\boldsymbol{\omega}$ in various coordinates, the physical components of the spin tensor $\mathbf{W} = \left(\mathbf{L} - \mathbf{L}^T\right)/2$, where $\mathbf{L}$ is the velocity gradient, can be found from

$$\mathbf{W} = \frac{1}{2}\begin{bmatrix} 0 & -\omega_3 & \omega_2 \\ \omega_3 & 0 & -\omega_1 \\ -\omega_2 & \omega_1 & 0 \end{bmatrix}. \tag{A2.10}$$

References

1. Huilgol RR, Phan-Thien N (1997) Fluids mechanics of viscoelasticity. Elsevier, Amsterdam
2. Rivlin RS, Ericksen JL (1955) Stress-deformation relations for isotropic materials. J Ration Mech Anal 4:323–425
3. Noll W (1955) On the continuity of the solid and fluid states. J Ration Mech Anal 4:3–81
4. Huilgol RR (1986) On the material description of a motion associated with a spatially steady velocity field. Zeit angew Math Phys 37:270–273
5. Martin AD, Mizel VJ (1966) Introduction to linear algebra. McGraw-Hill, New York
6. Frigaard IA, Ryan DP (2004) Flow of a visco-plastic fluid in a channel of slowly varying width. J Non-Newton Fluid Mech 123:67–83

Chapter 3
Fundamental Equations

The four fundamental equations of continuum mechanics are:

1. The conservation of mass;
2. The balance of linear momentum, which is Cauchy's first law of motion for continuous media extending Newton's second law and Euler's law of motion for rigid bodies;
3. The balance of angular momentum, which is Cauchy's second law of motion, extending Euler's law applicable to the rate of change of angular momentum;
4. Finally, the energy equation.

In deriving the pointwise equations from the above equations in integral form, sufficient smoothness of the various scalar and vector fields is assumed, as in Chap. 2. The derivation of the relevant equations is based on Reynolds' transport theorem, which is stated next without proof. A proof of this theorem is available in many books on continuum mechanics; for example, see Huilgol and Phan-Thien [1].

Reynolds Transport Theorem Let $\Phi(\mathbf{x}, t)$ be an nth order tensor field defined over the volume $\mathscr{V}$ occupied by the body $\mathscr{B}$ at time t. Then,

$$\frac{d}{dt}\int\limits_{\mathscr{V}} \Phi \, dv = \int\limits_{\mathscr{V}} (\dot{\Phi} + \Phi \, \nabla \cdot \mathbf{v}) \, dv, \tag{3.0.1}$$

where the material derivative $\dot{\Phi}$ is given by

$$\dot{\Phi} = \frac{\partial \Phi}{\partial t} + \nabla \Phi \cdot \mathbf{v}. \tag{3.0.2}$$

In Cartesian indicial notation, this means that

$$\dot{\Phi}_{i_1 \ldots i_n} = \frac{\partial \Phi_{i_1 \ldots i_n}}{\partial t} + \Phi_{i_1 \ldots i_n, j} v_j. \tag{3.0.3}$$

R.R. Huilgol, *Fluid Mechanics of Viscoplasticity*, DOI 10.1007/978-3-662-45617-0_3

The difficulty in proving Reynolds transport theorem arises from the fact that the volume $\mathscr{V}$ occupied by the body is, in general, changing with time t. This is overcome by converting the integral to that defined over the volume in the reference configuration, performing the time derivative in this setting and then reverting to the current one.

Applying the divergence theorem, one finds that

$$\frac{d}{dt}\int_{\mathscr{V}} \Phi \, dv = \int_{\mathscr{V}} (\dot{\Phi} + \Phi \nabla \cdot \mathbf{v}) \, dv = \int_{\mathscr{V}} \frac{\partial \Phi}{\partial t} \, dv + \int_{\mathscr{S}} (\Phi \mathbf{v}) \cdot \mathbf{n} \, dS, \tag{3.0.4}$$

where $\mathscr{S}$ is the surface bounding the volume $\mathscr{V}$ and $\mathbf{n}$ is the unit external normal to this surface. The above result is another form of Reynolds' transport theorem.

3.1 Conservation of Mass

In continuum mechanics, the conservation of mass is assumed to be a postulate. In other words, for all material volumes $\mathscr{V}$, i.e., those containing the same particles for all times,

$$\frac{d}{dt}\int_{\mathscr{V}} \rho \, dv = 0, \tag{3.1.1}$$

where $\rho = \rho(x, y, z, t)$ is the density at the point (x, y, z) at time t. By the transport theorem, the above equation reduces to

$$\int_{\mathscr{V}} \left[\frac{\partial \rho}{\partial t} + \nabla \cdot (\rho \mathbf{v}) \right] dv = 0. \tag{3.1.2}$$

Since the size and shape of the material volume is arbitrary, a necessary and sufficient condition for the *conservation of mass* is the *continuity equation*:

$$\frac{\partial \rho}{\partial t} + \nabla \cdot (\rho \mathbf{v}) = \dot{\rho} + \rho \, \nabla \cdot \mathbf{v} = 0, \tag{3.1.3}$$

where, as usual, the superposed dot denotes the material derivative.

In incompressible materials, only *isochoric*, i.e., volume preserving motions are possible and, since ρ is a constant everywhere, conservation of mass implies and is guaranteed by

$$\nabla \cdot \mathbf{v} = v^j{}_{;j} = 0. \tag{3.1.4}$$

However,

$$\nabla \cdot \mathbf{v} = \operatorname{tr} \mathbf{L} = \frac{1}{2} \operatorname{tr} \mathbf{A}, \tag{3.1.5}$$

where $\mathbf{L}$ is the velocity gradient and $\mathbf{A}$ is the first Rivlin-Ericksen tensor. Thus an assertion equivalent to the conservation of mass in isochoric motions is that $\operatorname{tr}\mathbf{L} = \operatorname{tr}\mathbf{A} = 0$.

3.2 Cauchy's First Law

In Newtonian mechanics, external forces act on a body and the rate of change of the linear momentum of the body is due to these forces. In Lagrangian mechanics, the external forces are classified into forces of constraint and the remainder. In continuum mechanics, the outside world acts on a body through contact forces, i.e., by direct touch with the surface of a body, and non-contact forces, which act at a distance; the latter are grouped together as body forces.

Let $\mathscr{V}$ denote the volume occupied by the body $\mathscr{B}$ at time t, $\mathbf{t}$ the contact force per unit area on its surface $\mathscr{S}$ exerted by the outside world, and $\mathbf{b}$ the body force per unit mass. Then Newton's second law of motion in an inertial frame of reference, as modified by Cauchy, states that the rate of change of the linear momentum is equal to the external forces on the body, i.e.,

$$\frac{d}{dt}\int_{\mathscr{V}} \rho\mathbf{v}\,dv = \int_{\mathscr{S}} \mathbf{t}\,dS + \int_{\mathscr{V}} \rho\mathbf{b}\,dv. \tag{3.2.1}$$

Using Reynolds' transport theorem, one finds that the left side is

$$\int_{\mathscr{V}} \left[\left(\frac{d\rho}{dt} + \rho\nabla\cdot\mathbf{v}\right)\mathbf{v} + \rho\mathbf{a}\right] dv. \tag{3.2.2}$$

If one assumes that mass is conserved, one can see immediately from (3.1.3) that the equation of motion for a continuous medium now becomes

$$\int_{\mathscr{V}} \rho\mathbf{a}\,dv = \int_{\mathscr{S}} \mathbf{t}\,dS + \int_{\mathscr{V}} \rho\mathbf{b}\,dv. \tag{3.2.3}$$

We wish to convert the surface integral in (3.2.3) to a volume integral through the divergence theorem in order to obtain a differential equation for the balance of linear momentum. To achieve this, note that on the boundary, the stress vector is given by

$$\mathbf{t} = \mathbf{t}(\mathbf{x}, t, \mathbf{n}) \qquad \mathbf{x} \in \mathscr{S}. \tag{3.2.4}$$

The real problem is how does this vector $\mathbf{t}$ depend on $\mathbf{n}$? Is the dependence linear in $\mathbf{n}$ or is it of a nonlinear[1] kind? Leaving aside the proof for the moment, let us

[1] An example of nonlinear dependence is $\mathbf{t} = f(\mathbf{x}\cdot\mathbf{n})\mathbf{n}$, where f is an arbitrary, scalar valued function.

accept Cauchy's stress principle that the stress vector and the unit normal are related linearly through the stress tensor $\mathbf{T}$. This is embodied in the following statement:

$$\mathbf{t}(\mathbf{x}, t, \mathbf{n}) = \mathbf{T}(\mathbf{x}, t)\mathbf{n}. \tag{3.2.5}$$

The meaning of Cauchy's stress principle is as follows:

1. Over the whole body, a stress tensor field $\mathbf{T}(\mathbf{x}, t)$ is defined.
2. If one wishes to find the force per unit area $\mathbf{t}$ exerted by the external world on the body, the above relation defines the stress vector at a point $\mathbf{x}$ on the boundary in terms of the stress tensor and the unit external normal at that boundary point.

Substituting the formula (3.2.5) into (3.2.3), we obtain:

$$\int_{\mathscr{V}} \rho\mathbf{a}\, dv = \int_{\mathscr{S}} \mathbf{T}\mathbf{n}\, dS + \int_{\mathscr{V}} \rho\mathbf{b}\, dv. \tag{3.2.6}$$

Appealing to the divergence theorem, the surface integral may be turned into a volume integral:

$$\int_{\mathscr{S}} T_{ij}n_j\, dS = \int_{\mathscr{V}} T_{ij,j}\, dv, \tag{3.2.7}$$

where $T_{ij,j}$ is the divergence of the stress tensor field. Hence we have *Cauchy's first law of motion*:

$$\int_{\mathscr{V}} \rho\mathbf{a}\, dv = \int_{\mathscr{V}} \nabla\cdot\mathbf{T}\, dv + \int_{\mathscr{V}} \rho\mathbf{b}\, dv, \tag{3.2.8}$$

from which one obtains the differential equations of motion:

$$\nabla\cdot\mathbf{T} + \rho\mathbf{b} = \rho\mathbf{a}, \tag{3.2.9}$$

$$T_{ij,j} + \rho b_i = \rho a_i. \tag{3.2.10}$$

The proof of Cauchy's stress principle is fairly complicated and an account can be found in many treatises on continuum mechanics; for example, see [1].

To put it in a more familiar context, let us adopt the convention that T_{ij} is the ith component of the stress vector acting on the outward (positive) side of the plane $x_j =$ const. Consider the plane $x = 0$ through the origin. Choose $\mathbf{n} = \mathbf{i}$, the unit vector in the x-direction. Then, the components of $\mathbf{t}$ are T_{11}, T_{21}, T_{31}, which is in accord with the rules of matrix multiplication. Thus, in general, we find that $t_{(\mathbf{n})k} = T_{km}n_m$, where the quantities T_{km} are independent of $\mathbf{n}$ and depend on $(\mathbf{x}, t)$ only. By the quotient law of tensors, T_{km} are the components of a Cartesian tensor of second order, and in general tensor notation,

$$t^k_{(\mathbf{n})} = T^{km}n_m\,, \qquad \mathbf{t}_{(\mathbf{n})} = \mathbf{T}\mathbf{n}. \tag{3.2.11}$$

Given the existence of the stress tensor, the equations of motion in the form given in (3.2.9) and (3.2.10) are valid. The important point to note is that there is no assumption of the symmetry of the stress tensor in the derivation of the above equations.

3.3 Cauchy's Second Law

Assuming that there do not exist any internal angular momentum, body couples, and couple stresses in the body, the balance of angular momentum equation with respect to an inertial frame for a material volume $\mathscr{V}$ says that the rate of change of the angular momentum is equal to the external torque on the body. There are two torques: those arising from the surface tractions and those from the body forces. Hence, this balance equation may be written as

$$\frac{d}{dt}\int_{\mathscr{V}} \mathbf{x}\times(\rho\mathbf{v})\,dv = \int_{\mathscr{S}} \mathbf{x}\times\mathbf{t}\,dS + \int_{\mathscr{V}} \mathbf{x}\times(\rho\mathbf{b})\,dv, \tag{3.3.1}$$

where $\mathbf{x}$ is the position vector of a particle from the fixed origin of the coordinate frame, and $\mathscr{S}$ is the surface of the volume $\mathscr{V}$. Using the transport theorem, we find that the left side of (3.3.1) takes the form

$$\frac{d}{dt}\int_{\mathscr{V}} \mathbf{x}\times(\rho\mathbf{v})\,dv = \int_{\mathscr{V}} (\dot{\rho}+\rho\nabla\cdot\mathbf{v})\,(\mathbf{x}\times\mathbf{v})\;dv + \int_{\mathscr{V}} \mathbf{x}\times(\rho\mathbf{a})\,dv, \tag{3.3.2}$$

when the identity $\dot{\mathbf{x}}\times\mathbf{v} = \mathbf{v}\times\mathbf{v} = \mathbf{0}$ is used, along with the fact that the material derivative of the velocity vector $\mathbf{v}$ is the acceleration vector $\mathbf{a}$. The continuity equation (3.1.3) shows that the first integral on the right is zero and hence the rate of change of the angular momentum is equal to the momentum of the inertia, i.e.,

$$\frac{d}{dt}\int_{\mathscr{V}} \mathbf{x}\times(\rho\mathbf{v})\,dv = \int_{\mathscr{V}} \mathbf{x}\times(\rho\mathbf{a})\,dv. \tag{3.3.3}$$

Examining the first integral on the right side of (3.3.1), the existence of the stress tensor $\mathbf{T}$ means that we may write this integral as

$$\int_{\mathscr{S}} \mathbf{x}\times\mathbf{t}\,dS = \int_{\mathscr{S}} (\mathbf{x}\times\mathbf{T}\mathbf{n})\,dS. \tag{3.3.4}$$

Introducing Cartesian coordinates for convenience, the right side of (3.3.4) is

$$\int_{\mathscr{S}} e_{ijk}\,x_j\,T_{km}\,n_m\,dS, \tag{3.3.5}$$

where e_{ijk} is the alternating tensor; see (2.4.13). By the divergence theorem, we have

$$\begin{aligned}\int_{\mathscr{S}} e_{ijk}\, x_j\, T_{km}\, n_m\, dS &= \int_{\mathscr{V}} \left(e_{ijk}\, x_j\, T_{km}\right)_{,m}\, dv \\ &= \int_{\mathscr{V}} \left(e_{ijk}\, \delta_{jm}\, T_{km} + e_{ijk}\, x_j\, T_{km,m}\right)\, dv \\ &= \int_{\mathscr{V}} \left(e_{ijk}\, T_{kj} + e_{ijk}\, x_j\, T_{km,m}\right)\, dv. \end{aligned} \tag{3.3.6}$$

Introducing the axial vector $\mathbf{t}^A$ corresponding to $\mathbf{T}$ through

$$(t^A)_i = e_{ijk}\, T_{kj}, \tag{3.3.7}$$

the balance of angular momentum equation now reads

$$\int_{\mathscr{V}} \mathbf{x} \times (\rho \mathbf{a})\, dv = \int_{\mathscr{V}} \left(\mathbf{t}^A + \mathbf{x} \times \nabla \cdot \mathbf{T}\right)\, dv + \int_{\mathscr{V}} \mathbf{x} \times (\rho \mathbf{b})\, dv. \tag{3.3.8}$$

Assuming that the balance of linear momentum holds in $\mathscr{V}$, i.e.,

$$\nabla \cdot \mathbf{T} + \rho \mathbf{b} = \rho \mathbf{a}, \tag{3.3.9}$$

Eq. (3.3.8) reduces to

$$\int_{\mathscr{V}} \mathbf{t}^A\, dv = \mathbf{0}. \tag{3.3.10}$$

Since $\mathscr{V}$ is arbitrary, we conclude that $\mathbf{t}^A = \mathbf{0}$ or that

$$e_{ijk}\, T_{kj} = 0. \tag{3.3.11}$$

Because of the property of the alternating tensor, it follows from the above that the stress tensor is symmetric, i.e.,

$$\mathbf{T} = \mathbf{T}^T. \tag{3.3.12}$$

Hence, in the absence of internal angular momentum, body couples and couple stresses, the necessary and sufficient condition for the balance of angular momentum, when the conservation of mass and balance of linear momentum equations are satisfied, is that (3.3.12) shall apply. This is *Cauchy's second law of motion*.

In this book it will always be assumed that the stress tensor is symmetric and thus the second law of motion is automatically satisfied. In engineering applications, there are occasions when one is called upon to calculate the angular momentum of

a fluid mass and equate it to the external torque to gain an additional insight into the flow field.

3.4 Conservation of Energy

Let $\mathscr{K}$ be the kinetic energy of the body and $\mathscr{E}$ its internal energy so that for any material volume $\mathscr{V}$,

$$\mathscr{K} = \int_{\mathscr{V}} \frac{1}{2}\rho|\mathbf{v}|^2\, dv\,, \qquad \mathscr{E} = \int_{\mathscr{V}} \rho\varepsilon\, dv, \tag{3.4.1}$$

where ε is the specific energy per unit mass. The mechanical power exerted by the outside world on the body is given by the rate at which the surface tractions and the body force do work on the body. These two are

$$\int_{\mathscr{S}} \mathbf{t}\cdot\mathbf{v}\, dS + \int_{\mathscr{V}} \rho\mathbf{b}\cdot\mathbf{v}\, dv. \tag{3.4.2}$$

Let the efflux of energy out of $\mathscr{S}$ be $\mathbf{q}$ per unit area and the energy supply be r per unit mass. Then one postulates the balance of energy equation as

$$\frac{d}{dt}\left\{\int_{\mathscr{V}} \left(\frac{1}{2}\rho\mathbf{v}\cdot\mathbf{v} + \rho\varepsilon\right) dv\right\} = \int_{\mathscr{S}} (\mathbf{t}\cdot\mathbf{v} - \mathbf{q}\cdot\mathbf{n})\, dS + \int_{\mathscr{V}} (\rho r + \rho\mathbf{b}\cdot\mathbf{v})\, dv. \tag{3.4.3}$$

Using the existence of the stress tensor, one obtains:

$$\frac{d}{dt}\left\{\int_{\mathscr{V}} \left(\frac{1}{2}\rho\mathbf{v}\cdot\mathbf{v} + \rho\varepsilon\right) dv\right\} = \int_{\mathscr{S}} (\mathbf{v}\cdot\mathbf{T}\mathbf{n} - \mathbf{q}\cdot\mathbf{n})\, dS + \int_{\mathscr{V}} \rho\,(\mathbf{b}\cdot\mathbf{v} + r)\, dv. \tag{3.4.4}$$

Assuming that mass is conserved and using the transport theorem, the left side of (3.4.4) can be written as

$$\int_{\mathscr{V}} \rho(\mathbf{v}\cdot\mathbf{a} + \dot{\varepsilon})\, dv, \tag{3.4.5}$$

where $\mathbf{a}$ is the acceleration and the superposed dot is the material derivative. The divergence theorem may be applied to the surface integral on the right side of (3.4.4) and, using Cartesian tensor notation to make the derivation easier, we find that

$$\int_{\mathscr{S}} (v_i\, T_{ij}\, n_j + q_i\, n_i)\, dS = \int_{\mathscr{V}} (T_{ij,j}\, v_i + T_{ij}\, v_{i,j} - q_{i,i})\, dv. \tag{3.4.6}$$

Hence, Eq. (3.4.4) now becomes

$$\int_{\mathscr{V}} \rho(\mathbf{v}\cdot\mathbf{a} + \dot{\varepsilon})\, dv = \int_{\mathscr{V}} [\mathbf{v}\cdot(\nabla\cdot\mathbf{T}) + \text{tr}\,\mathbf{T}\mathbf{L}^T - \nabla\cdot\mathbf{q}]\, dv + \int_{\mathscr{V}} \rho(\mathbf{v}\cdot\mathbf{b} + r)\, dv, \tag{3.4.7}$$

where $\mathbf{L}^T$ is the transpose of the velocity gradient and tr denotes the trace. Using the balance of linear momentum equation and the symmetry of the stress tensor implied by the balance of angular momentum, one finds that (3.4.7) may be simplified to

$$\int_{\mathscr{V}} \rho\dot{\varepsilon}\, dv = \int_{\mathscr{V}} (\text{tr}\,\mathbf{TD} - \nabla\cdot\mathbf{q} + \rho r)\, dv, \tag{3.4.8}$$

where $\mathbf{D}$ is the symmetric part of the velocity gradient. From this follows the differential equation of energy balance:

$$\rho\dot{\varepsilon} = \text{tr}\,\mathbf{TD} - \nabla\cdot\mathbf{q} + \rho r. \tag{3.4.9}$$

This can be replaced by

$$\rho\dot{\varepsilon} = \frac{1}{2}\text{tr}\,\mathbf{TA} - \nabla\cdot\mathbf{q} + \rho r. \tag{3.4.10}$$

In (3.4.10), the term tr $\mathbf{TA}/2$ is called the *stress power*.

The reader will note that the conservation of mass equation was basic. This is needed in obtaining Cauchy's first law of motion, and these two together are needed for Cauchy's second law of motion. All three are necessary to obtain the energy equation in the form given.

In dealing with constitutive relations, it is useful to replace tr $\mathbf{CD}$ with the notation $\mathbf{C} : \mathbf{D}$. Thus, tr $\mathbf{A}^2 = \mathbf{A} : \mathbf{A}$. In addition, one defines the second invariant $II(\mathbf{M})$ of a symmetric tensor $\mathbf{M}$ through

$$II(\mathbf{M}) = \frac{1}{2}\text{tr}\,\mathbf{M}^2 = \frac{1}{2}\mathbf{M} : \mathbf{M} = \frac{1}{2}||\mathbf{M}||^2. \tag{3.4.11}$$

In fact, the non-negative square root of the invariant $II(\mathbf{M})$ turns out to be more useful. And, in connection with this matter, we introduce the *kinematic invariant* or the *second invariant* $K(\mathbf{A})$ of the Rivlin-Ericksen tensor $\mathbf{A}$. This is defined through

$$K(\mathbf{A}) = [II(\mathbf{A})]^{1/2} = \frac{1}{\sqrt{2}}||\mathbf{A}|| \geq 0. \tag{3.4.12}$$

When deemed necessary, $K(\mathbf{A}(\mathbf{v}))$, where $\mathbf{A}(\mathbf{v})$ is derived from the velocity field $\mathbf{v}$, is expressed as $K(\mathbf{v})$. Note that in viscometric flows such as those listed in Sect. 2.5, it follows that

$$K(\mathbf{A}) = \dot{\gamma}, \tag{3.4.13}$$

where $\dot{\gamma}$ is the shear rate.

3.5 Control Volume and Control Surface

In several fluid mechanical problems encountered in engineering, the terms *control volume* and its bounding surface, *control surface*, are used quite regularly. The control volume is taken as a volume fixed in space, e.g., a pipe flow system, or one moving with a constant velocity, e.g., a jet engine. In order to apply the fundamental equations of continuum mechanics to the control volume cv, the basic idea is to assume that a material volume $\mathscr{V}$ occupies the control volume at a given time t. It is further assumed that the material is incompressible and that the flow is steady. In this case, there is no change in the mass of the fluid in the control volume, and the density ρ is a constant.

Thus, using the divergence theorem, (3.1.2) becomes

$$\int_{cv} \rho(\nabla \cdot \mathbf{v})\, dv = \int_{cs} \rho(\mathbf{v} \cdot \mathbf{n})\, dS = 0. \tag{3.5.1}$$

In essence, this equation says that the mass efflux into and out of the control volume occurs through the control surface cs, and that the net efflux is zero. If the control volume is moving with a constant velocity $\mathbf{v}^c$, one can assume that $\mathbf{v} = \mathbf{v}^c + \mathbf{w}$, where $\mathbf{w}$ is the relative velocity field. Clearly, one finds that (3.5.1) takes on the form:

$$\int_{cv} \rho(\nabla \cdot \mathbf{v})\, dv = \int_{cs} \rho(\mathbf{w} \cdot \mathbf{n})\, dS = 0. \tag{3.5.2}$$

Now, the acceleration vector is given by

$$a_i = v_{i,j} v_j = (v_i v_j)_{,j}, \tag{3.5.3}$$

for the flow is steady and the material is incompressible, i.e., $v_{j,j} = 0$. Thus,

$$\int_{\mathscr{V}} \rho a_i\, dv = \int_{cs} \rho v_i v_j n_j\, dS. \tag{3.5.4}$$

Hence, the rate of change of the linear momentum of the material volume $\mathscr{V}$ can be written as the efflux of the linear momentum into and out of the control volume through the control surface. Or, we obtain

$$\int_{\mathscr{V}} \rho \mathbf{a}\, dv = \int_{cs} \mathbf{v}(\rho \mathbf{v} \cdot \mathbf{n})\, dS. \tag{3.5.5}$$

This can be equated to the external forces acting on the control volume at that instant; see (3.2.3).

Clearly, when $\mathbf{v} = \mathbf{v}^c + \mathbf{w}$,

$$\int_{\mathscr{V}} \rho \mathbf{a}\, dv = \int_{cs} \mathbf{w}(\rho \mathbf{w} \cdot \mathbf{n})\, dS, \tag{3.5.6}$$

since $d\mathbf{v}/dt = d\mathbf{w}/dt$.

Finally, the rate of change of angular momentum is the integral of the integrand $(\mathbf{x} \times \rho \mathbf{a})$ over the material volume $\mathscr{V}$; see (3.3.3). Now, using the incompressibility of the material, the fact that the velocity field is steady and the property of the alternating tensor, it follows that

$$e_{ijk} x_j a_k = e_{ijk} x_j v_{k,m} v_m = e_{ijk} (x_j v_k v_m)_{,m}. \tag{3.5.7}$$

Hence, using the divergence theorem,

$$\int_{\mathscr{V}} e_{ijk} x_j (\rho a_k)\, dv = \int_{cs} e_{ijk} x_j v_k (\rho v_m n_m)\, dS. \tag{3.5.8}$$

Thus,

$$\int_{\mathscr{V}} \mathbf{x} \times (\rho \mathbf{a})\, dv = \int_{cs} \mathbf{x} \times \mathbf{v}(\rho \mathbf{v} \cdot \mathbf{n})\, dS, \tag{3.5.9}$$

which is the efflux of the angular momentum into and out of the control volume through the control surface; it can be equated to the external torques acting on the control volume at that instant through (3.3.1). Obviously, when $\mathbf{v} = \mathbf{v}^c + \mathbf{w}$, one finds that

$$\int_{\mathscr{V}} \mathbf{x} \times (\rho \mathbf{a})\, dv = \int_{cs} \mathbf{x} \times \mathbf{w}(\rho \mathbf{w} \cdot \mathbf{n})\, dS. \tag{3.5.10}$$

In the context of pumps and turbines, one obtains the Euler turbomachine equations from (3.3.1) and (3.5.9), or (3.3.1) and (3.5.10) depending on the specific nature of the problem.

Appendix

For the moment, assume that the total stress tensor $\mathbf{T} = -p\mathbf{1} + \mathbf{S}$, where p is the pressure and $\mathbf{S}$ is the extra stress tensor. The equations of motion (3.2.9) become

$$-\nabla p + \nabla \cdot \mathbf{S} + \rho\mathbf{b} = \rho\mathbf{a}, \tag{A3.1}$$

which have the following indicial form:

$$-p_{,i} + S_{ij;j} + \rho b_i = \rho a_i, \quad i, j = 1, 2, 3, \tag{A3.2}$$

in curvilinear coordinates. In (A3.2), S_{ij}, $p_{,i}$, b_i and a_i are the covariant components of the extra stress tensor, the pressure gradient vector, the body force vector and the acceleration vector respectively and the semi-colon (;) denotes the covariant derivative. The set of three equations in (A3.2) have to be cast in their respective physical component forms when problems in cylindrical or spherical coordinates have to be solved. For a complete coverage of these matters, see [1]. We list below the equations in Cartesian, cylindrical and spherical coordinates which are employed, as necessary, in the sequel.

Cartesian Coordinates

$$-\frac{\partial p}{\partial x} + \frac{\partial S_{xx}}{\partial x} + \frac{\partial S_{xy}}{\partial y} + \frac{\partial S_{xz}}{\partial z} + \rho b_x = \rho\left(\frac{\partial u}{\partial t} + u\frac{\partial u}{\partial x} + v\frac{\partial u}{\partial y} + w\frac{\partial u}{\partial z}\right), \tag{A3.3}$$

$$-\frac{\partial p}{\partial y} + \frac{\partial S_{xy}}{\partial x} + \frac{\partial S_{yy}}{\partial y} + \frac{\partial S_{yz}}{\partial z} + \rho b_y = \rho\left(\frac{\partial v}{\partial t} + u\frac{\partial v}{\partial x} + v\frac{\partial v}{\partial y} + w\frac{\partial v}{\partial z}\right), \tag{A3.4}$$

$$-\frac{\partial p}{\partial z} + \frac{\partial S_{xz}}{\partial x} + \frac{\partial S_{yz}}{\partial y} + \frac{\partial S_{zz}}{\partial z} + \rho b_z = \rho\left(\frac{\partial w}{\partial t} + u\frac{\partial w}{\partial x} + v\frac{\partial w}{\partial y} + w\frac{\partial w}{\partial z}\right). \tag{A3.5}$$

Cylindrical Coordinates

$$\begin{aligned} -\frac{\partial p}{\partial r} + \frac{\partial S_{rr}}{\partial r} + \frac{1}{r}\frac{\partial S_{r\theta}}{\partial \theta} + \frac{\partial S_{rz}}{\partial z} + \frac{S_{rr} - S_{\theta\theta}}{r} + \rho b_r \\ = \rho\left(\frac{\partial u}{\partial t} + u\frac{\partial u}{\partial r} + \frac{v}{r}\frac{\partial u}{\partial \theta} + w\frac{\partial u}{\partial z} - \frac{v^2}{r}\right), \end{aligned} \tag{A3.6}$$

$$\begin{aligned} -\frac{1}{r}\frac{\partial p}{\partial \theta} + \frac{\partial S_{r\theta}}{\partial r} + \frac{1}{r}\frac{\partial S_{\theta\theta}}{\partial \theta} + \frac{\partial S_{\theta z}}{\partial z} + \frac{2}{r}S_{r\theta} + \rho b_\theta \\ = \rho\left(\frac{\partial v}{\partial t} + u\frac{\partial v}{\partial r} + \frac{v}{r}\frac{\partial v}{\partial \theta} + w\frac{\partial v}{\partial z} + \frac{uv}{r}\right), \end{aligned} \tag{A3.7}$$

$$-\frac{\partial p}{\partial z}+\frac{\partial S_{rz}}{\partial r}+\frac{1}{r}\frac{\partial S_{\theta z}}{\partial \theta}+\frac{\partial S_{zz}}{\partial z}+\frac{1}{r}S_{rz}+\rho b_z = \rho\left(\frac{\partial w}{\partial t}+u\frac{\partial w}{\partial r}+\frac{v}{r}\frac{\partial w}{\partial \theta}+w\frac{\partial w}{\partial z}\right). \tag{A3.8}$$

Spherical Coordinates

$$-\frac{\partial p}{\partial r}+\frac{\partial S_{rr}}{\partial r}+\frac{1}{r}\frac{\partial S_{r\theta}}{\partial \theta}+\frac{1}{r\sin\theta}\frac{S_{r\phi}}{\partial \phi}+\frac{1}{r}[2S_{rr}-S_{\theta\theta}-S_{\phi\phi}+\cot\theta\, S_{r\theta}]+\rho b_r = \rho\left(\frac{\partial u}{\partial t}+u\frac{\partial u}{\partial r}+\frac{v}{r}\frac{\partial u}{\partial \theta}+\frac{w}{r\sin\theta}\frac{\partial u}{\partial \phi}-\frac{v^2+w^2}{r}\right), \tag{A3.9}$$

$$-\frac{1}{r}\frac{\partial p}{\partial \theta}+\frac{\partial S_{r\theta}}{\partial r}+\frac{1}{r}\frac{\partial S_{\theta\theta}}{\partial \theta}+\frac{1}{r\sin\theta}\frac{S_{\theta\phi}}{\partial \phi}+\frac{1}{r}[3S_{r\theta}+\cot\theta(S_{\theta\theta}-S_{\phi\phi})]+\rho b_\theta = \rho\left(\frac{\partial v}{\partial t}+u\frac{\partial v}{\partial r}+\frac{v}{r}\frac{\partial v}{\partial \theta}+\frac{w}{r\sin\theta}\frac{\partial v}{\partial \phi}+\frac{uv}{r}-\frac{w^2\cot\theta}{r}\right), \tag{A3.10}$$

$$-\frac{1}{r\sin\theta}\frac{\partial p}{\partial \phi}+\frac{\partial S_{r\phi}}{\partial r}+\frac{1}{r}\frac{\partial S_{\theta\phi}}{\partial \theta}+\frac{1}{r\sin\theta}\frac{S_{\phi\phi}}{\partial \phi}+\frac{1}{r}[3S_{r\phi}+2\cot\theta\, S_{\theta\phi}]+\rho b_\phi = \rho\left(\frac{\partial w}{\partial t}+u\frac{\partial w}{\partial r}+\frac{v}{r}\frac{\partial w}{\partial \theta}+\frac{w}{r\sin\theta}\frac{\partial w}{\partial \phi}+\frac{uw}{r}+\frac{vw\cot\theta}{r}\right). \tag{A3.11}$$

Typically, in fluid mechanics, the body force is assumed to be derived from a potential χ, or it is zero. In the former case, $\mathbf{b}=-\nabla\chi$ so that we have to solve the equations

$$-\nabla p+\nabla\cdot\mathbf{S}=\rho\mathbf{a}, \tag{A3.12}$$

where p includes the $\rho\chi$ term. Of course, when the body force is zero, we have to examine

$$-\nabla p+\nabla\cdot\mathbf{S}=\rho\mathbf{a}. \tag{A3.13}$$

Reference

1. Huilgol RR, Phan-Thien N (1997) Fluid mechanics of viscoelasticity. Elsevier, Amsterdam

Chapter 4
Constitutive Equations

In this chapter, we begin with a detailed examination of the response of a continuous medium to the constraint of incompressibility. It is shown that a unique isotropic tensor arises as a consequence; its non-zero component is commonly known as the pressure. From the existence of the pressure, it follows that in an incompressible medium, the total stress tensor is decomposed into this isotropic part and a traceless extra stress tensor, with the latter being defined through the kinematics of the motion.

In viscoplastic fluids, the extra stress tensor is undefined in the unyielded zone, while in the yielded region, it is a function of the Rivlin-Ericksen tensor and an explicit form, depending on the viscosity and the yield stress is proposed through a constitutive relation. In the unyielded zone, the rigid motion is a more severe restriction than that due to incompressibility, for the former is equivalent to $\mathbf{A} = \mathbf{0}$, while the latter is defined through $\mathrm{tr}\,\mathbf{A} = 0$; clearly, the former implies the latter trivially. Thus, one can replace the extra stress tensor in the rigid zone through a second constraint tensor, aptly termed the *viscoplasticity constraint tensor*. This tensor can be extended into the yielded region through the constitutive term for the relevant viscoplastic fluid involving the yield stress only. Hence, the constitutive relation for the viscoplastic fluid can be modified to consist of the pressure term, the viscous stress tensor and the viscoplasticity constraint tensor. The importance of this modification lies in the fact that the corresponding constitutive relation leads to efficient numerical schemes, explored later on in Chap. 10.

Next, two regularised models which have been developed to overcome the difficulties inherent in numerical modelling of viscoplastic fluids are discussed in Sect. 4.4. However, with the introduction of the augmented Lagrangian method and the operator-splitting scheme for the solution of the flow problems in viscoplastic fluids, it would appear that regularised models may become less relevant in the near future.

In Sect. 4.5, the constitutive relations for compressible viscoplastic fluids are derived. It is shown that the viscoplasticity constraint tensor plays a significant role here as well.

R.R. Huilgol, *Fluid Mechanics of Viscoplasticity*, DOI 10.1007/978-3-662-45617-0_4

Finally, in Sect. 4.6, one dimensional models for Bingham, Herschel-Bulkley and Casson fluids are listed along with their velocity and stress potentials. From these, their three dimensional analogues are obtained. These results are of importance in Chaps. 8 and 9.

4.1 Pressure and Incompressibility

What is the true meaning of *pressure* in the rheology of incompressible materials, whether they be elastic solids, or viscoelastic fluids or viscoplastic substances? Can it be defined uniquely? Further, can this pressure be incorporated into a constitutive equation? The answers to the above questions are found in Lagrangian mechanics, as applied to rigid bodies [1].[1]

To begin, consider the following decomposition of the total stress tensor T_{ij} in an incompressible fluid:

$$T_{ij} = -p\delta_{ij} + S_{ij}, \tag{4.1.1}$$

where S_{ij} is the extra stress tensor, defined through a constitutive relation, and p is the pressure. In order for the decomposition to be meaningful, it is essential to show that

1. The pressure at any point in an incompressible fluid can be defined uniquely, and it has a permanent significance.
2. A uniquely defined pressure imposes a restriction on the trace of the extra stress tensor in every deformation.
3. Just because the density of an incompressible fluid is not affected by pressure, it is not true that *pressure has no effect on rheological properties*. In fact, there exists a fully developed theory to incorporate this dependence [2].

We shall now turn to Lagrangian mechanics to demonstrate its relevance to rheology and its use in establishing the above three claims.

4.1.1 The Meaning of Pressure

In Lagrangian mechanics, the forces acting on a rigid body are split into two classes: those forces which arise due to externally imposed constraints and the rest, usually described as given forces. This decomposition, along with the associated kinematics, is sufficient to understand the definition of pressure in an incompressible body. Here is a simple example from dynamics which has a direct correspondence with continuum mechanics.

[1] The material in this section is a summary of that appearing in Huilgol [1].

1. Assume that a rigid box is dragged along a rough horizontal surface; this is the kinematical constraint on the motion.
2. In turn, the surface of constraint exerts a force of constraint, i.e., a normal reaction N on the body. All that can be said, at this point, is that this force N is parallel to the normal to the surface. Subsequently, the equations of motion reveal that the force N opposes the weight of the body. This point that the equations of motion determine whether N opposes the weight or not has its counterpart in continuum mechanics as will be shown below. Clearly, N does no work in this motion.
3. The body is acted on by a force which lies along the surface of constraint. This force F, due to friction, has to be defined by an equation. Typically, F is assumed to be that of the Coulomb type, i.e., $F = \mu N$, or it is proportional to the force of constraint. The frictional force is part of the non-constraint forces.
4. The dragging force D and the weight of the body also form part of the non-constraint forces.

We shall now make the connection between the motion of a rigid body, as described above, and the continuum mechanics of an incompressible body transparent. In doing so, we draw upon the work by Rajagopal and Srinivasa [2].

1. The kinematical constraint on the motion is given by the requirement that the velocity field $\mathbf{v}$ has zero divergence everywhere, i.e., $\nabla \cdot \mathbf{v} = 0$.
2. The surface of constraint exerts a stress on the body, given by C_{ij}, which is *parallel to the normal to the surface of constraint*. At this point, it is not obvious whether this tensor is of the *compressive* or *tensile* type.
3. The extra stress tensor is defined to lie along the surface of constraint; it is defined through a constitutive relation.
4. The body is acted upon by surface tractions and body forces.

Thus, the first question is this: can one define the constraint tensor in an incompressible material? Is this unique?

One approach, used extensively in continuum mechanics, is based on an extension of the fact that the reaction N does no work when the rigid body is dragged along the surface. So, one demands that the total stress tensor T_{ij} be determined to within a stress tensor π_{ij} which produces zero stress power in any motion meeting the kinematical constraint. So, let the total stress tensor T_{ij} be decomposed into two parts:

$$T_{ij} = S_{ij} + \pi_{ij}. \tag{4.1.2}$$

The stress power of π_{ij} is given by $(1/2)\pi_{ij}A_{ij}$, where $\mathbf{A}$ is the first Rivlin-Ericksen tensor. Since $v_{i,i} = \nabla \cdot \mathbf{v} = 0$ is the same as $A_{ii} = 0$, the condition that π_{ij} produces zero stress power in any motion meeting the latter constraint is that

$$\pi_{ij}A_{ij} = 0 \text{ for all } A_{ii} = 0. \tag{4.1.3}$$

The solution for π_{ij} in Eq. (4.1.3) is well known; for example, see [3]. Thus,

$$\pi_{ij} = p\delta_{ij}. \tag{4.1.4}$$

Unfortunately, as remarked by Rajagopal and Srinivasa [2], one can add a multiple of the Kronecker delta to S_{ij} in Eq. (4.1.2) and subtract it from π_{ij} without affecting the requirement of zero stress power. So, this method does not lead to a unique definition of p. In fact, this non-uniqueness has led to a general feeling that what one calls as the *pressure* is not very important, when one is dealing with incompressible materials. Just about every part of the stress proportional to the Kronecker delta is dumped into the pressure term. It is obvious that this practice causes no difficulties when the decomposition (4.1.1) is not crucial. This is not the situation in viscoplastic fluids and so, it behooves us to define the meaning of pressure precisely. It is this matter to which we turn next.

Once again, let us decompose the total stress tensor into two parts [2]:

$$T_{ij} = S_{ij} + C_{ij}, \tag{4.1.5}$$

where the stress tensor C_{ij} arises due to the incompressibility constraint $A_{ii} = 0$. Let us write the latter as defining the *surface of constraint*:

$$\phi(\mathbf{A}) = A_{ii} = 0. \tag{4.1.6}$$

Just as the level surface $f(x, y, z) = 0$ has a normal defined through ∇f, we can define a normal $\mathbf{N}$, which is a symmetric second order tensor, to the surface of constraint through:

$$\mathbf{N} = \frac{\partial \phi}{\partial \mathbf{A}}, \quad N_{ij} = \frac{\partial \phi}{\partial A_{ij}}. \tag{4.1.7}$$

Then, any motion of an incompressible material occurs on *the surface of constraint*, and the constitutive equation for the extra stress tensor defines it on this surface; see [2] for a discussion of this matter.

Since the tensor C_{ij} must be parallel to the normal N_{ij}, we have the unique decomposition of the total stress tensor T_{ij}, with $C_{ij} = \lambda N_{ij}$:

$$T_{ij} = S_{ij} + \lambda N_{ij}, \quad S_{ij} N_{ij} = 0. \tag{4.1.8}$$

Hence, the Lagrange multiplier λ is given by

$$\lambda = \frac{T_{ij} N_{ij}}{N_{kl} N_{kl}}. \tag{4.1.9}$$

It follows from (4.1.6) and (4.1.7) that the tensor $N_{ij} = \delta_{ij}$, so that one obtains:

$$T_{ij} = S_{ij} + \lambda \delta_{ij}, \tag{4.1.10}$$

$$S_{ij} \delta_{ij} = S_{ii} = 0, \tag{4.1.11}$$

$$\lambda = \frac{1}{3} T_{ii}. \tag{4.1.12}$$

So, λ exists and is uniquely defined through an application of Lagrangian mechanics to continuum mechanics. Usually, one replaces λ by $-p$, and calls p, the pressure.

In conclusion, the pressure p, now defined as the negative of the mean normal stress through Eq. (4.1.12), has a fundamental significance. It arises as a unique response due to the kinematic constraint on the velocity field in an incompressible material. So, we arrive at the following unambiguous decomposition of the total stress tensor in all incompressible bodies, including viscoplasticity:

$$T_{ij} = S_{ij} - p\delta_{ij}, \quad S_{ii} = 0. \tag{4.1.13}$$

Thus, we have a unique, working definition of *pressure*. It is common to call

$$p = -\frac{1}{3}T_{ii} \tag{4.1.14}$$

as the *mechanical pressure*. We note that as a consequence of the decomposition described above, the trace of the extra stress tensor S_{ij} is zero in all motions of an incompressible body. While the definition of the entity, called pressure, is unique, one has to determine it as a field through the equations of motion. This situation is similar to that in determining the normal force N in the example from rigid body mechanics mentioned earlier.

One point worth mentioning is that the pressure field p in a motion need not be positive everywhere, although in a fluid at rest it is always positive. An example of a flow where the pressure field is negative, one can refer to the flow of a Bingham fluid in a channel. Another example where the pressure is negative at the surface occurs in the flow of a viscoelastic fluid [4].

4.2 Incompressible Viscoplastic Fluids

Let the total stress tensor in an incompressible yield stress fluid be written as $\mathbf{T}$. As is well known, the flow domain is decomposed into two disjoint sets; one where the fluid has yielded and $\mathbf{A} \neq \mathbf{0}$, and the other where the fluid has not yielded and $\mathbf{A} = \mathbf{0}$. Let us examine the consequences of this demarcation closely next.

1. If the fluid has yielded, it has been shown in Sect. 4.1 above that there exists a uniquely defined pressure p such that $p = -(1/3)T_{ii}$. Thus, the decomposition of $\mathbf{T} = -p\mathbf{1} + \mathbf{S}$ is unique since the motion occurs under the constraint of incompressibility.
2. If the fluid has not yielded, the motion does not occur on the *plane* $A_{ii} = 0$; rather, it occurs in the *six-dimensional space* $A_{ij} = 0$. Hence, it is not possible to prove that the total stress tensor must have the unique decomposition $\mathbf{T} = -p\mathbf{1} + \mathbf{S}$, for the existence of a uniquely defined pressure p cannot be established. To circumvent this ambiguity, one extends the definition of $p = -(1/3)T_{ii}$ from the yielded zone into the unyielded zone. That is, the pressure p is now a continuously

defined entity in the whole flow domain. Consequently, it is possible to accept that one may express the total stress tensor as $\mathbf{T} = -p\mathbf{1} + \mathbf{S}$. Next, one connects the *second invariant* $T(\mathbf{S})$ of the extra stress tensor $\mathbf{S}$ with the rigidity of the flow through

$$\mathbf{A} = \mathbf{0}, \quad T(\mathbf{S}) \leq \tau_y, \quad T(\mathbf{S}) = (1/\sqrt{2})||\mathbf{S}||. \tag{4.2.1}$$

The above equation states that the fluid experiences a rigid motion, which includes being at rest as well, when the *magnitude* of the extra stress tensor stress is less than or equal to the yield stress. Note that the second invariant of the stress tensor, $T(\mathbf{S})$, is derived from (3.4.11).

When the magnitude of the extra stress tensor exceeds the yield stress, one defines $\mathbf{S}$ as a function of the Rivlin-Ericksen tensor $\mathbf{A}$. So, let

$$\mathbf{S} = \mathbf{f}(\mathbf{A}), \quad T(\mathbf{S}) > \tau_y. \tag{4.2.2}$$

It is well known that this function must satisfy the principle of frame indifference. That is, for all orthogonal tensors $\mathbf{Q}$, this requirement leads to the following:

$$\mathbf{Q}\mathbf{f}(\mathbf{A})\mathbf{Q}^T = \mathbf{f}(\mathbf{Q}\mathbf{A}\mathbf{Q}^T). \tag{4.2.3}$$

The solution of this restriction is also well understood and results in the following expansion:

$$\mathbf{f}(\mathbf{A}) = \sum_{i=0}^{2} \alpha_i \mathbf{A}^i, \quad \mathbf{A}^0 = \mathbf{1}. \tag{4.2.4}$$

Each coefficient α_i, $i = 0, 1, 2$, is a function of the following three invariants I, II, III of $\mathbf{A}$:

$$I(\mathbf{A}) = \operatorname{tr} \mathbf{A}, \quad II(\mathbf{A}), \quad III(\mathbf{A}) = \det \mathbf{A}. \tag{4.2.5}$$

In viscoplastic fluid mechanics, it is customary to assume that the coefficients α_0 and α_2 are zero. And that the coefficient α_1 depends on the invariant $II(\mathbf{A})$, or $K(\mathbf{A})$ only. Thus,

$$\mathbf{S} = \alpha_1 \mathbf{A}, \tag{4.2.6}$$

where

$$\alpha_1 = \eta(K(\mathbf{A})) + \frac{\tau_y}{K(\mathbf{A})}. \tag{4.2.7}$$

Hence, the extra stress tensor is given by

$$\mathbf{S} = \eta(K(\mathbf{A}))\mathbf{A} + \frac{\tau_y}{K(\mathbf{A})}\mathbf{A}, \quad T(\mathbf{S}) > \tau_y, \tag{4.2.8}$$

where $\eta(K(\mathbf{A}))$ and τ_y are, respectively, the viscosity and the yield stress, of which only the former is assumed to depend on the invariant $K(\mathbf{A}) \geq 0$; i.e., it is shear rate

dependent. Obviously, the extra stress tensor $\mathbf{S}$ has zero trace in an incompressible fluid, as required, since $I(\mathbf{A}) = \operatorname{tr}\mathbf{A} = 0$ in such materials. And, in a simple shearing flow (2.5.2), it is obvious that

$$K(\mathbf{A}) = \left[\frac{1}{2}\operatorname{tr}\mathbf{A}^2\right]^{1/2} = \dot{\gamma} \geq 0. \tag{4.2.9}$$

Thus, one says that the viscosity $\eta(K(\mathbf{A}))$ depends on $\dot{\gamma} \geq 0$, or is shear rate dependent.

Usually, one assumes that the viscosity is of the power law type:

$$\eta(\dot{\gamma}) = k\dot{\gamma}^{m-1}, \tag{4.2.10}$$

where $\dot{\gamma}$ is the shear rate in a viscometric flow, the consistency index $k > 0$ is a constant, and $0 < m \leq 1$. Since the constitutive equation of a Bingham fluid is given by

$$\mathbf{S} = \eta\mathbf{A} + \frac{\tau_y}{K(\mathbf{A})}\mathbf{A}, \quad T(\mathbf{S}) > \tau_y, \tag{4.2.11}$$

where η is a constant, the viscosity function in Eq. (4.2.10) reduces to that of a Bingham fluid when one chooses $m = 1$ and $k = \eta$.

When $0 < m < 1$, the fluid is said to be of the Herschel-Bulkley type. In these fluids, one notes that the viscosity $\eta(\dot{\gamma}) \to \infty$ as $\dot{\gamma} \to 0$, while the shear stress $\sigma(\dot{\gamma}) \to 0$.

In Casson fluids, the shear stress σ in a steady shearing flow is given by:

$$\sqrt{\sigma} = \sqrt{\tau}_y + \sqrt{k\dot{\gamma}}, \quad k > 0, \tag{4.2.12}$$

which may be rewritten as:

$$\sigma = \tau_y + [k + 2\sqrt{k\tau_y}\,\dot{\gamma}^{-1/2}]\dot{\gamma}. \tag{4.2.13}$$

Clearly, this results in the following viscosity function for the Casson fluid:

$$\eta(\dot{\gamma}) = k + 2\left(\sqrt{k\tau_y}\right)\dot{\gamma}^{-1/2}. \tag{4.2.14}$$

Of course, both the viscosity and the yield stress may depend on the temperature and such dependence is easily understood. However, the experimentally known fact that a material property such as viscosity depends on the pressure in an incompressible material needs some explanation. Once again, one recalls from the sliding motion of a rigid body on a plane that the force of constraint N acts normally to the plane. The frictional force F acting on the body is usually assumed to be of the Coulomb type, i.e., it is given by $F = \mu N$. That is, the force F is a function of the force of constraint, N, and it is defined on the surface of constraint, viz. the plane.

As explained in Sect. 4.1, the motion of an incompressible fluid occurs on the surface of constraint, defined by (4.1.6), and the constitutive equation for the stress tensor $\mathbf{S}$ is defined on this surface only. Thus, it is possible that the constitutive equation can depend on the incompressibility constraint tensor $-p\mathbf{1}$, or on the pressure p. In fact, Antman [5] has developed a comprehensive theory to explain the dependence of material properties on material constraints, such as incompressibility. That is, there are theoretical justifications to admit constitutive equations for incompressible fluids in which the viscosity and the yield stress may depend on the pressure.

4.2.1 Equations of Motion for Incompressible Materials

Now that the pressure term p has been unambiguously defined, one can replace the total stress tensor $\mathbf{T}$ by $-p\mathbf{1} + \mathbf{S}$. The equations of motion (3.2.9) become

$$-\nabla p + \nabla \cdot \mathbf{S} + \rho \mathbf{b} = \rho \mathbf{a}, \tag{4.2.15}$$

which have the following indicial form:

$$-p_{,i} + S_{ij;j} + \rho b_i = \rho a_i, \quad i, j = 1, 2, 3. \tag{4.2.16}$$

4.3 Viscoplasticity Constraint Tensor

Incompressibility is a material property and is equivalent to the condition $\nabla \cdot \mathbf{v} = 0$ on the velocity field, or that the Rivlin-Ericksen tensor $\mathbf{A}$ is traceless. In turn, the latter leads to a constraint on the stress tensor throughout the body as demonstrated in Sects. 4.1 and 4.2. That is, the total stress tensor $\mathbf{T}$ is decomposed into $\mathbf{T} = -p\mathbf{1} + \mathbf{S}$, in which the constraint tensor is given by $-p\mathbf{1}$, and the extra stress tensor $\mathbf{S}$ has zero trace, i.e., $\mathbf{1} : \mathbf{S} = 0$.

In an incompressible viscoplastic fluid, another material property, known as the yield stress τ_y, induces an additional constraint on the extra stress tensor $\mathbf{S}$. In fact, this property divides the flow domain into unyielded and yielded regions. In the former, $\mathbf{A} = \mathbf{0}$. Under this restriction on $\mathbf{A}$, the extra stress tensor $\mathbf{S}$ cannot be defined through a constitutive relation. However, using (4.2.1) as a guide, consider the following constraint on $\mathbf{S}$:

$$T(\mathbf{S}) < \tau_y, \quad \text{when } \mathbf{A} = \mathbf{0}. \tag{4.3.1}$$

Since $\mathbf{S}$ is unknown, there is no loss of generality in replacing it by

$$\mathbf{S} = \sqrt{2}\, \tau_y\, \boldsymbol{\Lambda}, \quad \mathbf{1} : \boldsymbol{\Lambda} = 0, \quad \text{when } \mathbf{A} = \mathbf{0}. \tag{4.3.2}$$

The advantage of defining the tensor $\boldsymbol{\Lambda}$ lies in the fact that

$$\boldsymbol{\Lambda} : \boldsymbol{\Lambda} < 1 \quad \text{when } \mathbf{A} = \mathbf{0}. \tag{4.3.3}$$

Whenever $\mathbf{A} \neq \mathbf{0}$, we know that (4.2.11) applies. Here, we note that

$$||\frac{\mathbf{A}}{K(\mathbf{A})}|| = \sqrt{2}. \tag{4.3.4}$$

Thus, we can replace the constitutive relation (4.2.11) by

$$\mathbf{S} = \eta\mathbf{A} + \sqrt{2}\,\tau_y\,\boldsymbol{\Lambda}, \quad \mathbf{1} : \boldsymbol{\Lambda} = 0, \tag{4.3.5}$$

with the requirement that

$$\boldsymbol{\Lambda} : \boldsymbol{\Lambda} = 1 \quad \text{when } \mathbf{A} \neq \mathbf{0}. \tag{4.3.6}$$

In sum, one can assume that a constitutive equation for an incompressible viscoplastic fluid holds throughout the flow domain and is given by

$$\mathbf{S}(\mathbf{v}) = \eta\mathbf{A}(\mathbf{v}) + \sqrt{2}\,\tau_y\,\boldsymbol{\Lambda}, \quad \mathbf{1} : \boldsymbol{\Lambda} = 0, \tag{4.3.7}$$

where one may call the second order, symmetric, tensor $\boldsymbol{\Lambda}$ the *viscoplasticity constraint tensor*. Note that the traceless condition $\mathbf{1} : \boldsymbol{\Lambda} = 0$ has been imposed on this tensor so that the stress tensor $\mathbf{S}$ satisfies the condition $\text{tr}\,\mathbf{S} = 0$. Since $\boldsymbol{\Lambda} : \boldsymbol{\Lambda} < 1$ in the unyielded zone and $\boldsymbol{\Lambda} : \boldsymbol{\Lambda} = 1$ in the yielded region, it follows that on the yield surface, where $\mathbf{A} = \mathbf{0}$, the tensor $\boldsymbol{\Lambda}$ must satisfy the condition $\boldsymbol{\Lambda} : \boldsymbol{\Lambda} < 1$. Thus, one can require that the tensor $\boldsymbol{\Lambda}$ meet the following conditions:

$$\boldsymbol{\Lambda} : \boldsymbol{\Lambda} = \begin{cases} < 1, & \mathbf{A} = \mathbf{0}, \\ 1, & \mathbf{A} \neq \mathbf{0}. \end{cases} \tag{4.3.8}$$

These conditions have been derived from those imposed on the stress tensor, viz., $T(\mathbf{S}) \leq \tau_y$ when $\mathbf{A} = \mathbf{0}$, and $\tau_y < T(\mathbf{S})$ when $\mathbf{A} \neq \mathbf{0}$. The problem of determining where the flow is rigid and where it is liquid-like has been shifted to finding the tensor $\boldsymbol{\Lambda}$ in the flow field such that is satisfies Eq. (4.3.8). Moreover, just as the magnitude of the shear stress σ satisfies $0 \leq \sigma < \tau_y$ in the rigid core in a shearing flow, it is found that $0 \leq ||\boldsymbol{\Lambda}|| < 1$ in the rigid core regions.

What has been proposed is important for the following reasons:

1. The constitutive Eqs. (4.3.7) and (4.3.8) are defined over the entire flow domain, not just where the fluid has yielded.
2. One searches for the solution velocity field $\mathbf{u}$ and the viscoplasticity constraint tensor $\boldsymbol{\Lambda}$ to determine the yielded/unyielded regions. There are no singularities because one is not trying to find the location of the yield surface(s) as the limit of $\mathbf{A}/K(\mathbf{A})$ as $\mathbf{A} \to \mathbf{0}$.

3. However, the equations of motion now involve two unknown fields: a vector field $\mathbf{u}$, and a symmetric tensor field $\boldsymbol{\Lambda}$. The latter requires that there should exist a connection between the velocity field $\mathbf{u}$ and $\boldsymbol{\Lambda}$. Under Dirichlet boundary conditions, it is possible to prove such a relation; see Sect. 8.9.
4. Given this, the problem of finding $\mathbf{u}$ can be decoupled from that of determining where $||\boldsymbol{\Lambda}|| < 1$ and where $||\boldsymbol{\Lambda}|| = 1$. This forms the basis of the operator-splitting method discussed in Chap. 10.

4.4 Regularisation

A glance at the constitutive equation (4.2.8) of a general viscoplastic fluid, or the Bingham fluid (4.2.11), shows that in numerical modelling, it is difficult to find the location of the free boundary separating the yielded zone from the unyielded zone, since $\mathbf{A} = \mathbf{0}$ on this boundary. One way to circumvent this is to employ (4.3.7) as the constitutive relation. The second one is to choose a non-Newtonian viscous fluid which mimics the existence of a yield stress. While there are a number of such models, only two will be highlighted here. The first is the bi-viscosity model [6] and the second is the Papanastasiou model [7]. These models are known as *regularised models*; they disguise the existence of the yield stress through two different types of non-Newtonian viscosity functions. A brief description of these follows next.

In the bi-viscosity model to approximate a Bingham fluid [6], the dependence of the shear stress σ on the shear rate is linear and very steep around $\dot{\gamma} = 0$, so that

$$\sigma = \eta_0 \dot{\gamma}, \quad \dot{\gamma} < \dot{\gamma}_c, \tag{4.4.1}$$

where $\dot{\gamma}_c$ is a *critical shear rate*. Beyond this, the shear stress is assumed to be given by

$$\sigma = \tau_y + \eta_p \dot{\gamma}, \quad \dot{\gamma} > \dot{\gamma}_c. \tag{4.4.2}$$

See Fig. 4.1 for an explanation of η_0 and η_p, where these are identified as the respective slopes of the shear stress-shear rate curves. Typically, one sets $\eta_0 = 1000\eta_p$ to perform numerical simulations. Thus, the constitutive equation for a Bingham fluid is replaced by

$$\mathbf{S} = \begin{cases} \eta_0 \mathbf{A}, & K(\mathbf{A}) \leq \dot{\gamma}_c, \\ \left[\eta_p + \frac{\tau_y}{K(\mathbf{A})}\right]\mathbf{A}, & K(\mathbf{A}) > \dot{\gamma}_c. \end{cases} \tag{4.4.3}$$

The major drawback of this model is that the viscosity function is not smooth at the critical shear rate $\dot{\gamma}_c$; see Fig. 4.1.

In the Papanastasiou model [7], the constitutive equation for an incompressible Bingham fluid is once again replaced by that of a material with a non-Newtonian viscosity. See Fig. 4.2. That is,

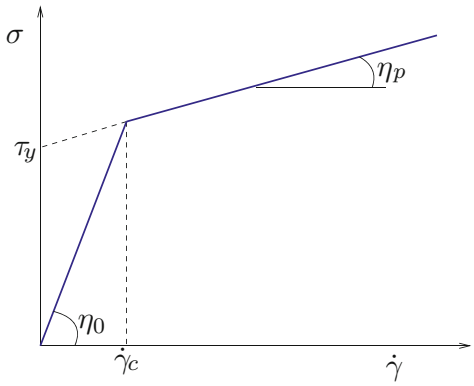

Fig. 4.1 The Bingham and Bi-viscosity models

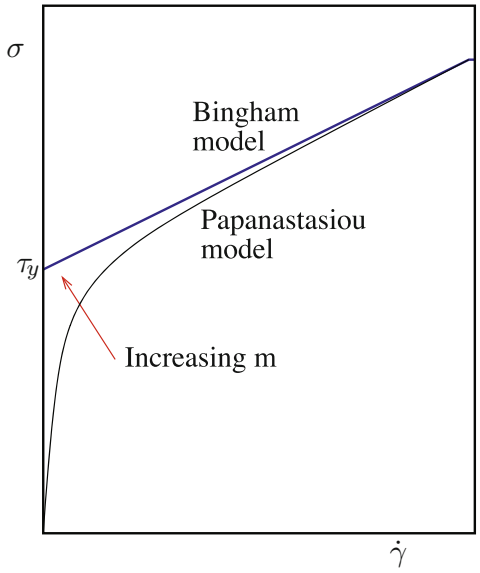

Fig. 4.2 The Bingham and Papanastasiou models

$$\mathbf{S} = \eta(K(\mathbf{A}))\mathbf{A}, \tag{4.4.4}$$

where the viscosity η is the sum of the constant Newtonian viscosity η_0, and a parameter dependent term. To be specific,

$$\eta(K(\mathbf{A})) = \eta_0 + \frac{\tau_y}{K(\mathbf{A})}\Big[1 - \exp(-mK(\mathbf{A}))\Big], \tag{4.4.5}$$

where $m > 0$ is the parameter which can be chosen arbitrarily. In a simple shearing flow in the x-direction described through $u = u(y)$, the viscosity $\eta(\dot{\gamma})$ and the shear stress σ are given by

$$\eta(\dot{\gamma}) = \eta_0 + \frac{\tau_y}{\dot{\gamma}}[1 - \exp(-m\dot{\gamma})], \quad \sigma = \eta_0 \frac{du}{dy} \pm \tau_y[1 - \exp(-m\dot{\gamma})], \tag{4.4.6}$$

where the $+$ (resp.$-$) sign applies if the shear rate du/dy is positive (resp. negative); note that $\dot{\gamma} = |du/dy| > 0$ here. As the parameter m increases, $\exp(-m\dot{\gamma}) \to 0$ and the shear stress approaches that of the Bingham fluid, which explains the presence of τ_y in the constitutive Eq. (4.4.5). Note that the viscosity function in (4.4.6) is a smooth function of the shear rate $|\dot{\gamma}|$.

As far as numerical modelling is concerned, one can employ (4.4.5) and choose an appropriate value for the parameter m. A search through the literature shows that m can be larger than 10^4; see Sect. 10.6.

4.5 Compressible Viscoplastic Fluids

In developing constitutive equations for compressible viscoplastic fluids, one has to include the density and the temperature as additional variables right from the beginning. Thus, one begins by writing the constitutive equation of a compressible viscoplastic fluid as

$$\mathbf{T} = -p\mathbf{1} + \mathbf{S}, \tag{4.5.1}$$

where the thermodynamic pressure p, the density ρ and the absolute temperature Θ satisfy an equation of state:

$$f(p, \rho, \Theta) = 0. \tag{4.5.2}$$

From the above implicit equation, we assume that we can solve for the density as a function of the pressure and the temperature, i.e.,

$$\rho = \rho(p, \Theta). \tag{4.5.3}$$

This equation permits one to replace the density ρ by the independent variables (p, Θ) as required.

Let the *non-thermodynamic stress tensor* $\mathbf{S}$ in a compressible yield stress fluid be given by:

$$\mathbf{A}(\mathbf{v}) = \mathbf{0}, \quad T(\mathbf{S}) \leq \tau_y, \tag{4.5.4}$$

$$\mathbf{S}(p, \Theta, \mathbf{v}) = \alpha(p, \Theta, I, II, III)\mathbf{1} + \eta(p, \Theta, I, II, III)\mathbf{A}(\mathbf{v}) + \frac{\tau_y(p, \Theta)}{K(\mathbf{v})}\mathbf{A}(\mathbf{v}), \quad T(\mathbf{S}) > \tau_y. \tag{4.5.5}$$

In Eq. (4.5.5), for brevity, we have introduced the following notation for the non-thermodynamic isotropic component α and the viscosity η:

$$\alpha(p, \Theta, I, II, III) = \alpha(p, \Theta, I(\mathbf{A}(\mathbf{v})), II(\mathbf{A}(\mathbf{v})), III(\mathbf{A}(\mathbf{v}))), \tag{4.5.6}$$

$$\eta(p, \Theta, I, II, III) = \eta(p, \Theta, I(\mathbf{A}(\mathbf{v})), II(\mathbf{A}(\mathbf{v})), III(\mathbf{A}(\mathbf{v}))), \tag{4.5.7}$$

In Eqs. (4.5.6) and (4.5.7), the invariants I, II, III appear and they have been defined earlier through (4.2.5).

To derive a fundamental inequality in Sect. 8.10, one has to impose the following constitutive restriction:

$$\alpha(p, \Theta, \mathbf{0}) = 0. \tag{4.5.8}$$

This says that when $\mathbf{A}(\mathbf{v}) = \mathbf{0}$, i.e., when the fluid particle is at rest or undergoing a rigid body motion, such as in a plug flow, the non-thermodynamic isotropic term is zero. On physical grounds, it would appear to be a very reasonable assumption, which has been employed by others as well. In the theory of laminar boundary layers in compressible fluids [8], it is common to demand that

$$\alpha(p, \Theta, \mathbf{A}(\mathbf{v})) = \frac{1}{2}(\xi - \frac{2}{3}\eta)I(\mathbf{A}(\mathbf{v})), \tag{4.5.9}$$

which means that Eq. (4.5.8) holds true. A similar assumption has been made by Vinay et al. [9]. Thus, without loss of generality, one can assume that in a state of rest, or in a rigid motion, $\alpha(p, \Theta, \mathbf{0}) = 0$.

As far as compressible fluids are concerned, one can make the same assumption as in Eq. (4.3.7) regarding the viscoplasticity constraint tensor, and propose the following as the constitutive equation:

$$\begin{aligned}\mathbf{S}(p, \Theta, \mathbf{v}) = {} & \alpha(p, \Theta, I, II, III)\mathbf{1} + \eta(p, \Theta, I, II, III)\mathbf{A}(\mathbf{v}) \\ & + \sqrt{2}\,\tau_y(p, \Theta)\boldsymbol{\Lambda}(\mathbf{v}),\end{aligned} \tag{4.5.10}$$

which is valid throughout the domain of the flow. Numerical modelling using the above form of the constitutive equation has been attempted; see Chap. 10.

4.6 Analogues for Incompressible Viscoplastic Fluids

In this section, one dimensional models along with their extensions to fully invariant, three dimensional models are listed. These extensions will be useful, in particular in Chap. 8, where variational principles and variational inequalities are derived.

4.6.1 One Dimensional Models

For the Bingham, Herschel-Bulkley and Casson models, the constitutive equations for the shear stress, the velocity and stress potentials are non-zero provided the shear rate $\dot{\gamma} > 0$, or equivalently, the magnitude of the shear stress $|\sigma| > \tau_y$.

1. Velocity Gradient:
$$\frac{du}{dy}. \tag{4.6.1}$$

2. Shear Rate:
$$\dot{\gamma} = \left|\frac{du}{dy}\right| \geq 0. \tag{4.6.2}$$

3. Constitutive Equation—Bingham fluid:
$$\frac{du}{dy} = 0, \quad |\sigma| \leq \tau_y, \tag{4.6.3}$$
$$\sigma = \eta\frac{du}{dy} + \frac{\tau_y}{\dot{\gamma}}\frac{du}{dy}, \quad |\sigma| = \eta\dot{\gamma} + \tau_y > \tau_y. \tag{4.6.4}$$

4. Velocity Potential—Bingham fluid:
$$\phi(\dot{\gamma}) = \begin{cases} 0, & \dot{\gamma} = 0, \\ \frac{1}{2}\eta\dot{\gamma}^2 + \tau_y\dot{\gamma}, & \dot{\gamma} > 0, \end{cases} \tag{4.6.5}$$
and
$$\frac{d\phi}{d\dot{\gamma}} = |\sigma|, \quad \dot{\gamma} > 0. \tag{4.6.6}$$

5. Stress Potential—Bingham fluid:
$$\Gamma(|\sigma|) = \frac{1}{8\eta}\Big(|\sigma - \tau_y| + \sigma - \tau_y\Big)^2, \tag{4.6.7}$$
and
$$\frac{d\Gamma}{d|\sigma|} = \dot{\gamma}, \quad |\sigma| > \tau_y. \tag{4.6.8}$$

6. Constitutive Equation—Herschel-Bulkley fluid:
$$\frac{du}{dy} = 0, \quad |\sigma| \leq \tau_y, \tag{4.6.9}$$
$$\sigma = k_b\dot{\gamma}^{m-1}\frac{du}{dy} + \frac{\tau_y}{\dot{\gamma}}\frac{du}{dy}, \quad |\sigma| = k_b(\dot{\gamma})^m + \tau_y > \tau_y. \tag{4.6.10}$$

7. Velocity Potential—Herschel-Bulkley fluid:

$$\phi(\dot{\gamma}) = \begin{cases} 0, & \dot{\gamma} = 0, \\ (k_b/(m+1))\dot{\gamma}^{m+1} + \tau_y\dot{\gamma}, & \dot{\gamma} > 0, \end{cases} \tag{4.6.11}$$

and

$$\frac{d\phi}{d\dot{\gamma}} = |\sigma|, \quad \dot{\gamma} > 0. \tag{4.6.12}$$

8. Stress Potential—Herschel-Bulkley fluid:

$$\Gamma(|\sigma|) = \frac{m}{(m+1)2^{(m+1)/m}}\left(\frac{1}{k_b}\right)^{1/m}\Big(|\sigma - \tau_y| + \sigma - \tau_y\Big)^{(m+1)/m}, \tag{4.6.13}$$

and

$$\frac{d\Gamma}{d|\sigma|} = \dot{\gamma}, \quad |\sigma| > \tau_y. \tag{4.6.14}$$

9. Constitutive Equation—Casson fluid:

$$\sqrt{|\sigma|} = \sqrt{k_c\dot{\gamma}} + \sqrt{\tau_y}, \tag{4.6.15}$$

$$\sigma = \left[k_c + 2\frac{\sqrt{k_c\tau_y}}{\sqrt{\dot{\gamma}}}\right]\frac{du}{dy} + \frac{\tau_y}{\dot{\gamma}}\frac{du}{dy}, \quad |\sigma| = [\sqrt{k_c\dot{\gamma}} + \sqrt{\tau_y}]^2. \tag{4.6.16}$$

10. Velocity Potential—Casson fluid:

$$\phi(\dot{\gamma}) = \begin{cases} 0, & \dot{\gamma} = 0, \\ \left[\frac{1}{2}k_c\dot{\gamma} + \frac{4}{3}(k_c\tau_y\dot{\gamma})^{1/2} + \tau_y\right]\dot{\gamma}, & \dot{\gamma} > 0, \end{cases} \tag{4.6.17}$$

and

$$\frac{d\phi}{d\dot{\gamma}} = |\sigma|, \quad \dot{\gamma} > 0. \tag{4.6.18}$$

11. Stress Potential—Casson fluid:

$$\Gamma(|\sigma|) = \begin{cases} 0, & |\sigma| \le \tau_y, \\ \frac{1}{k_c}\left[\frac{1}{2}|\sigma| - \frac{4}{3}(\tau_y|\sigma|)^{1/2} + \tau_y\right]|\sigma|, & |\sigma| > \tau_y, \end{cases} \tag{4.6.19}$$

and

$$\frac{d\Gamma}{d|\sigma|} = \dot{\gamma}, \quad |\sigma| > \tau_y. \tag{4.6.20}$$

4.6.2 Some Results from Tensor Analysis

To motivate the introduction of velocity and stress potentials in a three dimensional setting, we shall establish some simple results from tensor analysis next. Using Cartesian tensor notation, one finds that

$$\begin{aligned}\frac{\partial A_{ij}}{\partial A_{mn}} &= \frac{1}{2}\left(\frac{\partial A_{ij}}{\partial A_{mn}} + \frac{\partial A_{ji}}{\partial A_{mn}}\right)\\ &= \frac{1}{2}\left(\delta_{im}\delta_{jn} + \delta_{in}\delta_{jm}\right).\end{aligned} \tag{4.6.21}$$

Hence,

$$\frac{\partial (A_{ij}A_{ji})}{\partial A_{mn}} = \frac{\partial A_{ij}}{\partial A_{mn}}A_{ji} + A_{ij}\frac{\partial A_{ji}}{\partial A_{mn}} = 2A_{mn}. \tag{4.6.22}$$

That is,

$$\frac{\partial}{\partial \mathbf{A}}(\mathbf{A} : \mathbf{A}) = 2\mathbf{A}. \tag{4.6.23}$$

Recalling (3.4.12) and noting that $2K^2(\mathbf{A}) = \mathbf{A} : \mathbf{A}$, one finds that

$$\frac{\partial}{\partial \mathbf{A}}(2K^2(\mathbf{A})) = 4K(\mathbf{A})\frac{\partial K(\mathbf{A})}{\partial \mathbf{A}} = 2\mathbf{A}. \tag{4.6.24}$$

That is,

$$\frac{\partial K(\mathbf{A})}{\partial \mathbf{A}} = \frac{\mathbf{A}}{2K(\mathbf{A})}. \tag{4.6.25}$$

Similarly, for the extra stress tensor,

$$\frac{\partial T(\mathbf{S})}{\partial \mathbf{S}} = \frac{\mathbf{S}}{2T(\mathbf{S})}. \tag{4.6.26}$$

The velocity potential $\phi(K(\mathbf{A}))$ is defined so that it satisfies the following conditions:

$$\phi(K(\mathbf{A})) = 0, \quad K(\mathbf{A}) = 0, \tag{4.6.27}$$

$$\frac{d\phi}{dK(\mathbf{A})} = T(\mathbf{S}), \quad K(\mathbf{A}) > 0. \tag{4.6.28}$$

The stress potential $\Gamma(T(\mathbf{S}))$ is defined so that

$$\Gamma(T(\mathbf{S})) = 0, \quad T(\mathbf{S}) \leq \tau_y, \tag{4.6.29}$$

$$\frac{d\Gamma}{dT(\mathbf{S})} = K(\mathbf{A}), \quad T(\mathbf{S}) > \tau_y. \tag{4.6.30}$$

4.6.3 Three Dimensional Models

To derive the three dimensional versions from one-dimensional models, one replaces du/dy by $\mathbf{A}$; the shear rate $\dot{\gamma}$ by $K(\mathbf{A})$; the shear stress σ by $\mathbf{S}$; and, finally, the magnitude of the shear stress $|\sigma|$ by $T(\mathbf{S})$.

1. Rivlin-Ericksen tensor:
$$\mathbf{A}. \tag{4.6.31}$$

2. Kinematic or Second Invariant of the Rivlin-Ericksen tensor:
$$K(\mathbf{A}) = \frac{1}{\sqrt{2}}||\mathbf{A}||. \tag{4.6.32}$$

3. Constitutive Equation—Bingham fluid:
$$\mathbf{A} = 0, \quad T(\mathbf{S}) \leq \tau_y, \tag{4.6.33}$$
$$\mathbf{S} = \eta\mathbf{A} + \frac{\tau_y}{K(\mathbf{A})}\mathbf{A}, \quad T(\mathbf{S}) > \tau_y, \tag{4.6.34}$$
$$T(\mathbf{S}) = \eta K(\mathbf{A}) + \tau_y > \tau_y. \tag{4.6.35}$$

4. Velocity Potential—Bingham fluid:
$$\phi(K(\mathbf{A})) = \begin{cases} 0, & \mathbf{A} = \mathbf{0}, \\ \frac{1}{2}\eta K(\mathbf{A})^2 + \tau_y K(\mathbf{A}), & K(\mathbf{A}) > 0. \end{cases} \tag{4.6.36}$$

5. Stress Potential—Bingham fluid:
$$\Gamma(T(\mathbf{S})) = \frac{1}{8\eta}\Big(|T(\mathbf{S}) - \tau_y| + T(\mathbf{S}) - \tau_y\Big)^2. \tag{4.6.37}$$

6. Constitutive Equation—Herschel-Bulkley fluid:
$$\mathbf{A} = 0, \quad T(\mathbf{S}) \leq \tau_y, \tag{4.6.38}$$
$$\mathbf{S} = k_b K(\mathbf{A})^{m-1}\mathbf{A} + \frac{\tau_y}{K(\mathbf{A})}\mathbf{A}, \quad T(\mathbf{S}) > \tau_y, \tag{4.6.39}$$
$$T(\mathbf{S}) = k_b K(\mathbf{A})^m + \tau_y > \tau_y. \tag{4.6.40}$$

7. Velocity Potential—Herschel-Bulkley fluid:
$$\phi(K(\mathbf{A})) = \begin{cases} 0, & \mathbf{A} = \mathbf{0}, \\ (k_b/(m+1))K(\mathbf{A})^{m+1} + \tau_y K(\mathbf{A}), & K(\mathbf{A}) > 0. \end{cases} \tag{4.6.41}$$

8. Stress Potential—Herschel-Bulkley fluid:

$$\Gamma(T(\mathbf{S})) = \frac{m}{(m+1)2^{(m+1)/m}}\left(\frac{1}{k_b}\right)^{1/m}\left(|T(\mathbf{S}) - \tau_y| + T(\mathbf{S}) - \tau_y\right)^{(m+1)/m}. \tag{4.6.42}$$

9. Constitutive Equation—Casson fluid:

$$\mathbf{A} = 0, \quad T(\mathbf{S}) \leq \tau_y, \tag{4.6.43}$$

$$\mathbf{S} = \left[k_c + 2\frac{\sqrt{k_c\tau_y}}{\sqrt{K(\mathbf{A})}}\right]\mathbf{A} + \frac{\tau_y}{K(\mathbf{A})}\mathbf{A}, \quad T(\mathbf{S}) > \tau_y, \tag{4.6.44}$$

$$T(\mathbf{S}) = \left[\sqrt{k_c}K(\mathbf{A})^{1/2} + \sqrt{\tau_y}\right]^2, \quad T(\mathbf{S}) > \tau_y. \tag{4.6.45}$$

10. Velocity Potential—Casson fluid:

$$\phi(K(\mathbf{A})) = \begin{cases} 0, & \mathbf{A} = \mathbf{0}, \\ \left[\frac{1}{2}k_c K(\mathbf{A}) + \frac{4}{3}\left(k_c\tau_y K(\mathbf{A})\right)^{1/2} + \tau_y\right]K(\mathbf{A}), & K(\mathbf{A}) > 0. \end{cases} \tag{4.6.46}$$

11. Stress Potential—Casson fluid:

$$\Gamma(T(\mathbf{S})) = \begin{cases} 0, & T(\mathbf{A}) \leq \tau_y, \\ \frac{1}{k_c}\left[\frac{1}{2}T(\mathbf{S}) - \frac{4}{3}(\tau_y T(\mathbf{S}))^{1/2} + \tau_y\right]T(\mathbf{S}), & T(\mathbf{S}) > \tau_y. \end{cases} \tag{4.6.47}$$

References

1. Huilgol RR (2009) On the definition of pressure in rheology. Rheol Bull 78(2):12, 14–15, 29
2. Rajagopal KR, Srinivasa AR (2005) On the nature of constraints for continua undergoing dissipative processes. Proc R Soc A461:278–2795
3. Huilgol RR, Phan-Thien N (1997) Fluid mechanics of viscoelasticity. Elsevier, Amsterdam
4. Huilgol RR, Panizza, M, Payne LE (1993) On the rectilinear flow of a second order fluid and the role of the second normal stress difference. J Non-Newt Fluid Mech 50:331–348. Corrigenda (1994) J Non-Newt Fluid Mech 55:209–211
5. Antman SS (1981) Material constraints in continuum mechanics. Atti della Acc Naz Lincei, Rend Cl Sci Fiz Math Nat 70:256–264
6. O'Donovan EJ, Tanner RI (1984) Numerical study of the Bingham squeeze film problem. J Non-Newt Fluid Mech 15:74–83
7. Papanastasiou TC (1987) Flows of materials with yield. J Rheol 31:385–404
8. Stewartson K (1984) The theory of laminar boundary layers in compressible fluids. Clarendon, Oxford
9. Vinay G, Wachs A, Agassant J-F (2006) Numerical simulation of weakly compressible Bingham flows: the restart of pipeline flows of waxy crude oils. J Non-Newt Fluid Mech 136:93–105

Chapter 5
Analytic Solutions: Steady Flows

In this chapter, a collection of analytic solutions to the steady flows of Bingham fluids is presented. First of all, the steady velocity fields in a simple shearing flow, the flow down an inclined plane, that in a pipe of circular cross-section, in a concentric annulus, and in a Couette flow are derived. In each case, the role of the yield stress is emphasised. Next, the helical flow of a Bingham fluid is analysed and a general method to find a complete solution of this problem is presented. Attention is also drawn to the steady flows of non-Bingham fluids. Later on, a simple problem involving heat transfer in a shearing flow between parallel walls is included to illustrate the role played by the Nusselt number. Subsequently, attention is drawn to results pertaining to entry flows and those far downstream in a circular tube and between parallel walls in the presence of heat transfer.

In each shearing flow, except in the simple shearing flow, one is faced with the following difficulty which arises from the constitutive equation for the Bingham fluid. From (4.2.11), we see that

$$\mathbf{S} = \eta\mathbf{A} + \frac{\tau_y}{K(\mathbf{A})}\mathbf{A}, \quad T(\mathbf{S}) > \tau_y. \tag{5.0.1}$$

In a Bingham fluid, the viscosity is constant and in a shearing flow, such as that in a channel (2.5.4) where the velocity field is given by $\dot{x} = u(y)$, Eq. (5.0.1) turns into a simple expression for the shear stress $S_{12} = S_{21}$, given by

$$S_{12} = \eta u' + \frac{\tau_y}{\dot{\gamma}}u' = \eta u' + \frac{\tau_y}{|u'|}u'. \tag{5.0.2}$$

This formula shows that

$$S_{12} = \eta u' - \tau_y, \tag{5.0.3}$$

if $u' < 0$, and

$$S_{12} = \eta u' + \tau_y, \tag{5.0.4}$$

if $u' > 0$. The following examples depend on the descriptions of the shear stresses given above in the yielded zones. In the rigid core, the sign of the shear stress changes in a continuous manner from a positive value to a negative one as required.

R.R. Huilgol, *Fluid Mechanics of Viscoplasticity*, DOI 10.1007/978-3-662-45617-0_5

5.1 Simple Shearing Flow

The velocity field in a simple shearing flow is given in Cartesian coordinates through

$$\dot{x} = \dot{\gamma} y, \quad \dot{y} = \dot{z} = 0, \quad \dot{\gamma} > 0. \tag{5.1.1}$$

It occurs between two plates at $y = 0$ and $y = H$. Later on, we shall consider the situation when the shearing flow is supposed to occur in the half-space $0 \leq y < \infty$ in the context of an initial value problem. At present, it is easy to see that there is no unyielded region in $0 \leq y \leq H$ and the shear stress is given by

$$S_{12} = S_{21} = \eta \dot{\gamma} + \tau_y \tag{5.1.2}$$

throughout the region of the flow. The pressure function $p(x, y, z)$ may be assumed to be a constant, if body forces are ignored.

5.2 Flow in a Channel

The flow in a channel has been discussed at length in Chap. 1. To recall, the velocity field is given by

$$\dot{x} = u(y), \quad \dot{y} = \dot{z} = 0, \quad -H \leq y \leq H. \tag{5.2.1}$$

Depending on the pressure drop per unit length $G > G_c$, the latter being the critical value, this shearing flow occurs with a plug in the centre, situated between $y = \pm h$, moving as a rigid body. The shear stress changes sign from a positive value at $y = -H$ to a negative one at $y = H$, as shown earlier. That is:

$$S_{21} = S_{12} = \begin{cases} \eta u' + \tau_y, & -H \leq y \leq h, \\ -\tau_y y/h, & -h \leq y \leq h, \\ \eta u' - \tau_y, & h \leq y \leq H. \end{cases} \tag{5.2.2}$$

Note that $S_{21} = S_{12} = 0$ at $y = 0$ and that $u' = 0$, $-h \leq y \leq h$. The pressure field is given by $p(x, y, z) = -Gx + f(y, z)$, where $f(y, z)$ may be considered to be a constant when there are no body forces.

5.3 Flow Down an Inclined Plane

The flow down an inclined plane can be considered to be similar to that in the bottom half of a channel. See Fig. 5.1.

Let the Bingham fluid flow down the incline making an angle α with the horizontal. The depth of the flow is H and, by positioning the x-axis along the free surface and the y-axis normal to it, one can see that the shear stress $S_{21} = S_{12} = \sigma(y)$. Thus, the equations of motion are given by

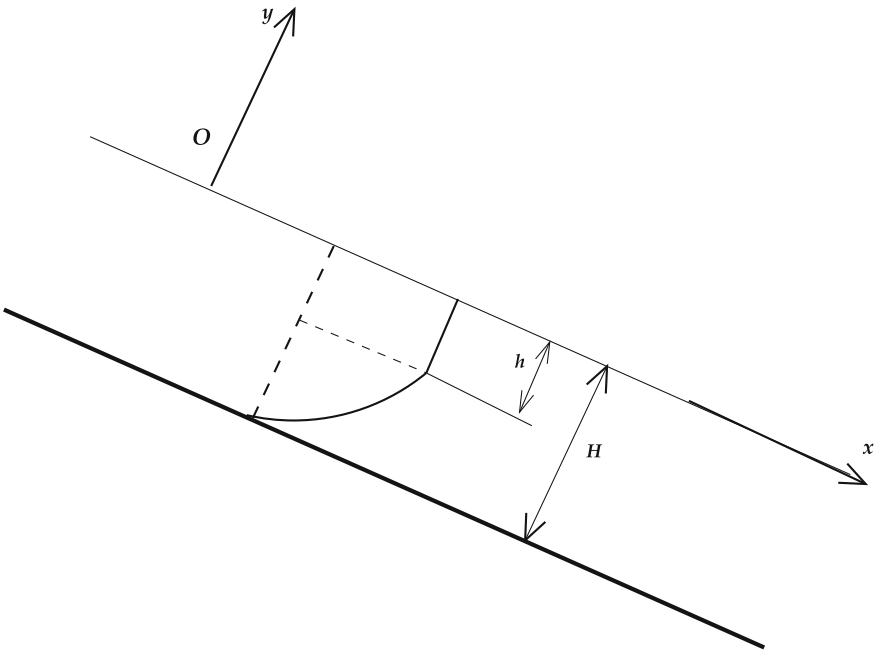

Fig. 5.1 Flow down an inclined plane

$$-\frac{\partial p}{\partial x}+\frac{\partial \sigma}{\partial y}+\rho g\sin\alpha=0, \tag{5.3.1}$$

$$-\frac{\partial p}{\partial y}-\rho g\cos\alpha=0. \tag{5.3.2}$$

These can be integrated and one obtains $p(x,y)=-\rho gy\cos\alpha$, $\sigma(y)=b-\rho gy\sin\alpha$, where b is a constant of integration. Assuming that the angle of inclination α is large enough, there will be a plug flow region at the top with a shearing flow below it. So, the shear stress distribution is given by

$$\sigma(y)=\begin{cases}-\tau_y y/h, & -h\le y\le 0,\\ \eta u'+\tau_y, & -H\le y\le -h.\end{cases} \tag{5.3.3}$$

Note that on the free surface at $y=0$, there is no shear stress as it should be. Thus, $\sigma(y)=b-\rho gy\sin\alpha$ leads to the result that $b=0$. The only matter of concern now is to determine the depth of the flow H or the width of the plug h, for a given value of α. To find this, we see that

$$\tau_y=\sigma(-h)=\rho gh\sin\alpha. \tag{5.3.4}$$

Hence, h has been found.

We shall now obtain a relationship between the flow rate Q and the depth H as follows. Integration by parts, using $u(-H) = 0$ due to the adherence condition and that $u' = 0,\ -h \le y \le 0$, leads to

$$Q = \int_{-H}^{0} u\, dy = -\int_{-H}^{-h} yu'\, dy. \tag{5.3.5}$$

Next, in $-H \le y \le -h$, one has

$$\sigma(y) = -\rho g y \sin\alpha = \eta u' + \tau_y = \eta u' + \rho g h \sin\alpha. \tag{5.3.6}$$

Thus,

$$u' = -\frac{\rho g \sin\alpha}{\eta}(y + h), \quad -H \le y \le -h. \tag{5.3.7}$$

Hence,

$$Q = \frac{\rho g \sin\alpha}{\eta} \int_{-H}^{-h} (y^2 + hy)\, dy \tag{5.3.8}$$

$$= \frac{\rho g H^3 \sin\alpha}{3\eta}\left[1 - \frac{3}{2}\left(\frac{h}{H}\right) + \frac{1}{2}\left(\frac{h}{H}\right)^3\right]. \tag{5.3.9}$$

Since the wall shear stress has the magnitude $\sigma_w = \rho g H \sin\alpha$, one can recast this in the form

$$Q = \frac{H^2 \sigma_w}{3\eta}\left[1 - \frac{3}{2}\left(\frac{\tau_y}{\sigma_w}\right) + \frac{1}{2}\left(\frac{\tau_y}{\sigma_w}\right)^3\right]. \tag{5.3.10}$$

Comparing this with (1.5.4), we see that this flow rate is exactly half of that for the flow in a channel as asserted earlier.

5.4 Flow in a Pipe of Circular Cross-Section

The axial flow in a pipe of circular cross-section is quite different from that in a channel because the shear stress field is negative throughout the cross-section. Of course, there will be a rigid plug in the centre of the pipe provided the applied pressure drop per unit length G exceeds the effect of the yield stress on the boundary of the pipe of inner radius R. The force acting on the Bingham fluid at rest per unit length of the pipe is given by $G \times \pi R^2$, while the yield stress τ_y opposes it with the force $\tau_y \times 2\pi R$. Thus, the critical pressure drop per unit length to initiate the flow is given by

$$G_c = \frac{2\tau_y}{R}. \tag{5.4.1}$$

Since the axial velocity field in a pipe of circular cross-section is best described through cylindrical coordinates, the steady flow has the form

$$\dot{r} = 0, \quad \dot{\theta} = 0, \quad \dot{z} = w(r), \quad 0 \leq r \leq R, \quad -\infty < z < \infty, \tag{5.4.2}$$

with $w(R) = 0$. Realising that there is no acceleration, the equation of motion relevant to the problem at hand is given by

$$-\frac{\partial p}{\partial z} + \frac{\partial S_{rz}}{\partial r} + \frac{S_{rz}}{r} = 0, \tag{5.4.3}$$

when the body force is ignored; or, if the flow is in a vertical direction, the body force can be incorporated into the pressure term.

If the pressure drop per unit length along the axis is $G > G_c > 0$, one sees that $p(r, \theta, z) = -Gz + f(r, \theta)$, where the latter function may be taken to be a constant, preferably zero. Thus, the shear stress distribution is given by

$$S_{rz} = -\frac{Gr}{2} + \frac{B}{r}, \tag{5.4.4}$$

where the constant B has to be found. If one assumes that the shear stress is bounded in $0 \leq r \leq R$, it follows that $B = 0$. Thus,

$$S_{rz} = -\frac{Gr}{2}, \quad 0 \leq r \leq R. \tag{5.4.5}$$

This shear stress is negative throughout the domain of the flow because on the surface of the pipe, the unit external normal $\mathbf{n}$ is radial. Since the shear stress σ_w on the wall opposes the flow, it is acting upstream. Thus, using Cauchy's stress principle, it follows that

$$[\mathbf{t}] = \begin{bmatrix} -p + S_{rr} & S_{r\theta} & S_{rz} \\ S_{r\theta} & -p + S_{\theta\theta} & S_{\theta z} \\ S_{rz} & S_{\theta z} & -p + S_{zz} \end{bmatrix} \begin{bmatrix} 1 \\ 0 \\ 0 \end{bmatrix} \tag{5.4.6}$$

$$= \begin{bmatrix} -p + S_{rr} \\ S_{r\theta} \\ S_{rz} \end{bmatrix} = \begin{bmatrix} -p \\ 0 \\ -\sigma_w \end{bmatrix}. \tag{5.4.7}$$

This shows clearly why the shear stress S_{rz} in the fluid is negative throughout. Assuming that the central plug has a radius ρ, we can describe the shear stress distribution through

$$S_{rz}(r) = \begin{cases} -\tau_y r/\rho, & 0 \leq r \leq \rho, \\ \eta w' - \tau_y, & \rho \leq r \leq R, \quad w' = dw/dr. \end{cases} \tag{5.4.8}$$

Next, the shear stress reaches the value τ_y on the boundary of the plug of radius ρ, when

$$\tau_y = \frac{G\rho}{2}. \tag{5.4.9}$$

Thus, the radius of the plug is given by $\rho = 2\tau_y/G$, whence it is easy to see that $\tau_y/\sigma_w = r/R$. These preliminaries provide enough information to determine the velocity distribution in the pipe and the flow rate. First of all, from (5.4.5), (5.4.7) and (5.4.8), we see that

$$\eta w' = \frac{G}{2}(\rho - r), \quad \rho \le r < R. \tag{5.4.10}$$

Hence,

$$w(r) = \frac{Gr}{4\eta}\Big[2\rho - r\Big] + B. \tag{5.4.11}$$

Since $w(R) = 0$, the constant of integration B is given by

$$B = \frac{GR}{4\eta}\Big[R - 2\rho\Big], \tag{5.4.12}$$

whence

$$w(r) = \frac{GR^2}{4\eta}\left(1 - \frac{r^2}{R^2}\right) - \frac{G\rho R}{2\eta}\left(1 - \frac{r}{R}\right), \quad \rho \le r \le R. \tag{5.4.13}$$

Using (5.4.9), this can be rewritten as

$$w(r) = \frac{GR^2}{4\eta}\left(1 - \frac{r^2}{R^2}\right) - \frac{\tau_y R}{\eta}\left(1 - \frac{r}{R}\right), \quad \rho \le r \le R. \tag{5.4.14}$$

This velocity distribution is parabolic and the velocity in the plug is a constant given by

$$w(r) = \frac{GR^2}{4\eta}\left(1 - \frac{\rho}{R}\right)^2, \quad 0 \le r \le \rho, \tag{5.4.15}$$

because $\tau_y = G\rho/2$. Finally, integration by parts and $w' = 0,\ 0 \le r \le \rho$, shows that the flow rate is given by

$$Q = \int_0^R 2\pi r w(r)\, dr = -\int_\rho^R \pi r^2 w'\, dr \tag{5.4.16}$$

$$= \frac{\pi G}{2\eta}\int_\rho^R r^2(r - \rho)\, dr \tag{5.4.17}$$

$$= \frac{\pi G R^4}{8\eta}\left[1 - \frac{4}{3}\left(\frac{\rho}{R}\right) + \frac{1}{3}\left(\frac{\rho}{R}\right)^4\right] \tag{5.4.18}$$

$$= \frac{\pi G R^4}{8\eta}\left[1 - \frac{4}{3}\left(\frac{\tau_y}{\sigma_w}\right) + \frac{1}{3}\left(\frac{\tau_y}{\sigma_w}\right)^4\right]. \tag{5.4.19}$$

5.4.1 The Buckingham Equation

To obtain the Buckingham equation, set $r_0 = \rho/R$. Next, from (5.4.9), it follows that $G = 2\tau_y/Rr_0$. Defining the Bingham number Bn through

$$\text{Bn} = \frac{\tau_y R}{\eta U}, \tag{5.4.20}$$

where $U = Q/\pi R^2$ is the velocity scale, Eq. (5.4.18) leads to the following Buckingham equation for r_0:

$$r_0^4 - 4\left(1 + \frac{3}{\text{Bn}}\right)r_0 + 3 = 0. \tag{5.4.21}$$

To show that there is a unique solution r_0 such that $0 < r_0 < 1$, we consider the fourth order equation:

$$x^4 - 4\left(1 + \frac{3}{\text{Bn}}\right)x + 3 = 0. \tag{5.4.22}$$

The discriminant $\triangle$ of this equation is given by

$$\triangle = 6912 - 6912\left(1 + \frac{3}{\text{Bn}}\right)^4 < 0. \tag{5.4.23}$$

Hence, (5.4.22) has four roots out of which two are real and the other two are complex conjugates. To prove that the real roots are both positive, consider the function:

$$f(x) = x^4 - 4\left(1 + \frac{3}{\text{Bn}}\right)x + 3. \tag{5.4.24}$$

Since $f(0) = 3$, $f(1) < 0$, it follows that there is a unique root of (5.4.22) given by $x = r_0$, such that $0 < r_0 < 1$. Moreover, $f(1) < 0$ and $f(x) \to \infty$ as $x \to \infty$ imply that the second, real root of (5.4.22) is larger than 1.

Finally, as in Sect. 1.8, the plug disappears as the Bingham number Bn $\to 0$; and the radius of the plug approaches 1 as Bn $\to \infty$. A regular perturbation analysis of (5.4.21) yields the result that [1]:

$$r_0 \sim \frac{1}{4}\text{Bn} - \frac{1}{12}\text{Bn}^2 \quad \text{as Bn} \to 0. \tag{5.4.25}$$

Similarly, using the method employed in (1.8.11), one can prove that the following asymptotic expansion [1] holds for large Bn:

$$r_0 \sim 1 - \frac{\sqrt{2}}{\mathrm{Bn}^{1/2}} + \frac{1}{3\ \mathrm{Bn}} + O(\mathrm{Bn}^{-3/2}). \tag{5.4.26}$$

5.5 Axial Flow in a Concentric Annulus

The axial flow in a concentric annulus is similar to that in a pipe of circular cross-section. The steady flow has the form

$$\dot{r} = 0, \quad \dot{\theta} = 0, \quad \dot{z} = w(r), \quad R_1 \le r \le R_2, \quad -\infty < z < \infty, \tag{5.5.1}$$

where $R_1 < R_2$ are the radii of the surfaces between which the flow occurs and $w(R_1) = w(R_2) = 0$.

Since there is no acceleration, the equation of motion relevant to the problem at hand is given by

$$-\frac{\partial p}{\partial z} + \frac{\partial S_{rz}}{\partial r} + \frac{S_{rz}}{r} = 0, \tag{5.5.2}$$

where the existence of the body force is dealt with in a manner similar to that in the flow of the Bingham fluid in a circular pipe. If the pressure drop per unit length along the axis is $G > G_c > 0$, one sees that $p(r, \theta, z) = -Gz + f(r, \theta)$, where the latter function may be taken to be a constant, preferably zero. Thus, the shear stress distribution is again given by

$$S_{rz} = -\frac{Gr}{2} + \frac{B}{r}, \tag{5.5.3}$$

where the constant B has to be found. Since the flow occurs between the surfaces at $r = R_1$ and $r = R_2$, the constant $B \neq 0$. In fact, as in the case of the flow in a channel, the shear stress $S_{rz} > 0$ on the surface $r = R_1$ and $S_{rz} < 0$ on $r = R_2$. This stress distribution means that the constant $B > 0$ and thus $dS_{rz}/dr < 0$ in $R_1 < r < R_2$. The latter has the following consequence: it is not possible for a flow to occur with the shear stress $S_{rz}(R_2) < -\tau_y$ and $0 < S_{rz}(R_1) < \tau_y$. To understand this, consider the following argument:

1. Let $0 < S_{rz}(R_1) < \tau_y$, $S_{rz}(R_2) < -\tau_y$.
2. Since the shear stress is a monotonically decreasing function of r, it follows that at some value of $r = R_0$, the stress $S_{rz}(R_0) = -\tau_y$.
3. If the flow were to occur in the annular region $R_0 \le r \le R_2$, Cauchy's stress principle proves that $S_{rz}(R_0) > 0$. So, there is a contradiction.

In a similar fashion, one can show that there is no flow if $-\tau_y < S_{rz}(R_2)$, $\tau_y < S_{rz}(R_1)$.

In other words, the critical pressure drop per unit length G_c needed to initiate the flow must satisfy

$$-G_c\frac{R_1}{2}+\frac{B}{R_1}=\tau_y, \tag{5.5.4}$$

$$-G_c\frac{R_2}{2}+\frac{B}{R_2}=-\tau_y. \tag{5.5.5}$$

Adding the two equations, one obtains

$$B=\frac{GR_1R_2}{2}. \tag{5.5.6}$$

Thus,

$$G_c=\frac{2\tau_y}{R_2-R_1}. \tag{5.5.7}$$

A different derivation of the same result using the Mosolov and Miasnikov Lemmas will be presented in Sect. 9.1.

Now, let $G > G_c$ so that a steady flow occurs in the concentric annulus. In order to determine the velocity field, which will contain a concentric annular plug flow within it, one has to find the radii ρ_1, ρ_2 of the plug such that $\rho_1 < \rho_2$; see Fig. 5.2. There will be a shearing flow within $R_1 < r < \rho_1$, and within $\rho_2 < r < R_2$, and the velocity distribution has to be found inside both of these annular domains.

Once again, the shear stress has the distribution:

$$S_{rz}(r)=-\frac{Gr}{2}+\frac{B}{r},\quad R_1\le r\le R_2. \tag{5.5.8}$$

As far as the plug between $\rho_1 \le r \le \rho_2$ is concerned, its boundaries are subjected to the yield stress τ_y in magnitude. Hence, one obtains:

$$B=\frac{G\rho_1\rho_2}{2},\quad G=\frac{2\tau_y}{\rho_2-\rho_1}. \tag{5.5.9}$$

In other words, we have derived a relation between ρ_1 and ρ_2, which is:

$$\rho_2-\rho_1=\frac{2\tau_y}{G}. \tag{5.5.10}$$

We need another to find these two radii. Here, we use the constitutive equations:

$$\eta w'+\tau_y=-\frac{Gr}{2}+\frac{B}{r},\quad R_1\le r\le \rho_1, \tag{5.5.11}$$

$$\eta w'-\tau_y=-\frac{Gr}{2}+\frac{B}{r},\quad \rho_2\le r\le R_2. \tag{5.5.12}$$

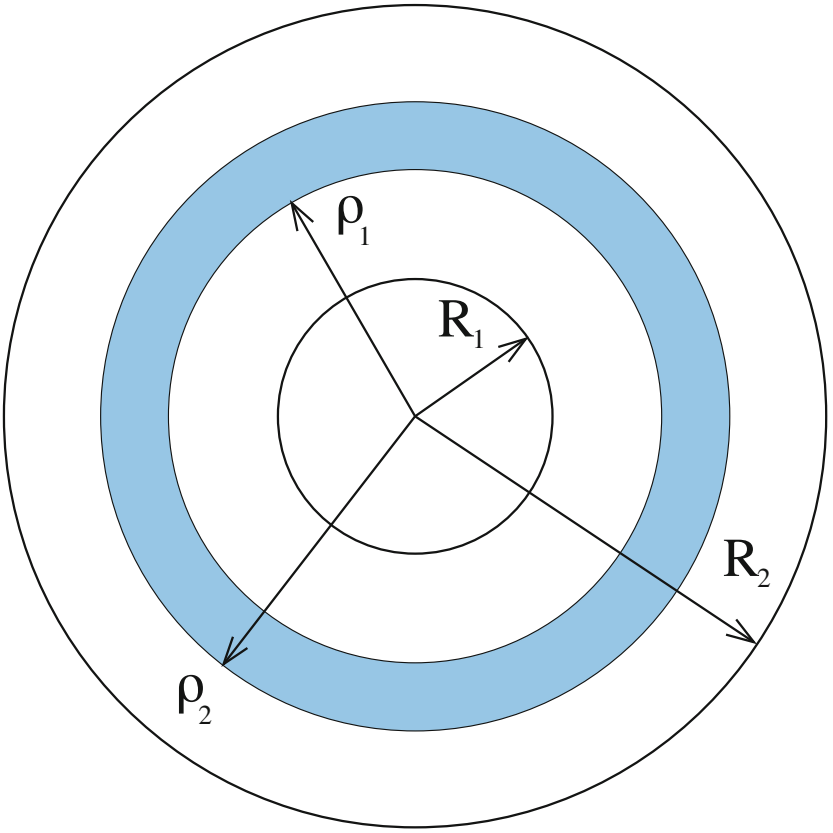

Fig. 5.2 Axial flow in a concentric annulus

That is:

$$\eta w' = -\frac{Gr}{2} - \frac{G}{2}(\rho_2 - \rho_1) + \frac{B}{r}, \quad R_1 \le r \le \rho_1, \tag{5.5.13}$$

$$\eta w' = -\frac{Gr}{2} + \frac{G}{2}(\rho_2 - \rho_1) + \frac{B}{r}, \quad \rho_2 \le r \le R_2. \tag{5.5.14}$$

Using the conditions that $w(R_1) = w(R_2) = 0$, one can integrate both and obtain:

$$\eta w(r) = -\frac{G}{4}(r^2 - R_1^2) - \frac{G}{2}(\rho_2 - \rho_1)(r - R_1) + \frac{G\rho_1\rho_2}{2} \ln\left(\frac{r}{R_1}\right), \quad R_1 \le r \le \rho_1, \tag{5.5.15}$$

$$\eta w(r) = \frac{G}{4}(R_2^2 - r^2) - \frac{G}{2}(\rho_2 - \rho_1)(R_2 - r) + \frac{G\rho_1\rho_2}{2} \ln\left(\frac{r}{R_2}\right), \quad \rho_2 \le r \le R_2. \tag{5.5.16}$$

Using the fact that the plug moves with a constant speed, one has $w(\rho_1) = w(\rho_2)$. This results in the second relationship between the radii ρ_1 and ρ_2, viz.,

$$\rho_1\rho_2 \ln\left(\frac{\rho_1}{R_1}\right) - \frac{1}{2}(\rho_1^2 - R_1^2) - (\rho_2 - \rho_1)(\rho_1 - R_1) = \rho_1\rho_2 \ln\left(\frac{\rho_2}{R_2}\right) + \frac{1}{2}(R_2^2 - \rho_2^2) - (\rho_2 - \rho_1)(R_2 - \rho_2). \tag{5.5.17}$$

Let $R_1 = \alpha R_2$, $\rho_1 = \beta_1 R_2$, $\rho_2 = \beta_2 R_2$. Define the Bingham number to be given by $\mathrm{Bn} = \tau_y / G R_2$. From Eq. (5.5.10), we see that

$$\beta_1 = \beta_2 - \mathrm{Bn}. \tag{5.5.18}$$

Dividing Eq. (5.5.17) through by R_2^2, one obtains:

$$\beta_1\beta_2 \ln\left(\frac{\beta_1}{\alpha}\right) - \frac{1}{2}(\beta_1^2 - \alpha^2) - (\beta_2 - \beta_1)(\beta_1 - \alpha) = \beta_1\beta_2 \ln \beta_2 + \frac{1}{2}(1 - \beta_2^2) - (\beta_2 - \beta_1)(1 - \beta_2). \tag{5.5.19}$$

Using (5.5.18), one can obtain an equation for β_2, which is

$$2\beta_2(\beta_2 - \mathrm{Bn}) \ln\left(\frac{\beta_2 - \mathrm{Bn}}{\alpha\beta_2}\right) + 2\mathrm{Bn}(1 - \beta_2) = 1 - (\mathrm{Bn} + \alpha)^2. \tag{5.5.20}$$

This equation has to be solved for β_2. Assuming that this has been done and β_1 found from (5.5.18), the flow rate can be obtained through integration by parts and using $w(R_1) = w(R_2) = 0$. One is led to the following:

$$Q = \int_{R_1}^{R_2} 2\pi r w(r)\, dr \tag{5.5.21}$$

$$= -\int_{R_1}^{\rho_1} \pi r^2 w'(r)\, dr - \int_{\rho_2}^{R_2} \pi r^2 w'(r)\, dr. \tag{5.5.22}$$

After much effort, one obtains:

$$Q = \frac{\pi G R_2^4}{8\eta}\Bigg[(1-\alpha)^4 - 2\beta_2(\beta_2 - \mathrm{Bn})(1-\alpha^2) - \frac{4}{3}(1+\alpha^3)\mathrm{Bn} + \frac{1}{3}\mathrm{Bn}(2\beta_2 - \mathrm{Bn})^3\Bigg]. \tag{5.5.23}$$

A complicated set of solutions exist when the inner wall at $r = R_1$ moves along its axis with a steady speed U_0. This motion may be in the direction of the pressure drop G or in the opposite direction. Given G and U_0, it has been found by Liu and Zhu [2] that eight different solutions exist depending on whether a plug flow region exists adjacent to the inner or the outer wall, or in between as discussed here, or whether the fluid is completely sheared in the annulus.

5.6 Couette Flow

The Couette flow is an azimuthal flow which occurs between two concentric circular cylindrical surfaces of infinite length. That is, the domain of the flow is given by

$$\Omega = \{(r,\theta,z) : R_1 \le r \le R_2,\ 0 \le \theta \le 2\pi,\ -\infty < z < \infty\}. \tag{5.6.1}$$

The velocity field is described through

$$\dot{r} = 0, \quad \dot{\theta} = \omega(r), \quad \dot{z} = 0. \tag{5.6.2}$$

There are a number of possibilities for the angular velocity ω; one of the two surfaces at $r = R_1$ and $r = R_2$ may be stationary, or both may rotate in the same direction or in opposite directions. The principle behind all of these flows is the same, viz., for a given set of boundary conditions, to determine the angular velocity distribution in the interior; in particular, to find the location of the rigid core, if any.

Regardless of the different boundary conditions, one can make some predictions about the flow field in (5.6.2). First of all, omitting the body force, the equations of motion are:

$$-\frac{\partial p}{\partial r} = -\rho\omega^2 r, \tag{5.6.3}$$

$$-\frac{1}{r}\frac{\partial p}{\partial \theta} + \frac{\partial S_{r\theta}}{\partial r} + \frac{2}{r}S_{r\theta} = 0, \tag{5.6.4}$$

$$-\frac{\partial p}{\partial z} = 0, \tag{5.6.5}$$

Note that these equations have been derived from (A3.6)–(A3.8), with $v = r\omega$; various stress components are zero because of the form of the tensor $\mathbf{A}$ in (2.5.12).

Since there are no pressure gradients in the azimuthal or the axial direction, the only equation of interest is (5.6.4) from which the velocity field $\omega = \omega(r)$ has to be found. Once this is known, one can find $p = p(r)$ from (5.6.3). Since (5.6.4) turns into the ordinary differential equation

$$\frac{dS_{r\theta}}{dr} + \frac{2}{r} S_{r\theta} = 0, \tag{5.6.6}$$

its solution is given by

$$S_{r\theta} = \frac{C}{r^2}, \tag{5.6.7}$$

where $C \neq 0$ is a constant, which is positive or negative.

Now, suppose that the magnitude of the applied moment per unit height on a cylindrical surface of radius r be $M > 0$. Thus,

$$M = |S_{r\theta}(r)| \cdot 2\pi r \cdot r, \tag{5.6.8}$$

which means that

$$|C| = \frac{M}{2\pi}. \tag{5.6.9}$$

This relation permits one to define the radial position R_0 of the yield surface through

$$R_0 = \left(\frac{M}{2\pi \tau_y} \right)^{1/2}. \tag{5.6.10}$$

Hence, one finds that

1. If $R_0 \leq R_1$, the fluid has to remain rigid. That is, no flow can occur.
2. If $R_1 < R_0 < R_2$, there will be a flow with part of the fluid moving as a rigid body.
3. If $R_2 \leq R_0$, the fluid flows like a viscous liquid.

We shall now consider two separate cases depending on the sign of the constant C.

$\underline{C > 0}$.

If $C > 0$, the shear stress is bounded as follows:

$$\frac{M}{2\pi R_2^2} \leq S_{r\theta} \leq \frac{M}{2\pi R_1^2}. \tag{5.6.11}$$

The constitutive equation for the shear stress leads to the result that

$$S_{r\theta} = \eta r \omega' + \tau_y = \frac{M}{2\pi r^2}, \tag{5.6.12}$$

or

$$\eta r\omega' = \frac{M}{2\pi r^2} - \tau_y. \tag{5.6.13}$$

Obviously, the yield surface is located at the radius R_0 given by

$$\frac{M}{2\pi} = \tau_y R_0^2. \tag{5.6.14}$$

Thus,

$$\omega' = \frac{T}{2\eta\pi r}\left[\frac{1}{r^2} - \frac{1}{R_0^2}\right], \quad R_1 < r < R_0, \tag{5.6.15}$$

which proves that $\omega' > 0$ in $R_1 < r < R_0$, reaching zero at $r = R_0$. That is, the yielded zone exists next to the inner cylinder and extends into the fluid. Between $R_0 \le r \le R_2$, the fluid is in a state of rigid motion.

Now, when is $C > 0$, or when is $S_{r\theta} > 0$ in $R_1 \le r \le R_2$? A simple answer is when the inner cylinder is stationary and the outer one rotates, i.e.,

$$\omega(R_1) = 0, \quad \omega(R_2) = \Omega_2 > 0. \tag{5.6.16}$$

Note that in this situation, the outer cylinder exerts a counter-clockwise shear stress on the fluid in the direction of rotation, while the inner cylinder exerts a shear stress in the clockwise direction. Using Cauchy's stress principle, one sees that the unit external normal on the outer cylindrical surface is radially outwards and thus, the shear stress in the fluid is positive at that surface. Similarly, it is positive on the inner cylindrical surface as well.

The angular velocity field is now given by

$$\omega(r) = A - \frac{M}{4\eta\pi}\left[\frac{1}{r^2} + \frac{2}{R_0^2}\ln r\right], \quad R_1 \le r \le R_0. \tag{5.6.17}$$

The constant of integration A can be found from $\omega(R_1) = 0$. Thus,

$$\omega(r) = \frac{M}{4\eta\pi}\left[\frac{1}{R_1^2} - \frac{1}{r^2} + \frac{2}{R_0^2}\ln\left(\frac{R_1}{r}\right)\right], \quad R_1 \le r \le R_0. \tag{5.6.18}$$

Since the fluid moves as a rigid body in $R_0 \le r \le R_2$, one finds that $\omega(R_0) = \Omega_2$. Hence,

$$\Omega_2 = \frac{M}{4\eta\pi}\left[\frac{1}{R_1^2} - \frac{1}{R_0^2} + \frac{2}{R_0^2}\ln\left(\frac{R_1}{R_0}\right)\right]. \tag{5.6.19}$$

$\underline{C < 0}$.

Obviously, when $C < 0$, the shear stress $S_{r\theta} < 0$ in $R_1 \le r \le R_2$. Here, the inner cylinder rotates and the outer one is at rest, i.e.,

$$\omega(R_1) = \Omega_1 > 0, \quad \omega(R_2) = 0. \tag{5.6.20}$$

In this situation, the constitutive equation for the shear stress leads to the result that

$$S_{r\theta} = \eta r\omega' - \tau_y = -\frac{M}{2\pi r^2}, \tag{5.6.21}$$

or

$$\eta r\omega' = \tau_y - \frac{M}{2\pi r^2}. \tag{5.6.22}$$

Obviously, the yield surface is located at the radius R_0 given by

$$\frac{M}{2\pi} = \tau_y R_0^2, \tag{5.6.23}$$

Thus,

$$\omega' = \frac{M}{2\eta\pi r}\left[\frac{1}{R_0^2} - \frac{1}{r^2}\right], \quad R_1 < r < R_0, \tag{5.6.24}$$

which proves that $\omega' < 0$ in $R_1 < r < R_0$, reaching zero at $r = R_0$. That is, once again, the yielded zone exists next to the inner cylinder and extends into the fluid. Between $R_0 \le r \le R_2$, the fluid is in a state of rigid motion. The above equation can be integrated as before; the details are omitted.

The interesting feature of the above two flows is that the rigid core lies next to the outer cylindrical surface. That is, the core has the same angular velocity as that of the outer cylinder.

When the cylinders rotate in the same or opposite directions, the resulting flow can also be studied in the manner indicated here. Finally, in order to complete the solution of the Couette flow problem, it is essential to find the pressure field $p = p(r)$ by integration of (5.6.3). That is,

$$p(r) = D + \int \rho\omega^2(r) r\, dr, \tag{5.6.25}$$

where D is a constant.

5.7 Helical Flow

In the helical flow or spiral flow, the velocity field is a superposition of Couette flow on the flow in a concentric annulus. Thus,

$$\dot{r} = 0, \quad \dot{\theta} = \omega(r), \quad \dot{z} = w(r), \quad R_1 \le r \le R_2, \quad 0 \le \theta \le 2\pi, \quad -\infty < z < \infty, \tag{5.7.1}$$

where $w(R_1) = w(R_2) = 0$, and $\omega(R_1) = \Omega_1$, $\omega(R_2) = \Omega_2$. The boundary conditions on $w(r)$ can be changed to include axial sliding of one or both cylinders;

see Peng and Zhu [3] for the case when $w(R_1) = U,\ w(R_2) = 0$, and there is no pressure gradient along the axis of the pipe.

In the helical flow, there are two non-zero shear stresses, viz., $S_{r\theta}$ and S_{rz}, and the equations of motion can be obtained from a combination of (5.5.2) and (5.6.3)–(5.6.5). Thus,

$$-\frac{\partial p}{\partial r} = -\rho\omega^2 r, \tag{5.7.2}$$

$$-\frac{1}{r}\frac{\partial p}{\partial \theta} + \frac{\partial S_{r\theta}}{\partial r} + \frac{2}{r}S_{r\theta} = 0, \tag{5.7.3}$$

$$-\frac{\partial p}{\partial z} + \frac{\partial S_{rz}}{\partial r} + \frac{S_{rz}}{r} = 0. \tag{5.7.4}$$

Let the pressure drop per unit length G exceed the critical value $G_c = 2\tau_y/(R_2 - R_1)$ derived above in (5.5.7). The shear stress S_{rz} in once again given by (5.5.3), i.e.,

$$S_{rz} = -\frac{Gr}{2} + \frac{B}{r}. \tag{5.7.5}$$

The second shear stress $S_{r\theta}$ is the same as that in (5.6.7), i.e.,

$$S_{r\theta} = \frac{C}{r^2}, \quad |C| = \frac{M}{2\pi}, \tag{5.7.6}$$

where $M > 0$ is magnitude of the applied moment per unit height on a cylindrical surface of radius r.

Note that the shear stress S_{rz} decreases from a positive maximum at $r = R_1$ to a negative minimum at $r = R_2$ as before, thereby attaining the value of zero somewhere in (R_1, R_2), say at $r = \rho_0$. Around this radius, there will be a domain in which this shear stress lies between $-\tau_y$ and τ_y. However, this is not the width of the rigid core due to the existence of the second shear stress $S_{r\theta}$ which is either positive or negative across the annular gap. Now, the stress invariant $T(\mathbf{S})$ is given by

$$T(\mathbf{S}) = [S_{r\theta}^2 + S_{rz}^2]^{1/2}. \tag{5.7.7}$$

Hence, the width of the core has to be found by solving the algebraic equation $T^2(\mathbf{S}) = \tau_y^2$, or the following:

$$G^2\pi^2 r^6 - 4\pi^2(GB + \tau_y^2)r^4 + 4B^2\pi^2 r^2 + M^2 = 0. \tag{5.7.8}$$

It is sufficient to look for the solutions of the cubic equation:

$$G^2\pi^2\xi^3 - 4\pi^2(GB + \tau_y^2)\xi^2 + 4B^2\pi^2\xi + M^2 = 0. \tag{5.7.9}$$

It is easy to see that the three roots ξ_1, ξ_2, ξ_3 are such that

$$\xi_1 + \xi_2 + \xi_3 = 4\pi^2(GB + \tau_y^2), \quad \xi_1\xi_2\xi_3 = -M^2. \tag{5.7.10}$$

Hence, the three roots are all real, with one negative root; or, there are two complex conjugate roots with positive real parts, and the third is real and negative. In general, a cubic equation will possess all real, distinct roots if its discriminant (cf. (1.8.6)) $\triangle > 0$; if $\triangle = 0$, it has three real roots, of which two coincide. In the case of helical flow, one is interested in the situation when $\xi_1 > 0, \xi_2 > 0$ only, for these lead to $\rho_1 = (\xi_1)^{1/2} > 0$, $\rho_2 = (\xi_2)^{1/2} > 0$. If the roots exist such that $\rho_1 < \rho_2$, one can see that when $\rho_1 > R_2$, the Bingham fluid will flow like a viscous fluid; there is no flow if $\rho_2 < R_1$. If $\rho_1 < R_1 < \rho_2 < R_2$, partial rigid body motion and partial shearing will occur. We shall analyse the simplest situation next.

Suppose that for a given G and M, there exist two meaningful roots ρ_1 and ρ_2, such that $R_1 < \rho_1 < \rho_2 < R_2$. While these roots depend on the constant B as in the case of the flow in an annulus (cf. (5.5.9)), a simple relationship is hard to find. In fact, the determination of the constant B in a shear rate dependent viscous or viscoelastic non-Newtonian fluid, without a yield stress, is also a difficult problem. Using the viscometric fluidity function,[1] an iterative procedure has been proposed in [4], with a summary appearing in [5]. Thus, it is not surprising that a complete analysis of the helical flow in a viscoplastic fluid is yet to be found. As far as the physics of the problem is concerned, the axial pressure gradient on its own forces the Bingham fluid to yield next to both cylinders, while the Couette flow causes the fluid to rotate rigidly next to the outer cylinder. It is this conflicting interplay which has to be addressed in solving the problem.

Assuming that the fluid has yielded in $R_1 < r < \rho_1$ and in $\rho_2 < r < R_2$, the azimuthal and axial velocity fields have to be found by solving the following coupled, nonlinear equations in these domains, when $C = M/2\pi > 0$:

$$S_{r\theta} = \frac{M}{2\pi r^2} = \left(\eta + \frac{\tau_y}{\dot{\gamma}}\right) r\omega', \tag{5.7.11}$$

$$S_{rz} = -\frac{Gr}{2} + \frac{B}{r} = \left(\eta + \frac{\tau_y}{\dot{\gamma}}\right) w', \tag{5.7.12}$$

$$\dot{\gamma} = [r^2\omega'^2 + w'^2]^{1/2} > 0. \tag{5.7.13}$$

Of course, the relevant boundary conditions on $\omega(r)$ and $w(r)$, along with $\omega(\rho_1) = \omega(\rho_2)$, $w(\rho_1) = w(\rho_2)$, need to be applied to obtain the solution.

[1] The viscometric fluidity function plays a crucial role in Hele-Shaw flows as well; see Sect. 7.3.

It is possible to decouple the differential equations as follows. First of all, when the fluid has yielded, the constitutive equation for the Bingham fluid is given by

$$\mathbf{S} = \eta\mathbf{A} + \frac{\tau_y}{K(\mathbf{A})}\mathbf{A}, \quad T(\mathbf{S}) > \tau_y. \tag{5.7.14}$$

From (4.6.35), we see that $K(\mathbf{A}) = [T(\mathbf{S}) - \tau_y]/\eta$. In the helical flow, $K(\mathbf{A}) = \dot{\gamma}$. Thus, in (5.7.11) and (5.7.12),

$$\begin{aligned}\dot{\gamma} &= \frac{[S_{r\theta}^2 + S_{rz}^2]^{1/2} - \tau_y}{\eta} \\ &= \frac{\left[\left(M/2\pi r^2\right)^2 + \left(-Gr/2 + B/r\right)^2\right]^{1/2} - \tau_y}{\eta}.\end{aligned} \tag{5.7.15}$$

Thus, one obtains a nonlinear equation for $\omega = \omega(r)$ and another one for $w = w(r)$, which are decoupled and, in principle, these problems can be solved. Replacing the annulus by a plane slot reduces the complexity of the problem at hand and such solutions exist [6].

As an example of a flow problem without any approximation, consider the motion of a Bingham fluid caused by the rotation of the cylindrical surfaces and the axial movement of the inner cylinder, in the absence of a pressure gradient [3]. In such a flow, the fluid outside the yield surface will be in a state of rigid body rotation only. Thus, the boundary conditions become:

$$\omega(R_1) = \Omega_1, \quad \omega(R_2) = \Omega_2, \quad w(R_1) = U, \quad w(\rho_0) = w(R_2) = 0, \tag{5.7.16}$$

where the yield surface is located at $r = \rho_0$, $R_1 < \rho_0 < R_2$. The location of the yield surface can be found from solving the following equation (cf. (5.7.9)) for ξ:

$$4\pi^2\tau^2\xi^2 - 4B^2\pi^2\xi - M^2 = 0, \tag{5.7.17}$$

which has a positive and a negative root. The former is given by

$$\xi_1 = \frac{1}{2\tau_y^2}\left[B^2 + \left(B^4 + (M^2\tau_y^2/\pi^2)\right)^{1/2}\right] = \rho_0^2. \tag{5.7.18}$$

Provided $R_1 < \rho_0 < R_2$, it is found that the fluid lying between ρ_0 and R_2 rotates as a rigid body. The fluid is sheared in the axial direction between R_1 and ρ_0.

Of course, no solution is complete without determining the pressure field:

$$p(r, z) = D - Gz + \int \rho\omega^2(r) r\, dr, \tag{5.7.19}$$

where D is a constant.

5.8 Steady Flows of General Viscoplastic Fluids

It is not easy to find closed form solutions to Herschel-Bulkley or Casson fluids, since the relationship between the shear stress and the shear rate is nonlinear when the fluid has yielded. Apart from the few steady flows listed in the Table IV of the review article [7], two longitudinal shear flow, mixed boundary value problems have been solved by Craster [8], demonstrating the complex nature of the methods used.

5.9 Heat Transfer Problems

Heat transfer between a fluid and its surroundings is usually assumed to fall into two separate categories: in the first one, the surroundings are at fixed temperatures, and in the second one, the heat transfer flux is constant. In both of these problems, the Nusselt number plays a crucial role and we shall examine a simple example of the first kind to illustrate this point.

5.9.1 Heat Transfer Between Two Parallel Plates

Let a Bingham fluid undergo a steady flow under the following conditions. The plate at $x = 0$ is fixed and maintained at a constant temperature T_0; the plate at $x = H$ is moving with a constant speed U in the x-direction and is at a fixed temperature T_1. The velocity field is that due to simple shear and is given by $u = Uy/H,\ 0 \leq y \leq H$. If one ignores the effects of viscous heating, the temperature profile would be entirely due to conduction and given by

$$\frac{T - T_0}{T_1 - T_0} = \frac{y}{H}. \tag{5.9.1}$$

The viscous heating changes this linear profile and it is this aspect we shall examine next.

Since the flow is steady, the energy equation (3.4.10) takes on a very simple form:

$$\frac{1}{2} T_{ij} A_{ij} - q_{i,i} = 0. \tag{5.9.2}$$

Here, the shear stress distribution and the shear rate are given by

$$T_{12} = \tau_y + \eta \frac{du}{dy} = \tau_y + \eta \frac{U}{H}, \quad A_{12} = \frac{U}{H}. \tag{5.9.3}$$

The heat conduction occurs in the y-direction and this is given by $q = -k(dT/dy)$, where $k > 0$ is the conductivity coefficient and $T = T(y)$ is the unknown temperature

profile. Assuming that the physical properties of the fluid, viz., η, τ_y, k, are all constants, the energy equation becomes

$$k\frac{d^2T}{dy^2} + D_v = 0, \quad D_v = \tau_y\frac{U}{H} + \eta\left(\frac{U}{H}\right)^2, \tag{5.9.4}$$

where D_v is the viscous dissipation rate. The differential equation for the temperature $T = T(y)$ can be solved quite easily and one obtains:

$$\frac{T - T_0}{T_1 - T_0} = \frac{y}{H} + \frac{D_v H^2}{2k(T_1 - T_0)}\left[\left(\frac{y}{H}\right) - \left(\frac{y}{H}\right)^2\right]. \tag{5.9.5}$$

Note that in this flow, it would appear that the yield stress does not play a significant role; the overall effect is as if the fluid possesses a non-Newtonian viscosity. This is not strictly true, for the yield stress is important in determining whether the heat transfer is dominated by conduction or convection. This will become transparent with the introduction of the Nusselt number which follows next.

5.9.1.1 Nusselt Number

Suppose that the temperature at the wall is T_w in a flow which occurs along the z-axis normal to a cross-section in the (x, y)-plane. Under steady flow conditions, the velocity field is given by $u = u(x, y)$, and the temperature through $T = T(x, y)$. The bulk temperature T_b is defined as the ratio of the temperature flux in the direction of motion divided by the volumetric flux. That is,

$$T_b = \frac{\int_{\mathscr{A}} T(x, y)u(x, y)\, da}{\int_{\mathscr{A}} u(x, y)\, da}, \tag{5.9.6}$$

where $\mathscr{A}$ represents the domain of the cross-section. Appealing to Newton's law of heat transfer by convection, the heat flux q_w through the wall is given by

$$q_w = h(T_w - T_b), \tag{5.9.7}$$

where h is the heat transfer coefficient, named after Newton. If, on the other hand, one were to consider the fluid as being stagnant, heat transfer at the wall would be due to conduction alone. In this case, the heat flux has the form

$$q_w = k\frac{(T_w - T_b)}{L}, \tag{5.9.8}$$

where L is a characteristic length, such as the gap H between parallel plates.

The Nusselt number, Nu, for the flow under consideration is defined as the ratio of the heat transfer due to convection divided by that due to conduction. Thus,

$$\mathrm{Nu} = \frac{2hL(T_w - T_b)}{k(T_w - T_b)} = \frac{2hL}{k}. \tag{5.9.9}$$

A Nusselt number of order unity means that the flow is very sluggish and is equivalent to heat transfer by conduction. A large Nusselt number means that convection is very efficient; in the turbulent flow in a pipe, the Nusselt number is of the order of 100–1,000. These are the reasons why the Nusselt number is important in heat transfer problems.

In viscoplastic fluids, the Bingham number determines whether the flow is dominated by viscosity or the yield stress. A small Bingham number would mean that viscous effects are dominant and heat transfer occurs due to convection. A large Bingham number means that the fluid behaves more like a solid and heat conduction is likely to occur. This observation is confirmed by the numerical modelling of the thermally driven flow of a Bingham fluid in a cavity; see Fig. 10.4 and Sect. 10.3.4.

5.9.2 More General Problems

We shall mention briefly some of the results available in the literature.

Flow in Circular Tubes: The basic assumptions in solving the heat transfer problems in a circular tube are: at the entry to the tube, the velocity field is that of a fully developed flow and the temperature is uniform. The wall of the tube is maintained at a constant temperature or the heat flux at the wall is constant. In either of the two cases, asymptotic solutions are obtained for small z along the axis of the flow, which means that only the radial conduction is considered. For large z, heat conduction is assumed to occur both radially and axially, with convection in the axial direction only. For these problems one can determine the Nusselt numbers, since the Bingham fluid acts as a non-Newtonian fluid. Full details of the methods of calculation have been published by Bird et al. [9]. These calculations are applicable to the Bingham fluid for the reasons just mentioned; see Bird et al. [7].

Flow between Parallel Plates: The basic assumptions in solving the heat transfer problem between parallel walls are the same as above. At the entry to the space between the parallel plates, the velocity field is that of a fully developed flow and the temperature is uniform. The walls are maintained at identical, constant temperatures or the heat flux at both walls is the same and constant. In either of the two cases, asymptotic solutions are obtained for small z along the axis of the flow, which means that conduction across the flow is considered. For large z, heat conduction is assumed to occur both across the flow and axially, with convection in the axial direction only.

For these problems one can determine the Nusselt numbers, since the Bingham fluid acts as a non-Newtonian fluid. For a complete description, see Bird et al. [7, 9].

Temperature Dependence: If the viscosity and the yield stress depend on the temperature, there is a vast literature on their influence on heat transfer. These are listed in Tables IX and X in the review article by Bird et al. [7].

Summary: Whether one is interested in free or forced convection problems, one finds that the analytical solutions are usually approximations to the exact solutions. If one looks at the numerical methods, the published results can be improved enormously because the earlier work was not based on the finite element method.

References

1. Nouar C, Frigaard IA (2001) Nonlinear stability of Poiseuille flow of a Bingham fluid: theoretical results and comparison with phenomenological criteria. J Non-Newt Fluid Mech 100:127–149
2. Liu Y-Q, Zhu K-Q (2010) Axial Couette-Poiseuille flow of Bingham fluids through concentric annuli. J Non-Newt Fluid Mech 165:1494–1504
3. Peng J, Zhu K-Q (2004) Linear stability of Bingham fluids in spiral Couette flow. J Fluid Mech 512:21–45
4. Huilgol RR (1990) Helical flow of non-Newtonian fluids. In: Proceeding of the 5th national conference Rheol, Melbourne, Australia, pp 43–46
5. Huilgol RR, Phan-Thien N (1997) Fluid mechanics of viscoelasticity. Elsevier, Amsterdam
6. Bittleston SH, Hassager O (1992) Flow of viscoplastic fluids in a rotating concentric annulus. J Non-Newt Fluid Mech 42:19–36
7. Bird RB, Dai GC, Yarusso B (1982) The rheology and flow of viscoplastic materials. Rev Chem Eng 1:1–70
8. Craster RV (1995) Solutions for Herschel-Bulkley flows. Q J Mech Appl Math 48:343–374
9. Bird RB, Armstrong RC, Hassager O (1987) Dynamics of polymeric liquids, vol 1: fluid mechanics, 2nd edn. Wiley-Interscience, New York

Chapter 6
Analytic Solutions: Unsteady Shearing Flows

In this chapter, we shall begin by studying the initial value problem of the start-up of the flow of a Bingham fluid in a channel from rest due to a constant applied pressure gradient; see Sect. 6.1. The material presented is mostly based on the work of Safronchik with some simplifications as needed. It is also shown that this problem cannot be solved through an application of the Laplace transform. Later on, a summary of the work done by Safronchik on the initiation of a Couette flow, followed by that in a pipe of circular cross-section is provided in Sect. 6.2.

The above unsteady flow problems have an interesting feature, viz., that the yield surface propagates into the fluid with a finite speed. Due to the incompressibility of the fluid, the motion of the yield surface is lateral to itself. And, across the propagating yield surface, not all of the temporal derivatives and spatial gradients of the velocity field and the shear stress distribution are continuous. Indeed, it turns out that the velocity and the acceleration are both continuous across the yield surface, while the derivative of the acceleration, known as the *jerk*, suffers a jump. These aspects of the kinematics have a corresponding impact on the shear stress and its temporal and spatial derivatives. These matters are fully explored in Sect. 6.3 through the theory of singular surfaces in motion.

6.1 Unsteady Flow in a Channel

Consider an incompressible Bingham fluid at rest in an infinitely long channel in the x-direction. The channel is symmetric about this axis and has a width $2H$ in the y-direction. Equivalently, the domain of the fluid is the infinite strip $-\infty < x < \infty$, $-H \leq y \leq H$. Suppose that the fluid is set in motion at time $t = 0^+$ with a suddenly applied, constant pressure drop of $G > 0$ per unit length in the x-direction. Assuming the velocity field to be given by $\dot{x} = u(y, t)$, the problem is to find the subsequent velocity field given the following initial and boundary conditions:

$$u(y, 0) = 0, \quad -H \leq y \leq H; \quad u(\pm H, t) = 0, \quad t \geq 0. \tag{6.1.1}$$

R.R. Huilgol, *Fluid Mechanics of Viscoplasticity*, DOI 10.1007/978-3-662-45617-0_6

The equation of motion for the problem is

$$-\frac{\partial p}{\partial x}+\frac{\partial \sigma}{\partial y}=\rho\frac{\partial u}{\partial t}, \tag{6.1.2}$$

where $p=-Gx$ is the pressure due to the constant pressure drop per unit length G, and $\sigma=\sigma(y,t)$ is the shear stress and ρ is the density of the fluid. Assuming that $G>G_c$, where the critical pressure drop per unit length $G_c=\tau_y/H$, an unsteady flow will be initiated and will develop into a shear flow $u=u(y,t)$ across the cross-section of the channel. Since the flow is symmetric about the x-axis, it is sufficient to solve the problem in the upper half only. Thus, we have to find $u=u(y,t),\ 0\le y\le H,\ t\ge 0$, satisfying the initial condition $u(y,0)=0$, and the adherence condition $u(H,t)=0$.

The flow will commence at the edge of the channel with a rigidly flowing core away from the wall and as time progresses, the fluid will accelerate with the core shrinking laterally until the flow become steady. This final velocity profile is that which appears in Sect. 1.4., viz.,

$$u(y)=\begin{cases} G[(H^2-y^2)-2h(H-y)]/2\eta, & h\le y\le H,\\ G(H-h)^2/2\eta, & 0\le y\le h. \end{cases} \tag{6.1.3}$$

Returning to the unsteady flow conditions, the shear stress distribution is linear in the rigid core. That is

$$\sigma=-\frac{\tau_y}{h(t)}y,\quad 0\le y\le h(t), \tag{6.1.4}$$

where $h(t)$ is the width of the core; it is assumed that $0\le h(t)<H$. And, in this core, the velocity $u=u(t)$ only, whence the equation of motion reduces to

$$\frac{du}{dt}=\frac{1}{\rho}\left[G-\frac{\tau_y}{h(t)}\right], \tag{6.1.5}$$

which can be integrated with respect to T and one obtains:

$$u(t)=\frac{1}{\rho}\left[Gt-\int_0^t\frac{\tau_y}{h(\xi)}\,d\xi\right]. \tag{6.1.6}$$

Of course, $u(y,t)=u(t),\ 0\le y\le h(t)$.

In the sheared region, the shear stress is given by

$$\sigma=\eta\frac{\partial u}{\partial y}-\tau_y,\quad h(t)\le y\le H,\ t\ge 0. \tag{6.1.7}$$

Consequently, the equation of motion is given by the following:

$$\eta \frac{\partial^2 u}{\partial y^2} = \rho \frac{\partial u}{\partial t} - G. \tag{6.1.8}$$

Noting that the flow commences from rest, the adherence condition at the wall of the channel and the fact that the velocity gradient is zero at the edge of the core, this partial differential equation has to be integrated with the following conditions:

$$u(y,0) = 0, \quad 0 \le y \le H; \quad u(H,t) = 0, \quad t \ge 0; \quad \frac{\partial u}{\partial y}(h(t),t) = 0, \quad t > 0. \tag{6.1.9}$$

The relevant equations can now be put in a non-dimensional form using the change of variables similar to those adopted in Sect. 1.7. That is:

$$\tilde{x} = \frac{x}{H}, \quad \tilde{y} = \frac{y}{H}, \quad \tilde{t} = \frac{\eta}{\rho H^2} t, \quad \delta(\tilde{t}) = \frac{h(t)}{H}, \tag{6.1.10}$$

$$\tilde{u} = \frac{u}{U}, \quad \tilde{\sigma} = \frac{H}{\eta U}\sigma, \quad \tilde{G} = \frac{H^2}{\eta U} G. \tag{6.1.11}$$

The partial differential equation (6.1.8) becomes:

$$\frac{\partial^2 \tilde{u}}{\partial \tilde{y}^2} = \frac{\partial \tilde{u}}{\partial \tilde{t}} - \tilde{G}. \tag{6.1.12}$$

After dropping the tildes, we obtain:

$$\frac{\partial^2 u}{\partial y^2} = \frac{\partial u}{\partial t} - G, \quad \delta(t) < y < 1, \ t > 0. \tag{6.1.13}$$

The following conditions apply:

$$u(y,0) = 0, \quad 0 \le y \le 1; \quad u(1,t) = 0, \quad t \ge 0; \quad \frac{\partial u}{\partial y}(\delta(t),t) = 0, \quad t > 0. \tag{6.1.14}$$

Regarding the velocity in the core, consider (6.1.6). Using (6.1.10, 6.1.11), we find that

$$\frac{Gt}{\rho} = \frac{1}{\rho} \cdot \frac{\eta U}{H^2} \tilde{G} \cdot \frac{\rho H^2}{\eta} \tilde{t} = U \tilde{G} \tilde{t}. \tag{6.1.15}$$

Next, in analogy with $t = (\rho H^2/\eta)\tilde{t}$, we let $\xi = (\rho H^2/\eta)\tilde{\xi}$. Then,

$$\frac{1}{\rho} \int_0^t \frac{\tau_y}{h(\xi)}\, d\xi = \frac{1}{\rho} \int_0^{\tilde{t}} \frac{\tau_y}{H\delta(\tilde{\xi})} \frac{\rho H^2}{\eta}\, d\tilde{\xi} = \int_0^{\tilde{t}} \frac{\tau_y H}{\eta \delta(\tilde{\xi})}\, d\tilde{\xi}. \tag{6.1.16}$$

Let the Bingham number be $\mathrm{Bn} = \tau_y H/\eta U$. Hence, the right side becomes

$$\int_0^{\tilde{t}} \frac{GH^2}{\eta\delta(\tilde{\xi})}\, d\tilde{\xi} = U\mathrm{Bn}\int_0^{\tilde{t}} \frac{1}{\delta(\tilde{\xi})}\tilde{G}\, d\tilde{\xi}. \tag{6.1.17}$$

Since $u = U\tilde{u}$, we can now drop the tildes from (6.1.15) and (6.1.17). The velocity in the core is given by (cf. (6.1.6)):

$$u(t) = Gt - \mathrm{Bn}\int_0^t \frac{1}{\delta(\xi)}\, d\xi. \tag{6.1.18}$$

The required equations have now been assembled. They are (6.1.13) and (6.1.14); their solution provides the velocity in the core (6.1.18), valid in $0 \le y \le \delta(t)$.

In order to solve the problem at hand, it is desirable to define a new function $\lambda(y, t)$ so that

$$u(y, t) = Gt + \lambda(y, t). \tag{6.1.19}$$

Noting the initial condition $u(y, 0) = 0$, the new function satisfies the following equations:

$$\frac{\partial^2\lambda}{\partial y^2} = \frac{\partial\lambda}{\partial t}, \quad \delta(t) < y < 1, \quad 0 < t \le t_0, \tag{6.1.20}$$

$$\lim_{t\to 0^+} \lambda(y, t) = 0, \tag{6.1.21}$$

$$\lim_{y\to 1^-} \lambda(y, t) = -Gt, \tag{6.1.22}$$

$$\lim_{y\to\delta(t)^+} \lambda(y, t) = -\mathrm{Bn}\int_0^t \frac{1}{\delta(\xi)}\, d\xi = \phi(t), \tag{6.1.23}$$

$$\lim_{y\to\delta(t)^+} \frac{\partial\lambda}{\partial y} = 0, \tag{6.1.24}$$

where the function $\phi(t)$ has been introduced in (6.1.23) for convenience. Obviously, one has to find $\lambda(y, t)$ as well as the location of the yield surface at $y = \delta(t)$ as parts of the solution, with $\delta(0) = 1$. Note that the boundary condition (6.1.22) means that the method of solution cannot be valid for all $t \in (0, \infty)$, or it is valid for a finite interval of time only.

6.1.1 The Solution

The solution to the problem of finding the function $\lambda(y, t)$ is due to Safronchik [1], who based it on the method of Kolodner [2]; the latter had shown that in linear

partial differential equations with free surfaces, it was possible to derive a functional equation to determine the location of the free surface without knowing the solution of the partial differential equation. Subsequently, this solution could be derived. It is this method that was applied by Safronchik to find a nonlinear integral equation satisfied by the position of the yield surface. From this, the velocity in the core and in the yielded region would follow. In fact, Safronchik considered a much more general problem than the one being discussed here; for instance, the Bingham fluid could begin the flow with a non-zero velocity profile, and the pressure gradient could be time dependent as well. Having obtained the solution for this extremely general case, Safronchik simplified his results to apply to the initial-boundary value problem listed in (6.1.20)–(6.1.24) above. It is this aspect of his solution that will be summarised here.

First of all, the domain of the sheared flow is given by

$$\mathscr{D}_+ = \{\delta(t) < y < 1,\ 0 < t < t_0\}. \tag{6.1.25}$$

Since the position of the free surface at $y = \delta(t)$ is unknown, the domain of the flow will be extended into its complement, viz.,

$$\mathscr{D}_- = \{-\infty < y < \delta(t),\ 0 < t < t_0\}. \tag{6.1.26}$$

Thus, the problem will now be solved in the semi-infinite strip

$$\mathscr{D} = \{-\infty < y < 1,\ 0 < t < t_0\}. \tag{6.1.27}$$

The important point to note is that the domain $\mathscr{D}$ is unaffected by the exact location of the yield surface at $y = \delta(t)$.

The relevant equations are:

$$\frac{\partial^2 \lambda}{\partial y^2} = \frac{\partial \lambda}{\partial t}, \quad -\infty < y < 1, \quad 0 < t < t_0, \tag{6.1.28}$$

$$\lim_{t \to 0^+} \lambda(y,t) = 0, \quad -\infty < y \le 1, \tag{6.1.29}$$

$$\lim_{y \to 1^-} \lambda(y,t) = -Gt, \quad 0 \le t \le t_0, \tag{6.1.30}$$

$$\lim_{y \to -\infty} \lambda(y,t) = 0, \quad 0 \le t \le t_0. \tag{6.1.31}$$

We can decompose the solution into two parts:

$$\lambda_+(y,t) = \lambda(y,t), \quad (y,t) \in \mathscr{D}_+, \tag{6.1.32}$$

$$\lambda_-(y,t) = \lambda(y,t), \quad (y,t) \in \mathscr{D}_-, \tag{6.1.33}$$

with $y = \delta(t)$ forming the boundary between $\mathscr{D}_+$ and $\mathscr{D}_-$.

The problem posed in (6.1.28)–(6.1.31) has a solution given by

$$\lambda(y,t) = I_1(y,t) + I_2(y,t) + I_3(y,t), \tag{6.1.34}$$

where the three functions are integrals depending on heat kernels as follows:

$$I_1 = -\frac{1}{2\sqrt{\pi}} \int_0^t \frac{G\sigma(1-y)}{(t-\sigma)^{3/2}} \exp\left[-\frac{(1-y)^2}{4(t-\sigma)} \right] d\sigma, \tag{6.1.35}$$

$$I_2 = \frac{1}{\sqrt{\pi}} \int_0^t \left\{ \phi(\sigma) \left[\frac{y-\delta(\sigma)}{4(t-\sigma)^{3/2}} - \frac{\delta'(\sigma)}{2(t-\sigma)^{1/2}} \right] \times \exp\left[-\frac{[y-\delta(\sigma)]^2}{4(t-\sigma)} \right] \right\} d\sigma, \tag{6.1.36}$$

$$I_3 = -\frac{1}{\sqrt{\pi}} \int_0^t \left\{ \phi(\sigma) \left[\frac{2-y-\delta(\sigma)}{4(t-\sigma)^{3/2}} - \frac{\delta'(\sigma)}{2(t-\sigma)^{1/2}} \right] \times \exp\left[-\frac{[2-y-\delta(\sigma)]^2}{4(t-\sigma)} \right] \right\} d\sigma, \tag{6.1.37}$$

for $t > \sigma$, and $\lambda(y,t) \equiv 0$ for $\sigma \le t$.

In his solution, Safronchik[1] proved the following results:

1. The integral I_1 has the following limiting behaviour:

$$I_1(1,t) = 0, \quad 0 \le t \le t_0 \tag{6.1.38}$$

$$\lim_{t \to 0^+} I_1(y,t) = 0, \quad -\infty < y \le 1, \tag{6.1.39}$$

$$\lim_{y \to 1^-} I_1(y,t) = -ct, \quad 0 \le t \le t_0. \tag{6.1.40}$$

$$\lim_{y \to -\infty} I_1(y,t) = 0, \quad 0 \le t \le t_0. \tag{6.1.41}$$

2. The derivative $\partial I_1/\partial y$ is bounded in the closure of $\mathscr{D}$, or in the region $\{-\infty < y \le 1,\ 0 \le t \le t_0\}$. In fact, it is continuous in this region.
3. The integral I_2 has the following limiting behaviour:

$$I_2(1,t) = 0, \quad 0 \le t \le t_0 \tag{6.1.42}$$

$$\lim_{t \to 0^+} I_2(y,t) = 0, \quad -\infty < y \le 1, \tag{6.1.43}$$

$$\lim_{y \to 1^-} I_2(y,t) = 0, \quad 0 \le t \le t_0, \tag{6.1.44}$$

$$\lim_{y \to -\infty} I_2(y,t) = 0, \quad 0 \le t \le t_0. \tag{6.1.45}$$

[1] In comparing the integrals listed here with those in [1] it must be noted that the integrals $I_1,\ I_2,\ I_3$ correspond to $J_1,\ J_2,\ J_4$ respectively, with modifications due to the fact the initial condition is assumed to be zero here. For this reason, the integral J_3 is not needed, for it is zero.

4. While the integral I_2 is bounded in $\{-\infty < y \leq 1,\ 0 \leq t \leq t_0\}$, it has a discontinuity across the curve $y = \delta(t)$. That is,

$$\lim_{y\to\delta(t)^+} I_2(y,t) = I_2(\delta(t),t) + \frac{1}{2}\phi(t), \tag{6.1.46}$$

$$\lim_{y\to\delta(t)^-} I_2(y,t) = I_2(\delta(t),t) - \frac{1}{2}\phi(t). \tag{6.1.47}$$

Hence,

$$\lim_{y\to\delta(t)^+} I_2(y,t) - \lim_{y\to\delta(t)^-} I_2(y,t) = \phi(t). \tag{6.1.48}$$

5. However,

$$\lim_{y\to\delta(t)^+} \frac{\partial I_2}{\partial y}(y,t) = \lim_{y\to\delta(t)^-} \frac{\partial I_2}{\partial y}(y,t). \tag{6.1.49}$$

6. Finally, the integral I_3 has the following limiting behaviour:

$$I_3(1,t) = 0, \quad 0 \leq t \leq t_0 \tag{6.1.50}$$

$$\lim_{t\to 0^+} I_3(y,t) = 0, \quad -\infty < y \leq 1, \tag{6.1.51}$$

$$\lim_{y\to 1^-} I_3(y,t) = 0, \quad 0 \leq t \leq t_0. \tag{6.1.52}$$

$$\lim_{y\to -\infty} I_3(y,t) = 0, \quad 0 \leq t \leq t_0. \tag{6.1.53}$$

7. The derivative $\partial I_3/\partial y$ is bounded in $\{-\infty < y \leq 1,\ 0 \leq t \leq t_0\}$. In fact, it is continuous in this region.

If we examine the above conditions in detail, it will be found that $\lambda(y,t) = I_1(y,t) + I_2(y,t) + I_3(y,t)$ satisfies all of the Eqs. (6.1.28)–(6.1.31). Now, one has yet to determine where the yield surface $y = \delta(t)$ is located.

To answer this, we note that the condition (6.1.47) can be used to demand that the solution $\lambda_-(y,t) \to 0$ as $y \to \delta(t)^-$. In fact, one can prove from this that $\lambda_-(y,t) \equiv 0$ in $\mathscr{D}_-$, for this function satisfies the heat equation, has a zero initial condition, and vanishes as $y \to -\infty$. Hence, it follows that

$$\lim_{y\to\delta(t)^-} \frac{\partial \lambda_-(y,t)}{\partial y} = 0. \tag{6.1.54}$$

Conversely, if the function $\lambda_-(y,t)$ satisfies the heat equation, has zero initial condition, vanishes at infinity and zero flux enters it at the other boundary (cf. (6.1.54)), then $\lambda_-(y,t) \equiv 0$ in $\mathscr{D}_-$. So, there are two ways to determine the location of the yield surface.

Since $\lambda_-(y,t) = \lambda(y,t)$ in $\mathscr{D}_-$, the first method is to solve the following equation:

$$\lim_{y\to\delta(t)^-} \lambda(y,t) = \lim_{y\to\delta(t)^-} \Big[I_1(y,t) + I_2(y,t) + I_3(y,t) \Big] = 0. \tag{6.1.55}$$

Noting that the partial derivatives of the three integrals with respect to y do not suffer a jump at the yield surface, the second approach is to solve:

$$\lim_{y\to\delta(t)} \frac{\partial\lambda(y,t)}{\partial y} = 0. \tag{6.1.56}$$

The latter equation will now be considered. To simplify it, one proceeds as follows:

1. In (6.1.35), let

$$\beta = \frac{1-y}{2\sqrt{t-\sigma}}, \quad y < 1,\ t \geq 0. \tag{6.1.57}$$

Thus,

$$\frac{d\beta}{d\sigma} = \frac{1-y}{4(t-\sigma)^{3/2}}. \tag{6.1.58}$$

Hence,

$$\frac{d}{d\sigma}\int_{\infty}^{\beta} e^{-\alpha^2}\,d\alpha = \frac{(1-y)}{4(t-\sigma)^{3/2}}\exp\left[-\frac{(1-y)^2}{4(t-\sigma)}\right]. \tag{6.1.59}$$

Consequently, using integration by parts,

$$I_1 = \frac{2G}{\sqrt{\pi}}\int_0^t \left(\int_{\infty}^{\beta} e^{-\alpha^2}\,d\alpha\right) d\sigma. \tag{6.1.60}$$

Thus,

$$\frac{\partial I_1}{\partial y} = -\frac{G}{\sqrt{\pi}}\int_0^t \frac{1}{\sqrt{t-\sigma}}\exp\left[-\frac{(1-y)^2}{4(t-\sigma)}\right] d\sigma. \tag{6.1.61}$$

2. In a similar fashion, one can rearrange I_2 and obtain

$$I_2 = -\frac{1}{\sqrt{\pi}}\int_0^t \phi'(\sigma)\left(\int_{z_1(y,t)}^{z_1(y,\sigma)} e^{-\beta^2} d\beta\right) d\sigma, \tag{6.1.62}$$

where

$$z_1(y,\sigma) = \frac{y-\delta(\sigma)}{2\sqrt{t-\sigma}}, \tag{6.1.63}$$

and

$$z_1(y,t) = \begin{cases} \infty, & y > \delta(t), \\ 0, & y = \delta(t), \\ -\infty, & y < \delta(t). \end{cases} \tag{6.1.64}$$

Thus,

$$\frac{\partial I_2}{\partial y} = -\frac{1}{2\sqrt{\pi}} \int_0^t \frac{\phi'(\sigma)}{\sqrt{t-\sigma}} \exp\left[-\frac{[y-\delta(\sigma)]^2}{4(t-\sigma)} \right] d\sigma. \tag{6.1.65}$$

3. Finally,

$$I_3 = \frac{1}{\sqrt{\pi}} \int_0^t \phi'(\sigma) \left(\int_{z_2(y,t)}^{z_2(y,\sigma)} e^{-\beta^2} d\beta \right) d\sigma, \tag{6.1.66}$$

where

$$z_2(y,\sigma) = \frac{2-y-\delta(\sigma)}{2\sqrt{t-\sigma}}, \tag{6.1.67}$$

and

$$z_2(y,t) = \begin{cases} \infty, & y > \delta(t), \\ 0, & y = \delta(t), \\ -\infty, & y < \delta(t). \end{cases} \tag{6.1.68}$$

Thus,

$$\frac{\partial I_3}{\partial y} = -\frac{1}{2\sqrt{\pi}} \int_0^t \frac{\phi'(\sigma)}{\sqrt{t-\sigma}} \exp\left[-\frac{[2-y-\delta(\sigma)]^2}{4(t-\sigma)} \right] d\sigma. \tag{6.1.69}$$

Hence, one obtains the following integral equation to determine the location of the yield surface at $y = \delta(t)$:

$$G \int_0^t \frac{1}{\sqrt{t-\sigma}} \exp\left[-\frac{[1-\delta(t)]^2}{4(t-\sigma)} \right] d\sigma \quad - \int_0^t \frac{\phi'(\sigma)}{2\sqrt{t-\sigma}}$$

$$\times \left\{ \exp\left[-\frac{[\delta(t)-\delta(\sigma)]^2}{4(t-\sigma)} \right] \quad + \exp\left[-\frac{[2-\delta(t)-\delta(\sigma)]^2}{4(t-\sigma)} \right] \right\} d\sigma = 0. \tag{6.1.70}$$

This is Kolodner's functional equation to determine the location of the yield surface at $y = \delta(t)$. As noted earlier, this equation does not require the velocity field in $0 \le y \le 1$ to solve for $\delta(t)$. Even so, this nonlinear integral equation has never been

solved. So, we shall obtain an approximate solution when t is very small, or when the yield surface $\delta(t)$ is close to 1.

6.1.2 Approximate Solution

From (6.1.23), it follows that $\phi'(\sigma) = \mathrm{Bn}/\delta(\sigma)$. Thus, (6.1.70) becomes:

$$G \int_0^t \frac{1}{\sqrt{t-\sigma}} \exp\left[-\frac{[1-\delta(t)]^2}{4(t-\sigma)}\right] d\sigma = \frac{\mathrm{Bn}}{2} \int_0^t \frac{1}{\delta(\sigma)\sqrt{t-\sigma}} \times \left\{\exp\left[-\frac{[\delta(t)-\delta(\sigma)]^2}{4(t-\sigma)}\right] + \exp\left[-\frac{[2-\delta(t)-\delta(\sigma)]^2}{4(t-\sigma)}\right]\right\} d\sigma. \quad (6.1.71)$$

For small values of t, assume that $\delta(\sigma) = \delta(0) = 1$ on the right side, whence the exponential terms can be replaced by the integer 2. Thus, the right side becomes

$$\mathrm{Bn} \int_0^t \frac{1}{\sqrt{t-\sigma}}\, d\sigma = 2\mathrm{Bn}\sqrt{t}. \quad (6.1.72)$$

Hence, we are left with

$$\int_0^t \frac{1}{\sqrt{t-\sigma}} \exp\left[-\frac{[1-\delta(t)]^2}{4(t-\sigma)}\right] d\sigma = \frac{2\mathrm{Bn}}{G}\sqrt{t}. \quad (6.1.73)$$

Now, let us introduce another substitution:

$$\alpha(\sigma) = \frac{1-\delta(t)}{2\sqrt{t-\sigma}}. \quad (6.1.74)$$

The left side of (6.1.73) can now be integrated by parts to obtain:

$$\int_0^t e^{-\alpha^2} \frac{1}{\sqrt{t-\sigma}}\, d\sigma = -\left[2e^{-\alpha^2}\sqrt{t-\sigma}\right]_0^t + 2\int_0^t \sqrt{t-\sigma}\left(\frac{d}{d\sigma}e^{-\alpha^2}\right) d\sigma. \quad (6.1.75)$$

Since

$$2\alpha(\sigma)\sqrt{t-\sigma} = 1-\delta(t) = 2\alpha(0)\sqrt{t}, \quad (6.1.76)$$

one can write the integral on the right side of (6.1.75) as

$$2\int_0^t \sqrt{t-\sigma}\left(\frac{d}{d\sigma}e^{-\alpha^2}\right)d\sigma = -4\alpha(0)\sqrt{t}\int_{\alpha(0)}^{\infty} e^{-\beta^2}\,d\beta. \tag{6.1.77}$$

Substituting the above into (6.1.73), cancelling $\sqrt{t}$, it follows that we have to determine $\alpha(0)$ as the solution of the transcendental equation:

$$\exp\left\{-[\alpha(0)]^2\right\} - 2\alpha(0)\int_{\alpha(0)}^{\infty} e^{-\beta^2}\,d\beta = \frac{\mathrm{Bn}}{G}. \tag{6.1.78}$$

Since $\delta(t) < 1$ for $t > 0$, it follows that this equation must have a positive solution for $\alpha(0)$. Assuming that this has been found, we obtain the position of the yield surface, valid for a very short interval of time only. This is given by

$$\delta(t) = 1 - 2\alpha(0)\sqrt{t}, \quad 0 \le t \le \frac{1}{4[\alpha(0)]^2}. \tag{6.1.79}$$

From (6.1.19) and (6.1.23), we see that the velocity of the rigid core is given by

$$\begin{aligned} u(t) &= Gt + \phi(t) = Gt - \mathrm{Bn}\int_0^t \frac{1}{\delta(\xi)}\,d\xi \\ &= Gt - \mathrm{Bn}\int_0^t \frac{1}{1-2\alpha(0)\sqrt{\xi}}\,d\xi \\ &= Gt - \mathrm{Bn}\int_0^{\sqrt{t}} \frac{2\sigma}{1-2\alpha(0)\sigma}\,d\sigma \\ &= Gt + \mathrm{Bn}\frac{1}{\alpha(0)}\sqrt{t} + \mathrm{Bn}\frac{1}{[2\alpha(0)]^2}\ln\left[1-2\alpha(0)\sqrt{t}\right]. \end{aligned} \tag{6.1.80}$$

Having found $\delta(t)$, it is possible to find the velocity field $u(y,t)$ in $\delta(t) \le y \le 1$; however, following Safronchik, this is omitted.

In sum, it is important to realise that as soon as the flow starts, a plug forms within the fluid; it occupies the region $0 \le y \le \delta(t)$. The velocity of the fluid in the plug is given by $u(t)$ above. In Sect. 6.3, the underlying kinematics and dynamics of the moving yield surface are examined using the theory of propagating singular surfaces due to Hadamard.

6.1.3 Laplace Transform

Given the partial differential equation in (6.1.13):

$$\frac{\partial^2 u}{\partial y^2} = \frac{\partial u}{\partial t} - G, \quad \delta(t) < y < 1, \ t > 0, \tag{6.1.81}$$

can one apply the Laplace transform to solve this equation? The answer is in the negative, for in order to apply this transform, every $y \in (\delta(t), 1)$ must be in the yielded part of the flow for *all* $t > 0$. This is clearly impossible, for as the yield surface moves laterally from $y(0) = 1$, points which lie in the unsheared region enter the yielded region at separate times.

To understand this, let the final width of the plug be $\delta_\infty < 1$. Consider a layer of fluid at $y = y_1$ such that $y_1 = \delta(t_1) > \delta_\infty$. This layer of fluid will lie in the sheared region for all $t > t_1$ only. Hence, the material in $y_1 < y < 1$ satisfies (6.1.81) for $t > t_1$ only; and, the initial velocity distribution across this domain is not given by $u(y, 0) = 0, \ y_1 \le y \le 1$. Rather, the latter depends on when the fluid layer enters the sheared zone; prior to that, this layer of the fluid experiences a plug flow.

6.1.4 Application of Maximum Principles

Using the maximum principles[2] for parabolic equations, Comparini [4] obtained bounds on the velocity, its spatial and temporal gradients in the initiation of the channel flow. Let $y = h$ be the location of the yield surface when the flow has reached steady state and let $u_\infty(y)$ be this velocity field given by (1.4.5, 1.4.6). Further, let there be an initial velocity distribution $u(y, 0) = u_0(y)$ such that

$$u_0(1) = 0, \quad u_0'(y) \le 0, \quad u_0''(y) \le 0, \quad 0 < h_0 \le y \le H. \tag{6.1.82}$$

Note that this requires the initial velocity distribution $u_0 = u_0(y)$ to be such that it has a yield surface at $y = h_0$. Further, it must satisfy the following conditions:

$$u_0'(y) \ge -\frac{G}{\eta}\left(y - \frac{\tau_y}{G}\right), \tag{6.1.83}$$

$$u_0''(y) \ge -\frac{G}{\eta}. \tag{6.1.84}$$

[2] Protter and Weinberger [3] have written a highly readable introduction to maximum principles.

Assuming that $h < h_0 < H$, Comparini proved the following results:

$$\frac{\tau_y}{G} < h(t), \tag{6.1.85}$$

$$0 \le u(y,t) \le u_\infty(y), \tag{6.1.86}$$

$$-\frac{G}{\eta}\left(y - \frac{\tau_y}{G}\right) \le u_y(y,t) \le 0, \tag{6.1.87}$$

$$0 \le u_t(y,t) \le \frac{G}{\rho}, \tag{6.1.88}$$

where $h < h(t) < h_0$. Note that $\tau_y/G < h(t)$ in (6.1.85) is simply a restatement of $h < h(t)$, meaning that the yield surface approaches the steady state value from above. The next one (6.1.86) says that the velocity $u(y,t)$ is evolving towards the steady velocity field $u_\infty(y)$ from below; and, this leads to the result that the velocity gradient is less negative than the final one (6.1.87). The last one becomes transparent when one looks at the equation of motion (6.1.2) and puts $G = -\partial p/\partial x > 0$, and notes that $\partial\sigma/\partial y \le 0$ in the upper half of the channel.

Several other results including a global existence theorem for the solution, its asymptotic behaviour and the effects of a time dependent pressure gradient have also been derived by Comparini [4].

6.2 Unsteady Couette and Poiseuille Flows

After solving the problem of the channel flow described above, Safronchik [5] considered the Couette flow problem. Let a rod of radius R, immersed in an infinite sea of Bingham fluid with an initial angular velocity distribution, be given a time dependent velocity starting at $t = 0^+$. Assuming that the angular velocity $\omega(r,t) \to 0$ as $r \to \infty$, this initial-boundary value problem was solved, after the location of the yield surface at $r = \rho$ was found through another application of Kolodner's method.

If one is interested in solving the flow in a concentric annulus of radii R_1 and $R_2 > R_1$, Safronchik pointed out that the solution for the infinite vat is also the solution to this problem as long as the location of the yield surface at $r = \rho$ is such that $\rho < R_2$ and $\omega(R_2) = 0$. Having pointed out that the method of solution fails for the case when $\rho \ge R_2$, he did not proceed further with it. In fact, as shown by Comparini and De Angelis [6], there are numerous possibilities. For instance, there may be regions where the shear rate becomes zero and changes sign. These aspects have also been explored by Comparini [7]. Simply put, it is not easy to predict what happens in an unsteady Couette flow in a concentric cylinder viscometer.

Turning next to the initial-boundary value problem of the flow in a pipe of circular cross-section, Safronchik [8] has also solved this problem. Again, the Bingham fluid has an initial velocity distribution $w(r,0) = F(r)$, and is subjected to a time dependent pressure gradient beginning at $t = 0^+$. The subsequent flow was fully determined, basing the location of the yield surface on Kolodner's method. There

is much wealth of analysis and detail in this work, making it difficult to summarise it here.

6.3 Unsteady Flow in a Half-Space

In this section, an unsteady flow of a Bingham fluid in the half-space $-\infty < x < \infty$, $0 \leq y < \infty$ is explored in depth. The flow begins as a steady, simple shearing flow with a constant shear rate $\dot{\gamma} > 0$. At time $t = 0^+$, the magnitude of the shear stress on the boundary at $y = 0$ is reduced to a value below that of the yield stress. This reduction causes a plug to form adjacent to this boundary and the size of the plug increases with time, since the flow as $y \to \infty$ is not affected by this change in the shear stress.

There are two aspects to the solution to this problem. The first one is to find the velocity field in the plug flow and the yielded region [9] and this is studied in Sect. 6.3.1. The second one is to examine the continuity and discontinuity in the velocity and the shear stress fields and their temporal and spatial gradients across the yield surface, and the interrelations between them. In particular, it will be shown that the velocity and the local acceleration are continuous, while the time derivative of the acceleration, known as *jerk*, suffers a jump across the yield surface. These results [10] are obtained by applying the theory of propagating singular surfaces, originally due to Hadamard. A full exposition of the theory and its applications is provided below in Sects. 6.3.2–6.3.4.

6.3.1 An Initial Value Problem

In this sub-section, the initial value problem solved by Sekimoto [9] will be considered. Here, one begins by considering the shearing flow $u = u(y, t)$ of a Bingham fluid in the semi-infinite region $y > 0$. In the absence of a pressure gradient, the equation of motion becomes

$$\rho \frac{\partial u}{\partial t} = \frac{\partial \sigma}{\partial y}. \tag{6.3.1}$$

The initial condition for the velocity field is that of a steady, simple shearing flow:

$$u(y, 0) = \dot{\gamma} y, \quad 0 \leq y < \infty, \tag{6.3.2}$$

where $\dot{\gamma} > 0$ is a constant shear rate. On the boundary $y = 0$, the shear stress is given by $\sigma(0, t) = \eta\dot{\gamma} + \tau_y$ for $t < 0$. At $t = 0^+$, we reduce this stress to a constant value τ_0 so that subsequently

$$\sigma(0, t) = \tau_0, \quad t > 0, \tag{6.3.3}$$

where $|\tau_0| < \tau_y$.

To complete the specification of the problem, it is assumed that the velocity field as y tends to infinity is not affected by this diminution in the shear stress so that

$$|u(y,t) - \dot{\gamma} y| \to 0, \quad y \to \infty. \tag{6.3.4}$$

Now, the reduction in the magnitude of the shear stress on the boundary will cause the fluid adjacent to the boundary to move as a plug, with the width of the plug increasing in time; and, it is the speed of propagation of the yield surface that is also of interest. Importantly, it will be seen below that this speed is finite for $t > 0$. Hence, the yield surface is supposed to be at $y = y_c(t)$ for $t \geq 0$; the fluid is expected to move as a plug in $0 \leq y < y_c(t)$ and to undergo a shearing flow in $y_c(t) < y < \infty$. Since the equation of motion Eq. (6.3.1) becomes the heat equation

$$\frac{\partial u}{\partial t} = \nu \frac{\partial^2 u}{\partial y^2}, \quad y_c(t) < y < \infty, \tag{6.3.5}$$

where $\nu = \eta/\rho$ is the kinematic viscosity, the solution is of the form:

$$y_c(t) = \theta \cdot (\nu t)^{1/2}, \tag{6.3.6}$$

$$u(y,t) = \dot{\gamma} y f\left(\frac{y}{(\nu t)^{1/2}}, \theta\right), \quad y_c \leq y < \infty, \tag{6.3.7}$$

where $\theta > 0$ is a dimensionless parameter to be determined along with the function $f(\cdot, \cdot)$. In order to do so, we shall use the fact that the velocity $u(y,t)$ is continuous at the yield surface and that $\partial u/\partial y = 0$ on this surface.

In the rigid core, the acceleration $\partial u/\partial t$ is independent of y. Hence, the equation of motion Eq. (6.3.1) leads to the result that the shear stress distribution in the core is linear, i.e.,

$$\sigma(y,t) = \frac{\tau_y - \tau_0}{y_c(t)} y + \tau_0, \quad 0 \leq y \leq y_c(t). \tag{6.3.8}$$

That is, the gradient of the shear stress $\partial\sigma/\partial y = (\tau_y - \tau_0)/y_c(t)$ in the core. Using this, integrating (6.3.1), noting that $u(0,0) = 0$ and that

$$u(y_c(t), t) = \dot{\gamma} y_c f(\theta, \theta), \tag{6.3.9}$$

we obtain

$$\rho \dot{\gamma} y_c f(\theta, \theta) = \int_0^t \frac{\tau_y - \tau_0}{y_c(\sigma)} \, d\sigma = 2 \frac{\tau_y - \tau_0}{\theta^2 \nu} y_c(t). \tag{6.3.10}$$

Define the constant

$$\zeta = \frac{\tau_y - \tau_0}{\eta \dot{\gamma}}. \tag{6.3.11}$$

Using $\eta = \rho\nu$, (6.3.10) turns into a relationship between θ and the function $f(\theta, \theta)$:

$$\theta^2 f(\theta, \theta) = \zeta. \tag{6.3.12}$$

At the yield surface $y = y_c(t)$, the velocity gradient $\partial u/\partial y = 0$ as $y \to y_c(t)^-$ since the velocity gradient is zero in the rigid zone. Since the shear stress is equal to the yield stress on the yield surface, one finds that $\partial u/\partial y = 0$ as $y \to y_c(t)^+$. Thus, from (6.3.7), we obtain:

$$f(\theta, \theta) + \theta f'(\theta, \theta) = 0, \tag{6.3.13}$$

where $f'(s, \theta) = \partial f(s, \theta)/\partial s$. Obviously, Eqs. (6.3.12, 6.3.13) provide a set of conditions which $f(s, \theta)$ must meet. And, (6.3.4) says that

$$\lim_{s\to\infty} f(s, \theta) = 1. \tag{6.3.14}$$

However, one needs a differential equation which must be satisfied by $f(s, \theta)$. Here, one uses the fact that the shear stress is given by

$$\sigma = \tau_y + \eta \frac{\partial u}{\partial y}, \quad y_c(t) < y < \infty, \tag{6.3.15}$$

which can be used in the equation of motion (6.3.1) to obtain:

$$\eta \frac{\partial^2 u}{\partial y^2} = \rho \frac{\partial u}{\partial t}, \quad y_c(t) < y < \infty. \tag{6.3.16}$$

From (6.3.7), one finds that

$$\rho \frac{\partial u}{\partial t} = -\frac{1}{2}\eta\dot{\gamma} \frac{1}{(\nu t)^{1/2}} s^2 f'(s, \theta), \tag{6.3.17}$$

$$\eta \frac{\partial u^2}{\partial y^2} = \eta\dot{\gamma} \frac{1}{(\nu t)^{1/2}} \Big[2f'(s, \theta) + sf''(s, \theta) \Big], \tag{6.3.18}$$

where $f''(s, \theta) = \partial^2 f(s, \theta)/\partial s^2$. Hence, the function $f(s, \theta)$ satisfies the differential equation:

$$sf''(s, \theta) + \left[\frac{s^2}{2} + 2 \right] f'(s, \theta) = 0. \tag{6.3.19}$$

The solution of this equation is given by

$$f(s, \theta) = 1 + \frac{2\exp(-s^2/4) - s\sqrt{\pi}\ \mathrm{erfc}(s/2)}{s\sqrt{\pi}\ \mathrm{erfc}(\theta/2)}, \tag{6.3.20}$$

where $\operatorname{erfc}(x)$ is the complementary error function defined through

$$\operatorname{erfc}(x) = \frac{2}{\sqrt{\pi}} \int_x^\infty \exp(-t^2)\, dt. \tag{6.3.21}$$

Hence, the velocity field $u = u(y, t)$ has now been found.

The condition (6.3.12) can now be made more explicit:

$$\zeta = \frac{\theta \exp(\theta^2/4)}{\sqrt{\pi}\, \operatorname{erfc}(\theta/2)}. \tag{6.3.22}$$

It can be shown that one can find the following asymptotic relations for θ:

$$\theta = \begin{cases} \zeta\sqrt{\pi}, & \zeta << 1, \\ (2\zeta)^{1/2}, & \zeta >> 1. \end{cases} \tag{6.3.23}$$

We shall now explore the kinematics and dynamics of the lateral motion of the yield surface through the study of singular surfaces in motion.

6.3.2 Singular Surfaces in Motion

Suppose that in the shearing flow of an incompressible fluid in the x-direction defined through the velocity field $u = u(y, t)$, there is a surface at $y = y_c(t)$, across which certain kinematical and stress related quantities suffer jumps. If this singular surface propagates through the fluid, it must do so laterally; this is a consequence of the incompressibility of the material; see p. 525 in [11]. The following nomenclature applies to different types of singular surfaces in motion:

1. Propagating Vortex Sheet. This is a singular surface across which the shearing velocity $u = u(y, t)$ suffers a jump, along with the shear stress $\sigma = \sigma(y, t)$. An example of such a motion can be found in the solution of the Rayleigh problem due to Huilgol [12, 13] for the Lodge model [14], which is of importance in the flows of viscoelastic fluids.
2. Acceleration Wave. This is a surface across which $u = u(y, t)$ and $\sigma = \sigma(y, t)$ are continuous while $\partial u/\partial t$, $\partial u/\partial y$, $\partial\sigma/\partial t$ and $\partial\sigma/\partial y$ suffer jumps. Examples of such waves arise in viscoelastic materials [15–17].
3. Jerk Wave. This is a surface across which $u = u(y, t)$, $\sigma = \sigma(y, t)$, and their first order derivatives $\partial u/\partial t$, $\partial u/\partial y$, $\partial\sigma/\partial t$ and $\partial\sigma/\partial y$ are all continuous, while the second order derivatives $\partial^2 u/\partial t^2$, $\partial^2 u/\partial t\partial y$, $\partial^2 u/\partial y^2$, and $\partial^2\sigma/\partial t^2$, $\partial^2\sigma/\partial t\partial y$ and $\partial^2\sigma/\partial y^2$ all suffer jumps. Using two specific examples, it will be shown below that the lateral movement of the yield surfaces in both of these flows of a Bingham fluid satisfies all of the above requirements. Moreover, the description of such a

wave as a *jerk wave* is appropriate, for the time derivative of the acceleration $a = \partial u/\partial t$ is known as jerk, and $\partial a/\partial t = \partial^2 u/\partial t^2$. It is further shown that a jerk wave propagation occurs in the shearing flows of all viscoplastic fluids.

The speed of propagation $U = U(t)$ of a singular surface obeys a compatibility condition proved in a Lemma due to Hadamard; see p. 492 in [11]. To describe this, let the jump $[f]$ of an entity $f = f(y,t)$ across the singular surface be defined through

$$\left[f \right](t) = f^+ - f^-, \tag{6.3.24}$$

where

$$f^+ = \lim_{y \to y_c^+} f(y,t) \tag{6.3.25}$$

is the limiting value as y approaches $y = y_c(t)$ from above, while

$$f^- = \lim_{y \to y_c^-} f(y,t) \tag{6.3.26}$$

is the limiting value as y approaches $y = y_c(t)$ from below. Then, Hadamard's Lemma states that

$$\frac{d}{dt}\left[f \right] = \left[\dot{f} \right] + U\left[\partial f/\partial y \right], \tag{6.3.27}$$

where $\dot{f}$ is the material derivative of f, and $U = U(t)$ is the speed of propagation of the singular surface. In the shearing flow under consideration, $\dot{f} = \partial f/\partial t$, and one obtains:

$$\frac{d}{dt}\left[f \right] = \left[\partial f/\partial t \right] + U\left[\partial f/\partial y \right]. \tag{6.3.28}$$

Some consequences of the Hadamard Lemma as it affects unidirectional shearing flows will be derived next.

6.3.3 Hadamard Lemma and Unsteady Shearing Flows in Viscoplastic Fluids

Consider the unsteady shearing flow $u = u(y,t)$ of a viscoplastic fluid in the x-direction. The equation of motion is given by

$$\rho \frac{\partial u}{\partial t} = \frac{\partial \sigma}{\partial y} - \frac{\partial p}{\partial x}, \tag{6.3.29}$$

where ρ is the density of the fluid. Clearly, $\partial p/\partial x = P(t)$, where $P(t)$ is a function of time t only. Thus, we have to consider

$$\rho \frac{\partial u}{\partial t} = \frac{\partial \sigma}{\partial y} - P(t). \tag{6.3.30}$$

At time t, let the yield surface be located at $y = y_c(t)$. On the yield surface, the velocity field is continuous and the shear stress is equal to the yield stress. That is,

$$\Big[u\Big](t) = 0, \quad \Big[\sigma\Big](t) = 0. \tag{6.3.31}$$

If the yield surface moves with a finite speed $U = dy_c/dt$ such that $0 < |U(t)| < \infty$, it follows from the Hadamard Lemma Eq. (6.3.28) that

$$\frac{d}{dt}\Big[u\Big] = \Big[\partial u/\partial t\Big] + U\Big[\partial u/\partial y\Big] = 0, \tag{6.3.32}$$

$$\frac{d}{dt}\Big[\sigma\Big] = \Big[\partial \sigma/\partial t\Big] + U\Big[\partial \sigma/\partial y\Big] = 0. \tag{6.3.33}$$

At the yield surface, it is known that $\partial u/\partial y = 0$, or $\Big[\partial u/\partial y\Big] = 0$. Hence, Eq. (6.3.32) shows that the local acceleration is also continuous at the yield surface, or $\Big[\partial u/\partial t\Big] = 0$. If one applies the jump condition to the equation of motion Eq. (6.3.30), one obtains

$$\left[\frac{\partial u}{\partial t}\right] = \left[\frac{\partial \sigma}{\partial y}\right] = 0, \tag{6.3.34}$$

for the pressure gradient $P(t)$ is independent of y. That is, at the moving yield surface, the gradient of the shear stress is continuous, which in turn implies through Eq. (6.3.33) that $\Big[\partial \sigma/\partial t\Big] = 0$ as well.

Hence, we conclude that in a unidirectional, unsteady shearing flow of a viscoplastic fluid in which the yield surface propagates with a finite speed, all of the first order temporal and spatial derivatives of u and σ are continuous i.e., $\Big[\partial u/\partial t\Big] = 0$, $\Big[\partial u/\partial y\Big] = 0$, $\Big[\partial \sigma/\partial t\Big] = 0$, $\Big[\partial \sigma/\partial y\Big] = 0$. Thus, Hadamard's Lemma implies that at the propagating singular surface, the following equations must hold true:

$$\frac{d}{dt}\left[\frac{\partial u}{\partial t}\right] = \Big[\partial^2 u/\partial t^2\Big] + U\Big[\partial^2 u/\partial t \partial y\Big] = 0, \tag{6.3.35}$$

$$\frac{d}{dt}\left[\frac{\partial u}{\partial y}\right] = \left[\partial^2 u/\partial t \partial y\right] + U\left[\partial^2 u/\partial y^2\right] = 0, \tag{6.3.36}$$

$$\frac{d}{dt}\left[\frac{\partial \sigma}{\partial t}\right] = \left[\partial^2 \sigma/\partial t^2\right] + U\left[\partial^2 \sigma/\partial t \partial y\right] = 0, \tag{6.3.37}$$

$$\frac{d}{dt}\left[\frac{\partial \sigma}{\partial y}\right] = \left[\partial^2 \sigma/\partial t \partial y\right] + U\left[\partial^2 \sigma/\partial y^2\right] = 0, \tag{6.3.38}$$

where $U = U(t) \neq 0$ is the finite speed of propagation of the wave.

As an example where the above conditions are met, let us reconsider the unsteady shearing flow of a Bingham fluid studied in Sect. 6.3.1. One possible method to prove that the above four equations are satisfied lies in determining the six second order derivatives from the solutions already obtained, find their jumps across the yield surface and verify that Eqs. (6.3.35)–(6.3.38) hold true. A more elegant method is to observe that if one of the derivatives, say $\partial^2 u/\partial y^2$, suffers a jump across the yield surface, which has a finite, non-zero speed of propagation, then automatically the above conditions will be met. This is because a jump in $\partial^2 u/\partial y^2$ leads to discontinuities in $\partial^2 u/\partial t \partial y$ and $\partial^2 u/\partial t^2$ through Eqs. (6.3.35, 6.3.36).

Next, from the equation of motion Eq. (6.3.30), it is obvious that

$$\rho\left[\frac{\partial^2 u}{\partial t^2}\right] = \left[\frac{\partial^2 \sigma}{\partial t \partial y}\right]. \tag{6.3.39}$$

Thus, the discontinuity of $\partial^2 u/\partial t^2$ implies the discontinuities in the other second order derivatives, viz., $\partial^2 \sigma/\partial t \partial y$, $\partial^2 \sigma/\partial t^2$ and $\partial^2 \sigma/\partial y^2$ through Eqs. (6.3.37, 6.3.38), which means that the yield surface propagates as a jerk wave.

So, one is led to discover the mechanism for $\partial^2 u/\partial y^2$ to suffer a jump. A simple explanation, valid for all viscoplastic fluids follows next.

1. In the core region, $\partial u/\partial y = 0$ which means that $(\partial^2 u/\partial y^2)^- = 0$.
2. In the core, if the fluid has a constant yield stress τ_y, the shear stress distribution is linear in y, and $\partial \sigma/\partial y \neq 0$ and is a function of t only. Moreover, Eq. (6.3.34) shows that this gradient is continuous at the yield surface.
3. Using the constitutive equation of a viscoplastic fluid, one can show that $\partial \sigma/\partial y \neq 0$ at the yield surface implies that $(\partial^2 u/\partial y^2)^+ \neq 0$.
4. In the absence of a pressure gradient, the equation of motion Eq. (6.3.30) shows that $\partial \sigma/\partial y \neq 0$ is equivalent to $\partial u/\partial t \neq 0$. Hence, in such a flow, a non-zero acceleration of the core and a change in its size is sufficient for the propagating yield surface to be termed a jerk wave.

We shall now apply the above reasoning to the flow covered in some detail in Sect. 6.3.1.

6.3.4 Implications of the Continuity of $\partial\sigma/\partial y$ at the Yield Surface

In this part, we shall examine the solution to the unsteady shearing flow problem in Sect. 6.3.1 and the implications arising from the fact that $\partial\sigma/\partial y$ is continuous on the yield surface.

From Eq. (6.3.7), it is obvious that the yield surface propagates into the fluid with a velocity $U(t) = \theta \cdot (\nu/t)^{1/2}/2 > 0,\ t > 0$. In the rigid core, the acceleration $\partial u/\partial t$ is independent of y. Recalling that the shear stress distribution in the core is linear, i.e.,

$$\sigma(y,t) = \frac{\tau_y - \tau_0}{y_c(t)} y + \tau_0, \quad 0 \le y \le y_c(t), \tag{6.3.40}$$

the gradient of the shear stress $\partial\sigma/\partial y = (\tau_y - \tau_0)/y_c(t)$ in the core. Consequently, the limiting value at the yield surface is given by

$$\left(\frac{\partial\sigma}{\partial y}\right)^- = \frac{\tau_y - \tau_0}{y_c(t)} > 0, \quad t > 0. \tag{6.3.41}$$

Now, we know from Eq. (6.3.34) above that $\partial\sigma/\partial y$ is continuous at the yield surface. Hence,

$$\frac{\partial\sigma}{\partial y} = \left(\frac{\partial\sigma}{\partial y}\right)^+ = \left(\frac{\partial\sigma}{\partial y}\right)^- = \frac{\tau_y - \tau_0}{y_c(t)} > 0, \quad t > 0. \tag{6.3.42}$$

Now, from the constitutive relation Eq. (6.3.15), it follows that

$$\left(\frac{\partial^2 u}{\partial y^2}\right)^+ = \frac{1}{\eta}\frac{\partial\sigma}{\partial y} = \frac{\tau_y - \tau_0}{\eta y_c(t)} > 0, \quad t > 0. \tag{6.3.43}$$

Since $U(t) > 0$, it is obvious that the yield surface moves as a jerk wave through the fluid.

6.3.5 Extensions to Other Shearing Flows

So far, a single shearing flow in an unbounded domain has been used to show that the yield surface propagates as a jerk wave in a Bingham fluid. In this section, we shall examine whether it is possible to identify other unsteady, unidirectional shearing flows where the yield surface moves as a jerk wave. In a bounded domain, the flows in a channel, or a circular pipe or the Couette flow between concentric circular cylinders fall into the class of unidirectional shearing flows. In an unbounded domain, the solution to the shearing flow provided by Sekimoto [9], the Couette flow studied by Safronchik [1], or the Rayleigh problem [18] belong here.

The above flows can be separated into two classes: those where the width of the rigid zone is finite, and where it is not. In the former category, one sees that the flows in a channel, and a circular pipe will contain a symmetric region of unyielded fluid in the middle. In a Couette flow, the situation can be very complicated indeed for, as shown by Comparini and De Angelis [6], multiple liquid-rigid-liquid-rigid zones may exist. In an unbounded domain, we have already examined the flow by Sekimoto as falling into this class of flows. In the work of Safronchik [5], one can find the Couette flow induced by a rotating rod in a sea of Bingham fluid; that is, an infinite zone of unyielded fluid remains. Similarly, in the Rayleigh problem when the plane at $y = 0$ acquires a constant velocity in the x-direction, it is clear that an infinite amount of unsheared fluid must lie ahead of the moving yield surface, if it exists.

Clearly the start-up from rest of the flow of a Bingham fluid in a channel under a suddenly applied, constant pressure gradient has a finite core which contracts with time. To be specific, as explained in Sect. 6.1, the location of the yield surface is given, over a short time period, by

$$y_c(t) = H - 2\alpha(\nu t)^{1/2}, \quad 0 \le t \le H^2/4\alpha\nu. \tag{6.3.44}$$

In Eq. (6.3.44), H is the half-channel width, and $\alpha(0) > 0$ is the solution of the transcendental equation:

$$\exp[-\alpha(0)^2] - 2\alpha(0) \int_{\alpha(0)}^{\infty} e^{-\beta^2}\, d\beta = \mathrm{Bn}/G. \tag{6.3.45}$$

As mentioned earlier, the solution in Eq. (6.3.44) is valid for a short time period only, i.e., as long as $0 \le y_c(t) \le H$. The speed of propagation of the yield surface is given by $U(t) = -\alpha(0)(\nu/t)^{1/2} < 0,\ t > 0$ which corresponds to the yield surface moving from the channel wall into the fluid with a finite speed.

In the core, the shear stress is given by

$$\sigma(y, t) = -\frac{\tau_y}{y_c(t)} y, \quad 0 \le y \le y_c(t), \tag{6.3.46}$$

so that $(\partial\sigma/\partial y)^- = -\tau_y/y_c(t) < 0$. In the yielded region, it is clear that $(\partial\sigma/\partial y)^+ = \eta(\partial^2 u/\partial y^2)^+$. Since, $\partial\sigma/\partial y$ is continuous at $y = y_c(t)$, we note that

$$\left[\frac{\partial^2 u}{\partial y^2}\right](t) = \left(\frac{\partial^2 u}{\partial y^2}\right)^+ = -\frac{\tau_y}{\eta y_c(t)} < 0, \quad t > 0, \tag{6.3.47}$$

or $\partial^2 u/\partial y^2$ suffers a jump across the yield surface, which means that the yield surface moves as a jerk wave. The same argument can be made regarding the cessation of a flow in the channel, for the core expands to choke off the flow in a finite amount of

time. Obviously, in other viscoplastic fluids, such as Casson and Herschel-Bulkley fluids, the jerk wave phenomena persist in the channel flow.

As an example where a propagating yield surface does not exist, consider the Rayleigh problem for a Bingham fluid. Here, the fluid occupies the half-space $y > 0$. At time $t = 0^+$, let the plane at $y = 0$ acquire a constant velocity V in the x-direction and let this boundary condition be maintained for all $t > 0$. Let us begin by assuming that the yield surface propagates into $y > 0$ with a speed $U(t) > 0$. If at time t, the yield surface is located at $y = y_c(t)$, we see that the fluid is at rest in $y_c(t) \leq y < \infty$. This means that $u(y, t)$ and all of its temporal and spatial gradients are all zero in the rigid core. This requires that the shear stress $\sigma(y, t) = \tau_y$ in $y_c(t) \leq y < \infty$, or there is no gradient of the shear stress ahead of the moving front; so, $(\partial\sigma/\partial y)^+ = 0$. By the continuity of this gradient or that of $\partial u/\partial t$ at the yield surface, it follows that $(\partial^2 u/\partial y^2)^- = 0$ behind the wave front. Hence, the yield surface cannot propagate as a jerk wave. In fact, it has been shown that it cannot move as a wave of higher order either. That is, the flow of the Bingham fluid is identical to that of the Newtonian fluid in this initial value problem [18].

6.3.6 Open Ended Problems

Arising from the jerk wave analysis, one can pose the following questions:

1. Given a set of initial conditions with a yield surface, will the latter propagate or remain stationary?
2. What is the asymptotic nature of the velocity field near a point where the yield surface begins to propagate?
3. What can be said in more than one space dimension?

We offer the following comments:

1. The Hadamard Lemma has the simple form given by Eq. (6.3.28) above in a special class of shearing flows only, for the material particles situated on the moving yield surface do not possess a velocity component in the direction of propagation. In order for this propagation to occur, the examples in the literature show that if the flow domain is finite, the fluid must be set in motion by the sudden movement of a boundary, or through a suddenly imposed pressure gradient; if the flow domain is infinite, the core has to be finite in size. Examples of propagating yield surfaces in these situations are available in the channel flow studied by Safronchik, the cessation of the channel flow and that in a pipe of circular cross-section, and the flow examined in Sect. 6.3.1. Numerical simulation of the cessation of a simple shearing motion, channel and Poiseuille flows using the Papanastasiou model shows that the yield surface moves laterally and expands till the fluid comes to a halt [19]. Clearly, in these motions, the movement of the yield surface can be classified as a jerk wave. When the flow domain is infinite and the core is also

infinite and at rest, as in the Rayleigh problem, propagation of a yield surface cannot occur as shown above.

2. There is no unique answer to the asymptotic nature of the velocity field near a point where the yield surface begins to propagate. Since the velocity field is continuous across the yield surface, it suffices to consider the velocity in the core only. For instance, one may turn to the study of the initiation of the flow in a channel discussed above in Sect. 6.1. It has been mentioned that the velocity in the core has the form

$$u(t) = Gt + \mathrm{Bn}\frac{1}{\alpha(0)}\sqrt{t} + \mathrm{Bn}\frac{1}{[2\alpha(0)]^2}\ln\left[1 - 2\alpha(0)\sqrt{t}\right]. \tag{6.3.48}$$

Clearly, the velocity in the core is not directly proportional to $t^{1/2}$. If we now compare the above with that obtained from Eq. (6.3.7) in the examination of the unsteady simple shear flow in an unbounded domain, one finds that the velocity in the core is given by:

$$u(t) = \dot{\gamma}\theta f(\theta, \theta)(\nu t)^{1/2}, \tag{6.3.49}$$

which is proportional to $t^{1/2}$.

3. The start-up of the flow of a Bingham fluid in a pipe of square cross-section provides an example of a two dimensional flow. When the flow starts, pockets of fluid at rest in the corners arise with a moving plug at the centre, which will be surrounded by the yielded material. It is impossible to show analytically that the yield surfaces propagate into the corners and towards the centre of the pipe as jerk waves. Clearly, this start-up flow provides an opportunity to test the jerk wave hypothesis through numerical simulation. This is because the shape and location of each one of the propagating surfaces, which is likely to be curved, is unknown, as is its instantaneous speed of propagation relative to the material particles situated on it. Obviously, the numerical modelling will have to meet the kinematical and dynamical compatibility conditions, derived by Hadamard in 1903. For a more recent exposition, see pp. 492–530 in [11]. A simplified version, applicable to elastic solids, has also been provided by Eringen [20].

References

1. Safronchik AI (1959) Non-steady flow of a visco-plastic material between parallel walls. J Appl Math Mech (PMM) 23:1314–1327
2. Kolodner II (1956) Free Boundary problem for the heat equation with applications to problems of change of phase. Commun Pure Appl Math 9:1–31
3. Protter MH, Weinberger HF (1967) Maximum principles in differential equations. Prentice-Hall, Englewood Cliffs
4. Comparini E (1992) A one-dimensional Bingham flow. J Math Anal Appl 169:127–139
5. Safronchik AI (1959) Rotation of a cylinder with a variable angular velocity in a visco-plastic medium. J Appl Math Mech (PMM) 23:1504–1511

6. Comparini E, De Angelis E (1996) Flow of a Bingham fluid in a concentric cylinder viscometer. Adv Math Sci Appl 6:97–116
7. Comparini E (1997) Regularization procedures of singular free boundary problems in rotational Bingham flows. Zeit angew Math Mech 77:543–554
8. Safronchik AI (1960) Unsteady flow of visco-plastic material in a circular tube. J Appl Math Mech (PMM) 24:200–207
9. Sekimoto K (1991) An exact non-stationary solution of simple shear flow in a Bingham fluid. J Non-Newton Fluid Mech 39:107–113
10. Huilgol RR (2010) On the description of the motion of the yield surface in unsteady shearing flows of a Bingham fluid as a jerk wave. J Non-Newton Fluid Mech 165:65–69
11. Truesdell C, Toupin RA (1960) The classical field theories In: Flügge S (ed) Encyclopedia of Physics III/1. Springer, New York
12. Huilgol RR (1981) Propagation of a vortex sheet in viscoelastic fluids—the Rayleigh problem. J Non-Newton Fluid Mech 8:337–347
13. Huilgol RR (1983) Corrections and extensions to [12]. J Non-Newton Fluid Mech 12:249–251
14. Lodge AS (1964) Elastic liquids. Academic Press, New York
15. Coleman BD, Gurtin ME, Herrera IR (1965) The velocity of one-dimensional shock and acceleration waves. Arch Ration Mech Anal 19:1–19
16. Coleman BD, Gurtin ME (1968) On the stability against shear waves of steady flows of nonlinear viscoelastic fluids. J Fluid Mech 33:165–181
17. Huilgol RR (1973) Acceleration waves in isotropic simple materials. Arch Mech Stos 25:365–376
18. Huilgol RR (2004) On kinematic conditions affecting the existence and non-existence of a moving yield surface in unsteady unidirectional flows of Bingham fluids. J Non-Newton Fluid Mech 123:215–221
19. Chatzimina M, Georgiou GC, Argyropaidas I, Mitsoulis E, Huilgol RR (2005) Cessation of Couette and Poiseuille flows of a Bingham plastic and finite stopping times. J Non-Newton Fluid Mech 129:117–127
20. Eringen AC (1962) Nonlinear theory of continuous media. McGraw-Hill, New York

Chapter 7
Analytical Approximation Techniques

Convened by The Institution of Mechanical Engineers, London, a committee headed by Beauchamp Tower was asked to investigate the lubrication of journal bearings. In its report, submitted in 1883, the committee came to the conclusion that *profuse* hydrodynamic lubrication of the bearings reduced the friction to an extremely small value. Moreover, at the end of the oil bath experiments, the committee was surprised to realise, quite by accident, that the lubricating oil developed considerable pressure around the periphery of the bearing and that this pressure was responsible for supporting the load.

It was left to Reynolds [1] to put Tower's findings on a rigorous mathematical basis and to explain the action of the hydrodynamic forces which produced the necessary lift. In doing so, he derived the now famous partial differential equation for the pressure distribution around the circumference of the bearing, connecting the film thickness and pressure at any point, the viscosity of the oil, and the velocities of the rubbing surfaces and their normal velocity.[1] For a journal bearing under a steady load, he simplified this equation to the following:

$$\frac{\partial}{\partial x}\left(h^3\frac{\partial p}{\partial x}\right)+\frac{\partial}{\partial z}\left(h^3\frac{\partial p}{\partial z}\right)=6\eta U\frac{\partial h}{\partial x}. \tag{7.0.1}$$

It is assumed here that the x-axis lies along the fixed surface of the outer casing, the z-axis is along the axis of the bearing and that the very small film thickness lies in the y-direction, given by $h = h(x, z)$. Of course, $p = p(x, z)$ is the pressure, U is the azimuthal speed of the bearing and η is the viscosity of the fluid.

In order to obtain (7.0.1), Reynolds assumed that the flow is essentially two-dimensional, is well described by the velocity components (u, w) in the (x, z) directions respectively, and that the Navier-Stokes equations reduce to:

[1] This equation has received much attention in the literature. For the first solution of the problem of full film lubrication in a bearing of finite length, see Tao [2]. For a solution including cavitation effects and employing a variational inequality, see Cimatti [3].

R.R. Huilgol, *Fluid Mechanics of Viscoplasticity*, DOI 10.1007/978-3-662-45617-0_7

$$\frac{\partial^2 u}{\partial y^2} = \frac{1}{\eta}\frac{\partial p}{\partial x}, \tag{7.0.2}$$

$$\frac{\partial^2 w}{\partial y^2} = \frac{1}{\eta}\frac{\partial p}{\partial z}. \tag{7.0.3}$$

That is, while $u = u(x, y, z),\ w = w(x, y, z)$, the only derivatives that matter are $\partial^2 u/\partial y^2,\ \partial^2 w/\partial y^2$; the rest can be ignored. Using the boundary conditions to integrate these two equations and employing the continuity equation, Reynolds was able to produce (7.0.1). Clearly, this is the beginning of the *lubrication approximation*.

In this chapter, this approximation is used to examine the lubrication paradox which leads to the conclusion that a plug flow will exist in a Bingham fluid provided the walls of a channel are parallel and not otherwise. In order to disprove this, the steady flow of a Bingham fluid in a small amplitude, long wavelength perturbation of a uniform channel is explored. Next, the Hele-Shaw flow equations are derived through the viscometric fluidity function which is applicable to both viscous and viscoplastic fluids. Recently, these equations have been applied to injection moulding problems.

Finally, the stability of the channel flow of a Bingham fluid is examined when subjected to one, two or three dimensional disturbances which may be modal or non-modal. A summary of the available results is offered. Simply put, it is found that instability depends on the Bingham number with the critical Reynolds number increasing almost linearly with it. That is, the Bingham fluid is more stable in this flow than its Newtonian counterpart. Surprisingly, the opposite is true in the case of a helical flow.

7.1 The Lubrication Paradox

If one were to apply the lubrication approximation to the one-dimensional flow of a Bingham fluid in a symmetric channel of varying width, say $-H(x) \le y \le H(x),\ -\infty < x < \infty$, the equations of motion are:

$$-\frac{\partial p}{\partial x} + \frac{\partial \sigma}{\partial y} = 0, \tag{7.1.1}$$

where $p = p(x)$ only. If there is a yield surface at $y = h(x)$, it is easy to see that

$$h(x) = -\tau_y/p',\ p' = dp/dx. \tag{7.1.2}$$

Suppose that the velocity field $u = u(x, y)$ across the gap. Since the flow is symmetric about the x-axis, it is quite straightforward to show that (cf. (1.4.5)):

$$u(x, y) = -\frac{p'}{2\eta}\Big(H^2(x) - y^2\Big) - \frac{\tau_y}{\eta}\Big(H(x) - y\Big),\quad h(x) \le y \le H(x). \tag{7.1.3}$$

The plug velocity given by $u_p = u(x, h(x))$ is a constant in $0 \le y \le h(x)$ and, using the continuity of $u = u(x, y)$ at the yield surface, one has

$$u_p = -\frac{p'}{2\eta}\Big(H^2(x) - h^2(x)\Big) - \frac{\tau_y}{\eta}\Big(H(x) - h(x)\Big), \quad 0 \le y \le h(x). \tag{7.1.4}$$

Since $h(x) = -\tau_y/p'$, one can rewrite the above as

$$2\eta u_p = \tau_y h(x) - 2\tau_y H(x) - p' H^2(x). \tag{7.1.5}$$

Since the fluid is incompressible, the flow rate Q per unit width is constant and given by

$$Q = 2u_p h(x) + 2\int_{h(x)}^{H(x)} u\, dy. \tag{7.1.6}$$

Substituting (7.1.2) and (7.1.3) in the above, one finds that

$$3\eta Q = -3\tau_y H^2(x) - 2p' H^3(x) - p' h^3(x). \tag{7.1.7}$$

Hence, we have three equations, viz., (7.1.2), (7.1.5) and (7.1.7), which connect $p', h(x), H(x)$. It is conceivable that these are indeed non-constant functions of x. It will be shown next that this is impossible [4], for it leads to a contradiction. The proof is more direct than that advanced in [5].

The first step is to multiply (7.1.5) by p', use (7.1.2) and suppress the dependence on x for convenience, leading to

$$H^2 p'^2 + 2(\eta u_p + \tau_y H)p' + \tau_y^2 = 0. \tag{7.1.8}$$

This is a quadratic equation for p'. Let its roots be α and β. Clearly these roots must satisfy

$$\alpha + \beta = -\frac{2(\eta u_p + \tau_y H)}{H^2}, \quad \alpha\beta = \frac{\tau_y^2}{H^2}. \tag{7.1.9}$$

Note that the two roots are both real and negative; this is as is should be, for the pressure gradient $p' < 0$.

Secondly, multiply (7.1.7) by p'^2 and obtain the cubic equation

$$2H^3 p'^3 + 3(\tau_y H^2 + \eta Q)p'^2 - \tau_y^3 = 0. \tag{7.1.10}$$

If there is a set of unique solutions to p', then the roots of (7.1.10) are the two previous roots α, β and a new one, γ. It follows quite easily that

$$\alpha + \beta + \gamma = -\frac{3(\tau_y H^2 + \eta Q)}{2H^3}, \quad \alpha\beta\gamma = \frac{\tau_y^3}{2H^3}. \tag{7.1.11}$$

Comparing $(7.1.9)_2$ and $(7.1.11)_2$, we find that $p' = \gamma = \tau_y/2H > 0$. This is a contradiction, for the pressure gradient cannot be positive. Note that (7.1.5) and (7.1.7) reduce to tautologies if, for example, $H(x)$ is constant.

Hence, a plug flow in an incompressible Bingham fluid cannot occur, within the lubrication approximation, if the channel boundary is not parallel to the x-axis. This is the lubrication paradox and confirms the view expressed by Lipscomb and Denn [5]. Of course, one cannot rule out the existence of a plug flow if the lubrication approximation is not used. This is illustrated in the next section through an examination of the flow in an undulating channel.

7.2 Steady Flow in a Wavy Channel—The Periodic Case

Apart from resolving the lubrication paradox, the problem to be studied here is of interest in several industries; for example, in studying the effects of uneven well bore geometry on drilling and primary cementing processes in oil and gas well construction, as well as in food processing. The occurrence of fouling layers [6], i.e., those deposits which lie in the recesses of the walls and do not move, is not an acceptable outcome in such situations. In order to model this situation, the flow of a Bingham fluid in a slowly varying channel with a periodic boundary is studied here; see Fig. 7.1. The half-width of the channel is H and the period of the wavy channel is L. Scaling all lengths with respect to H, it is assumed that the boundary of the channel is given by $y = y_w(x) = 1 - h\cos 2\pi x$. The flow is two-dimensional with the velocity field given by $\mathbf{u} = u(x, y)\mathbf{i} + v(x, y)\mathbf{j}$. The boundary conditions are:

$$v = 0, \quad S_{xy} = 0, \quad y = 0, \tag{7.2.1}$$

$$u = 0, \quad v = 0, \quad y = 1 - h\cos 2\pi x. \tag{7.2.2}$$

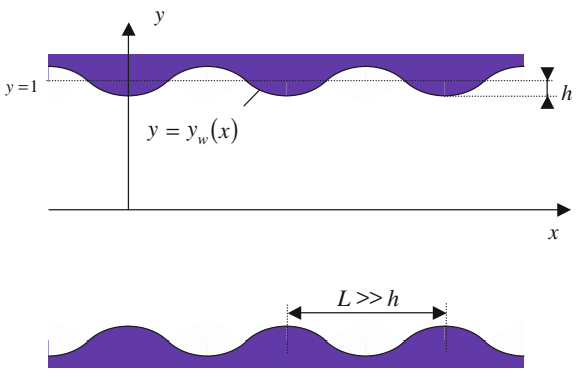

Fig. 7.1 Slowly varying channel geometry

The Reynolds and Bingham numbers are given by

$$\mathrm{Re} = \frac{\rho U H}{\eta}, \quad \mathrm{Bn} = \frac{\tau_y H}{\eta U}, \tag{7.2.3}$$

where U is the average velocity along the channel. Let the aspect ratio δ be given by

$$\delta = \frac{H}{L}. \tag{7.2.4}$$

Scaling the pressure p and the shear stress S_{xy} with $\eta U/H$, and the normal stresses $S_{xx} = -S_{yy}$ with $\delta \eta U/H$, one can derive the following set of non-dimensional equations:

$$-\frac{\partial p}{\partial x} + \delta^2 \frac{\partial S_{xx}}{\partial x} + \frac{\partial S_{xy}}{\partial y} = \delta \,\mathrm{Re}\left(u\frac{\partial u}{\partial x} + v\frac{\partial u}{\partial y}\right), \tag{7.2.5}$$

$$-\frac{\partial p}{\partial y} + \delta^2 \frac{\partial S_{xy}}{\partial y} + \delta^2 \frac{\partial S_{yy}}{\partial y} = \delta^3 \,\mathrm{Re}\left(u\frac{\partial v}{\partial x} + v\frac{\partial v}{\partial y}\right), \tag{7.2.6}$$

$$\frac{\partial u}{\partial x} + \frac{\partial v}{\partial y} = 0. \tag{7.2.7}$$

The non-dimensional form of the extra stress tensor in a Bingham fluid is given by

$$\mathbf{S} = \left(1 + \frac{\mathrm{Bn}}{K(\mathbf{A})}\right)\mathbf{A}, \quad T(\mathbf{S}) > \mathrm{Bn}, \tag{7.2.8}$$

where

$$A_{xy} = \frac{\partial u}{\partial y} + \delta^2 \frac{\partial v}{\partial x}, \tag{7.2.9}$$

$$A_{xx} = 2\frac{\partial u}{\partial x} = -2\frac{\partial v}{\partial y} = -A_{yy}, \tag{7.2.10}$$

$$K(\mathbf{A}) = \left[A_{xy}^2 + \delta^2 A_{xx}^2\right]^{1/2}, \quad T(\mathbf{S}) = \left[S_{xy}^2 + \delta^2 S_{xx}^2\right]^{1/2}. \tag{7.2.11}$$

Finally, the scaled velocity $u = u(x, y)$ is such that

$$\int_0^{y_w(x)} u(x, y)\, dy = 1. \tag{7.2.12}$$

In order to seek a solution, one assumes that as $h \to 0$, the velocity field must reduce to that in a channel with straight walls. Secondly, there will be a yielded flow next to the wall; this is an *outer solution*. In the centre of the channel, there will

be a plug flow moving with a speed u_p which has to be determined. The transition from one solution to the other occurs at an approximate position of the *perturbed yield surface* found by an inner solution and matching conditions; see Frigaard and Ryan [7]. A summary follows next.

7.2.1 Zeroth Order Solution

The zeroth order solution $u_0(x, y)$ is given by

$$u_0(x,y) = \begin{cases} \text{Bn}\,(y_w - y_y)^2/2y_y, & y \in [0, y_y], \\ \text{Bn}\Big[(y_w - y_y)^2 - (y - y_y)^2\Big]/2y_y, & y \in (y_y, y_w]. \end{cases} \tag{7.2.13}$$

where the location of the pseudo-yield surface y_y is found from:

$$y_y = \frac{\text{Bn}}{|p_{0,x}|}. \tag{7.2.14}$$

Next, it can be shown that $y_y = y_w/\xi$, where $\xi = \xi(B^*)$ is the single root of the Buckingham equation:

$$2\xi^3 - \left(3 + \frac{6}{B^*}\right)\xi^2 + 1 = 0, \quad B^* = \text{Bn}\; y_w, \tag{7.2.15}$$

with the requirement that $\xi > 1$ and $B^* = \text{Bn}\; y_w^2$. Replacing y_0 by $1/\xi$, this equation can also be obtained from (1.8.3).

The pressure gradient $p_{0,x}$ is now found from (7.2.14) and the velocity field from (7.2.13). Thus, the entire leading order solution depends on the Bingham number Bn and the function defining the wall, $y_w(x)$. The interesting conclusion is that the pressure gradient adjusts itself to maintain the unit flow rate through the narrower parts of the channel; in turn, the pseudo-plug is narrower.

The axial variation in the velocity is similar to that in the centre of the channel. If the pseudo-plug velocity is $u_{pp}(x)$, it must equal that at the edge of the plug, i.e.,

$$u_{pp}(x) = u_0(x, y_y) = \frac{\text{Bn}}{2y_y}(y_w - y_y)^2. \tag{7.2.16}$$

Next, one notes from $y_w = 1 + O(\delta)$ that the perturbed Bingham number $B^* = \text{Bn} + O(\delta)$ and, thus $\xi = (1/y_0) + O(\delta)$, where y_0 is the location of the yield surface in the flat, plane channel. Hence, the location of the pseudo-yield surface, $y_y(x)$, and the pseudo-plug velocity, $u_{pp}(x)$ are $O(\delta)$ perturbations of the flat, plane channel values. In sum, the solution is similar to that of the flow in a flat, plane channel; the variations lie in the fact that the channel walls are periodic with a very

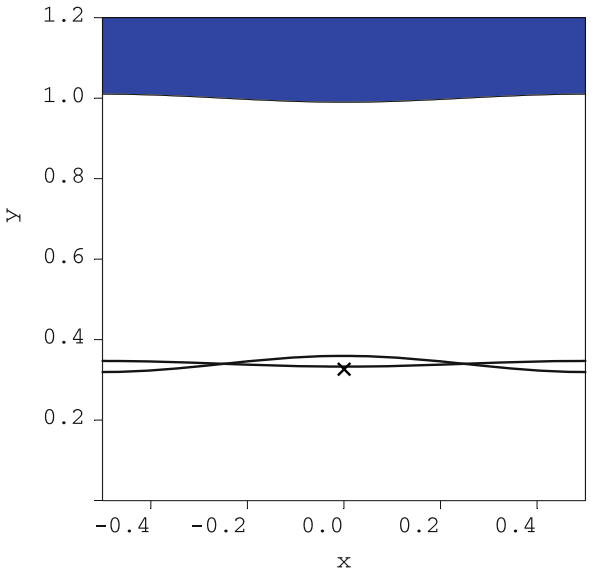

Fig. 7.2 Composite asymptotic solution compared with the zeroth order outer approximation

shallow depression. In Fig. 7.2, which is Fig. 7c in [7], the curve with the mark '×' is the curve $y_y(x)$, when $\delta = 0.05$, $h = 0.01$ and Bn = 2. The pseudo-yield surface is almost parallel to the undulating wall surface. The region $y \in [0, y_y]$ is not a true plug domain, since the leading order velocity $u_0(x, y)$ varies in the x-direction, which is another manifestation of the lubrication paradox for yield stress fluids.

Since the pseudo-yield surface is almost parallel to the wall, one can see that $y_y(0) < y_y(\pm 1/2)$. From (7.2.16), one can observe that the pseudo-plug velocity $u_{pp}(0) > u_{pp}(x)$ for any $x \in (0, 1/2)$. That is, the pseudo-plug velocity is a maximum when the wavy wall is closest to the centre of the channel.

Now, we turn to the first order corrections to show that there is a true plug across the channel.

7.2.2 First Order Corrections

The first assumption is that for sufficiently small $h = O(\delta)$, there is a true plug which is intact along the length of the channel and is bounded by the yield surface $y = y_T(x)$. Next, this surface may be assumed to lie within $O(\delta)$ of the pseudo-yield surface $y_y(x)$. Now, the true plug velocity u_p is a constant which means that one can expect it to equal a particular value of the pseudo-plug velocity. Since the flow is symmetric about the centreline of the channel, there exists $x_p \in [0, 1/2]$ such that

$$u_p = u_{pp}(x_p), \quad x \in [-1/2, 1/2]. \tag{7.2.17}$$

It is easy to observe that for the corrected velocity field, the largest velocity at each x will be the plug velocity u_p, reached at $y_T(x)$.

Now, at any fixed x, consider the case when $u_{pp}(x) > u_p$. From the observation made earlier, this means that $|x| < x_p$. This leads to the outer solution u_0 being faster than the true plug solution in the pseudo-plug. To correct this situation, the first order correction must be such that it increases the velocity in the sheared layer, or the true plug must be wider than the pseudo-plug in $|x| < x_p$. The opposite happens when $u_{pp}(x) < u_p$. That is, one has $|x| > x_p$.

Consider the first case: $u_{pp}(x) < u_p,\ y_T(x) < y_y(x)$. Assume that

$$y_y(x) \sim y_T(x) + \delta\xi_T(x) + O(\delta^2). \tag{7.2.18}$$

Here, $\xi_T(x)$ is the first order perturbation from $y_y(x)$. The two outer solutions are matched in a transition layer of order $O(\delta)$ by the composite solution of the form:

$$u \sim \begin{cases} u_p, & 0 \le y \le y_T, \\ u_p + \delta^2 u_2^i(x, y) + \cdots, & y_T < y \le y_y, \\ u_0(x, y) + \delta u_1(x, y) + \delta^2 u_2(x, y) + \cdots, & y_y < y \le y_w. \end{cases} \tag{7.2.19}$$

The outer solutions u_1 and u_2 and the inner solution u_2^i are found by paying careful attention to the required matching conditions. Since the majority of interest lies at the yield surface, the results for the inner solution u^i and the outer solution u are;

$$u^i(x, y_y) \sim u_p - \delta^2 \frac{\mathrm{Bn}}{2y_y}\xi_T^2 + O(\delta^3), \tag{7.2.20}$$

$$u(x, y_y) \sim u_{pp}(x) + \delta u_1^* + \delta^2 u_2^* + O(\delta^3), \tag{7.2.21}$$

$$u_1^* = \frac{1}{\delta}[u_p - u_{pp}(x)], \tag{7.2.22}$$

$$u_2^* = -\frac{\mathrm{Bn}}{2y_y}\xi_T^2, \tag{7.2.23}$$

$$\xi_T = \frac{u_1^*(y_y + 2y_w)}{u_{pp}}. \tag{7.2.24}$$

The conclusions that can be drawn from the above are as follows:

- The first order velocity correction u_1^* in (7.2.22) compensates for the discrepancy in the plug speeds. This is positive, while the second order correction u_2^* is negative.
- The yield surface correction ξ_T is $O(1)$ and positive. That is, the $y_y > y_T$ in (7.2.18) as required.

The solution for the second case: $u_{pp}(x) > u_p,\ y_T(x) > y_y(x)$ has a structure similar to the first one. Finally, the solutions depend on the true plug speed u_p which has to be determined. This leads to the solution of the following equation for x_p:

$$F(x_p) = \int_0^{1/2} \left([y_T(x) - y_y(x)] \frac{\partial p_0}{\partial x}(x) + \delta y_T(x) \frac{\partial p_1}{\partial x}(x) \right) dx = 0. \tag{7.2.25}$$

In order to find the solution $x_p \in (0, 1/2)$, the pressure gradients $\partial p_i / \partial x$, $i = 0, 1$, have to be found [7]. Finally, one notes that x_p delivers the true plug velocity u_p through $u_{pp}(x_p) = u_p$. Interestingly, the width of the true plug is larger in the narrow portion of the channel and smaller in the wider part; see Fig. 7.2, reproduced from Fig. 7c in [7]. Numerical solution [8] of the wavy channel flow confirms the above theoretical predictions, viz., that there is a true rigid plug in a small amplitude, long wavelength perturbation of the uniform channel.

7.2.3 Breaking the Unyielded Plug

Suppose that there is a critical value of the amplitude h_c so that if $h > h_c$, the plug will break. That is, the plug will be replaced by a pseudo-plug. Within the broken pseudo-plug, the flow will be of an extensional character and one can determine the corresponding stresses, viz., S_{xx}. At a fixed point $x_b \in [0, 1/2]$, define the mean extensional stress integral:

$$I(x_b) = \delta \int_0^{x_b} S_{xx}(x_b, y)\, dy. \tag{7.2.26}$$

A sufficient condition for the plug to break at a point $x = x_b$ is that

$$|I(x_b)| > \text{Bn}\ y_T(x_b). \tag{7.2.27}$$

This result can be improved further to lead to the following condition:

$$\left| \int_0^{x_p} \left[p_{0,x}(x) \frac{[y_t(x) - y_y(x)]}{\delta} + p_{1.x}(x) y_T(x) \right] dx \right| > \text{Bn}\ y_T(x_b). \tag{7.2.28}$$

Numerical modelling [8] shows that these predictions are fairly accurate.

7.3 Hele-Shaw Flow Problems

In order to explain the phenomenon of viscous fingering where a fluid of lower viscosity, e.g., water, protrudes into a fluid of higher viscosity, e.g., oil, in a pressure driven flow, Saffman and Taylor [9] employed the Hele-Shaw flow equations; it was

assumed that this intrusion was due to a symmetric flow occurring between two parallel planes of infinite extent of a Newtonian fluid.[2] In the symmetric case, the Hele-Shaw flow approximation is based on the lubrication theory as follows:

1. The flow is essentially two dimensional with a velocity field given by $\mathbf{u} = u\mathbf{i}+v\mathbf{j}$, where
$$u = u(x, y, z), \quad v = v(x, y, z), \tag{7.3.1}$$
in a Cartesian coordinate system with $-H \leq z \leq H$. Here, $2H$ denotes the gap between the parallel plates. The velocity field vanishes along the plates, i.e., $\mathbf{u}(x, y, \pm H) = \mathbf{0}$. Moreover, the velocity gradient is zero along the mid-plane, i.e., $\partial_z \mathbf{u}(x, y, 0) = \mathbf{0}$.
2. The rate of change of the velocity field with respect to the coordinates x and y can be ignored when compared with that associated with the z coordinate.
3. The effects of body forces and inertia are irrelevant.
4. The flow is isothermal and the material properties are not dependent on the shear rate history either.

Hence, one may ignore the equation of motion in the z-direction completely and the resulting equations are:
$$\nabla_2 p = \partial_z \mathbf{s}, \tag{7.3.2}$$
where ∇_2 is the two-dimensional gradient operator $\mathbf{i}\partial(\cdot)/\partial x + \mathbf{j}\partial(\cdot)/\partial y$. The shear stress vector on the right side is given by $\mathbf{s} = s_{xz}\mathbf{i} + s_{yz}\mathbf{j}$. It too vanishes along the mid-plane, i.e., $\mathbf{s}(x, y, 0) = \mathbf{0}$.

The next step is to define the average velocity field $\overline{\mathbf{u}}$ through
$$\overline{\mathbf{u}}(x, y) = \frac{1}{2H} \int_{-H}^{H} \mathbf{u}(x, y, z)\, dz. \tag{7.3.3}$$
The Hele-Shaw equations connect $\overline{\mathbf{u}}$ with $\nabla_2 p$ through a constitutive relation between the stress vector $\mathbf{s}$ and the velocity gradient $\partial_z \mathbf{u}$.

When the flow is asymmetric, it takes place between two curves defined by $z = h^-(x, y)$ and $z = h^+(x, y)$. Here, the datum $z = 0$ lies along the cavity centreline, with $z = h^+(x, y)$ lying above the mid-plane and $z = h^-(x, y)$ lying below it. That is, instead of Eq. (7.3.3), we have
$$\overline{\mathbf{u}}(x, y) = \frac{1}{h^+ - h^-} \int_{h^-}^{h^+} \mathbf{u}(x, y, z)\, dz. \tag{7.3.4}$$
Note that we do not have to assume that $h^+(x, y) = -h^-(x, y)$ to obtain the average velocity field.

[2] For experimental results on viscous fingering in a yield stress fluid, see [10].

7.3.1 The Viscometric Fluidity Function

In a viscometric flow, such as the channel, Couette and Poiseuille flows, the viscometric fluidity function [11, 12] appears and it provides a way of defining the shear rate in terms of the shear stress. That is, let $\dot{\gamma}$ be the shear rate, and the viscosity $\eta = \eta(|\dot{\gamma}|)$. The shear stress σ in a viscometric flow is given by $\sigma = \eta(|\dot{\gamma}|)\dot{\gamma}$. The *viscometric fluidity function* ϕ is a function of the magnitude of the shear stress $|\sigma|$, and we define it through

$$\dot{\gamma} = \phi(|\sigma|)\sigma. \tag{7.3.5}$$

In purely viscous fluids, it follows from (7.3.5) that

$$\dot{\gamma} = \phi(|\sigma|)\sigma = \phi(|\sigma|)\eta(|\dot{\gamma}|)\dot{\gamma}, \tag{7.3.6}$$

which means that the viscometric fluidity function is the reciprocal of the viscosity function.

In viscoplastic fluids, this reciprocity does not hold because the shear rate is zero till the shear stress exceeds the yield stress. Nevertheless, the shear rate is a unique function of the shear stress in such fluids; see Fig. 7.3. That is, for viscoplastic fluids, there is a unique relation between $\dot{\gamma}$ and the shear stress σ through the function $\phi(|\sigma|)$ even when the fluid has not yielded. This is exploited in what follows through several examples.[3]

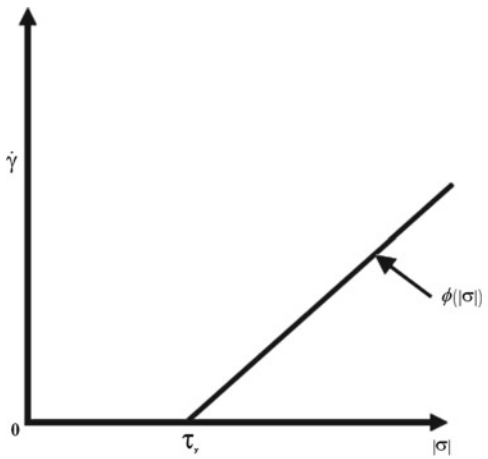

Fig. 7.3 The fluidity function for a Bingham fluid

[3] The material in the remainder of this section is derived from [13], with minor modifications and additions.

In a power law fluid, the two functions are:

$$\eta(|\dot{\gamma}|) = K|\dot{\gamma}|^{m-1}, \quad \phi(|\sigma|) = \left(\frac{1}{K}\right)^{1/m} |\sigma|^{(1-m)/m}, \tag{7.3.7}$$

where $K > 0$ is a constant and $m > 0$ is the power law index. For $m = 1$, we get the Newtonian fluid and $K = \eta$, the constant viscosity of the fluid.

If the fluid is viscoplastic, then the shear rate is zero when the magnitude of the shear stress is below the yield stress, and is non-zero otherwise. Hence, the viscometric fluidity function must be zero in the former instance and non-zero when the magnitude of the shear stress exceeds the yield stress. So, in a Bingham fluid, the fluidity function is defined through

$$\phi(|\sigma|) = 0, \quad |\sigma| \leq \tau_y, \quad \phi(|\sigma|) = \frac{|\sigma| - \tau_y}{\eta|\sigma|}, \quad |\sigma| \geq \tau_y, \tag{7.3.8}$$

where η is the viscosity and τ_y is the yield stress. Both of these are constants, of course. In a Herschel-Bulkley fluid, the corresponding fluidity function can be obtained from the constitutive relation for the shear stress-shear rate, which is:

$$\sigma = \tau_y + k_b|\dot{\gamma}|^{m-1}\dot{\gamma}, \quad \sigma \geq \tau_y. \tag{7.3.9}$$

Thus,

$$\phi(|\sigma|) = 0, \quad |\sigma| \leq \tau_y, \quad \phi(|\sigma|) = \left(\frac{|\sigma| - \tau_y}{k_b}\right)^{1/m} \cdot \frac{1}{|\sigma|}, \quad |\sigma| \geq \tau_y. \tag{7.3.10}$$

Clearly, the Bingham model is recovered if $m = 1$ and $k_b = \eta$. Next, for the Casson fluid, the constitutive relation is given by:

$$\sqrt{\sigma} = \sqrt{\tau_y} + \sqrt{k_c\dot{\gamma}}, \tag{7.3.11}$$

where $\dot{\gamma} \geq 0$. Thus, the fluidity function is

$$\phi(|\sigma|) = 0, \quad |\sigma| \leq \tau_y, \quad \phi(|\sigma|) = \frac{\left(\sqrt{|\sigma|} - \sqrt{\tau_y}\right)^2}{k_c|\sigma|}, \quad |\sigma| \geq \tau_y. \tag{7.3.12}$$

7.3.2 Papanastasiou Model

The Papanastasiou model requires some analysis because one has to invert an exponential function. Recall from (4.4.6) that the shear stress is given by

$$\sigma = \eta_0 \dot{\gamma} + \tau_y [1 - \exp(-m\dot{\gamma})], \tag{7.3.13}$$

when $\dot{\gamma} \geq 0$. The non-dimensional form of the above equation is to be preferred here and introducing a characteristic length scale L and a velocity scale U, the Bingham number $\mathrm{Bn} = \tau_y L/\eta_0 U$, and scaling the shear stress accordingly, the non-dimensional form of the above equation becomes:

$$|\sigma| = |\dot{\gamma}| + \mathrm{Bn}\,[1 - \exp(-m|\dot{\gamma}|)]. \tag{7.3.14}$$

Thus,

$$|\dot{\gamma}| + \mathrm{Bn} - |\sigma| = \mathrm{Bn} \exp(-m|\dot{\gamma}|). \tag{7.3.15}$$

Multiplying throughout by $m \exp\left[m\left(|\dot{\gamma}| + \mathrm{Bn} - |\sigma|\right)\right]$, one obtains

$$m\left(|\dot{\gamma}|+\mathrm{Bn}-|\sigma|\right) \exp\left[m\left(|\dot{\gamma}|+\mathrm{Bn}-|\sigma|\right)\right] = m\,\mathrm{Bn} \exp\left[m\left(\mathrm{Bn}-|\sigma|\right)\right]. \tag{7.3.16}$$

This equation is of the form $We^W = z$, where z may be complex. The solution $W = W(z)$ is called the Lambert W function [14], and we find that [15]

$$m\left(|\dot{\gamma}| + \mathrm{Bn} - |\sigma|\right) = W\left(m\ \mathrm{Bn} \exp\left[m\left(\mathrm{Bn} - |\sigma|\right)\right]\right). \tag{7.3.17}$$

Thus,

$$|\dot{\gamma}| = |\sigma| - \mathrm{Bn} + \frac{1}{m} W\left(m\ \mathrm{Bn} \exp\left[m\left(\mathrm{Bn} - |\sigma|\right)\right]\right). \tag{7.3.18}$$

Since $|\dot{\gamma}| = \phi(|\sigma|)|\sigma|$, it follows that the fluidity function is given by

$$\phi(|\sigma|) = \frac{1}{|\sigma|}\left[|\sigma| - \mathrm{Bn} + \frac{1}{m} W\left(m\ \mathrm{Bn} \exp\left[m\left(\mathrm{Bn} - |\sigma|\right)\right]\right)\right]. \tag{7.3.19}$$

Some comments are in order here. First of all, on the right side of Eq. (7.3.16), the numbers m, Bn and $\exp[m(\mathrm{Bn}-|\sigma|)]$ are all positive. Hence, in (7.3.17), the Lambert W function is such that $W = W(x) > 0$, since $x > 0$ [14]. In this situation, it is also known that the Lambert W function is single valued as well. Thus, one does not have to consider multiple branches of this function.

Secondly, if $|\sigma| = 0$ in Eq. (7.3.18), one has

$$|\dot{\gamma}| = -\mathrm{Bn} + \frac{1}{m} W\left(m\ \mathrm{Bn} \exp\left[m\ \mathrm{Bn}\right]\right). \tag{7.3.20}$$

Now, it is known that $W(\alpha \exp[\alpha]) = \alpha$. Using this, one can see that $|\dot{\gamma}| = 0$ in (7.3.20). In other words, just as Eq. (7.3.14) shows that $|\sigma| = 0$ when $|\dot{\gamma}| = 0$, the

solution (7.3.18), expressed in terms of the Lambert W function, proves the converse, as it should.

7.3.3 The Symmetric Case

Let us now return to Eq. (7.3.2) and integrate it to obtain

$$\mathbf{s}(x, y, z) = z\nabla_2 p(x, y), \tag{7.3.21}$$

where the vanishing of the shear stress vector along the centreline, i.e., $\mathbf{s}(x, y, 0) = \mathbf{0}$ has been used. The above equation tells us that $|\mathbf{s}| = |z\nabla_2 p|$ is defined, which permits us to extend the definition of the viscometric fluidity function to two-dimensional flows so that

$$\partial_z \mathbf{u} = \phi(|\mathbf{s}|)\mathbf{s}. \tag{7.3.22}$$

Noting that in the one-dimensional shear flow, the velocity $u = u(z)$ is positive when $-\partial p/\partial x = G > 0$, it follows from Eqs. (7.3.2), (7.3.21) and (7.3.22) that

$$\mathbf{u}(x, y, z) = -\left(\int_{-H}^{z} \phi(|\zeta \nabla_2 p|)\zeta \, d\zeta \right) \nabla_2 p, \tag{7.3.23}$$

where we have used the fact that the velocity field vanishes at $z = -H$. Hence, we obtain the average velocity field:

$$\overline{\mathbf{u}}(x, y) = -\frac{1}{H}\left(\int_{-H}^{0} \phi(|z\nabla_2 p|)z \, dz \right) \nabla_2 p, \tag{7.3.24}$$

where the symmetry of the velocity field about $z = 0$ has been employed. From this result, we find that $\nabla_2 \cdot \overline{\mathbf{u}} = 0$ leads to a partial differential equation for $p = p(x, y)$ as in the case of the Newtonian fluid [9].

7.3.4 The Average Velocity Field in the Symmetric Case

In order to derive the average velocity field, we turn to a unidirectional Hele-Shaw flow with a constant pressure gradient $G > 0$. That is, let $\mathbf{u} = u(z)\mathbf{i}$, where $-H \leq z \leq H$. The equation of motion now becomes

$$\frac{\partial p}{\partial x} = -G = \frac{\partial \sigma}{\partial z}. \tag{7.3.25}$$

Thus,

$$\sigma = -Gz, \quad -H \le z \le H. \tag{7.3.26}$$

Next, the average velocity is given by

$$\overline{u} = \frac{1}{H}\int_{-H}^{0} u(z)\,dz = -\frac{1}{H}\int_{-H}^{0} zu'(z)\,dz, \tag{7.3.27}$$

where we have used integration by parts and that $u(-H) = 0$. Now, it is obvious that in $-H \le z \le 0$, the shear stress $\sigma = -Gz \ge 0$, and $u' \ge 0$ as well. Hence, in this region, $u' = \phi(\sigma)\sigma$. Thus, for a viscous fluid, we obtain the average velocity field:

$$\overline{u} = \frac{1}{G^2 H}\int_{0}^{\sigma_w} \phi(\sigma)\sigma^2\,d\sigma, \tag{7.3.28}$$

where $\sigma_w = GH$ is the shear stress at the wall.

For a power law fluid, we use Eqs. (7.3.7) and (7.3.28) to obtain

$$\overline{u} = \frac{Hm}{1+2m}\Big(GH/K\Big)^{1/m}. \tag{7.3.29}$$

From this, one can solve for G:

$$G = \frac{K(1+2m)^m \overline{u}^m}{H^{m+1} m^m}, \tag{7.3.30}$$

which has been derived by Alexandrou and Entov [16]; see their Eq. (5).

In order to convert (7.3.29) to a form suitable for the averaged velocity field $\overline{\mathbf{u}}$, one writes $G^{1/m} = G^{(1-m)/m} \cdot G$, where $G = -\partial p/\partial x > 0$. Thus, one obtains

$$\overline{\mathbf{u}} = -\left[\frac{Hm}{1+2m}\Big(H/K\Big)^{1/m} |\nabla_2 p|^{(1-m)/m}\right]\nabla_2 p, \tag{7.3.31}$$

a result obtained by Aronsson and Janfalk [17]. In particular, for a Newtonian fluid, $m = 1$ and $K = \eta_0$, the constant viscosity. Thus,

$$\overline{\mathbf{u}} = -\frac{H^2}{3\eta_0}\nabla_2 p, \tag{7.3.32}$$

which means that the averaged velocity field is derivable from a potential.

If the fluid is viscoplastic with a constant yield stress τ_y, then $u' = 0$ in the region $-h \le z \le 0$, where $h = \tau_y/G \le H$. In this case, we find that

$$\overline{u} = \frac{1}{G^2 H} \int_{\tau_y}^{\sigma_w} \phi(\sigma)\sigma^2 \, d\sigma. \tag{7.3.33}$$

For a Bingham fluid, the average velocity can deduced from Eqs. (7.3.8) and (7.3.33):

$$\overline{u} = \frac{H\sigma_w}{3\eta}\left[1 - \frac{3}{2}\left(\frac{\tau_y}{\sigma_w}\right) + \frac{1}{2}\left(\frac{\tau_y}{\sigma_w}\right)^3\right], \quad \sigma_w > \tau_y. \tag{7.3.34}$$

Of course, one can rewrite Eq. (7.3.34) by using $\sigma_w = GH$ and derive

$$\overline{u} = \frac{GH^2}{3\eta}\left[1 - \frac{3}{2}\left(\frac{\tau_y}{GH}\right) + \frac{1}{2}\left(\frac{\tau_y}{GH}\right)^3\right], \quad GH > \tau_y. \tag{7.3.35}$$

From the above result, it is obvious that $\overline{\mathbf{u}} = \mathbf{0}$ if $|\nabla_2 p| \leq \tau_y/H$, and

$$\overline{\mathbf{u}} = -\frac{H^2}{3\eta}\left[1 - \frac{3}{2}\left(\frac{\tau_y}{H|\nabla_2 p|}\right) + \frac{1}{2}\left(\frac{\tau_y}{H|\nabla_2 p|}\right)^3\right]\nabla_2 p, \quad |\nabla_2 p| > \tau_y/H. \tag{7.3.36}$$

Needless to say, the corresponding results for the Herschel-Bulkley and Casson fluids can be established in a manner similar to that used in the derivation of Eqs. (7.3.33) and (7.3.34). However, the task of obtaining the average velocity field $\overline{\mathbf{u}}$ for the Papanastasiou model has yet to be completed. Note that one has to substitute the expression for $\phi(|\sigma|)$ into (7.3.28) to obtain the average velocity field.

7.3.5 Hele-Shaw Flow Equations

If the material is an incompressible Newtonian fluid, the Hele-Shaw flow equations can be derived from (7.3.32) and one finds that the pressure field satisfies the Laplace's equation:

$$\nabla \cdot \overline{\mathbf{u}} = \frac{\partial^2 p}{\partial x^2} + \frac{\partial^2 p}{\partial y^2} = 0, \quad \nabla_2^2 p = 0. \tag{7.3.37}$$

Of course, the average velocity field can also be obtained from the stream function $\psi = \psi(x, y)$, such that $\overline{u} = \partial\psi/\partial y$, $\overline{v} = -\partial\psi/\partial x$. Since p is harmonic, it follows that ψ is also harmonic, and these two functions are conjugate functions of each other.

In the case of a power law fluid, one obtains [17]

$$\nabla_2 \cdot \left(|\nabla_2 p|^{(1-m)/m}\nabla_2 p\right) = 0. \tag{7.3.38}$$

The stream function satisfies

$$\nabla_2 \cdot \left(|\nabla_2 \psi|^{m-1} \nabla_2 \psi \right) = 0. \tag{7.3.39}$$

For a comprehensive discussion of the solutions of these equations, see [17].

7.3.6 The Asymmetric Case

In several applications of injection moulding [18], the Hele-Shaw flow is assumed to occur between two parallel planes at $z = \pm H$ once again; however, adjacent to each wall, there is a frozen layer of material so that the molten plastic flows between two curves $z = h^-(x, y)$ and $z = h^+(x, y)$. The equations of motion are again given by

$$\nabla_2 p = \partial_z \mathbf{s}. \tag{7.3.40}$$

Integration with respect to z leads to

$$\mathbf{s}(z) = z\nabla_2 p + \mathbf{s}(h^-) - h^- \nabla_2 p, \tag{7.3.41}$$

where, for brevity, we have suppressed the dependence on (x, y) so that $\mathbf{s}(z) = \mathbf{s}(x, y, z)$, $h^- = h^-(x, y)$, and so on. Applying the viscometric fluidity function and letting $\phi(z)$ stand for $\phi(|\mathbf{s}(z)|)$, we find that

$$\partial_z \mathbf{u} = -\phi(z) z \nabla_2 p - \phi(z)\mathbf{A}, \tag{7.3.42}$$

where $\mathbf{A} = \mathbf{A}(x, y)$ is the vector

$$\mathbf{A} = \mathbf{s}(h^-) - h^- \nabla_2 p. \tag{7.3.43}$$

Thus, using the no-slip condition at $z = h^-$, we obtain the velocity field:

$$\mathbf{u}(z) = -\nabla_2 p \left(\int_{h^-}^{z} \phi(\zeta)\zeta \, d\zeta \right) - \mathbf{A} \int_{h^-}^{z} \phi(\zeta) \, d\zeta. \tag{7.3.44}$$

Since $\mathbf{u} = \mathbf{0}$ on $z = h^+$ as well, we find that

$$\nabla_2 p \left(\int_{h^-}^{h^+} \phi(z) z \, dz \right) + \mathbf{A} \int_{h^-}^{h^+} \phi(z) \, dz = \mathbf{0}. \tag{7.3.45}$$

It is now obvious that the vector $\mathbf{A}$ arises when the flow is not symmetric about the centreline $z = 0$. To prove this, let us consider the symmetric case where $h^+ = -h^- = H$ and $\phi(z) = \phi(-z),\ 0 \le z \le H$. It is easy to see that the integrand $\phi(z)z$ is an odd function of z. Hence,

$$\int_{-H}^{H} \phi(z) z \, dz = 0. \tag{7.3.46}$$

Consequently, from Eq. (7.3.45), we see that the vector $\mathbf{A} = \mathbf{0}$ under symmetric flow conditions and we recover Eq. (7.3.23) for the velocity field $\mathbf{u}(z)$ from Eq. (7.3.44).

Returning to the asymmetric case and assuming that the flow is not totally frozen, i.e., that

$$\int_{h^-}^{h^+} \phi(z) \, dz \neq 0, \tag{7.3.47}$$

we find from Eq. (7.3.45) that the vector $\mathbf{A} = -C\nabla_2 p$, where the function $C = C(x, y)$ is given by

$$C = \frac{\int_{h^-}^{h^+} \phi(z) z \, dz}{\int_{h^-}^{h^+} \phi(z) \, dz}. \tag{7.3.48}$$

Hence, Eq. (7.3.39) may be rewritten as

$$\mathbf{u}(z) = \left[\int_{h^-}^{z} \phi(\zeta)\zeta \, d\zeta - C \int_{h^-}^{z} \phi(\zeta) \, d\zeta \right] \nabla_2 p. \tag{7.3.49}$$

From this, the average velocity field $\overline{\mathbf{u}}$ can be obtained as follows:

$$[h^+ - h^-]\overline{\mathbf{u}} = \left[\int_{h^-}^{h^+} \left(\int_{h^-}^{z} \phi(\zeta)\zeta \, d\zeta \right) dz - C \int_{h^-}^{h^+} \left(\int_{h^-}^{z} \phi(\zeta) \, d\zeta \right) dz \right] \nabla_2 p. \tag{7.3.50}$$

Integration by parts shows that

$$\int_{h^-}^{h^+} \left(\int_{h^-}^{z} \phi(\zeta)\zeta \, d\zeta \right) dz = \int_{h^-}^{h^+} \phi(z)[h^+ z - z^2] \, dz, \tag{7.3.51}$$

and

$$\int_{h^-}^{h^+} \left(\int_{h^-}^{z} \phi(\zeta)\, d\zeta \right) dz = \int_{h^-}^{h^+} \phi(z)[h^+ - z]\, dz. \tag{7.3.52}$$

Consequently,

$$[h^+ - h^-]\overline{\mathbf{u}} = \left[\int_{h^-}^{h^+} \phi(z)[h^+ z - z^2]\, dz - C \int_{h^-}^{h^+} \phi(z)[h^+ - z]\, dz \right] \nabla_2 p. \tag{7.3.53}$$

Replacing C by its form in Eq. (7.3.48), we obtain

$$[h^+ - h^-]\overline{\mathbf{u}} = \left[-\int_{h^-}^{h^+} \phi(z) z^2\, dz + \frac{\left(\int_{h^-}^{h^+} \phi(z) z\, dz \right)^2}{\int_{h^-}^{h^+} \phi(z)\, dz} \right] \nabla_2 p. \tag{7.3.54}$$

In injection moulding, this relation is expressed through the *fluidity function* S_2 as follows:

$$\overline{\mathbf{u}} = -\frac{2S_2}{h^+ - h^-} \nabla_2 p, \tag{7.3.55}$$

where

$$S_2 = \frac{1}{2} \left[\int_{h^-}^{h^+} \phi(z) z^2\, dz - \frac{\left(\int_{h^-}^{h^+} \phi(z) z\, dz \right)^2}{\int_{h^-}^{h^+} \phi(z)\, dz} \right]. \tag{7.3.56}$$

The derivation of S_2 given here follows closely that in Sect. 5.3 of the book by Kennedy [18]. In it, attention is focussed on viscous fluids only and the viscosity function $\eta(|\dot{\gamma}|)$ is employed instead of the viscometric fluidity function. Clearly, the derivation of the relevant equations for the Hele-Shaw flows, as presented here, applies to both viscous and viscoplastic fluids.

It is obvious that one can obtain the fluidity function S_2 for the symmetric case from Eq. (7.3.56), which leads to

$$S_2 = \frac{1}{2} \int_{-H}^{H} \phi(z) z^2\, dz. \tag{7.3.57}$$

For purely viscous fluids, this takes the familiar form [9, 18]

$$S_2 = \frac{1}{2} \int_{-H}^{H} \frac{z^2}{\eta(z)}\, dz, \tag{7.3.58}$$

because, as demonstrated in Eq. (7.3.6) above, the viscometric fluidity function is the reciprocal of the viscosity in this case.

At present, there are no applications of the viscometric fluidity function to the Hele-Shaw flows of viscoplastic fluids. However, it has been used to study the filling problem in injection moulding; see Chap. 3 in [19].

7.4 Linearised Stability Analysis

In the linearised theory of stability, time dependent disturbances of order $O(\varepsilon)$ are imposed on a given steady main flow and the stability of the latter is examined.[4] For example, consider the steady flow of a Newtonian fluid in a channel under a constant pressure drop per unit length. The linearised stability theory of this flow is classical and a great deal of research has been done due to the large discrepancy which exists between the critical Reynolds number computed for linearised stability and those observed experimentally. For the channel flow, Squire's theorem [21] implies that three-dimensional infinitesimal disturbances are more stable than two-dimensional disturbances for all wave numbers. Accurate numerical solution of the corresponding Orr-Sommerfeld problem, due to Orszag [22], gives the linearised stability limit for the Reynolds number Re* = 5722.4, where Re* is computed from the maximal velocity in the channel and its half-width. Experimental observations indicate that instability occurs at Re* $\approx$ 1,000. Attempts to remove this discrepancy resulted in research into weakly nonlinear stability theory and additional work on linearised stability theory, with the latter being more successful in explaining the transition to turbulence. See Chapman [23] for a comprehensive discussion of this matter. Thus, the study of the linearised stability of the channel flow of a Bingham fluid has a great deal of merit and is important.

To begin, consider the steady flow of a Bingham fluid in a channel under a constant pressure drop per unit length. The velocity field is given by (1.4.5) in the sheared region and by (1.4.6) in the plug, with the location of the yield surface derived in (1.4.1). For a channel of width H, which is the chosen length scale, and a wall shear stress of magnitude σ_w, a velocity scale can be chosen through

$$U_0 = \frac{H\sigma_w}{2\eta}\left(1 - \frac{\tau_y}{\sigma_w}\right)^2. \tag{7.4.1}$$

One can now scale the pressure and stress fields with respect to ρU_0^2.

The Reynolds number is $\mathrm{Re} = \rho U_0 H/\eta$, and the Bingham number is $\mathrm{Bn} = \tau_y H/\eta U_0$. Let $\mathbf{A}$ be the non-dimensional form of the first Rivlin-Ericksen tensor. Using this, the non-dimensional form of the constitutive equation for the Bingham fluid is more conveniently written as

[4] An excellent introduction to linearised hydrodynamic stability theory of the flows of Newtonian fluids has been written by Lin [20].

$$\mathbf{S} = \frac{1}{\mathrm{Re}}\eta(K(\mathbf{A})), \quad \eta(K(\mathbf{A})) = \eta + \frac{\mathrm{Bn}}{K(\mathbf{A})}, \quad T(\mathbf{S}) > \frac{\mathrm{Bn}}{\mathrm{Re}}, \tag{7.4.2}$$

with

$$\mathbf{A} = \mathbf{0}, \quad T(\mathbf{S}) \leq \frac{\mathrm{Bn}}{\mathrm{Re}}. \tag{7.4.3}$$

Finally, the base flow solution has the pressure field given by

$$P(x) = -\frac{\sigma_w}{\tau_y} \cdot \frac{\mathrm{Bn}}{\mathrm{Re}}\, x, \tag{7.4.4}$$

and the velocity field $\mathbf{U} = U_0(y)\mathbf{j}$, where

$$U_0(y) = \begin{cases} 1, & 0 \leq |y| \leq \tau_y/\sigma_w, \\ 1 - \Big([|y| - \tau_y/\sigma_w]/[1 - \tau_y/\sigma_w]\Big)^2, & \tau_y/\sigma_w \leq |y| \leq 1. \end{cases} \tag{7.4.5}$$

Now, consider an infinitesimal disturbance of the form $(\varepsilon p, \varepsilon \mathbf{u})$, $\varepsilon << 1$, superimposed on the primary flow $(P, \mathbf{U})$ described above. The perturbed flow field satisfies the following equations [24]:

$$\nabla \cdot [\mathbf{U} + \varepsilon \mathbf{u}] = 0, \tag{7.4.6}$$

$$\varepsilon \mathbf{u}_t + \Big((\mathbf{U} + \varepsilon \mathbf{u}) \cdot \nabla\Big)\Big(\mathbf{U} + \varepsilon \mathbf{u}\Big) = -\nabla(P + \varepsilon p) + \nabla \cdot (\mathbf{S} + \varepsilon \mathbf{S}^*). \tag{7.4.7}$$

Whenever $T(\mathbf{S} + \varepsilon \mathbf{S}^*) > \mathrm{Bn}/\mathrm{Re}$, one notes that $\mathbf{S}$ is derived from the base flow and $\mathbf{S}^*$ is obtained from the disturbance to the primary velocity field. The equations of motion for the linearised disturbances can be derived, retaining terms of order ε only. These are:

$$\nabla \cdot \mathbf{u} = 0, \tag{7.4.8}$$

$$u_t + vU_y + Uu_x = -p_x + \frac{1}{\mathrm{Re}}\nabla^2 u + \frac{\mathrm{Bn}}{\mathrm{Re}}\left(\frac{\nabla^2 u - u_{yy} - v_{yx}}{K(\mathbf{u})}\right), \tag{7.4.9}$$

$$\begin{aligned} v_t + Uv_x &= -p_y + \frac{1}{\mathrm{Re}}\nabla^2 v \\ &\quad + \frac{\mathrm{Bn}}{\mathrm{Re}}\left(2v_y \frac{d}{dy}\left[\frac{1}{K(\mathbf{u})}\right] + \frac{\nabla^2 v - v_{xx} - u_{yx}}{K(\mathbf{u})}\right), \end{aligned} \tag{7.4.10}$$

$$\begin{aligned} w_t + Uw_x &= -p_z + \frac{1}{\mathrm{Re}}\nabla^2 w \\ &\quad + \frac{\mathrm{Bn}}{\mathrm{Re}}\left((v_z + w_y)\frac{d}{dy}\left[\frac{1}{K(\mathbf{u})}\right] + \frac{\nabla^2 w}{K(\mathbf{u})}\right), \end{aligned} \tag{7.4.11}$$

where ∇^2 is the three dimensional Laplacian, and $U_y = dU/dy$, $u_x = \partial u/\partial x$, etc.

At the fixed boundaries of the flow region, there is no slip, i.e., $\mathbf{u} = \mathbf{0}$ on $y = \pm 1$. The perturbation $(\varepsilon p, \varepsilon \mathbf{u})$ is assumed to be periodic in the x- and z-directions, say with periods $2X$ and $2Z$ respectively. Just as in the case of the flow in a wavy channel, it is assumed that the yield surfaces change slightly to

$$y_+ = (\tau_y/\sigma_w) + \varepsilon h_+(x, z, t), \quad y_- = (\tau_y/\sigma_w) + \varepsilon h_-(x, z, t), \tag{7.4.12}$$

where h_+ and h_- are also periodic in x and z. The linearisations for the temporal and spatial derivatives of the perturbations are quite complicated to obtain, for one has to consider the perturbation of the yield surface as well as the equations of motion. The first requirement is that at the yield surface, the following holds:

$$K(\mathbf{A}(\mathbf{U} + \varepsilon \mathbf{u})) = 0, \quad \text{at } y = y_+, \ y_-. \tag{7.4.13}$$

Writing $\mathbf{A}(\mathbf{U} + \varepsilon \mathbf{u}) = \mathbf{A}(\mathbf{U}) + \varepsilon \mathbf{A}(\mathbf{u})$, the components of the latter tensor can be determined at the locations $(x, \pm(\tau_y/\sigma_w), z, t)$. It turns out that each component is zero, except

$$\begin{aligned} A_{xy}(x, \tau_y/\sigma_w, z, t) &= u_y(x, \tau_y/\sigma_w, z, t) + v_y(x, \tau_y/\sigma_w, z, t) \\ &= \frac{2h_+(x, z, t)}{(1 - \tau_y/\sigma_w)^2}, \end{aligned} \tag{7.4.14}$$

$$\begin{aligned} A_{xy}(x, -\tau_y/\sigma_w, z, t) &= u_y(x, -\tau_y/\sigma_w, z, t) + v_y(x, -\tau_y/\sigma_w, z, t) \\ &= -\frac{2h_-(x, z, t)}{(1 - \tau_y/\sigma_w)^2}. \end{aligned} \tag{7.4.15}$$

The second is that Cauchy's equations of motion, viz.,

$$\int_{\Omega} \rho \frac{d(\mathbf{U} + \varepsilon \mathbf{u})}{dt} \, dv = \int_{\partial\Omega} \mathbf{T}\mathbf{n} \, dS \tag{7.4.16}$$

be linearised as well. Here, we note that $d\mathbf{U}/dt = \mathbf{0}$ for the base flow. Hence, the total stress tensor meets $\nabla \cdot \mathbf{T}(\mathbf{U}) = \mathbf{0}$, where $T(\mathbf{U}) = -P\mathbf{1} + \mathbf{S}(\mathbf{U})$ is the stress tensor associated to the base flow. Of course, for the perturbed flow, one has

$$T(\mathbf{U} + \varepsilon \mathbf{u}) = -P\mathbf{1} - \varepsilon p\mathbf{1} + \mathbf{S}(\mathbf{U} + \varepsilon \mathbf{u}). \tag{7.4.17}$$

In addition, one has to realise that the unit normal vector $\mathbf{n}$ to the perturbed yield surface occurs in (7.4.16), and that $d(\varepsilon \mathbf{u})/dt = \varepsilon \partial \mathbf{u}/\partial t + O(\varepsilon^2)$.

Next, the periodicity of the perturbation $\mathbf{u}$ in x and z permits one to obtain the value of $d(\varepsilon \mathbf{u})/dt$ by averaging over the volume: $-X \le x \le X$, $-(\tau_y/\sigma_w + \varepsilon h_-) \le y \le (\tau_y/\sigma_w + \varepsilon h_+)$, $-Z \le z \le Z$. Thus, to the first order,

$$\int_{-X}^{X}\int_{-Z}^{Z}\int_{-\tau_y/\sigma_w-\varepsilon h_-}^{\tau_y/\sigma_w+\varepsilon h_+}\frac{d(\varepsilon\mathbf{u})}{dt}\,dv=\varepsilon\frac{8XZ\tau_y}{\sigma_w}\frac{\partial\mathbf{u}}{\partial t}(x,\pm\frac{\tau_y}{\sigma_w},z,t)+O(\varepsilon^2). \tag{7.4.18}$$

The unit external normal $\mathbf{n}$ to the upper perturbed surface has the components:

$$\mathbf{n}=\left(\varepsilon\frac{\partial h_+}{\partial x},1,\varepsilon\frac{\partial h_+}{\partial z}\right)+O(\varepsilon^2), \tag{7.4.19}$$

while that normal to the lower surface has the components:

$$\mathbf{n}=\left(\varepsilon\frac{\partial h_-}{\partial x},1,\varepsilon\frac{\partial h_-}{\partial z}\right)+O(\varepsilon^2). \tag{7.4.20}$$

Omitting additional details, the outcome of the linearisation is:

$$u_t(x,\pm\tau_y/\sigma_w,z,t)=\frac{\sigma_w^2\,\mathrm{Bn}}{\tau_y^2\,\mathrm{Re}}\frac{1}{8XZ}\int_{-X}^{X}\int_{-Z}^{Z}[h_+(x',z',t)+h_-(x',z',t)]\,dx'\,dz', \tag{7.4.21}$$

$$v_t(x,\pm\tau_y/\sigma_w,z,t)=\frac{\sigma_w}{\tau_y}\frac{1}{8XZ}\int_{-X}^{X}\int_{-Z}^{Z}[p(x',-\tau_y/\sigma_w,z',t)-p(x',\tau_y/\sigma_w,z',t)]\,dx'\,dz', \tag{7.4.22}$$

$$w_t(x,\pm\tau_y/\sigma_w,z,t)=0. \tag{7.4.23}$$

The final results are:

- Consider one-dimensional perturbations of the type:

$$(p,\mathbf{u},h_+,h_-)\sim(p(y),\mathbf{u}(y),h_+,h_-)e^{\sigma t},\quad \sigma=\mu+i\nu. \tag{7.4.24}$$

  If $\sigma=0$, the flow is simply a variant of the steady channel flow with a change in $u(y)$ due to a variation of the pressure drop per unit length. This normal mode corresponds to a straightforward expansion or contraction of the plug region. If $\sigma\neq 0$, it turns out that $\mu<0$ for all values of the Reynolds number. In conclusion, this normal mode is unconditionally linearly stable.
- If two dimensional perturbations are to be examined, introduce a stream function $\psi=\psi(x,y,t)$ and let $u=\partial\psi/\partial y$, and $v=-\partial\psi/\partial x$. In normal mode, the solution may be written as

$$(\psi,p,h_+,h_-)=(f(y),p(y),h_+,h_-)e^{i\alpha(x-\sigma t)}. \tag{7.4.25}$$

Considering the case when $\alpha > 0$, this leads to an Orr-Sommerfeld equation for the Bingham fluid which has to be solved numerically to find the phase velocity σ. Note that the flow will be stable if the imaginary part of σ is negative, i.e., $\nu < 0$.

- The minimum Reynolds number for the two dimensional perturbations increases almost linearly with increasing Bingham number i.e., Re = O(Bn). That is, the flow in a channel of a Bingham fluid is more stable than that of a Newtonian fluid with Bn = 0.
- The linear stability bounds provide a theoretical upper bound on the Reynolds number needed for transition [25]; see Sect. 9.5.

If one considers three dimensional disturbances, where each component of the perturbation has the form:

$$q(x, y, z, t) = f(y)e^{i(\alpha x+\beta z-\sigma t)}, \tag{7.4.26}$$

the following results can be obtained [26]:

- For short wave lengths, the flow in a Bingham fluid will be more stable for larger Reynolds numbers than that for a Newtonian fluid.
- As the Bingham number Bn $\to \infty$, the critical Reynolds number is of the form Re = $O(\text{Bn}^{3/4})$.
- For long wave lengths, this bound can be improved to Re = O(Bn), which is identical to the result obtained in the study of two-dimensional disturbances.

Additional research [27] into the stability of the flow in a channel using both modal and non-modal disturbances has led to the following conclusions:

- The modal approach shows that the channel flow is linearly stable. In particular, if one considers stream wise perturbations, i.e., changes to (v, w) only are considered with $\beta = 0$ in (7.4.26), the effect of the Bingham number is less significant than that for span wise perturbations for (u, v) with $\alpha = 0$, and oblique perturbations of either (u, v) or (v, w) when $\alpha \neq 0,\ \beta \neq 0$.
- Regarding non-modal disturbances, it is found that the Bingham yield stress dissipation terms reduce the degree of non-normality. This is because the vanishing of the disturbances at the yield surface and the increased viscous dissipation reduce the energy transient growth compared with that in a Newtonian fluid for all wave numbers. In particular, the effect of the Bingham number is much weaker for a stream wise perturbation than for a span wise or oblique one.

In conclusion, one can assert that the channel flow of a Bingham fluid is more stable than that in a Newtonian fluid, and that the critical Reynolds number Re increases with the Bingham number Bn.

Thus, it is surprising to discover that the helical flow of a Bingham fluid due to a co-rotating regime and the axial motion of the inner cylinder is less stable than that of a Newtonian fluid [28, 29]. To make this precise, denote the azimuthal, basic flow by $v = V(r)$ in the cylindrical geometry. Let the velocity perturbations in the radial, azimuthal and axial directions along with that of the pressure be of the modal form:

$$(u, v, w, p) \sim (u(r), v(r), w(r), p(r))e^{i(kz-\sigma t)}. \tag{7.4.27}$$

Deriving the relevant eigenvalue problems for (u, v), it has been found that the critical inner Reynolds number does not increase monotonically with the Bingham number Bn, over a range of small to moderate Bn. The reason for the reduction in the Reynolds number is due to an increase in the rate of strain of the basic flow which, in turn, amplifies the transfer of energy to the perturbation through the inertial terms in the energy equation [28, 29]. For larger Bn, the yielded region contracts as expected and the inertial energy transfer is bounded by the yield stress dissipation, similar to that found in the case of non-modal disturbances of the channel flow.

7.5 Summary

To pose the problem concerned with the flow in a wavy channel, or the Hele-Shaw flows, or that concerned with the linearised stability of a channel or a helical flow is, as shown above, not an easy task. Their solution requires, once again, a great deal of ingenuity and hard analysis, followed by some highly challenging numerical implementation.

References

1. Reynolds O (1886) On the theory of lubrication and its application to Mr. Beauchamp Tower's experiments, including an experimental determination of the viscosity of olive oil. Philos Trans R Soc Lond 177:157–234
2. Tao LN (1959) General solution of the Reynolds equation for a journal bearing of finite width. Q Appl Math 17:129–136
3. Cimatti G (1977) On a problem of the theory of lubrication governed by a variational inequality. Appl Math Optim 3:227–242
4. Huilgol RR (1994) Some comments on the paper by Lipscomb and Denn. Department of Mathematics and Statistics, Flinders University, Research Report
5. Lipscomb GG, Denn MM (1984) Flow of Bingham fluid in complex geometries. J Non-Newton Fluid Mech 14:337–346
6. Roustaei A, Frigaard IA (2013) The occurrence of fouling layers in the flow of a yield stress fluid along a wavy-walled channel. J Non-Newton Fluid Mech 198:109–124
7. Frigaard IA, Ryan DP (2004) Flow of a visco-plastic fluid in a channel of slowly varying width. J Non-Newton Fluid Mech 123:67–83
8. Putz A, Frigaard IA, Martinez DM (2009) On the lubrication paradox and the use of the regularisation methods for lubrication flows. J Non-Newton Fluid Mech 163:62–77
9. Saffman PG, Taylor GI (1958) The penetration of a fluid into a porous medium or Hele-Shaw cell containing a more viscous liquid. Proc R Soc Lond A 245:312–329
10. Lindner A, Coussot P, Bonn D (2000) Viscous fingering in a yield stress fluid. Phys Rev Lett 85:314–317
11. Pipkin AC, Tanner RI (1972) A survey of theory and experiment in viscometric flows of viscoelastic liquids. In: Nemat-Nasser S (ed), Mechanics Today, vol 1, pp 262–321
12. Huilgol RR, Phan-Thien N (1997) Fluid mechanics of viscoelasticity. Elsevier, Amsterdam
13. Huilgol RR (2006) On the derivation of the symmetric and asymmetric Hele-Shaw flow equations for viscous and viscoplastic fluids using the viscometric fluidity function. J Non-Newton Fluid Mech 138:209–213

14. Corless RM, Gonnet GH, Hare DEG, Jeffrey DJ, Knuth DE (1996) On the Lambert W function. Adv Comput Math 5:329–359
15. You Z, Huilgol RR, Mitsoulis E (2008) Application of the Lambert W function to steady shearing flows of the Papanastasiou model. Int J Eng Sci 46:799–808
16. Alexandrou AN, Entov V (1997) On the steady-state advancement of fingers and bubbles in a Hele-Shaw cell filled by a non-Newtonian fluid. Eur J Appl Math 8:73–87
17. Aronsson G, Janfalk U (1992) On Hele-Shaw flow of power-law fluids. Eur J Appl Math 3:343–366
18. Kennedy P (1995) Flow analysis of injection molds. Hanser Verlag, Munich
19. Zheng R, Tanner RI, Fan X-J (2011) Injection molding: integration of theory and modeling methods. Springer, Heidelberg
20. Lin CC (1966) The theory of hydrodynamic stability. Cambridge University Press, Cambridge
21. Squire HB (1933) On the stability for three-dimensional disturbances of viscous fluid flow between parallel walls. Proc R Soc Lond, Ser A 142:621–628
22. Orszag SA (1971) Accurate solution of the Orr-Sommerfeld stability equation. J Fluid Mech 50:689–703
23. Chapman SJ (2002) Subcritical transition in channel flows. J Fluid Mech 451:35–97
24. Frigaard IA, Howison SD, Sobey IJ (1994) On the stability of Poiseuille flow of a Bingham fluid. J Fluid Mech 263:133–150
25. Nouar C, Frigaard IA (2001) Nonlinear stability of Poiseuille flow of a Bingham fluid: theoretical results and comparison with phenomenological criteria. J Non-Newton Fluid Mech 100:127–149
26. Frigaard I, Nouar C (2003) On three-dimensional linear stability of Poiseuille flow of Bingham fluids. Phys Fluids 15:2843–2851
27. Nouar C, Kabouya N, Dusek J, Mamou M (2007) Modal and non-modal linear stability of the plane Bingham-Poiseuille flow. J Fluid Mech 577:211–239
28. Peng J, Zhu K-Q (2004) Linear stability of Bingham fluids in spiral Couette flow. J Fluid Mech 512:21–45
29. Landry MP, Frigaard IA, Martinez DM (2006) Stability and instability of Taylor-Couette flows of a Bingham fluid. J Fluid Mech 560:321–353

Chapter 8
Variational Principles and Variational Inequalities

In this chapter, we shall derive two variational principles and variational inequalities for incompressible viscoplastic fluids. There is a variational principle for the velocity field and another one for the stress tensor; in both, it is necessary to ignore inertia as shown in Sect. 8.1. Surprisingly, variational inequalities can be derived even if both the body force and inertia are present under the assumption that there exists a velocity field which satisfies the equations of motion; see Sect. 8.2. This derivation is purely formal and does not address the questions of existence and uniqueness of the relevant solutions. From this inequality, it is shown in Sect. 8.3 that a general energy balance equation can be derived under fairly general conditions on the velocity field. Next, the fundamental inequality is extended to non-isochoric trial velocity fields in Sect. 8.4, and to flows in the presence of wall slip in Sect. 8.5.

In Sect. 8.6, questions regarding the existence and uniqueness of solutions to the variational principles and the variational inequality are answered through an appeal to convex analysis. In broad terms, the solution found from one is the same as that found from the other, i.e., they are equivalent when inertia is ignored; see Sect. 8.6.5. In the next section Sect. 8.7, it is shown that under certain conditions the solution of the variational inequality satisfies the equations of motion when the fluid has yielded; this derivation complements that found earlier in Sect. 8.6.5. In addition, the boundary conditions under which the variational inequality and the trilinear functional associated to the convected acceleration terms can be simplified are addressed in Sect. 8.8.

Next, the *viscoplasticity constraint tensor* $\boldsymbol{\Lambda}$ is reintroduced in Sect. 8.9 and relations between this tensor, the solution velocity field $\mathbf{u}$ and any admissible velocity field $\mathbf{v}$ are mentioned. In turn, the use of this tensor leads to an operator-splitting method for the solution of Dirichlet type boundary value problems, a topic covered in Sect. 10.3.

Finally, the fundamental inequality is extended to compressible viscoplastic fluids in Sect. 8.10. Applications of this are discussed later in Sects. 10.4 and 10.5.

R.R. Huilgol, *Fluid Mechanics of Viscoplasticity*, DOI 10.1007/978-3-662-45617-0_8

8.1 Minimum and Maximum Principles for Incompressible Viscoplastic Fluids

It is well known that in continuum mechanics, there are two different variational principles for incompressible fluids. While a precise description of the various terms will be given later, here are the statements of these principles:

1. *Of all kinematically admissible velocity fields* $\mathbf{v}$, *the solution velocity field* $\mathbf{u}$ *minimises a functional* $\Phi(\mathbf{v})$, *defined for all* $\mathbf{v}$.
2. *Of all statically admissible stress fields* $\mathbf{T}^*$, *the solution stress field* $\mathbf{T}$ *maximises a functional* $\Psi(\mathbf{T}^*)$, *defined for all* $\mathbf{T}^*$.

In the first one, the solution velocity field $\mathbf{u}$ arises as a minimum of a suitably chosen functional, whereas in the second one, the actual stress field $\mathbf{T}$ maximises a totally different functional. Thus, we have to define these functionals and prove the two principles enunciated above, with the functionals varying from one material to another; the primary focus here is on viscoplastic fluids, of course. To begin, one has to define *a kinematically admissible velocity field* and *a statically admissible stress field*.

8.1.1 Basic Definitions and Principle of Virtual Power

Suppose that an incompressible fluid occupies a domain Ω with a smooth boundary $\partial\Omega$. This boundary is decomposed into two mutually disjoint subsets $\partial\Omega_u$ and $\partial\Omega_t$ such that

$$\partial\Omega = \partial\Omega_u \cup \partial\Omega_t; \quad \partial\Omega_u \cap \partial\Omega_t = \emptyset. \tag{8.1.1}$$

On the part $\partial\Omega_u$, the velocity vector $\mathbf{U}$ is given, whereas on $\partial\Omega_t$, the external stress vector $\mathbf{t}$ is prescribed. We are now in a position to define a kinematical admissible velocity field and a statically admissible stress field.

1. **Definition** A kinematically admissible velocity field is continuous, and has piecewise continuous partial derivatives with respect to $\mathbf{x} \in \Omega$ and all $t > 0$, obeys the boundary condition on $\partial\Omega_u$, and is divergence free.
2. **Definition** A statically admissible stress field is continuous, and has piecewise continuous partial derivatives with respect to $\mathbf{x} \in \Omega$ and all $t > 0$, satisfies the equations of motion in the absence of inertia, and obeys the boundary condition on $\partial\Omega_t$.

To prove the variational principles, one needs the principle of virtual power which follows next.

Consider any stress field $\mathbf{T}$ which satisfies the equations of motion in the absence of inertia; let the solution velocity field be $\mathbf{u}$. Using

$$T_{ij,j} + \rho b_i = 0, \tag{8.1.2}$$

form the dot product of this equation with an arbitrary velocity field $\mathbf{v}$, and integrate the equation over the domain Ω. One obtains:

$$\int_{\Omega} T_{ij,j}(\mathbf{u})v_i\,dv = \int_{\Omega} (T_{ij}(\mathbf{u})v_i)_{,j}\,dv - \int_{\Omega} T_{ij}(\mathbf{u})v_{i,j}\,dv$$
$$= \int_{\partial\Omega} T_{ij}(\mathbf{u})v_i n_j\,dS - \frac{1}{2}\int_{\Omega} T_{ij}(\mathbf{u})A_{ij}(\mathbf{v})\,dv, \tag{8.1.3}$$

where $A_{ij}(\mathbf{v}) = (v_{i,j} + v_{j,i})$. Hence, (8.1.2) leads to the following:

$$\frac{1}{2}\int_{\Omega} T_{ij}(\mathbf{u})A_{ij}(\mathbf{u})\,dv = \int_{\partial\Omega} T_{ij}(\mathbf{u})v_i n_j\,dS + \int_{\Omega} \rho b_i v_i\,dv. \tag{8.1.4}$$

Using the fact that $T_{ij}n_j = t_i$, which is the stress vector on the boundary $\partial\Omega$, we obtain the *principle of virtual power*:

$$\frac{1}{2}\int_{\Omega} T_{ij}(\mathbf{u})A_{ij}(\mathbf{v})\,dv = \int_{\partial\Omega} t_i(\mathbf{u})v_i\,dS + \int_{\Omega} \rho b_i v_i\,dv. \tag{8.1.5}$$

In direct notation,

$$\frac{1}{2}\int_{\Omega} \mathbf{T}(\mathbf{u}) : \mathbf{A}(\mathbf{v})\,dv = \int_{\partial\Omega} \mathbf{t}(\mathbf{u})\cdot\mathbf{v}\,dS + \int_{\Omega} \rho\mathbf{b}\cdot\mathbf{v}\,dv. \tag{8.1.6}$$

In incompressible materials, $\mathbf{T} = -p\mathbf{1} + \mathbf{S}$, and all velocity fields are divergence free. The principle of virtual power becomes:

$$\frac{1}{2}\int_{\Omega} \mathbf{S}(\mathbf{u}) : \mathbf{A}(\mathbf{v})\,dv = \int_{\partial\Omega} \mathbf{t}(\mathbf{u})\cdot\mathbf{v}\,dS + \int_{\Omega} \rho\mathbf{b}\cdot\mathbf{v}\,dv. \tag{8.1.7}$$

It follows readily from this that

$$\frac{1}{2}\int_{\Omega} \mathbf{S}(\mathbf{u}) : [\mathbf{A}(\mathbf{v}) - \mathbf{A}(\mathbf{u})]\,dv = \int_{\partial\Omega} \mathbf{t}(\mathbf{u})\cdot[\mathbf{v}-\mathbf{u}]\,dS + \int_{\Omega} \rho\mathbf{b}\cdot[\mathbf{v}-\mathbf{u}]\,dv. \tag{8.1.8}$$

A second version of the principle of virtual power can be proved under the assumption that two separate stress fields $\mathbf{T}$ and $\mathbf{T}^*$ satisfy the equations of equilibrium subject to the same body force field $\mathbf{b}$. If the respective, corresponding extra stress tensor fields are $\mathbf{S}$ and $\mathbf{S}^*$, one finds from (8.1.7) that

$$\frac{1}{2}\int_{\Omega} [\mathbf{S} - \mathbf{S}^*] : \mathbf{A}(\mathbf{u})\,dv = \int_{\partial\Omega} [\mathbf{t} - \mathbf{t}^*]\cdot\mathbf{u}\,dS. \tag{8.1.9}$$

8.1.2 The Velocity and Stress Functionals

To be specific, the solution velocity field $\mathbf{u}$ is kinematically admissible and gives rise to a stress tensor field $\mathbf{T}(\mathbf{u})$ which satisfies the equations of motion in the absence of inertia; the body force $\mathbf{b}$ is assumed to be non-zero. Thus,

$$\nabla \cdot \mathbf{T}(\mathbf{u}) + \rho \mathbf{b} = \mathbf{0}. \tag{8.1.10}$$

Let us now consider viscoplastic fluids, such Herschel-Bulkley or Casson fluids, which are different from the Bingham fluid. It is known that these fluids have a shear rate dependent viscosity and a constant yield stress. Can the minimum and maximum principles, originally proved by Prager [1] for Bingham fluids, be extended to such fluids? This matter will be considered next.

To begin, let the constitutive equation be expressed in terms of the tensor $\mathbf{A}$ derived from the velocity field $\mathbf{v}$ as follows:

$$\mathbf{A} = \mathbf{0}, \quad T(\mathbf{S}) \leq \tau_y, \tag{8.1.11}$$

$$\mathbf{S} = \eta(K(\mathbf{A}))\mathbf{A} + \frac{\tau_y}{K(\mathbf{A})}\mathbf{A}, \quad T(\mathbf{S}) > \tau_y. \tag{8.1.12}$$

Thus,

$$T(\mathbf{S}) \leq \tau_y, \ K(\mathbf{A}) = 0; \quad T(\mathbf{S}) = \eta(K(\mathbf{A}))K(\mathbf{A}) + \tau_y, \ K(\mathbf{A}) > 0. \tag{8.1.13}$$

From (8.1.11) and (8.1.12), it is obvious that the stress tensor $\mathbf{S}(\mathbf{u})$, defined through $\mathbf{A} = \mathbf{A}(\mathbf{u})$, and the kinematic tensor $\mathbf{A}(\mathbf{u})$ are *parallel*. Thus, replacing $K(\mathbf{A}(\mathbf{u}))$ by $K(\mathbf{u})$ for the sake of simplicity, one obtains:

$$\mathbf{S}(\mathbf{u}) : \mathbf{A}(\mathbf{u}) = ||\mathbf{S}(\mathbf{u})|| \cdot ||\mathbf{A}(\mathbf{u})|| = 2T(\mathbf{S}(\mathbf{u}))K(\mathbf{u}), \tag{8.1.14}$$

whereas, from the Cauchy-Schwarz inequality,

$$\mathbf{S}(\mathbf{u}) : \mathbf{A}(\mathbf{v}) \leq 2T(\mathbf{S}(\mathbf{u}))K(\mathbf{v}), \tag{8.1.15}$$

where $\mathbf{v}$ is any admissible velocity field.

The velocity potential $\phi(K(\mathbf{A}))$ is defined, as in Sect. 4.6, so that it satisfies the following conditions:

$$\phi(K(\mathbf{A})) = 0, \quad K(\mathbf{A}) = 0, \tag{8.1.16}$$

$$\frac{d\phi}{dK(\mathbf{A})} = T(\mathbf{S}), \quad K(\mathbf{A}) > 0. \tag{8.1.17}$$

Since $T(\mathbf{S})$ is a function of $K(\mathbf{A})$ when the fluid has yielded, it is convenient to use a simpler notation and let $K(\mathbf{A}) = \xi, \ T = \hat{T}(\xi), \xi > 0$, so that

$$\hat{T}(\xi) = \eta(\xi)\xi + \tau_y, \quad \xi > 0. \tag{8.1.18}$$

The potential associated to the stress tensor in (8.1.12) is given by (cf. (8.1.16) and (8.1.17)):

$$\phi(K(\mathbf{A})) = \int_0^{K(\mathbf{A})} \hat{T}(\xi)\, d\xi. \tag{8.1.19}$$

Now, define a new stress power functional $\Phi(\mathbf{v})$ in which one subtracts from the potential in (8.1.19), the power due to the body force $\mathbf{b}$ and the external power due to the surface traction vector $\mathbf{t}$, which acts on the boundary $\partial\Omega_t$ of the domain Ω. Thus,

$$\Phi(\mathbf{v}) = \int_{\Omega} \phi(K(\mathbf{v}))\, dv - \int_{\Omega} \rho\mathbf{b}\cdot\mathbf{v}\, dv - \int_{\partial\Omega_t} \mathbf{t}\cdot\mathbf{v}\, dS. \tag{8.1.20}$$

The minimum principle asserts that:

Theorem 8.1.1 *Of all kinematically admissible velocity fields* $\mathbf{v}$, *the solution velocity field* $\mathbf{u}$ *minimises the functional* $\Phi(\mathbf{v})$.

Clearly, the proof of the above Theorem is complete if one can show that $\Phi(\mathbf{v}) \geq \Phi(\mathbf{u})$, which requires that $T(\xi)$ be a convex function, i.e., it meets the following condition [2, 3]:

$$\frac{dT(\xi)}{d\xi} \geq 0, \quad \xi > 0. \tag{8.1.21}$$

See Sect. 8.1.3 below for a proof of the minimum principle using this condition.

In order to derive a maximum principle, one requires a stress potential $\Gamma(T(\mathbf{S}))$, similar to that defined in Sect. 4.6. It must satisfy the following conditions:

$$\Gamma(T(\mathbf{S})) = 0, \quad T(\mathbf{S}) \leq \tau_y, \tag{8.1.22}$$

$$\frac{d\Gamma}{dT(\mathbf{S})} = K(\mathbf{A}), \quad T(\mathbf{S}) > \tau_y. \tag{8.1.23}$$

Such a functional can be constructed provided one can invert $(8.1.13)_2$ and express $K(\mathbf{A})$ in terms of $T(\mathbf{S})$. To make this transparent, consider the case of the Herschel-Bulkley fluid and recall that (cf. (4.6.40)):

$$T(\mathbf{S}) = k_b K(\mathbf{A})^m + \tau_y, \quad K(\mathbf{A}) > 0, \quad 0 < m \leq 1. \tag{8.1.24}$$

This can be inverted and one obtains

$$K(\mathbf{A}) = \left(\frac{T(\mathbf{S}) - \tau_y}{k_b}\right)^{1/m}, \quad T(\mathbf{S}) > \tau_y. \tag{8.1.25}$$

Thus, in general, $K(\mathbf{A})$ will be assumed to be a function of the invariant $T(\mathbf{S})$, when $T(\mathbf{S}) > \tau_y$. Expressing this as $\hat{K}(\tau)$, $T(\mathbf{S}) = \tau > \tau_y$, we define the stress potential as follows:

$$\Gamma(T(\mathbf{S})) = \int_{\tau_y}^{T(\mathbf{S})} \hat{K}(\tau)\, d\tau. \tag{8.1.26}$$

The maximum principle states that:

Theorem 8.1.2 *Of all statically admissible stress fields, the true stress field* $\mathbf{T} = -p\mathbf{1} + \mathbf{S}$ *will maximise the stress power functional*

$$\Psi(\mathbf{T}^*) = \int_{\partial\Omega_u} \mathbf{t}^* \cdot \mathbf{U}\, dS - \int_{\Omega} \Gamma(T(\mathbf{S}^*))\, dv. \tag{8.1.27}$$

In order to prove this, one has to demand that the function $\hat{K}(\tau)$ be a non-decreasing function, i.e., it meets the following condition [2, 3]:

$$\frac{d\hat{K}(\tau)}{d\tau} \geq 0, \quad \tau > \tau_y. \tag{8.1.28}$$

This inequality holds once again for the Herschel-Bulkley fluid; see (8.1.25) above.

Finally, the result in (8.1.14) can be given another useful interpretation. One can consider the area of a rectangle of the kinematic and stress norms, i.e., $K(\mathbf{A}) \times T(\mathbf{S})$, and observe that it can be split into two sub-areas as in Fig. 8.1, leading to

$$K(\mathbf{A}) \times T(\mathbf{S}) = \int_0^{K(\mathbf{A})} \hat{T}(\xi)\, d\xi + \int_{\tau_y}^{T(\mathbf{S})} \hat{K}(\tau)\, d\tau = \phi(K(\mathbf{A})) + \Gamma(T(\mathbf{S})). \tag{8.1.29}$$

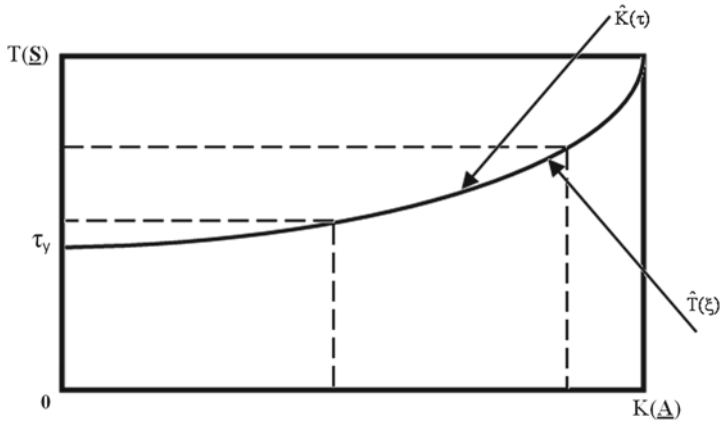

Fig. 8.1 The kinematic and stress norm rectangle

8.1.3 Proofs of the Theorems

In this sub-section, detailed proofs are provided for the two theorems stated above. The first one is the minimum principle which asserts that:

Theorem 8.1.1 *Of all kinematically admissible velocity fields* $\mathbf{v}$, *the solution velocity field* $\mathbf{u}$ *minimises the stress power functional* $\Phi(\mathbf{v})$, *given by*

$$\Phi(\mathbf{v}) = \int_{\Omega} \phi(K(\mathbf{v}))\, dv - \int_{\partial\Omega_t} \mathbf{t}\cdot\mathbf{v}\, dS - \int_{\Omega} \rho\mathbf{b}\cdot\mathbf{v}\, dv. \tag{8.1.30}$$

Clearly, the proof of the above Theorem is complete if one can show that $\Phi(\mathbf{v}) \geq \Phi(\mathbf{u})$.

Proof First of all, one recalls that the solution velocity field $\mathbf{u}$ satisfies the equations of motion given above in (8.1.2). On the surface of the body, the traction vector $\mathbf{t}$ is prescribed on $\partial\Omega_t$ only. However, it is related to the stress tensor $\mathbf{T}(\mathbf{u})$ which exists throughout the body, and the unit, external normal $\mathbf{n}$ defined everywhere on the bounding surface $\partial\Omega$ through

$$\mathbf{t} = \mathbf{t}(\mathbf{u}) = \mathbf{T}(\mathbf{u})\mathbf{n}. \tag{8.1.31}$$

Since $\mathbf{v} = \mathbf{u} = \mathbf{U}$ on the complement of $\partial\Omega_t$, that is on the set $\partial\Omega_u$, it follows that

$$\int_{\partial\Omega_t} \mathbf{t}(\mathbf{u})\cdot(\mathbf{v}-\mathbf{u})\, dS = \int_{\partial\Omega} \mathbf{t}\cdot(\mathbf{v}-\mathbf{u})\, dS. \tag{8.1.32}$$

Using the principle of virtual power (8.1.7), we are led to proving that

$$\Phi(\mathbf{v}) - \Phi(\mathbf{u}) = \int_{\Omega} \Big[\phi(K(\mathbf{v})) - \phi(K(\mathbf{u})) - \frac{1}{2}\mathbf{S}(\mathbf{u}) : [\mathbf{A}(\mathbf{v}) - \mathbf{A}(\mathbf{u})]\Big]\, dv \geq 0, \tag{8.1.33}$$

where $\mathbf{S}(\mathbf{u})$ is derived from the constitutive equation (8.1.11), using the relevant tensor $\mathbf{A}(\mathbf{u})$.

In fact, appealing to (8.1.13) and (8.1.14), it follows that one has to prove

$$\Phi(\mathbf{v}) - \Phi(\mathbf{u}) \geq \int_{\Omega} \Big[\phi(K(\mathbf{v})) - \phi(K(\mathbf{u})) - T(\mathbf{S}(\mathbf{u}))[K(\mathbf{v}) - K(\mathbf{u})]\Big]\, dv \geq 0. \tag{8.1.34}$$

From its definition in (8.1.18), it is easy to see that the integrand in (8.1.34) is itself expressible as the following integral:

$$\mathscr{I} = \int_{K(\mathbf{u})}^{K(\mathbf{v})} \left[\hat{T}(\xi) - T(\mathbf{S}(\mathbf{u})) \right] d\xi. \tag{8.1.35}$$

In verifying the above, note that $T(\mathbf{S}(\mathbf{u}))$ is constant, as far as the integration with respect to ξ is concerned. Thus, it is sufficient to show that $\mathscr{I} \geq 0$.

We shall now impose the condition mentioned earlier in (8.1.21):

$$\frac{d\hat{T}(\xi)}{d\xi} \geq 0, \quad 0 < \xi < \infty, \tag{8.1.36}$$

which is equivalent to demanding that $\hat{T}(\xi)$ is a *non-decreasing function* of ξ.

Examination of (8.1.35) shows that there are three cases to consider:

- At a point in the flow domain, the two invariants are equal, i.e., $K(\mathbf{u}) = K(\mathbf{v})$. In this case, the integral $\mathscr{I} = 0$.
- Next, suppose that $K(\mathbf{v}) > K(\mathbf{u}) \geq 0$. Then, the inequality (8.1.36) proves that $\mathscr{I} \geq 0$.
- Finally, let $K(\mathbf{u}) > K(\mathbf{v}) \geq 0$. Then, not only is the integrand in (8.1.35) non-positive, the lower limit in (8.1.35) is larger than the upper one. Thus, the integral $\mathscr{I} \geq 0$.

In conclusion, it has been established that

$$\Phi(\mathbf{v}) - \Phi(\mathbf{u}) \geq \int_{\Omega} \mathscr{I}\, dv \geq 0, \tag{8.1.37}$$

which proves the minimum principle. That is, of all kinematically admissible velocity fields $\mathbf{v}$, the solution vector $\mathbf{u}$ minimises the functional $\Phi(\mathbf{v})$.

Remark From (8.1.33), it follows that one can replace the functional $\Phi(\mathbf{v})$ by the following:

$$\Phi(\mathbf{v}) = \int_{\Omega} \left[\phi(K(\mathbf{v})) - \frac{1}{2}\mathbf{S}(\mathbf{u}) : \mathbf{A}(\mathbf{v}) \right] dv. \tag{8.1.38}$$

Thus, the solution vector field $\mathbf{u}$ minimises the above functional.

We shall now turn to the proof of the maximum principle, which is:

Theorem 8.1.2 *Of all statically admissible stress fields, the true stress field* $\mathbf{T} = -p\mathbf{1} + \mathbf{S}$ *will maximise the stress power functional*

$$\Psi(\mathbf{T}^*) = \int_{\partial\Omega_u} \mathbf{t}^* \cdot \mathbf{U}\, dS - \int_{\Omega} \Gamma(T(\mathbf{S}^*))\, dv, \tag{8.1.39}$$

where the stress potential $\Gamma(T(\mathbf{S}^*))$ has been defined for all admissible stress fields $\mathbf{S}^*$ *in* (8.1.22), (8.1.23) *and* (8.1.26).

Proof Let $\mathbf{T}$ be the admissible stress tensor which is the true solution. By definition, every admissible stress field gives rise to the same external stress vector on $\partial\Omega_t$. Appealing to the principle of virtual power (8.1.7) and observing that for any velocity field $\mathbf{u}$ which equals $\mathbf{U}$ on $\partial\Omega_u$, one finds that

$$\int_{\partial\Omega_u} (\mathbf{t} - \mathbf{t}^*) \cdot \mathbf{U}\, dS = \int_{\partial\Omega} (\mathbf{t} - \mathbf{t}^*) \cdot \mathbf{u}\, dS = \frac{1}{2} \int_{\Omega} [\mathbf{S} - \mathbf{S}^*] : \mathbf{A}(\mathbf{u})\, dv. \tag{8.1.40}$$

Hence, we have to prove that

$$\Psi(\mathbf{T}) - \Psi(\mathbf{T}^*) = \int_{\Omega} \frac{1}{2}(\mathbf{S} - \mathbf{S}^*) : \mathbf{A}(\mathbf{u})\, dv$$

$$- \int_{\Omega} [\Gamma(T(\mathbf{S})) - \Gamma(T(\mathbf{S}^*))]\, dv \geq 0. \tag{8.1.41}$$

Now, let $\mathbf{u}$ be the solution velocity field. Appealing once again to (8.1.13) and (8.1.14), the proof reduces to showing that

$$\Psi(\mathbf{T}) - \Psi(\mathbf{T}^*) \geq \int_{\Omega} [T(\mathbf{S}) - T(\mathbf{S}^*)] K(\mathbf{u})\, dv$$

$$- \int_{\Omega} [\Gamma(T(\mathbf{S})) - \Gamma(T(\mathbf{S}^*))]\, dv \geq 0. \tag{8.1.42}$$

Consider the integrand above and use (8.1.26) to obtain:

$$\mathscr{I} = [T(\mathbf{S}) - T(\mathbf{S}^*)] K(\mathbf{u}) - [\Gamma(T(\mathbf{S})) - \Gamma(T(\mathbf{S}^*))]$$

$$= \int_{T(\mathbf{S}^*)}^{T(\mathbf{S})} \left[K(\mathbf{u}) - \hat{K}(\tau) \right] d\tau. \tag{8.1.43}$$

As in the case of the minimum principle, there are three cases to consider.

- At a point in the flow domain, the two invariants are equal, i.e., $T(\mathbf{S}) = T(\mathbf{S}^*)$. In this case, the integral $\mathscr{I} = 0$.
- Next, suppose that $T(\mathbf{S}) > T(\mathbf{S}^*)$. Then, the inequality (8.1.28) proves that $\mathscr{I} \geq 0$.
- Finally, let $T(\mathbf{S}^*) > T(\mathbf{S})$. Then, not only is the integrand non-positive, the lower limit in (8.1.43) is larger than the upper one. Thus, the integral $\mathscr{I} \geq 0$.

Thus, it has been established that

$$\Psi(\mathbf{T}) - \Psi(\mathbf{T}^*) \geq \int_{\Omega} \mathscr{I}\, dv \geq 0, \tag{8.1.44}$$

which proves the maximum principle. That is, of all admissible stress fields $\mathbf{T}^*$, the solution stress tensor $\mathbf{T}$ maximises the functional $\Psi(\mathbf{T}^*)$.

Remark Just as in the case of the minimum principle, an examination of (8.1.41) shows that the true stress field $\mathbf{T} = -p\mathbf{1} + \mathbf{S}$ maximises the functional

$$\Psi(\mathbf{S}^*) = \int_{\Omega} \left[\frac{1}{2}\mathbf{S}^* : \mathbf{A}(\mathbf{u}) - \Gamma(T(\mathbf{S}^*))\right] dv. \tag{8.1.45}$$

8.1.4 Equality of $\Phi(\mathbf{u})$ and $\Psi(\mathbf{T})$

Let us assume that the velocity field $\mathbf{u}$ minimises the stress power functional, $\Phi(\mathbf{v})$, and that the stress field $\mathbf{T}$ maximises the corresponding stress power functional, $\Psi(\mathbf{T}^*)$. Appealing to (8.1.30) and (8.1.39), one finds that

$$\begin{aligned}\Phi(\mathbf{u}) - \Psi(\mathbf{T}) = &\int_{\Omega} \phi(K(\mathbf{u}))\, dv - \int_{\partial\Omega_t} \mathbf{t}\cdot\mathbf{u}\, dS - \int_{\Omega} \rho\mathbf{b}\cdot\mathbf{u}\, dv \\ &- \int_{\partial\Omega_u} \mathbf{t}\cdot\mathbf{U}\, dS + \int_{\Omega} \Gamma(T(\mathbf{S}))\, dv.\end{aligned} \tag{8.1.46}$$

Now, one can combine the stress power integrals to obtain the stress power over the whole body, i.e.,

$$\int_{\partial\Omega_t} \mathbf{t}\cdot\mathbf{u}\, dS + \int_{\partial\Omega_u} \mathbf{t}\cdot\mathbf{U}\, dS = \int_{\partial\Omega} \mathbf{t}\cdot\mathbf{u}\, dS. \tag{8.1.47}$$

Next, the relationship between $T(\mathbf{S}(\mathbf{u}))$ and $K(\mathbf{u})$ in (8.1.14) and (8.1.29) leads to the result that

$$\begin{aligned}\int_{\Omega} \phi(K(\mathbf{u}))\, dv + \int_{\Omega} \Gamma(T(\mathbf{S}))\, dv &= \int_{\Omega} K(\mathbf{u}) \times T(\mathbf{S}(\mathbf{u}))\, dv \\ &= \frac{1}{2}\int_{\Omega} \mathbf{S}(\mathbf{u}) : \mathbf{A}(\mathbf{u})\, dv.\end{aligned} \tag{8.1.48}$$

From the principle of virtual power (8.1.7), (8.1.46) and (8.1.47), it is easy to see that $\Phi(\mathbf{u}) = \Psi(\mathbf{T})$.

The two principles just proven can be summarised as:

$$\Psi(\mathbf{T}^*) \leq \Psi(\mathbf{T}) = \Phi(\mathbf{u}) \leq \Phi(\mathbf{v}) \tag{8.1.49}$$

for all statically admissible stress fields $\mathbf{T}^*$ and all kinematically admissible velocity fields $\mathbf{v}$.

8.1.5 Shear Rate Dependent Yield Stress

In a couple of papers [3, 4], it has been claimed that the minimum and maximum principles hold even if the yield stress depends on the shear rate, i.e., that $\tau_y = \tau_y(K(\mathbf{A}))$ is valid. If one looks at the definition of the potential associated with the stress tensor in (8.1.18) and (8.1.19), there is no difficulty in replacing a constant yield stress τ_y by one that depends on the shear rate and modifying the proof of the minimum principle. However, when one looks at the stress potential in (8.1.26), the lower limit of the integral, viz., τ_y, cannot be shear rate dependent; otherwise, the proof of the maximum principle will fail. Consequently, incorporating the shear rate dependence of the yield stress into the constitutive equations of viscoplastic fluids fails to deliver the result that $\Phi(\mathbf{u}) = \Psi(\mathbf{T})$.

8.1.6 Steady Flow in a Pipe of Uniform Cross-Section

As an application of the variational principle for the velocity field, consider the flow of a Bingham fluid along the axis of a pipe of uniform cross-section due to a constant pressure drop per unit length $G > G_c > 0$. Assuming that the axis of the pipe points in the z-direction, we may assume without loss of generality that each permissible velocity field has the form $\mathbf{v} = w(x, y)\mathbf{k}$, with the proviso that $w(x, y)$ is zero on the boundary of the pipe. Considering a unit length of the pipe, the external unit normal vectors at the inlet and outlet are given by $\mathbf{n} = \pm\mathbf{k}$, with the positive sign indicating that this vector points in the direction of the flow. Now, the stress distribution on the end planes is given by

$$\mathbf{t} = \pm(S_{xz}\mathbf{i} + S_{yz}\mathbf{j} - p\mathbf{k}), \tag{8.1.50}$$

where $p = -Gz$ is the pressure. Across the end planes at $z = z_2$, $z = z_1$, with $z_2 - z_1 = 1$, one finds that

$$\mathbf{t} \cdot \mathbf{v}_{|z=z_2} - \mathbf{t} \cdot \mathbf{v}_{|z=z_1} = Gw(x, y). \tag{8.1.51}$$

From (2.5.9), we see that

$$2K^2(\mathbf{A}) = \mathbf{A}(\mathbf{v}) : \mathbf{A}(\mathbf{v}) = 2\left[\left(\frac{\partial w}{\partial x}\right)^2 + \left(\frac{\partial w}{\partial y}\right)^2\right] = 2\nabla w \cdot \nabla w. \tag{8.1.52}$$

Next, one notes from (8.1.19) that in a Bingham fluid,

$$\phi(K(\mathbf{A})) = \frac{1}{2}\eta K(\mathbf{A})^2 + \tau_y K(\mathbf{A}). \tag{8.1.53}$$

Thus, the stress power functional to be minimised becomes:

$$\Phi(w) = \frac{1}{2}\eta a(w, w) + \tau_y j(w) - (G, w), \tag{8.1.54}$$

where

$$a(w, w) = \int_{\Omega} \nabla w \cdot \nabla w \, da, \tag{8.1.55}$$

$$j(w) = \int_{\Omega} |\nabla w| \, da, \tag{8.1.56}$$

$$(G, w) = \int_{\Omega} Gw \, da, \tag{8.1.57}$$

with Ω representing the cross-section of the pipe. A much simpler version of the functional $\Phi(w)$ arises when one considers the flow in a channel, leading to (1.9.3)–(1.9.5).

For Herschel-Bulkley and Casson fluids, one can appeal to (4.6.41) and (4.6.46) respectively to determine the relevant functional $\Phi(w)$ to be minimised.

8.2 Virtual Power and the Basic Inequality for Incompressible Viscoplastic Fluids

As mentioned in Chap. 1, the flow of a Bingham fluid in a channel is governed by a variational inequality. In this section, we shall derive a fundamental inequality for the flows of viscoplastic fluids, which are more general than Bingham fluids. It will be shown that the inequality includes both inertia and the body force, based on the derivation by Huilgol [5] closely. The procedure is purely formal and produces a general inequality, employing the Cauchy-Schwarz inequality as its basic tool.

8.2.1 A Point-Wise Inequality: Isochoric Velocity Fields

In order to obtain such an inequality, we shall use the constitutive relations Eqs. (4.2.1)–(4.2.8) as follows. Let the flow domain Ω be a bounded or an unbounded set in the three dimensional Euclidean space in general, and let it be decomposed into two disjoint subsets Ω_1 and Ω_0, such that

$$\Omega = \Omega_1 \cup \Omega_0, \quad \Omega_1 \cap \Omega_0 = \emptyset, \tag{8.2.1}$$

where

$$\Omega_1 = \{\mathbf{x} \in \Omega : \mathbf{A}(\mathbf{u}) \neq \mathbf{0}\}, \quad \Omega_0 = \{\mathbf{x} \in \Omega : \mathbf{A}(\mathbf{u}) = \mathbf{0}\}. \tag{8.2.2}$$

That is, Ω_1 is the region where the fluid has yielded, and Ω_0 is where it moves as a rigid body or is at rest. Note that in Eq. (8.2.2), either Ω_1 or Ω_0 may be empty.

Now, suppose that $\mathbf{u}$ is the velocity field which satisfies the equations of motion in Ω, i.e.,

$$\nabla \cdot \mathbf{T}(\mathbf{u}) + \rho \mathbf{b} = \rho \mathbf{a}, \quad \mathbf{a} = \frac{\partial \mathbf{u}}{\partial t} + \mathbf{u} \cdot \nabla \mathbf{u}, \tag{8.2.3}$$

where ρ is the density of the fluid, which is assumed to be incompressible, $\mathbf{a}$ is the acceleration vector derived from $\mathbf{u}$, and $\mathbf{b}$ is the body force. Let $\mathbf{v}$ be any other velocity field that is isochoric, i.e., $\nabla \cdot \mathbf{v} = 0$. Then, in the set Ω_1, where the fluid has yielded, one finds from the constitutive equation (4.2.8) that the *pseudo-stress power* is given by:

$$\frac{1}{2}\mathbf{T}(\mathbf{u}) : \mathbf{A}(\mathbf{v}) = \frac{1}{2}\mathbf{S}(\mathbf{u}) : \mathbf{A}(\mathbf{v}) = \frac{1}{2}\eta(K(\mathbf{u}))\mathbf{A}(\mathbf{u}) : \mathbf{A}(\mathbf{v}) + \frac{1}{2}\frac{\tau_y}{K(\mathbf{u})}\mathbf{A}(\mathbf{u}) : \mathbf{A}(\mathbf{v}). \tag{8.2.4}$$

Employing the Cauchy-Schwarz inequality on the term involving the yield stress contribution, we find that in the set Ω_1,

$$\frac{1}{2}\mathbf{T}(\mathbf{u}) : \mathbf{A}(\mathbf{v}) \leq \frac{1}{2}\eta(K(\mathbf{u}))\mathbf{A}(\mathbf{u}) : \mathbf{A}(\mathbf{v}) + \tau_y K(\mathbf{v}). \tag{8.2.5}$$

On the other hand, in the set Ω_0, one uses Eq. (4.2.1) and the Cauchy-Schwarz inequality to derive that

$$\frac{1}{2}\mathbf{T}(\mathbf{u}) : \mathbf{A}(\mathbf{v}) \leq \tau_y K(\mathbf{v}). \tag{8.2.6}$$

Thus, Eq. (8.2.5) applies in Ω_0 as well, because $\mathbf{A}(\mathbf{u}) = 0$ in that set. In other words, Eq. (8.2.5) is valid in the whole region Ω.

The corresponding results for the solution velocity field $\mathbf{u}$ can be obtained quite easily. One finds that in the set Ω_1, the true stress power is given by:

$$\frac{1}{2}\mathbf{T}(\mathbf{u}) : \mathbf{A}(\mathbf{u}) = \frac{1}{2}\eta(K(\mathbf{u}))\mathbf{A}(\mathbf{u}) : \mathbf{A}(\mathbf{u}) + \tau_y K(\mathbf{u}) \tag{8.2.7}$$

while in the set Ω_0,

$$\frac{1}{2}\mathbf{T}(\mathbf{u}) : \mathbf{A}(\mathbf{u}) = 0. \tag{8.2.8}$$

Thus, Eq. (8.2.7) is valid in Ω.

Consequently, at every point in the entire flow domain Ω,

$$\frac{1}{2}\mathbf{T}(\mathbf{u}) : [\mathbf{A}(\mathbf{v}) - \mathbf{A}(\mathbf{u})] \leq \frac{1}{2}\eta(K(\mathbf{u}))\mathbf{A}(\mathbf{u}) : [\mathbf{A}(\mathbf{v}) - \mathbf{A}(\mathbf{u})] + \tau_y[K(\mathbf{v}) - K(\mathbf{u})]. \tag{8.2.9}$$

Now, the definition of the tensor $\mathbf{A}$ means that

$$\mathbf{A}(\mathbf{v}) - \mathbf{A}(\mathbf{u}) = \mathbf{A}(\mathbf{v} - \mathbf{u}). \tag{8.2.10}$$

Thus, we obtain

$$\frac{1}{2}\mathbf{T}(\mathbf{u}) : \mathbf{A}(\mathbf{v} - \mathbf{u}) \leq \frac{1}{2}\eta(K(\mathbf{u}))\mathbf{A}(\mathbf{u}) : \mathbf{A}(\mathbf{v} - \mathbf{u}) + \tau_y[K(\mathbf{v}) - K(\mathbf{u})]. \tag{8.2.11}$$

This point-wise inequality, which is a hybrid measure of the stress power in the trial and actual velocity fields, will be used below to derive a fundamental inequality that applies to all flows of yield stress fluids. The crucial point to observe is that the point-wise inequality has been obtained by replacing the yield stress term by its upper bound, for the yield stress term is not a differentiable function of its argument K when $K = 0$, depending as it does on the square root of the second invariant of the Rivlin-Ericksen tensor.

8.2.2 The Integral Inequality

Now, turn to the equations of motion Eq. (8.2.3) and take its dot product with the vector $(\mathbf{v} - \mathbf{u})$. We obtain

$$\rho(\mathbf{a} - \mathbf{b}) \cdot (\mathbf{v} - \mathbf{u}) + \frac{1}{2}\mathbf{T}(\mathbf{u}) : \mathbf{A}(\mathbf{v} - \mathbf{u}) - \nabla \cdot [(\mathbf{v} - \mathbf{u}) \cdot \mathbf{T}(\mathbf{u})] = 0. \tag{8.2.12}$$

Using the inequality Eq. (8.2.11), we can convert Eq. (8.2.12) into the following:

$$\rho(\mathbf{a} - \mathbf{b}) \cdot (\mathbf{v} - \mathbf{u}) + \frac{1}{2}\eta(K(\mathbf{u}))\mathbf{A}(\mathbf{u}) : \mathbf{A}(\mathbf{v} - \mathbf{u}) + \tau_y[K(\mathbf{v}) - K(\mathbf{u})] \geq \nabla \cdot ((\mathbf{v} - \mathbf{u}) \cdot \mathbf{T}). \tag{8.2.13}$$

This inequality holds at all points in the flow domain, and will be transformed into one that applies over the flow region by integration with respect to its volume.

To accomplish this, following Duvaut and Lions [6, 7], let us define some functionals. First of all, the *viscous dissipation rate integral* for any scalar field $K(\mathbf{u})$,

and two velocity fields $\mathbf{v}$ and $\mathbf{w}$ is:

$$a(K(\mathbf{u}), \mathbf{v}, \mathbf{w}) = \frac{1}{2} \int_{\Omega} \eta(K(\mathbf{u}))\mathbf{A}(\mathbf{v}) : \mathbf{A}(\mathbf{w})\, dv. \tag{8.2.14}$$

It should be noted that $a(K(\mathbf{u}), \mathbf{v}, \mathbf{w})$ is always linear in its second and third arguments $\mathbf{v}$ and $\mathbf{w}$, and not in its first argument $K(\mathbf{u})$ unless the viscosity, η, is a constant. Next, the *yield stress dissipation rate integral* is:

$$\tau_y j(\mathbf{v}) = \tau_y \int_{\Omega} K(\mathbf{v})\, dv. \tag{8.2.15}$$

Also, the bilinear functional is the familiar inner product, i.e.,

$$(\mathbf{v}, \mathbf{w}) = \int_{\Omega} \mathbf{v} \cdot \mathbf{w}\, dv. \tag{8.2.16}$$

Finally, the trilinear functional for any three vector fields $\mathbf{u}$, $\mathbf{v}$ and $\mathbf{w}$ is:

$$b(\mathbf{u}, \mathbf{v}, \mathbf{w}) = \int_{\Omega} u_j v_{i,j} w_i\, dv. \tag{8.2.17}$$

Expressing the acceleration vector $\mathbf{a}$ in terms of $\mathbf{u}$ as in Eq. (8.2.3), one can integrate Eq. (8.2.13) over the flow domain Ω, and derive

$$\rho\left(\frac{\partial \mathbf{u}}{\partial t}, \mathbf{v} - \mathbf{u}\right) + \rho b(\mathbf{u}, \mathbf{u}, \mathbf{v} - \mathbf{u}) - \rho(\mathbf{b}, \mathbf{v} - \mathbf{u}) + a(K(\mathbf{u}), \mathbf{u}, \mathbf{v} - \mathbf{u}) + \tau_y[j(\mathbf{v}) - j(\mathbf{u})] \geq \int_{\Omega} \nabla \cdot ((\mathbf{v} - \mathbf{u}) \cdot \mathbf{T})\, dv. \tag{8.2.18}$$

Employing the divergence theorem on the right side, one finds that

$$\rho\left(\frac{\partial \mathbf{u}}{\partial t}, \mathbf{v} - \mathbf{u}\right) + \rho b(\mathbf{u}, \mathbf{u}, \mathbf{v} - \mathbf{u}) - \rho(\mathbf{b}, \mathbf{v} - \mathbf{u}) + a(K(\mathbf{u}), \mathbf{u}, \mathbf{v} - \mathbf{u}) + \tau_y[j(\mathbf{v}) - j(\mathbf{u})] \geq \int_{\partial\Omega} (\mathbf{v} - \mathbf{u}) \cdot \mathbf{T}\mathbf{n}\, dS, \tag{8.2.19}$$

where $\mathbf{n}$ is the external unit normal to the boundary $\partial\Omega$ of the flow domain.

Decomposing the boundary $\partial\Omega$ into the union of two disjoint subsets $\partial\Omega_u$, where the velocity vector $\mathbf{U}$ is prescribed, and $\partial\Omega_t$, where the stress vector $\mathbf{T}\mathbf{n} = \mathbf{t}$ is given, one sees that

$$\int_{\partial\Omega} (\mathbf{v} - \mathbf{u}) \cdot \mathbf{T}\mathbf{n}\, dS = \int_{\partial\Omega_t} (\mathbf{v} - \mathbf{u}) \cdot \mathbf{t}\, dS. \tag{8.2.20}$$

Thus, in any given flow, the exact form of the *stress power difference*, which is the integral on the right side of Eq. (8.2.20), leads to the specific form of the inequality applicable to that flow. Thus, in what follows, we shall refer to the following inequality repeatedly:

$$\rho\left(\frac{\partial \mathbf{u}}{\partial t}, \mathbf{v}-\mathbf{u}\right)+\rho b(\mathbf{u}, \mathbf{u}, \mathbf{v}-\mathbf{u})-\rho(\mathbf{b}, \mathbf{v}-\mathbf{u})+a(K(\mathbf{u}), \mathbf{u}, \mathbf{v}-\mathbf{u}) + \tau_y[j(\mathbf{v})-j(\mathbf{u})] \geq \int_{\partial \Omega_t}(\mathbf{v}-\mathbf{u}) \cdot \mathbf{t}\, dS. \tag{8.2.21}$$

The integral inequality in Eq. (8.2.19) is in the form of a *variational principle,* for it says that for all trial velocity fields $\mathbf{v}$, the left side is never less than the right side, and in the event that $\mathbf{v}=\mathbf{u}$, an equality results. As long as the assumed solution vector $\mathbf{u}$ exists, there is an inequality for the flow under investigation, with the latter following directly from the Cauchy-Schwarz inequality applied to the yield stress dissipation rate integral. Note that the derivation of (8.2.19), the *basic inequality*, has been accomplished without any initial/boundary conditions being imposed on the solution vector $\mathbf{u}$, or the trial velocity field $\mathbf{v}$. Further, the non-differentiability of $j(\mathbf{u})$ at $\mathbf{u}=\mathbf{0}$ is not a matter of concern either.

8.3 A General Energy Balance Equation for Viscoplastic Fluids

In a number of problems, the function spaces are such that in the fundamental inequality (8.2.19), one can replace the trial velocity field $\mathbf{v}$ by either $\mathbf{v}=2\mathbf{u}$, or $\mathbf{v}=\mathbf{0}$. In the former instance, the inequality becomes

$$\rho\left(\frac{\partial \mathbf{u}}{\partial t}, \mathbf{u}\right)+\rho b(\mathbf{u}, \mathbf{u}, \mathbf{u})-\rho(\mathbf{b}, \mathbf{u})+a(K(\mathbf{u}), \mathbf{u}, \mathbf{u}) + \tau_y j(\mathbf{u}) \geq \int_{\partial \Omega}\mathbf{u} \cdot \mathbf{T}\mathbf{n}\, dS. \tag{8.3.1}$$

On the other hand, if one puts $\mathbf{v}=\mathbf{0}$, the inequality has the form

$$-\left[\rho\left(\frac{\partial \mathbf{u}}{\partial t}, \mathbf{u}\right)+\rho b(\mathbf{u}, \mathbf{u}, \mathbf{u})-\rho(\mathbf{b}, \mathbf{u})+a(K(\mathbf{u}), \mathbf{u}, \mathbf{u}) + \tau_y j(\mathbf{u})\right] \geq -\int_{\partial \Omega}\mathbf{u} \cdot \mathbf{T}\mathbf{n}\, dS. \tag{8.3.2}$$

Hence, one is led to the general energy balance equation:

$$\rho\left(\frac{\partial \mathbf{u}}{\partial t}, \mathbf{u}\right) + \rho b(\mathbf{u}, \mathbf{u}, \mathbf{u}) - \rho(\mathbf{b}, \mathbf{u}) + a(K(\mathbf{u}), \mathbf{u}, \mathbf{u}) + \tau_y j(\mathbf{u}) - \int_{\partial\Omega} \mathbf{u} \cdot \mathbf{T}\mathbf{n}\, dS = 0. \tag{8.3.3}$$

An example of this will be exhibited in Sect. 8.8.2; another example appears in Sect. 9.2 in examining the motion of a Herschel-Bulkley fluid due to a rising bubble. A third one occurs in the motion of a solid body under creeping flow conditions; see Sect. 9.3.

8.4 Fundamental Inequality: Non-isochoric Trial Velocity Fields

In numerical modelling, it is quite often necessary to consider trial velocity fields which may be non-isochoric. That is, a trial velocity field $\mathbf{v}$ is such that $\nabla \cdot \mathbf{v} = 0$ may not be satisfied. Hence, we consider afresh the equations of motion satisfied by the solution vector $\mathbf{u}$:

$$-\nabla p + \nabla \cdot \mathbf{S}(\mathbf{u}) + \rho\mathbf{b} = \rho\mathbf{a}, \quad \nabla \cdot \mathbf{u} = 0. \tag{8.4.1}$$

Thus, instead of (8.2.11), we obtain:

$$\frac{1}{2}\mathbf{T}(\mathbf{u}) : \mathbf{A}(\mathbf{v} - \mathbf{u}) \leq -p\nabla \cdot (\mathbf{v} - \mathbf{u}) + \frac{1}{2}\eta(K(\mathbf{u}))\mathbf{A}(\mathbf{u}) : [\mathbf{A}(\mathbf{v} - \mathbf{u})] + \tau_y[K(\mathbf{v}) - K(\mathbf{u})]. \tag{8.4.2}$$

This leads to two separate inequalities, one for the extra stress tensor $\mathbf{S}$ and another one for the total stress tensor $\mathbf{T}$:

$$\int_{\Omega} \frac{1}{2}\mathbf{S}(\mathbf{u}) : \mathbf{A}(\mathbf{v} - \mathbf{u})\, dv \leq a(K(\mathbf{u}), \mathbf{u}, \mathbf{v} - \mathbf{u}) + \tau_y[j(\mathbf{v}) - j(\mathbf{u})], \tag{8.4.3}$$

and

$$\int_{\Omega} \frac{1}{2}\mathbf{T}(\mathbf{u}) : \mathbf{A}(\mathbf{v} - \mathbf{u})\, dv \leq -\int_{\Omega} p\nabla \cdot (\mathbf{v} - \mathbf{u})\, dv + a(K(\mathbf{u}), \mathbf{u}, \mathbf{v} - \mathbf{u}) + \tau_y[j(\mathbf{v}) - j(\mathbf{u})]. \tag{8.4.4}$$

The latter inequality will be employed later on in Sect. 10.2.2 under the assumption that both $\mathbf{u}$ and $\mathbf{v}$ obey the same boundary conditions on $\partial\Omega$. That is, one has (cf. (8.2.19)):

$$\rho\left(\frac{\partial \mathbf{u}}{\partial t}, \mathbf{v}-\mathbf{u}\right)+\rho b(\mathbf{u}, \mathbf{u}, \mathbf{v}-\mathbf{u})-\rho(\mathbf{b}, \mathbf{v}-\mathbf{u})-\int_{\Omega} p\nabla\cdot(\mathbf{v}-\mathbf{u})\,dv$$
$$+a(K(\mathbf{u}), \mathbf{u}, \mathbf{v}-\mathbf{u})+\tau_y[j(\mathbf{v})-j(\mathbf{u})]\geq 0. \tag{8.4.5}$$

For an incompressible Bingham fluid, the above inequality has the form:

$$\rho\left(\frac{\partial \mathbf{u}}{\partial t}, \mathbf{v}-\mathbf{u}\right)+\rho b(\mathbf{u}, \mathbf{u}, \mathbf{v}-\mathbf{u})-\rho(\mathbf{b}, \mathbf{v}-\mathbf{u})-\int_{\Omega} p\nabla\cdot(\mathbf{v}-\mathbf{u})\,dv$$
$$+\frac{1}{2}\eta\int_{\Omega}\mathbf{A}(\mathbf{u}):\mathbf{A}(\mathbf{v}-\mathbf{u})\,dv+\tau_y[j(\mathbf{v})-j(\mathbf{u})]\geq 0. \tag{8.4.6}$$

8.5 Variational Principles and Fundamental Inequality in the Presence of Wall Slip

The task of incorporating the effect of wall slip in the flow of an incompressible Bingham fluid in a channel has been illustrated in Chap. 1. This example leads to one partition the boundary $\partial\Omega$ of the flow domain Ω into three disjoint subsets: two subsets on which the stress vector is prescribed, while the velocity is tangential to the bounding surface on one and arbitrary on the second, and the third subset on which the velocity vector is given. The first one may be termed the *slip boundary* and the second the *flow boundary*, with the last being the *velocity boundary*. That is, in the case of a channel of finite length, the slip boundary consists of its walls and the flow boundary consists of the entry and exit regions; there is no velocity boundary. The shear stress on the bounding walls determines whether the fluid slips or not, while the applied pressure drop across the flow boundaries causes the flow to occur; for emphasis, see Sect. 1.11.

Hence, in general, the boundary $\partial\Omega$ of the flow domain is decomposed into three disjoint subsets as follows:

$$\partial\Omega=\partial\Omega_u\cup\partial\Omega_t\cup\partial\Omega_s;\quad \partial\Omega_u\cap\partial\Omega_t\cap\partial\Omega_s=\emptyset. \tag{8.5.1}$$

Here, on $\partial\Omega_u$, the velocity is prescribed; on $\partial\Omega_t$, the stress vector is given whereas on $\partial\Omega_s$, the slip boundary conditions are stated. In order to describe them, let $\mathbf{n}$ be the external, unit normal to the surface $\partial\Omega_s$. It will be assumed that on this part of the boundary, the velocity vector is orthogonal to it, i.e.,

$$\mathbf{u}\cdot\mathbf{n}=0. \tag{8.5.2}$$

Hence, the tangential component $\mathbf{u}^t = \mathbf{u} - (\mathbf{u}\cdot\mathbf{n})\mathbf{n} = \mathbf{u}$ on $\partial\Omega_s$. Next, the tangential component of the traction vector $\mathbf{t}^t$ is given on this surface through

$$\mathbf{t}^t = \mathbf{T}\mathbf{n} - (\mathbf{T}\mathbf{n}\cdot\mathbf{n})\mathbf{n}. \tag{8.5.3}$$

Hence, it is obvious that $\mathbf{t}\cdot\mathbf{u} = \mathbf{t}^t\cdot\mathbf{u}^t$ on $\partial\Omega_s$.

The boundary conditions to be imposed on $\partial\Omega_s$ are similar to those in (1.11.1). That is:

$$\mathbf{u}^t = \mathbf{0}, \quad |\mathbf{t}^t| \le g(0) = \tau_c, \tag{8.5.4}$$

$$\mathbf{t}^t = -\left(c_f(|\mathbf{u}^t|) + \frac{g(|\mathbf{u}^t|)}{|\mathbf{u}^t|}\right)\mathbf{u}^t, \quad |\mathbf{t}^t| > g(0). \tag{8.5.5}$$

Here, $g(0) = \tau_c$ is the critical value of the shear stress on the wall which determines whether slip will occur. And, just as in (1.11.4), it will be assumed that (8.5.5) can be inverted so that there is a unique solution for $\mathbf{u}^t$ in terms of $\mathbf{t}^t$.

It is a simple matter to recast the minimum and maximum principles to incorporate the presence of wall slip. Out of all admissible velocity field $\mathbf{v}$, one seeks the minimum of (cf. (8.1.20)):

$$\Phi(\mathbf{v}) = \int_{\Omega} \phi(K(\mathbf{v})\,dv - \int_{\partial\Omega_t} \mathbf{t}\cdot\mathbf{v}\,dS - \int_{\partial\Omega_s} \mathbf{t}^t\cdot\mathbf{v}^t\,dS - \int_{\Omega} \rho\mathbf{b}\cdot\mathbf{v}\,dv. \tag{8.5.6}$$

To obtain a maximum principle, one has to modify the definition of the class of statically admissible stress fields as follows:

Definition *A statically admissible stress field is continuous, and has piecewise continuous partial derivatives with respect to* $\mathbf{x} \in \Omega$ *and all* $t > 0$, *satisfies the equations of motion in the absence of inertia, and obeys the boundary conditions on* $\partial\Omega_t$ *and* $\partial\Omega_s$.

Using this definition, one can state that out of all statically admissible stress fields $\mathbf{T}^*$, one finds the maximum of (cf. (8.1.27)):

$$\Psi(\mathbf{T}^*) = \int_{\partial\Omega_u} \mathbf{t}^*\cdot\mathbf{U}\,dS - \int_{\Omega} \Gamma(K(\mathbf{S}^*))\,dv. \tag{8.5.7}$$

The proofs of the two principles are omitted for they are similar to those provided in Sect. 8.1.3.

As far as the integral inequality (8.2.19) is concerned, no modification is required for it has been derived without any reference to the imposed boundary conditions. Thus, the fundamental inequality in (8.2.19) is unchanged. However, it can be

modified as in (8.2.21) to obtain:

$$\rho\left(\frac{\partial \mathbf{u}}{\partial t}, \mathbf{v}-\mathbf{u}\right)+\rho b(\mathbf{u}, \mathbf{u}, \mathbf{v}-\mathbf{u})-\rho(\mathbf{b}, \mathbf{v}-\mathbf{u})+a(K(\mathbf{u}), \mathbf{u}, \mathbf{v}-\mathbf{u})$$
$$+\tau_y[j(\mathbf{v})-j(\mathbf{u})] \geq \int_{\partial\Omega_t}(\mathbf{v}-\mathbf{u})\cdot\mathbf{t}\,dS-\int_{\partial\Omega_s}(\mathbf{v}^t-\mathbf{u}^t)\cdot\mathbf{t}^t\,dS. \tag{8.5.8}$$

Now that the variational principle and the fundamental inequality have been derived for various conditions, it is necessary to explore the questions concerning the existence and uniqueness of solutions when they are employed. These matters are explored through convex analysis next.

8.6 Convex Analysis and Its Applications

It has been shown in Sect. 8.1.6 that the steady velocity field of a Bingham fluid in a pipe of uniform cross-section minimises the stress power functional

$$\Phi(w)=\frac{1}{2}\eta a(w,w)+\tau_y j(w)-(G,w), \tag{8.6.1}$$

subject to the condition $w(x, y) = 0$ on the boundary of the pipe.

A number of questions arise:

1. Is there a function that minimises the functional $\Phi(w)$? This is an *existence problem*.
2. If such a function exists, is it the only one? This is the *uniqueness problem*.
3. If there exists a unique function which minimises $\Phi(w)$, is this function the solution of the original problem? That is, in which sense does the minimiser satisfy the equations of motion governing the flow of the Bingham fluid in a pipe of uniform cross-section?
4. It is likely that in the cross-section of the pipe, one can observe the existence of rigid zones where the fluid may be at rest, or move as a plug. How smooth is the boundary separating a yielded zone from its neighbouring unyielded region?
5. To which function space does the solution belong?

As far as the inequality (8.2.19) or (8.2.21) is concerned, the questions posed above arise as well as the following.

1. Does it have to meet any specific conditions before one can it a *variational inequality*?
2. If it satisfies the required conditions, is it equivalent to any other, more useful forms?

Indeed, the answers exist. However, providing the detailed proofs is not attempted here, for these are available in the literature. Instead, we shall provide a summary documenting the relevant references where the answers can be found.

The first item in this list is the importance of lower semi-continuity and this is illustrated through its role in the Direct Method which follows next.

8.6.1 The Direct Method

Riemann investigated whether there exists a function $u = u(x, y)$ that has continuous second order partial derivatives and satisfies Laplace's equation:

$$\frac{\partial^2 u}{\partial x^2} + \frac{\partial^2 u}{\partial y^2} = 0 \tag{8.6.2}$$

in a given domain Ω and coincides with a given continuous function on the boundary of the specified region. Since the Laplace's equation is the Euler equation for the functional

$$J(u) = \int\int_{\Omega} \left[\left(\frac{\partial u}{\partial x} \right)^2 + \left(\frac{\partial u}{\partial y} \right)^2 \right] dx\, dy, \tag{8.6.3}$$

which assumes non-negative values only, Riemann considered it as obvious that the functional $J(u)$ has a minimum, and that this proved the existence of a solution to (8.6.2), satisfying the given boundary conditions. This idea was called the *Dirichlet principle* by Riemann, a student of Dirichlet.[1]

Weierstrass found a serious flaw in Riemann's argument. He pointed out that a functional bounded from below implies only that it has a greatest lower bound; it does not ensure that this lower bound is the minimiser of the functional in the given class of functions. To be specific, consider the following example due to Weierstrass. Let

$$J(y) = \int_{-1}^{1} x^2 y'^2\, dx, \quad y(-1) = -1,\ y(1) = 1. \tag{8.6.4}$$

Choose the following admissible function:

$$y_a(x) = \frac{\arctan(x/a)}{\arctan(1/a)}, \quad a > 0. \tag{8.6.5}$$

Then,

$$J(y_a) = \frac{a^2}{[\arctan(1/a)]^2} \int_{-1}^{1} \frac{x^2}{(x^2 + a^2)^2}\, dx$$

[1] The material in this sub-section is based on the exposition in Akhiezer [8].

$$< \frac{a^2}{[\arctan(1/a)]^2} \int_{-1}^{1} \frac{1}{(x^2+a^2)^2}\, dx$$

$$= \frac{2a}{\arctan(1/a)}. \tag{8.6.6}$$

As $a \to 0$, the right side approaches zero implying that this particular calculus of variations problem has no solution.

To overcome Weierstrass's objection, the *Direct Method* came into being in the calculus of variations. This method is based on the assumption that a functional $J(y)$ is finite and that it has a greatest lower bound which is actually attained on one of the admissible functions. That is, let $\mathscr{D}$ be the set of admissible functions and assume that

$$\inf_{y \in \mathscr{D}} J(y) = L > -\infty. \tag{8.6.7}$$

According to the definition of the lower bound, there exists a sequence of functions $y_1, y_2, \ldots, y_n \ldots$, known as the minimising sequence Σ, such that

$$\lim_{n \to \infty} J(y_n) = L. \tag{8.6.8}$$

Suppose that the limiting function $\hat{y}$ of the sequence exists and belongs to $\mathscr{D}$. If the equation

$$J(\hat{y}) = \lim_{n \to \infty} J(y_n) \tag{8.6.9}$$

holds, it follows that

$$J(\hat{y}) = L, \tag{8.6.10}$$

which means that the function $\hat{y}$ furnishes an absolute minimum. Obviously, (8.6.10) holds if $J(y)$ is a continuous functional, i.e., if the inequality

$$|J(y) - J(\hat{y})| < \varepsilon \tag{8.6.11}$$

is met by every function y in some ε-neighbourhood of $\hat{y}$. Unfortunately, $J(y)$ may not be a continuous functional. Indeed, it was noted by Lebesgue that *lower semi-continuity* is sufficient for the proof of (8.6.10). In the sequel, lower semi-continuity is denoted by l.s.c.

Now, suppose that $J(y)$ is l. s. c and that there exists a minimising sequence Σ which converges to $\hat{y} \in \mathscr{D}$. The definition of L means that

$$L \leq J(\hat{y}), \tag{8.6.12}$$

while lower semi-continuity ensures that

$$J(y_n) \geq J(\hat{y}) - \hat{\varepsilon}, \tag{8.6.13}$$

if y_n lies in a sufficiently small neighbourhood of $\hat{y}$. Since (8.6.13) holds for any $\hat{\varepsilon}$, we may write

$$L \geq J(\hat{y}) - \hat{\varepsilon}. \tag{8.6.14}$$

Comparing (8.6.12) and (8.6.14), we see that

$$J(\hat{y}) = L. \tag{8.6.15}$$

In sum, the direct method consists of the following four steps:

1. Proving the existence of the greatest lower bound for the given functional.
2. The construction of a minimising sequence within the chosen class of admissible functions. Great advances were made by Ritz and Galerkin to construct such sequences; in particular, Galerkin's ideas led to the finite and spectral element methods.
3. Proof that the limiting function of this sequence lies in the class of admissible functions.
4. Proof of the lower semi-continuity of the functional at this limiting function.

These matters are discussed next.

8.6.2 Convex Set and Convex Functionals

In any numerical scheme, questions regarding the choice of the set of admissible functions have to be settled. In fluid mechanics, the flow problems fall into three separate categories. In the first case, the velocity is prescribed over the boundary, i.e., one has a Dirichlet problem. In the second class, the external normal derivative of the velocity is defined over the boundary, i.e., one has a Neumann problem; for example, on a free boundary, this normal derivative is zero. In the third category, the boundary consists of the union of two mutually disjoint sets and on one part the Dirichlet boundary condition is prescribed, and in the other the Neumann condition is given.

The function space that is relevant in all of the above problems is the Sobolev space $W^{m,p}$ of integer order $m \geq 0$ on $L^p(\Omega)$, where Ω is an open set in $\mathbb{R}^d$, and d denotes the dimension of the space, $d \in [2, 3]$. In brief, one needs the following:

1. $L^p(\Omega)$ is the space of measurable functions f such that for $1 \leq p < \infty$,

$$||f||_{L^p(\Omega)} = \left(\int_{\Omega} |f(x)|^p \, dx \right)^{1/p} < \infty. \tag{8.6.16}$$

2. By $D^\alpha v$, one means

$$D^\alpha v = \frac{\partial^{\alpha_1 + \cdots + \alpha_n}}{\partial x_1^{\alpha_1} \ldots \partial x_n^{\alpha_n}} v, \quad \alpha = \{\alpha_1, \ldots, \alpha_n\}. \tag{8.6.17}$$

That is, $D^\alpha v$ is a partial, perhaps mixed, derivative of v of order α. Note that $0 \le \alpha_j \le d,\ j = 1, \ldots, d$. Of course, it is understood that $D^0 v = v$. That is, the zeroth derivative of a function is itself. Next, $D^1 v = Dv$ is the *gradient* of v, and so on. Moreover, the derivatives in (8.6.17) have to be regarded in the sense of *distributions.*

3. Let
$$|\alpha| = \sum_{j=1}^{d} \alpha_j. \tag{8.6.18}$$

4. The Sobolev space of order m on $L^p(\Omega)$, denoted by $W^{m,p}(\Omega)$, is defined through
$$W^{m,p}(\Omega) = \{v | v \in L^p(\Omega),\ D^\alpha v \in L^p(\Omega),\ |\alpha| \le m\}. \tag{8.6.19}$$

5. With the norm
$$||v||_{W^{m,p}(\Omega)} = \left(\sum_{|\alpha| \le m} ||D^\alpha v||^p_{L^p(\Omega)} \right)^{1/p}, \tag{8.6.20}$$
the space $W^{m,p}(\Omega)$ is a Banach space. Since reflexivity of the Banach space is required in Sect. 8.6.5, it will be assumed that $1 < p < \infty$.

6. If one sets $m = 1,\ p = 2$ one defines the Hilbert space $H^1(\Omega)$, which is of great importance in the flow of Bingham fluids. To be explicit,
$$(u, v)_{H^1(\Omega)} = \int_\Omega \left[uv + \sum_{j=1}^{d} \frac{\partial u}{\partial x_j} \frac{\partial v}{\partial x_j} \right] dv, \tag{8.6.21}$$
with the norm
$$||u||_{H^1(\Omega)} = \left(\int_\Omega \left[u^2 + |\nabla u|^2 \right] dv \right)^{1/2}. \tag{8.6.22}$$
That is, both $u \in L^2(\Omega)$ and $|\nabla u| \in L^2(\Omega)$.

7. The *trace* of a function v is the set of its boundary values. As remarked by Duvaut and Lions [7], the knowledge of v on the boundary $\partial\Omega$ implies the knowledge of its tangential derivatives on the boundary. Thus, one can define the trace γv as the set:
$$\gamma v = \{v, \partial v/\partial n\} \in L^2(\partial\Omega), \quad \text{if } v \in H^1(\Omega), \tag{8.6.23}$$
where $\partial v/\partial n$ is the normal derivative.

8. The space $H_0^1(\Omega)$ is the space of functions in $H^1(\Omega)$ such that $v = 0$ on the boundary $\partial\Omega$.

The above material is relevant to scalar valued functions only. In viscoplastic fluid mechanics, we have to consider vector and tensor valued functions, and their derivatives. This extension is not unduly problematic, for we can assume that if v_i are the components of a velocity field and that $v_{i,j}$ are the components of its gradient,

then each one is an element of $L^2(\Omega)$. Thus, the norm in (8.6.22) is replaced by

$$||\mathbf{v}||_{(H^1(\Omega)^d)} = \left(\int_\Omega \left[\sum_{i=1}^{d} |v_i|^2 + \sum_{i,j=1}^{d} |v_{i,j}|^2 \right] dv \right)^{1/2}, \tag{8.6.24}$$

where $d \in [2, 3]$ represents the two or three-dimensional space in which the problem is posed.

For other viscoplastic fluids, the selection of the function space is determined by the integrability of the derivative of the highest order in a given problem. In simple terms, this guarantees the integrability of the lower order derivates as well as that of the function itself. Here, the integrability of an exponent of $K(\mathbf{u})$ is required, as illustrated by the following two cases:

1. In connection with the integrability of the velocity functional:

$$\int_\Omega \phi(K(\mathbf{u}))\, dv. \tag{8.6.25}$$

2. The viscous and yield stress dissipation rate integrals:

$$a(K(\mathbf{u}), \mathbf{u}, \mathbf{v}) = \frac{1}{2} \int_\Omega \eta(K(\mathbf{u}))\mathbf{A}(\mathbf{u}) : \mathbf{A}(\mathbf{v})\, dv, \tag{8.6.26}$$

$$j(\mathbf{v}) = \int_\Omega K(\mathbf{v})\, dv. \tag{8.6.27}$$

For Bingham fluids, the viscosity is constant and the relevant function space is either $(H^1(\Omega))^d$ or $(H_0^1(\Omega))^d$. For Herschel-Bulkley fluids, one can observe from (4.6.39) and (4.6.41) that the integrability of $K(\mathbf{v})^{m+1}$ is important. Here, excluding the case $m = 1$, which corresponds to the Bingham fluid, one is faced with $m \in (0, 1)$. That is, the function space is now $W^{1,p}$, where $p = m + 1$. For Casson fluids, one can see from (4.6.44) and (4.6.46) that $p = 2$. Thus, assuming $p > 1$, the relevant norm is given by

$$||\mathbf{v}|| = \left(\int_\Omega \left[\sum_{i=1}^{d} |v_i|^p + \sum_{i,j=1}^{d} |v_{i,j}|^p \right] dv \right)^{1/p}. \tag{8.6.28}$$

Next, the class of admissible functions may form a subspace or belong to a *convex set* in the chosen function space. Recall that a set $\mathscr{S}$ is *convex* whenever for any two elements in it, the elements that lie along the *line* joining them also belong to $\mathscr{S}$. That is, $w \in \mathscr{S}$, whenever

$$w = (1 - t)u + tv \in \mathscr{S}, \quad 0 \le t \le 1, \quad \forall u, v \in \mathscr{S}. \tag{8.6.29}$$

As an example, consider the Dirichlet problem, and assume that two functions u and v satisfy the given boundary conditions. Clearly, any function $w = (1-t)u + tv$, $0 \leq t \leq 1$ satisfies the given boundary conditions as well.

The final piece in the jigsaw puzzle is to define the conditions which must be met by a functional Φ defined over $\mathscr{S}$. Firstly, it must be *convex*. That is, for every $u, v \in \mathscr{S}$,

$$\Phi((1-t)u + tv) \leq (1-t)\Phi(u) + t\Phi(v), \quad 0 \leq t \leq 1, \tag{8.6.30}$$

whenever the right-hand side is defined. The functional Φ is said to be *strictly convex*, if it is convex and $\forall u, v \in \mathscr{S}$, $u \neq v$, the above inequality is strict, i.e.,

$$\Phi((1-t)u + tv) < (1-t)\Phi(u) + t\Phi(v), \quad 0 < t < 1. \tag{8.6.31}$$

The above definition is an extension of what one learns in the calculus of a function of a single variable. That is $y = f(x)$ is strictly convex over $[a, b]$ means that the graph of the function lies below the straight line joining $[a, f(a)]$ to $[b, f(b)]$. In this case, one notes further that the function $y = f(x)$ attains its global minimum at a single point in $[a, b]$; this reasoning applies here too.

Next, a convex functional is said to be *proper*, meaning that it nowhere takes the value $-\infty$ and is not identically equal to $+\infty$.

8.6.3 Existence and Uniqueness

Here, we shall recall the fundamental theorem governing the existence and uniqueness of the solution to the problem of minimising a functional Φ over $\mathscr{S}$. Suppose that

$$\Phi \text{ is convex, l.s.c. and proper.} \tag{8.6.32}$$

In addition to the above condition, the fundamental theorem assumes the following:

$$\text{Either the set } \mathscr{S} \text{ is bounded,} \tag{8.6.33}$$

or that the functional Φ *is coercive over* $\mathscr{S}$, i.e., that

$$\lim \Phi(u) = +\infty, \quad u \in \mathscr{S}, \quad ||u|| \to \infty. \tag{8.6.34}$$

This theorem says that there *exists at least one solution* to the problem of minimising $\Phi(u)$, $u \in \mathscr{S}$. If the functional Φ is l.s.c, proper and strictly convex over S, the minimisation problem has a *unique solution*. For a proof, see Proposition 1.2, Chap. II, in [9].

In fluid mechanics, in general, the set $\mathscr{S}$ is not bounded, and thus one has to prove that the functional Φ is coercive over this set.

For example, this argument applies when one wishes to prove the existence and uniqueness of the minimiser of the functional $\Phi(w)$ in (8.1.54), which arises when one considers the steady flow of a Bingham fluid in a pipe of arbitrary cross-section due to a constant pressure gradient.

To be precise, we can now formulate this problem as follows: Find the minimum of

$$\Phi(w) = \frac{1}{2}\eta a(w, w) + \tau_y j(w) - (G, w), \quad \forall\, w \in H_0^1(\Omega), \tag{8.6.35}$$

where Ω is the cross-section of the pipe.

8.6.4 Variational Inequality

Turning next to the basic inequality (8.2.21), here are the requirements before one can call it a *variational inequality*.

1. The vector fields $\mathbf{u}, \mathbf{v}, \mathbf{w}$ must be elements of $W^{1,p}(\Omega) \times (0, T)$, where $(0, T)$ denotes the time interval. Note that if $p = 2$, the linear space is $H^1(\Omega)$.
2. Every element of $W^{1,p}(\Omega) \times (0, T)$ is divergence free.
3. Each velocity field satisfies the same boundary condition on $\partial\Omega \times (0, T)$, with a prescribed initial condition in Ω. That is, each velocity field lies in a subspace or a convex set.
4. Recall the viscous dissipation rate integral (8.2.14):

$$a(K(\mathbf{u}), \mathbf{v}, \mathbf{w}) = \frac{1}{2}\int_{\Omega} \eta(K(\mathbf{u}))\mathbf{A}(\mathbf{v}) : \mathbf{A}(\mathbf{w})\, dv, \tag{8.6.36}$$

   where η is the viscosity which depends on the second invariant of the Rivlin-Ericksen tensor $\mathbf{A}$, derived from the velocity field $\mathbf{u}$. In simple shearing flows, this invariant is simply the shear rate $\dot{\gamma}$; see (2.5.1) and (3.4.12). Using this idea, it will be assumed that the shear stress $\sigma = \eta(\dot{\gamma})\dot{\gamma}$ is a non-decreasing function in $\dot{\gamma} \geq 0$ satisfying

$$c_1\dot{\gamma}^{m-1} \leq \eta(\dot{\gamma})\dot{\gamma} \leq c_2\dot{\gamma}^{m-1}, \tag{8.6.37}$$

   for some positive constants c_1, c_2 and $m > 1$. See Kato [10] for the reasons behind this requirement. Obviously, the Bingham, Herschel-Bulkley and Casson fluids meet (8.6.37).
5. Next, recall the yield stress dissipation rate integral given by (8.2.15):

$$\tau_y j(\mathbf{v}) = \tau_y \int_{\Omega} K(\mathbf{v})\, dv. \tag{8.6.38}$$

   This functional has to be proved to be l.s.c, proper and convex. For the hint of a proof when $\mathbf{v} \in (H_0^1(\Omega))^2$, see p. 78 in [11].

The existence and uniqueness of the solution to a given variational inequality is a topic which requires an enormous amount of space and cannot be explained in simple terms. However, the above requirements, strengthened by demanding that the shear stress $\eta(\dot{\gamma})\dot{\gamma}$ is strictly convex in $\dot{\gamma} \geq 0$, seem to be sufficient; see Ekeland and Temam [9], Lions [12] and Kato [10].

If a given problem does not meet the above conditions, the basic inequality may still be solvable through numerical methods. In this situation, all that can be said is that one is *performing numerical experiments* [13].

8.6.5 *Equivalence of the Minimiser and the Solution of the Variational Inequality*

It would be desirable to prove that the minimiser $\mathbf{u}$ of the functional $\Phi(\mathbf{v})$ in (8.1.30) is the same as the solution $\mathbf{u}$ of the variational inequality (8.2.21); obviously, inertia has to be ignored to proceed. The reasons behind the congruence of the solutions are discussed below.

First of all, the functional Φ is split into $\Phi = \Phi_1 + \Phi_2$, where both Φ_1, Φ_2 are l.s.c convex functionals with Φ_1 being Gateaux-differentiable with a differential Φ_1'. Thus, consider the situation when

$$\Phi_1(\mathbf{v}) = \int_{\Omega} \left(\int_0^{K(\mathbf{v})} \eta(\xi)\xi \, d\xi \right) dv. \tag{8.6.39}$$

Formally, recalling from Sect. 4.6 that $\partial K/\partial \mathbf{A} = \mathbf{A}/2K$, and given some smoothness assumptions, one can show that Φ_1' leads to the following:

$$\begin{aligned} \langle \Phi_1'(\mathbf{u}), \mathbf{w} \rangle &= \frac{1}{2} \int_{\Omega} \eta(K(\mathbf{u}))\mathbf{A}(\mathbf{u}) : \mathbf{A}(\mathbf{w}) \, dv \\ &= a(K(\mathbf{u}), \mathbf{u}, \mathbf{w}). \end{aligned} \tag{8.6.40}$$

The reason behind this lies in the fact that the Gateaux derivative is a directional derivative and produces a functional by its action on $\mathbf{w}$. To see this clearly, consider the Bingham fluid with

$$\Phi_1(\mathbf{v}) = \frac{1}{2}\eta \int_{\Omega} K^2(\mathbf{A}(\mathbf{v})) \, dv. \tag{8.6.41}$$

Now,

$$\lim_{\varepsilon \to 0} \frac{K^2(\mathbf{A}(\mathbf{u} + \varepsilon \mathbf{w})) - K^2(\mathbf{A}(\mathbf{u}))}{\varepsilon} = \mathbf{A}(\mathbf{u}) : \mathbf{A}(\mathbf{w}). \tag{8.6.42}$$

That is, (8.6.40) is valid.

Next, define the l.s.c functional

$$\Phi_2(\mathbf{v}) = \tau_y j(\mathbf{v}) - \int_{\partial\Omega_t} \mathbf{t}\cdot\mathbf{v}\,dS - \int_{\Omega} \rho\mathbf{b}\cdot\mathbf{v}\,dv. \tag{8.6.43}$$

The basic result is that the minimiser $\mathbf{u}$ of $\Phi(\mathbf{v})$ is the same as the solution of the variational inequality

$$\langle \Phi_1'(\mathbf{u}), \mathbf{v}-\mathbf{u}\rangle + \Phi_2(\mathbf{v}) - \Phi_2(\mathbf{u}) \geq 0. \tag{8.6.44}$$

For a proof, see Proposition 2.2 in Chap. II [9]. Here , the reflexivity of the underlying Banach space $W^{1,p}$ is required, meaning that $1 < p < \infty$.

As an example, consider the steady flow of a Bingham fluid in a pipe of arbitrary cross-section under a constant pressure gradient. The solution w to this problem can be obtained by minimising the functional $\Phi(v)$ in (8.1.54), repeated here for convenience:

$$\Phi(v) = \frac{1}{2}\eta a(v,v) + \tau_y j(v) - (G,v), \quad \forall\, v \in H_0^1(\Omega), \tag{8.6.45}$$

where Ω is the domain defining the cross-section of the pipe.

From (8.2.21), it can be shown that the corresponding variational inequality for the solution w is given by

$$\eta a(w, v-w) + \tau_y[j(v) - j(w)] \geq (G, v-w), \quad \forall\, v, w \in H_0^1(\Omega). \tag{8.6.46}$$

Here the three functionals appearing in (8.6.45) and (8.6.46) are:

$$a(w,v) = \int_{\Omega} (\nabla w\cdot\nabla v)\,da, \tag{8.6.47}$$

$$j(w) = \int_{\Omega} |\nabla w|\,da, \tag{8.6.48}$$

$$(G,w) = \int_{\Omega} Gw\,da. \tag{8.6.49}$$

Hence, the solution of w obtained from (8.6.45) will be identical to that derived from (8.6.46).

More generally, if the flow is steady and inertia is ignored, one can subtract the energy equation (8.3.3) from the equation satisfied by the minimiser (cf. (8.1.30)) to obtain

$$\Phi(\mathbf{u}) = \Phi_1(\mathbf{u}) - a(K(\mathbf{u}),\mathbf{u},\mathbf{u}) + \int_{\partial\Omega_u} \mathbf{U}\cdot\mathbf{t}\,dS. \tag{8.6.50}$$

Obviously, if $\mathbf{U} = \mathbf{0}$, a further simplification of this result occurs.

8.7 Equivalence of the Solution of the Variational Inequality and the Equations of Motion

In 1948, Rivlin proved that for any chosen, static, finite deformation to be possible in an incompressible, isotropic elastic body, it was sufficient to exhibit a pressure field which satisfied the equations of equilibrium.[2] Subsequently, this idea was exploited in non-Newtonian fluid mechanics and has made its way into finite element modelling. Thus, for an assumed velocity field to be possible in a viscoplastic fluid, one has to demonstrate that a pressure field exists which satisfies the equations of motion. As shown in Sect. 4.1, the pressure term can be defined uniquely when the fluid has yielded. And, of course, in such a domain, the viscoplastic fluid satisfies a constitutive relation which makes the task easier.

As shown above, if a solution vector $\mathbf{u}$ satisfies the equations of motion in a given problem, it satisfies the variational inequality (8.2.19). Conversely, if one can prove that a velocity field $\mathbf{u}$, which meets the variational inequality, satisfies the equations of motion as well for it leads to the existence of a pressure field in a given problem, the two solutions are identical. The demonstration of this equality is based on two separate ideas.

- Suppose that ϕ is scalar and that $\mathbf{v}$ is any velocity field such that $\nabla \cdot \mathbf{v} = 0$ in a domain Ω, and $\mathbf{v} \cdot \mathbf{n} = 0$ on its boundary $\partial\Omega$. In this situation, the divergence theorem leads to the result that

$$\int_{\Omega} \nabla\phi \cdot \mathbf{v}\, dv = \int_{\Omega} \nabla \cdot (\phi\mathbf{v})\, dv = \int_{\partial\Omega} \phi(\mathbf{v} \cdot \mathbf{n})\, dS = 0. \tag{8.7.1}$$

  Is it possible to establish the converse? That is, suppose that $\mathbf{f}$ is any vector field such that for all divergence free vector fields $\mathbf{v}$, satisfying the given boundary condition, the following holds:

$$\int_{\Omega} \mathbf{f} \cdot \mathbf{v}\, dv = 0. \tag{8.7.2}$$

  Can one now prove that $\mathbf{f}$ is the gradient of a scalar ϕ? In principle, the proof of this result has been given by Ladyzhenskaya [15] in connection with Navier-Stokes equations which describe the flows of incompressible Newtonian fluids.
- The second idea is to assume that a solution $\mathbf{u}$ to the variational inequality exists and to turn the inequality into an equality. Now, suppose that $S_{ij}(\mathbf{u})$ are the corresponding components of the extra stress tensor in a viscoplastic fluid such that the following holds true for all divergence free vector fields $\mathbf{v}$:

$$\int_{\Omega} \left[(S_{ij}(\mathbf{u}))_{,j} + \rho b_i - \rho\left(\frac{\partial u_i}{\partial t} + u_{i,j}u_j \right) \right] v_i\, dv = 0. \tag{8.7.3}$$

[2] For a survey, see [14].

Assuming that the above holds, it follows that the vector f_i given by

$$f_i = (S_{ij}(\mathbf{u}))_{,j} + \rho b_i - \rho\left(\frac{\partial u_i}{\partial t} + u_{i,j}u_j\right) \tag{8.7.4}$$

is the gradient of a scalar p, which is commonly known as the pressure. That is, the solution $\mathbf{u}$ of the variational inequality is the same as that of the equations of motion. The following example, based on that in [7], illustrates the method. The proof is formal and assumes that on the boundary, the velocity field is zero.

Suppose that in such a flow, the variational inequality has the form (8.2.21) with $\mathbf{a} = \partial\mathbf{u}/\partial t + (\mathbf{u}\cdot\nabla)\mathbf{u}$, and $\mathbf{u} = \mathbf{v} = \mathbf{0}$ on $\partial\Omega$. Hence, we obtain

$$\rho(\mathbf{a}, \mathbf{v}-\mathbf{u}) - \rho(\mathbf{b}, \mathbf{v}-\mathbf{u}) + a(K(\mathbf{u}), \mathbf{u}, \mathbf{v}-\mathbf{u}) + \tau_y[j(\mathbf{v}) - j(\mathbf{u})] \geq 0. \tag{8.7.5}$$

Next, replace $\mathbf{v}$ by $\mathbf{u} + \varepsilon\mathbf{v}$. Thus, when $\mathbf{A}(\mathbf{u}) \neq \mathbf{0}$, one can derive the following (cf. (4.6.25)):

$$\lim_{\varepsilon\to 0}\frac{j(\mathbf{u}+\varepsilon\mathbf{v}) - j(\mathbf{u})}{\varepsilon} = \int_{\Omega}\frac{1}{2K(\mathbf{u})}\mathbf{A}(\mathbf{u}) : \mathbf{A}(\mathbf{v})\, dv. \tag{8.7.6}$$

Hence, replacing $\mathbf{v}$ by $\mathbf{u}+\varepsilon\mathbf{v}$ in (8.7.5), dividing by ε and taking the limit as $\varepsilon \to 0$, we obtain:

$$\begin{aligned}&\rho(\mathbf{a}, \mathbf{v}-\mathbf{u}) - \rho(\mathbf{b}, \mathbf{v}-\mathbf{u}) + a(K(\mathbf{u}), \mathbf{u}, \mathbf{v})\\ &\quad + \tau_y\int_{\Omega}\frac{1}{2K(\mathbf{u})}\mathbf{A}(\mathbf{u}) : \mathbf{A}(\mathbf{v})\, dv \geq 0.\end{aligned} \tag{8.7.7}$$

Replacing $\mathbf{v}$ by $-\mathbf{v}$, which is permissible, one finds that the solution $\mathbf{u}$ of the variational inequality now satisfies the following equation:

$$\rho(\mathbf{a}-\mathbf{b}, \mathbf{v}) + a(K(\mathbf{u}), \mathbf{u}, \mathbf{v}) + \tau_y\int_{\Omega}\frac{1}{2K(\mathbf{u})}\mathbf{A}(\mathbf{u}) : \mathbf{A}(\mathbf{v})\, dv = 0, \tag{8.7.8}$$

where

$$a(K(\mathbf{u}), \mathbf{u}, \mathbf{v}) = \frac{1}{2}\int_{\Omega}\eta(K(\mathbf{u}))\mathbf{A}(\mathbf{u}) : \mathbf{A}(\mathbf{v})\, dv. \tag{8.7.9}$$

The constitutive equation for the visoplastic fluid under consideration is given by

$$S_{ij}(\mathbf{u}) = \left[\eta(K(\mathbf{u})) + \frac{\tau_y}{K(\mathbf{u})}\right]A_{ij}(\mathbf{u}). \tag{8.7.10}$$

Now, $\mathbf{v} = \mathbf{0}$ on $\partial\Omega$ means that

$$\int_{\Omega}[S_{ij,j}v_i + S_{ij}v_{i,j}]\, dv = \int_{\Omega}[S_{ij}v_i]_{,j}\, dv = \int_{\partial\Omega}S_{ij}n_jv_i\, dS = 0. \tag{8.7.11}$$

Hence,

$$-\int_{\Omega}(S_{ij}(\mathbf{u}))_{,j}v_i\,dv=\int_{\Omega}S_{ij}(\mathbf{u})v_{i,j}\,dv=\frac{1}{2}\int_{\Omega}S_{ij}(\mathbf{u})A_{ij}(\mathbf{v})\,dv. \tag{8.7.12}$$

Comparing (8.7.8), (8.7.9) and (8.7.12) and suppressing the dependence on $\mathbf{u}$ for brevity, it has been proved that

$$\int_{\Omega}\Big[\rho a_i-\rho b_i-S_{ij,j}\Big]v_i\,dv=0 \tag{8.7.13}$$

for all divergence free velocity fields $\mathbf{v}$, vanishing on $\partial\Omega$. Hence, the velocity field $\mathbf{u}$ is such that

$$\rho a_i-\rho b_i-S_{ij,j}=p_{,i}, \tag{8.7.14}$$

where p is a scalar. In other words, the solution $\mathbf{u}$ of the variational inequality is also the solution of the equations of motion in the given problem. Such a problem has been named the *reservoir problem* in [7].

- A different method to prove that the solution of the variational inequality for the steady flow in a pipe of uniform, arbitrary cross-section satisfies the equations of motion in a Bingham fluid appears in [9]; see Chap. IV, Sect. 3.

Thus, while there are some results which prove the equivalence, there is no universal theorem guaranteeing that the solution of a variational inequity is congruent with that obtained from the equations of motion in all problems. Nevertheless, there is enough substantive support to accept that the two are identical in several problems of interest.

8.8 Special Cases of the Variational Inequality

In this section, it is shown that a simplification of the variational inequality (8.2.21) occurs in a number of flows. These are examined next.

8.8.1 Flows with Zero Stress Power Difference

The right side of Eq. (8.2.19) or (8.2.21) is zero in number of problems of interest. Consequently, one has:

$$\rho\left(\frac{\partial\mathbf{u}}{\partial t},\mathbf{v}-\mathbf{u}\right)+\rho b(\mathbf{u},\mathbf{u},\mathbf{v}-\mathbf{u})-\rho(\mathbf{b},\mathbf{v}-\mathbf{u})$$
$$+a(K(\mathbf{u}),\mathbf{u},\mathbf{v}-\mathbf{u})+\tau_y[j(\mathbf{v})-j(\mathbf{u})]\geq 0. \tag{8.8.1}$$

Here is a list of such flows.

1. Let both $\mathbf{u}$ and $\mathbf{v}$ meet the same boundary conditions, i.e., one has a Dirichlet problem, e.g., in the lid driven flow in a cavity, or in a reservoir where the velocity is zero. The reservoir problem appears in [7].
2. Consider the case of a solid body, or a number of bodies, at rest in a flow with the velocity given by $U(t)\mathbf{i}$ at infinity. Then, Ω is the unbounded domain with a rigid body, or many such bodies, inside of it. It is now easy to see that the surface integral in Eq. (8.2.21) vanishes on the boundary of every solid, because the trial velocity field $\mathbf{v}$, and the true velocity field $\mathbf{u}$ are both zero on it. Also, at infinity, every kinematically admissible field is equal to $U(t)\mathbf{i}$, or $\mathbf{v} = \mathbf{u}$ there. Hence, the surface integral in Eq. (8.2.21) is zero over the entire flow domain as required, and Eq. (8.8.1) is the correct form of this inequality.
3. Finally, let us turn to a class of free surface problems. Here, the boundary $\partial\Omega$ consists of two disjoint parts: $\partial\Omega_u$, where the velocity vector is prescribed, and $\partial\Omega_t$, where the stress vector is prescribed. On the part $\partial\Omega_u$, where the velocity is prescribed, it is clear that $\mathbf{v} - \mathbf{u} = \mathbf{0}$. If the remaining part, $\partial\Omega_t$, is such that it is open to the atmosphere, i.e., it is a free surface, then the stress vector will be zero on it. Hence, Eq. (8.8.1) is valid.

   An example of such a flow arises in the unsteady squeezing disk flow, where the top and bottom plates move together with a prescribed speed, while the lateral surface is open to the atmosphere. The same argument can be applied to the torsional flow. Other instances include the flow in a capillary rheometer, the slump test, the weir rupture test and the mud flow down an incline. In every flow mentioned here, there exist parts of the boundary where the velocity is prescribed, while on the remaining parts of the boundary, the stress vector is zero. For example, consider the mud flow down an incline as an initial value problem. Here, the velocity is prescribed upstream, it is zero on the inclined plane, and the mud surface open to the atmosphere is stress free. Interestingly enough, in all of the free surface flows mentioned here, the domain Ω occupied by the fluid changes with time.

8.8.2 Flows with Non-zero Stress Power Difference

Consider the unsteady axial flow in an infinitely long pipe of uniform cross-section, which may be simply or multiply-connected, and in which all velocity fields, such as $\mathbf{u}$ and $\mathbf{v}$, have a non-zero component in the axial direction only. That is, the solution velocity field is given by $\mathbf{u} = w(x, y, t)\mathbf{k}$, and $\mathbf{v} = v(x, y, t)\mathbf{k}$. In this case, it is easily shown that the shear stresses S_{xz} and S_{yz} depend on (x, y, t) only, while the normal stress $S_{zz} = 0$. The pressure term is given by $p = -G(t)z$, where $G(t) > 0$ is the pressure drop per unit length and the pressure is measured from a datum where it may be set to zero. Next, consider a pipe of unit length, lying between $z = 0$ and $z = 1$. Now, it is easily seen that on these end planes, $\mathbf{n} = \pm\mathbf{k}$, and

$$\mathbf{t} = \mathbf{T}\mathbf{n} = \pm(S_{xz}\mathbf{i} + S_{yz}\mathbf{j} - p\mathbf{k}). \tag{8.8.2}$$

Using the above and the adherence condition by which the velocity fields $\mathbf{u}$ and $\mathbf{v}$ vanish on the surface of the pipe, it is found that

$$\int_{\partial\Omega} (\mathbf{v} - \mathbf{u}) \cdot \mathbf{t}\, da = G(t) \int_{\Omega} (v(x, y, t) - w(x, y, t))\, da, \tag{8.8.3}$$

where Ω is the domain of cross-section of the pipe. Note that it is not essential that one knows the shear stresses S_{xz} and S_{yz}; what is needed is the inner product $(\mathbf{v} - \mathbf{u}) \cdot \mathbf{t}$.

Let us now derive the complete form of the variational inequality for unsteady flows in a pipe. For the assumed velocity fields,

$$\mathbf{A}(\mathbf{u}) : \mathbf{A}(\mathbf{v} - \mathbf{u}) = 2\nabla w \cdot \nabla(v - w), \tag{8.8.4}$$

and

$$K^2(w) = \nabla w \cdot \nabla w, \tag{8.8.5}$$

where ∇ is the two-dimensional gradient operator.

Now, set the body force $\mathbf{b} = \mathbf{0}$, or absorb it into the pressure term, if the body force is that due to gravity. Also, note that the acceleration vector is given by

$$\mathbf{a} = \frac{\partial w}{\partial t}\mathbf{k}, \tag{8.8.6}$$

which means that the trilinear functional in Eq. (8.2.21) vanishes. Let us now define four new integrals which follow from Eqs. (8.2.14)–(8.2.17). They are:

$$a\Big(K(w), w, v - w\Big) = \int_{\Omega} \eta\Big(K(w)\Big)\nabla w \cdot \nabla(v - w)\, da, \tag{8.8.7}$$

$$\tau_y[j(v) - j(w)] = \tau_y \int_{\Omega} \Big[\, |\nabla v| - |\nabla w| \,\Big]\, da, \tag{8.8.8}$$

$$\Big(G(t), v - w\Big) = \int_{\Omega} G(t)(v - w)\, da, \tag{8.8.9}$$

$$\Big(\frac{\partial w}{\partial t}, v - w\Big) = \int_{\Omega} \frac{\partial w}{\partial t}(v - w)\, da. \tag{8.8.10}$$

Thus, one is led to the fundamental inequality for the unsteady flows in a pipe:

$$\rho\Big(\frac{\partial w}{\partial t}, v - w\Big) + a\Big(K(w), w, v - w\Big) + \tau_y[j(v) - j(w)] \geq \Big(G(t), v - w\Big), \quad \forall v, w \in (H_0^1(\Omega))^2. \tag{8.8.11}$$

In the above inequality, the trial velocity field v may be steady or unsteady. All that is needed is that v must obey the same smoothness and boundary conditions as those applicable to w. From this inequality, the equations of energy balance can be derived as in (8.3.3) above and this results in the following:

$$\rho\left(\frac{\partial w}{\partial t}, w\right) + a\Big(K(w), w, w\Big) + \tau_y j(w) = \Big(G(t), w\Big). \tag{8.8.12}$$

Additional examples where the stress power difference is non-zero arise in the rise of bubbles and in the motions of rigid bodies in viscoplastic fluids. These matters are discussed fully in Sects. 9.2 and 9.3 below.

8.8.3 The Trilinear Functional Involving Acceleration Terms

When one looks at Eq. (8.2.21), the trilinear functional $b(\mathbf{u}, \mathbf{u}, \mathbf{v} - \mathbf{u})$ is seen to appear. By its definition in Eq. (8.2.17), this has the form

$$b(\mathbf{u}, \mathbf{u}, \mathbf{v} - \mathbf{u}) = \int_{\Omega} u_j u_{i,j}(v_i - u_i)\, dv, \tag{8.8.13}$$

and includes the convected terms of the acceleration vector. We shall examine how one may replace the above integral by another one to develop a suitable numerical scheme. Additionally, as shown by Duvaut and Lions [6, 7] and Kato [10], for example, a crucial step in proving the existence and uniqueness of solutions relies on replacing the functional $b(\mathbf{u}, \mathbf{u}, \mathbf{v})$ by $b(\mathbf{u}, \mathbf{v}, \mathbf{u})$, because the term $u_{i,j}$ is replaced by the known gradient $v_{i,j}$ of the trial velocity field. It is seen that such a replacement is possible in some instances, and we shall discuss this next.

Suppose that $\mathbf{u}$, $\mathbf{v}$ and $\mathbf{w}$ are any three smooth vector fields which are all divergence free. Then, it is trivial to verify that

$$\int_{\Omega} (u_j v_i w_i)_{,j}\, dv = b(\mathbf{u}, \mathbf{v}, \mathbf{w}) + b(\mathbf{u}, \mathbf{w}, \mathbf{v}). \tag{8.8.14}$$

Consequently, by the divergence theorem,

$$b(\mathbf{u}, \mathbf{v}, \mathbf{u}) + b(\mathbf{u}, \mathbf{u}, \mathbf{v}) = \int_{\partial\Omega} (\mathbf{v} \cdot \mathbf{u})(\mathbf{u} \cdot \mathbf{n})\, dS. \tag{8.8.15}$$

Thus,

$$2b(\mathbf{u}, \mathbf{u}, \mathbf{u}) = \int_{\partial\Omega} (\mathbf{u} \cdot \mathbf{u})(\mathbf{u} \cdot \mathbf{n})\, dS. \tag{8.8.16}$$

Since,

$$b(\mathbf{u}, \mathbf{u}, \mathbf{v} - \mathbf{u}) = b(\mathbf{u}, \mathbf{u}, \mathbf{v}) - b(\mathbf{u}, \mathbf{u}, \mathbf{u}), \tag{8.8.17}$$

we obtain:

$$b(\mathbf{u}, \mathbf{u}, \mathbf{v} - \mathbf{u}) = \frac{1}{2} \int_{\partial\Omega} [(2\mathbf{v} - \mathbf{u}) \cdot \mathbf{u}](\mathbf{u} \cdot \mathbf{n})\, da - b(\mathbf{u}, \mathbf{v}, \mathbf{u}) \tag{8.8.18}$$

in any given problem, which is valid in all continuous media. The crucial point is that the integral involving the local acceleration term, i.e., $(\partial\mathbf{u}/\partial t, \mathbf{v} - \mathbf{u})$, is quadratic in $\mathbf{u}$. With the above modification, the functional $b(\mathbf{u}, \mathbf{u}, \mathbf{v} - \mathbf{u})$, which is of a cubic order in $\mathbf{u}$, can be replaced by $b(\mathbf{u}, \mathbf{v}, \mathbf{u})$, that is also quadratic in $\mathbf{u}$, with an additional term given by a surface integral. It turns out that the latter is known in many cases.

Clearly, it is desirable to investigate when

$$\frac{1}{2} \int_{\partial\Omega} [(2\mathbf{v} - \mathbf{u}) \cdot \mathbf{u}](\mathbf{u} \cdot \mathbf{n})\, dS = 0. \tag{8.8.19}$$

There are several examples which satisfy the above condition. We shall mention some of them only. They are:

1. The reservoir problem, where $\mathbf{u} = \mathbf{v} = \mathbf{0}$ on the boundary.
2. The cavity driven flow, where on three parts of the boundary, the $\mathbf{u} = \mathbf{v} = \mathbf{0}$, and on the moving part, $\mathbf{u} \cdot \mathbf{n} = 0$.
3. The third example is the flow past a body/bodies at rest in a uniform flow at infinity. Here, $\mathbf{v} = \mathbf{u} = U(t)\mathbf{i}$, and $\mathbf{u} \cdot \mathbf{n} = \pm U(t)$ at infinity. And, on each solid surface, $\mathbf{u} \cdot \mathbf{n} = 0$.
4. The next one is the case of the torsional flow, where $\mathbf{u} \cdot \mathbf{n} = 0$ on the rotating disks, and on the free surface. Hence, Eq. (8.8.19) holds true. Moreover, it holds true in the case of a pipe flow, whether it is steady or unsteady. Given this, it would seem that in these five flows, it might be possible to prove existence and uniqueness theorems for general visco-plastic fluids. As far as the flow of a Bingham fluid in a pipe is concerned, such theorems do exist [6, 7, 13].

Now, let us look at those situations when the surface integral in Eq. (8.8.18) is not zero. In the case of a mud flow down an incline, the integral is determined fully by prescribing the upstream velocity whereby $\mathbf{v} = \mathbf{u}$; note that on the inclined plane and the free surface, $\mathbf{u} \cdot \mathbf{n} = 0$, and the contribution to this integral from these two parts of the boundary is zero. Thus, in the energy inequality for mud flows, it is possible to replace $b(\mathbf{u}, \mathbf{u}, \mathbf{v})$ by $b(\mathbf{u}, \mathbf{v}, \mathbf{u})$, with an additional known term.

Turning now to the case of the squeezing disk flow, it is worth recalling that on the free surface, two sets of boundary conditions are needed for all fluids–Newtonian or non-Newtonian. In the flow under discussion, the following two sets of boundary conditions have to be imposed on the free surface: the first is a global condition determined by the conservation of mass, which equates the rate of fluid squeezed by

the movement of the disks with the rate at which the free surface is bulging outwards; the second one arises from demanding that the stress vector be zero at every point on the surface. Thus, in the squeezing disk flow, the surface integral in Eq. (8.8.18) cannot be determined à priori. This would suggest that this particular flow is likely to cause problems in developing a numerical scheme for its solution as shown by the numerous attempts to solve it.

8.9 Viscoplasticity Constraint Tensor: The Final Equivalence

It has been shown earlier that in an incompressible material, the constraint of incompressibility leads to the existence of the pressure p, and the total stress tensor $\mathbf{T}$ is determined to within an isotropic stress tensor $-p\mathbf{1}$; see (4.1.13). Similarly, the existence of the yield stress is a constraint on the response of an incompressible viscoplastic fluid to a given motion. That is, one may expect a second *constraint tensor* $\boldsymbol{\Lambda}$ to arise in these materials. This matter has been explored earlier in Sect. 4.4 to explain why and how such a tensor can arise and why it is important.

As noted in Sect. 4.3, one has to establish a connection between the solution velocity field $\mathbf{u}$ and the tensor $\boldsymbol{\Lambda}$ to solve a given flow problem. Unfortunately, such a connection is hard to find, even in the case of a Bingham fluid. For such a fluid, it was proved by Duvaut and Lions that the tensor $\boldsymbol{\Lambda}$ exists under zero Dirichlet boundary conditions; see Sect. 9, Chap. VI in [7], where this tensor is identified as the *multiplier* $\mathbf{m}$. Moreover, this tensor, when it exists, satisfies the following conditions:

$$\boldsymbol{\Lambda} : \boldsymbol{\Lambda} \leq 1, \tag{8.9.1}$$

$$\boldsymbol{\Lambda} : \mathbf{A}(\mathbf{v}) \leq [\mathbf{A}(\mathbf{v}) : \mathbf{A}(\mathbf{v})]^{1/2}, \tag{8.9.2}$$

$$\boldsymbol{\Lambda} : \mathbf{A}(\mathbf{u}) = [\mathbf{A}(\mathbf{u}) : \mathbf{A}(\mathbf{u})]^{1/2}, \tag{8.9.3}$$

where $\mathbf{v}$ is any trial velocity field and $\mathbf{u}$ is the solution velocity field. Note that Eq. (8.9.3) provides the crucial relation between $\boldsymbol{\Lambda}$ and $\mathbf{u}$; this cannot be established by arguments based on constraints alone, a fact recognised in Sect. 4.3. More recently, Glowinski [13] has pointed out that the tensor $\boldsymbol{\Lambda}$ may be non-unique; the proof of its existence is harder if the boundary conditions are non-zero. However, $\nabla \cdot \boldsymbol{\Lambda}$ is unique [16], a fact that is crucial in connection with the equations of motion; see (8.9.6) below.

Obviously, there is much to be gained when one employs the tensor $\boldsymbol{\Lambda}$ in solving a given flow problem, for its magnitude separates the yielded zone from the rigid zone in the following fashion. To be specific, let $\boldsymbol{\Lambda} : \boldsymbol{\Lambda} < 1$. In this situation, Eq. (8.9.3) and the Cauchy-Schwarz inequality show that:

$$\begin{aligned}[A_{ij}(\mathbf{u})A_{ij}(\mathbf{u})]^{1/2} = \Lambda_{ij}A_{ij}(\mathbf{u}) &\leq [\Lambda_{kl}\Lambda_{kl}]^{1/2}[A_{ij}(\mathbf{u})A_{ij}(\mathbf{u})]^{1/2} \\ &< [A_{ij}(\mathbf{u})A_{ij}(\mathbf{u})]^{1/2}.\end{aligned} \tag{8.9.4}$$

The only solution to this inequality is that $A_{ij}(\mathbf{u}) = \mathbf{0}$. That is, wherever $\boldsymbol{\Lambda} : \boldsymbol{\Lambda} < 1$, the motion must be rigid. Thus, the domain of the flow can be decomposed into two mutually disjoint sets: one where $\boldsymbol{\Lambda} : \boldsymbol{\Lambda} < 1$ and the flow is rigid; and, another where $\boldsymbol{\Lambda} : \boldsymbol{\Lambda} = 1$ and the fluid has yielded, as shown earlier in Sect. 4.3.

In sum, under Dirichlet boundary conditions, one may adopt the constitutive equation of a Bingham fluid to be given by (4.3.7), viz.,

$$\mathbf{S}(\mathbf{v}) = \eta \mathbf{A}(\mathbf{v}) + \sqrt{2}\, \tau_y\, \boldsymbol{\Lambda}(\mathbf{v}), \quad \mathbf{1} : \boldsymbol{\Lambda} = 0, \tag{8.9.5}$$

with $\boldsymbol{\Lambda}$ obeying (8.9.1)–(8.9.3). Since the constitutive equation (8.9.5) holds throughout the flow domain, one may substitute it into Cauchy's equations of motion (4.2.15) to solve this class of flow problems. Thus, one obtains:

$$-\nabla p + \eta \nabla \cdot \mathbf{A}(\mathbf{v}) + \sqrt{2}\tau_y \nabla \cdot \boldsymbol{\Lambda} + \rho \mathbf{b} = \rho \mathbf{a}. \tag{8.9.6}$$

Let us assume that this problem has a unique solution $\mathbf{u}$. Substituting this into the fundamental inequality (8.2.19) and using (8.9.2) and (8.9.3), one can show that $\mathbf{u}$ satisfies the following variational inequality:

$$\rho\left(\frac{\partial \mathbf{u}}{\partial t}, \mathbf{v} - \mathbf{u}\right) + \rho b(\mathbf{u}, \mathbf{u}, \mathbf{v} - \mathbf{u}) - \rho(\mathbf{b}, \mathbf{v} - \mathbf{u}) + \frac{1}{2}\eta \int_{\Omega} \mathbf{A}(\mathbf{u}) : \mathbf{A}(\mathbf{v} - \mathbf{u})\, dv$$

$$+ \tau_y[j(\mathbf{v}) - j(\mathbf{u})] \geq 0, \tag{8.9.7}$$

because $\mathbf{v} = \mathbf{u}$ on the boundary $\partial\Omega$.

It was shown by Duvaut and Lions [7] that the solution of this variational inequality, under zero Dirichlet boundary conditions, is equivalent to solving the problem using (8.9.1)–(8.9.3), (8.9.5) and (8.9.6); for non-zero boundary conditions, the congruence of the two solutions has been established by Glowinski [13]. This is the *final equivalence*, and it will be exploited in the context of operator-splitting methods in Chap. 10.

For all non-Bingham incompressible viscoplastic fluids, the existence of the tensor $\boldsymbol{\Lambda}$ under Dirichlet boundary conditions has not been proved, which means that numerical modelling is of an *experimental nature*, once again.

8.10 The Basic Inequality for Compressible Viscoplastic Fluids

The derivation of the the variational inequality for compressible fluids follows the same procedures as that for the incompressible fluid, drawing upon the work of Huilgol and You [17]. Once again, let the flow domain Ω be a bounded or an unbounded set in the three dimensional Euclidean space in general, and let it be decomposed into two disjoint subsets Ω_1 and Ω_0 as in Eq. (8.2.2) above. That is, Ω_1 is the region where the fluid has yielded, and Ω_0 is where it moves as a rigid body or is at rest. Note that either Ω_1 or Ω_0 may be empty.

Using the constitutive equation for a compressible viscoplastic fluid, it follows that the pseudo-stress power is given by:

$$\begin{aligned}\frac{1}{2}\mathbf{T}(p,\Theta,\mathbf{u}):\mathbf{A}(\mathbf{v}) &= -p\nabla\cdot\mathbf{v}+\frac{1}{2}\mathbf{S}(p,\Theta,\mathbf{u}):\mathbf{A}(\mathbf{v})\\ &= [\alpha(p,\Theta,I,II,III)-p](\nabla\cdot\mathbf{v})\\ &\quad+\frac{1}{2}\eta(p,\Theta,I,II,III)\mathbf{A}(\mathbf{u}):\mathbf{A}(\mathbf{v})\\ &\quad+\frac{1}{2}\frac{\tau_y(p,\Theta)}{K(\mathbf{u})}\mathbf{A}(\mathbf{u}):\mathbf{A}(\mathbf{v}),\end{aligned}\tag{8.10.1}$$

where the invariants I, II, III depend on $\mathbf{A}(\mathbf{u})$. Next, by the Cauchy-Schwarz inequality, it follows that in the set Ω_1,

$$\begin{aligned}\frac{1}{2}\mathbf{T}(p,\Theta,\mathbf{u}):\mathbf{A}(\mathbf{v}) &\le [\alpha(p,\Theta,I,II,III)-p](\nabla\cdot\mathbf{v})\\ &\quad+\frac{1}{2}\eta(p,\Theta,I,II,III)\mathbf{A}(\mathbf{u}):\mathbf{A}(\mathbf{v})\\ &\quad+\tau_y(p,\Theta)K(\mathbf{v})).\end{aligned}\tag{8.10.2}$$

As in the case of incompressible fluids, it can be shown that Eq. (8.10.2) is valid in the whole region Ω.

Once again, the corresponding results for the solution velocity field $\mathbf{u}$ can be obtained quite easily. One finds that in the set Ω_1, the true stress power is given by:

$$\begin{aligned}\frac{1}{2}\mathbf{T}(p,\Theta,\mathbf{u}):\mathbf{A}(\mathbf{u}) &= [\alpha(p,\Theta,I,II,III)-p](\nabla\cdot\mathbf{u})\\ &\quad+\frac{1}{2}\eta(p,\Theta,I,II,III)\mathbf{A}(\mathbf{u}):\mathbf{A}(\mathbf{u})\\ &\quad+\tau_y(p,\Theta)K(\mathbf{u}).\end{aligned}\tag{8.10.3}$$

One can show, yet again, that Eq. (8.10.3) is valid in Ω. Hence, following the procedure for incompressible fluids, we obtain

$$\begin{aligned}\rho(\mathbf{a}-\mathbf{b})\cdot(\mathbf{v}-\mathbf{u})+[\alpha(p,\Theta,I,II,III)-p]\nabla\cdot(\mathbf{v}-\mathbf{u})&\\ +\frac{1}{2}\eta(p,\Theta,I,II,III)\mathbf{A}(\mathbf{u}):\mathbf{A}(\mathbf{v}-\mathbf{u})&\\ +\tau_y(p,\Theta)[K(\mathbf{v}))-K(\mathbf{u})]&\\ \ge\nabla\cdot((\mathbf{v}-\mathbf{u})\cdot\mathbf{T}).&\end{aligned}\tag{8.10.4}$$

This inequality holds at all points in the flow domain, and can be transformed into one that applies over the flow region by integration with respect to its volume just as in the case for incompressible fluids.

To accomplish this, a couple of changes are necessary. First of all, the *viscous dissipation rate integral* for any three velocity fields $\mathbf{u}$, $\mathbf{v}$ and $\mathbf{w}$ is:

$$a\Big(\mathbf{u}, \mathbf{v}, \mathbf{w}\Big) = \frac{1}{2}\int\limits_{\Omega} \eta(p, \Theta, I, II, III)\mathbf{A}(\mathbf{v}) : \mathbf{A}(\mathbf{w})\, dv. \tag{8.10.5}$$

Next, the *yield stress dissipation rate integral* is:

$$j(\mathbf{v}) = \int\limits_{\Omega} \tau_y(p, \Theta)K(\mathbf{v})\, dv. \tag{8.10.6}$$

Recalling the earlier definitions in Eqs. (8.2.16) and (8.2.17), one can integrate Eq. (8.10.4) over the flow domain Ω, and derive

$$\begin{aligned}\rho\Big(\frac{\partial \mathbf{u}}{\partial t}, \mathbf{v} - \mathbf{u}\Big) + \rho b\Big(\mathbf{u}, \mathbf{u}, \mathbf{v} - \mathbf{u}\Big) - \rho\Big(\mathbf{b}, \mathbf{v} - \mathbf{u}\Big) \\ + \int\limits_{\Omega} [\alpha(p, \Theta, I, II, III) - p][\nabla \cdot (\mathbf{v} - \mathbf{u})]\, dv + a\Big(\mathbf{u}, \mathbf{u}, \mathbf{v} - \mathbf{u}\Big) \\ + j(\mathbf{v}) - j(\mathbf{u}) \geq \int\limits_{\Omega} \nabla \cdot ((\mathbf{v} - \mathbf{u}) \cdot \mathbf{T})\, dv.\end{aligned} \tag{8.10.7}$$

Employing the divergence theorem on the right side, one finds that

$$\begin{aligned}\rho\Big(\frac{\partial \mathbf{u}}{\partial t}, \mathbf{v} - \mathbf{u}\Big) + \rho b\Big(\mathbf{u}, \mathbf{u}, \mathbf{v} - \mathbf{u}\Big) - \rho\Big(\mathbf{b}, \mathbf{v} - \mathbf{u}\Big) \\ + \int\limits_{\Omega} [\alpha(p, \Theta, I, II, III) - p][\nabla \cdot (\mathbf{v} - \mathbf{u})]\, dv + a\Big(\mathbf{u}, \mathbf{u}, \mathbf{v} - \mathbf{u}\Big) \\ + j(\mathbf{v}) - j(\mathbf{u}) \geq \int\limits_{\partial\Omega} (\mathbf{v} - \mathbf{u}) \cdot \mathbf{T}\mathbf{n}\, dS,\end{aligned} \tag{8.10.8}$$

where $\mathbf{n}$ is the external unit normal to the boundary $\partial\Omega$ of the flow domain.

Once again, decomposing the boundary $\partial\Omega$ into the union of two disjoint subsets $\partial\Omega_u$, where the velocity vector $\mathbf{U}$ is prescribed, and $\partial\Omega_t$, where the stress vector $\mathbf{T}\mathbf{n} = \mathbf{t}$ is given, one sees that

$$\int\limits_{\partial\Omega} (\mathbf{v} - \mathbf{u}) \cdot \mathbf{T}\mathbf{n}\, dS = \int\limits_{\partial\Omega_t} (\mathbf{v} - \mathbf{u}) \cdot \mathbf{t}\, dS. \tag{8.10.9}$$

Thus, in any given flow, the exact form of the *stress power difference*, which is the integral on the right side of Eq. (8.10.9), leads to the specific form of the inequality applicable to that flow. Thus, we arrive at the following inequality:

$$\rho\left(\frac{\partial \mathbf{u}}{\partial t}, \mathbf{v}-\mathbf{u}\right)+\rho b\Big(\mathbf{u}, \mathbf{u}, \mathbf{v}-\mathbf{u}\Big)-\rho\Big(\mathbf{b}, \mathbf{v}-\mathbf{u}\Big) + \int_{\Omega}[\alpha(p, \Theta, I, II, III)-p][\nabla \cdot(\mathbf{v}-\mathbf{u})]\, dv + a\Big(\mathbf{u}, \mathbf{u}, \mathbf{v}-\mathbf{u}\Big) + j(\mathbf{v})-j(\mathbf{u}) \geq \int_{\partial \Omega_t}(\mathbf{v}-\mathbf{u}) \cdot \mathbf{t}\, da. \tag{8.10.10}$$

Now, we shall turn to the continuity and energy equations. The former is given by

$$\frac{d\rho}{dt}+\rho \nabla \cdot \mathbf{u}=0, \tag{8.10.11}$$

which in view of Eq. (4.5.3) becomes:

$$\frac{\partial \rho}{\partial p}\frac{dp}{dt}+\frac{\partial \rho}{\partial \Theta}\frac{d\Theta}{dt}+\rho(p, \Theta)\nabla \cdot \mathbf{u}=0. \tag{8.10.12}$$

Recalling the balance of energy equation as:

$$\rho\frac{de}{dt}=\frac{1}{2}\mathbf{T}:\mathbf{A}-\nabla \cdot \mathbf{q}+\rho r, \tag{8.10.13}$$

where e is the internal energy function, $\mathbf{q}$ is the heat flux vector and r is the radiation supply, one finds that constitutive equations for e and $\mathbf{q}$ are needed. Here, in analogy with Eq. (4.5.6), we assume that

$$e=e(p, \Theta, I, II, III), \tag{8.10.14}$$

$$\mathbf{q}=-k(p, \Theta, I, II, III)\nabla \Theta, \tag{8.10.15}$$

where $k>0$ is the conductivity coefficient.

In injection moulding, one finds that the energy equation is replaced by

$$\rho c_p\frac{d\Theta}{dt}=\frac{1}{2}\mathbf{T}:\mathbf{A}-\nabla \cdot \mathbf{q}, \tag{8.10.16}$$

where c_p is the heat capacity at constant pressure.

Now, all of the main equations, including the basic inequality for the velocity field $\mathbf{u}$, have been assembled. From these, one can devise a numerical scheme to solve flow problems of interest.

References

1. Prager W (1954) On slow visco-plastic flow. Studies in Mathematics and Mechanics presented to Richard von Mises, Studies in Mathematics and Mechanics. Academic Press, New York, pp 208–216
2. Zwick KJ, Ayyaswamy PS, Cohen IM (1996) Variational analysis of the squeezing flow of a yield stress fluid. J Non-Newton Fluid Mech 63:179–199
3. Huilgol RR, Nguyen QD (2000) Variational principles and variational inequalities for the unsteady flows of a yield stress fluid. Int J Non-Linear Mech 36:49–67
4. Huilgol RR (1998) Variational principle and variational inequality for a yield stress fluid in the presence of slip. J Non-Newton Fluid Mech 75:231–251
5. Huilgol RR (2002) Variational inequalities in the flows of yield stress fluids including inertia: theory and applications. Phys Fluids 14:1269–1283
6. Duvaut G, Lions JL (1972) Les inéquations on mécanique et en physique. Dunod, Paris
7. Duvaut G, Lions JL (1976) Inequalities in mechanics and physics. Springer, New York
8. Akhiezer NI (1962) The calculus of variations. Blaisdell, New York
9. Ekeland I, Temam R (1976) Convex analysis and variational problems. North-Holland, Amsterdam
10. Kato Y (1993) Variational inequalities of Bingham type in three dimensions. Nagoya Math J 129:53–95
11. Glowinski R (1984) Numerical methods for nonlinear variational problems. Springer, New York
12. Lions JL (1968) Quelques des méthodes de résolution des problèmes aux limites non linéaires. Dunod and Gauthier-Villars, Paris
13. Glowinski R (2003) Finite element methods for incompressible viscous flows. In: Ciarlet PG, Lions J-L (eds) Handbook of numerical analysis, vol IX. North-Holland, Amsterdam
14. Rivlin RS (1960) Some topics in finite elasticity. In: Goodier JN, Hoff NJ (eds) Structural mechanics: proceedings of the first symposium on naval structural mechanics. Pergamon, Oxford, pp 169–198
15. Ladyzhenskaya OA (1963) The mathematical theory of viscous incompressible flow. Gordon and Breach, New York
16. Dean EJ, Glowinski R, Guidoboni G (2007) On the numerical simulation of Bingham visco-plastic flow: old and new results. J Non-Newton Fluid Mech 142:36–62
17. Huilgol RR, You Z (2009) Prolegomena to variational inequalities and numerical schemes for compressible viscoplastic fluids. J Non-Newton Fluid Mech 158:113–126

Chapter 9
Energy Methods in Action: Equality, Inequality and Stability

This chapter is concerned with five types of problems in which energy principles play a significant role. The first one is to determine the minimum pressure drop per unit length to initiate a steady flow of a Bingham fluid in a pipe of arbitrary cross-section; here, it is found that the variational principle developed in the previous chapter furnishes the necessary tool. In the next two sections, the conditions under which bubbles remain static when trapped in a viscoplastic fluid and the motion of a rigid body in such a fluid are discussed. Subsequently, the initiation and cessation of unsteady shearing flows in a channel or a pipe of arbitrary cross-section are examined through the application of variational inequalities. The time estimate for the fluid to attain a steady flow is found to be infinitely large; in contrast, the steady flow in a Bingham fluid comes to rest in a finite amount of time provided the pressure drop falls below a critical value. The latter result, as mentioned earlier in Chap. 1, provides a crucial difference between the cessation behaviour of Newtonian and Bingham fluids. Similar outcomes have been proven for more general viscoplastic fluids and attention is drawn to them as well.

Finally, the Orr-Sommerfeld energy equation is used to investigate the nonlinear stability of the steady flow of a Bingham fluid in a channel or a circular pipe.

9.1 Axial Flow in a Pipe of Arbitrary Cross-Section

In this section, a formula for the minimum pressure drop per unit length $G_c > 0$ to initiate a steady flow in a pipe of arbitrary cross-section is derived. Next, assuming such a flow occurs, the shape of a stagnant zone next to the boundary of a pipe with corners is depicted, and bounds on the magnitude of the core and the maximum velocity in it are also obtained.

R.R. Huilgol, *Fluid Mechanics of Viscoplasticity*, DOI 10.1007/978-3-662-45617-0_9

9.1.1 The Minimum Pressure Drop per Unit Length to Initiate a Steady Flow

Consider a pipe of arbitrary cross-section defined through Ω in (x, y) coordinates, with its boundary defined by Γ. Suppose that a steady axial flow of a Bingham fluid exists in this pipe with the velocity field defined through

$$\dot{x} = 0, \quad \dot{y} = 0, \quad \dot{z} = w(x, y) \geq 0, \quad w(x, y)\Big|_{\Gamma} = 0. \tag{9.1.1}$$

This flow is assumed to occur under a constant pressure drop, i.e., $\partial p/\partial z = -Gz$, $G > 0$. The relevant Rivlin-Ericksen tensor for the velocity field (9.1.1) is given by (2.5.9); it implies that two shear stresses exist in the yielded region. They are

$$S_{xz} = S_{zx} = \eta w_{,x} + \frac{\tau_y}{|\nabla w|} w_{,x}, \quad S_{yz} = S_{zy} = \eta w_{,y} + \frac{\tau_y}{|\nabla w|} w_{,y}, \tag{9.1.2}$$

since (cf. (2.5.10)):

$$K(\mathbf{A}) = |\nabla w|, \tag{9.1.3}$$

where

$$\nabla w = w_{,x}\mathbf{i} + w_{,y}\mathbf{j}. \tag{9.1.4}$$

Obviously, shear stresses exist in the unyielded regions as well and in them, they obey the inequality:

$$0 \leq T(\mathbf{S}) = \left[S_{xz}^2 + S_{yz}^2\right]^{1/2} \leq \tau_y. \tag{9.1.5}$$

The main problem for the flow in a pipe of arbitrary cross-section may now be posed: Is there a minimum pressure drop per unit length to initiate the flow? The answer to this question can be found from the Lemmas 2.2 and 2.3 proved by Mosolov and Miasnikov [1]. In order to apply these Lemmas, one has to begin with the energy equation for the flow of a Bingham fluid in a pipe of arbitrary cross-section. Thus, modifying the energy equation (8.8.12) as necessary for the steady flow of of a Bingham fluid, one obtains:

$$\frac{1}{2}\eta \int_{\Omega} |\nabla w|^2 \, da + \tau_y \int_{\Omega} |\nabla w| \, da = \int_{\Omega} Gw \, da. \tag{9.1.6}$$

The basic idea is to turn the above into an inequality by replacing the right side by an upper bound. In order to achieve this, two Lemmas will now be stated.

Lemma 1 *If $h(x, y)$ is a smooth function satisfying the condition*

$$h(x, y)\Big|_{\Gamma} = 0, \tag{9.1.7}$$

where Γ is the boundary of the cross-section, then

$$M \int_{\Omega} |\nabla h| \, da \geq \int_{\Omega} h \, da, \quad M = \sup_{\Omega' \subseteq \Omega} \frac{A(\Omega')}{P(\Omega')}. \tag{9.1.8}$$

Here, Ω' is an arbitrary sub-domain of Ω with a boundary Γ'. Next, $A(\Omega')$ is the area of this sub-domain and $P(\Omega')$ is its perimeter. One notes that there is no restriction that Ω should possess a symmetric cross-section. This Lemma can be applied to the right side of (9.1.6) and results in the following inequality:

$$\frac{1}{2}\eta \int_{\Omega} |\nabla w|^2 \, da + \tau_y \int_{\Omega} |\nabla w| \, da \leq MG \int_{\Omega} |\nabla w| \, da. \tag{9.1.9}$$

Obviously, there will be an infinite number of sub-domains of Ω. Unless one finds a specific sub-domain which delivers the bound M, the above Lemma is not of much use. The following Lemma provides the clue regarding the shape of this sub-domain.

Lemma 2 *There exists a sub-domain Ω_1 with boundary Γ_1 for which*

$$M = \frac{A(\Omega_1)}{P(\Omega_1)}, \tag{9.1.10}$$

where, if Q is a point on Γ_1 not on Γ, then the connected part of the set $\Gamma_1 \backslash \Gamma$, containing Q, is the arc of a circle touching Γ.

This says in essence that if a point Q lies on the boundary Γ_1 and not on the boundary Γ, then the arc on which Q lies is circular and this arc is tangential to Γ when it meets it. See Fig. 9.1. The procedure to find M relies on this observation. Note that the given domain Ω may, in itself, be the optimal one as in the case of a circular disk. Otherwise, an interior one exists which furnishes M.

The importance of finding the sub-domain Ω_1 and its boundary Γ_1 arises from the fact that in 1967, Mosolov and Miasnikov [2] proved in Theorem 5 the following result:

Theorem *Let Ω be a simply connected domain in which the supremum M is obtained on a single closed curve Γ_1 bounding the sub-domain Ω_1. Then, if the motion exists in a Bingham fluid, the stagnant zones must lie outside Ω_1.*

Thus, a stagnant zone, when it exists, lies in the corner of a pipe and a circular arc separates it from the rest of the pipe.

Turning to the inequality (9.1.9), one notes that the constant M depends on the shape of the cross-section Ω only and is a geometric property. Rewriting this inequality as

$$\frac{1}{2}\eta \int_{\Omega} |\nabla w|^2 \, da \leq (MG - \tau_y) \int_{\Omega} |\nabla w| \, da, \tag{9.1.11}$$

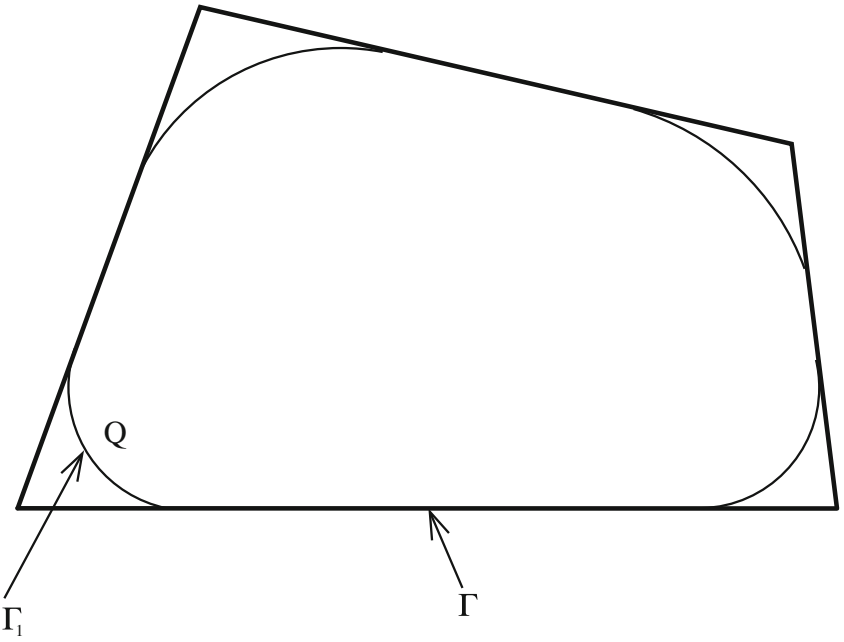

Fig. 9.1 Subdomain with a circular arc

one sees that if $MG - \tau_y \leq 0$, then

$$\eta \int_{\Omega} |\nabla w|^2 \, da \leq 0. \tag{9.1.12}$$

Since $|\nabla w| \geq 0$, the only way to satisfy the above inequality is to demand that $\nabla w = 0$ throughout Ω. That is, $w(x, y) = C$, a constant; however, the vanishing of this velocity field on the boundary Γ means that $w(x, y) \equiv 0$ in Ω. In simple terms, if $MG - \tau_y \leq 0$, then no flow can occur. Hence, we have arrived at the following:

Conclusion: A pressure drop per unit length G will sustain the steady flow in a pipe of arbitrary cross-section if

$$G > G_c = \frac{\tau_y}{M}, \tag{9.1.13}$$

where G_c is the critical pressure drop per unit length.

Obviously, for a given cross-section, the task is now to find M. While this is not simple in all cases, one can use Lemma 2 of Mosolov and Miasnikov to obtain the critical pressure drop per unit length in a few pipes of symmetric cross-section quite easily as shown by Huilgol [3].

To illustrate this method, consider a pipe of square cross-section with a side of length a each. See Fig. 9.2.

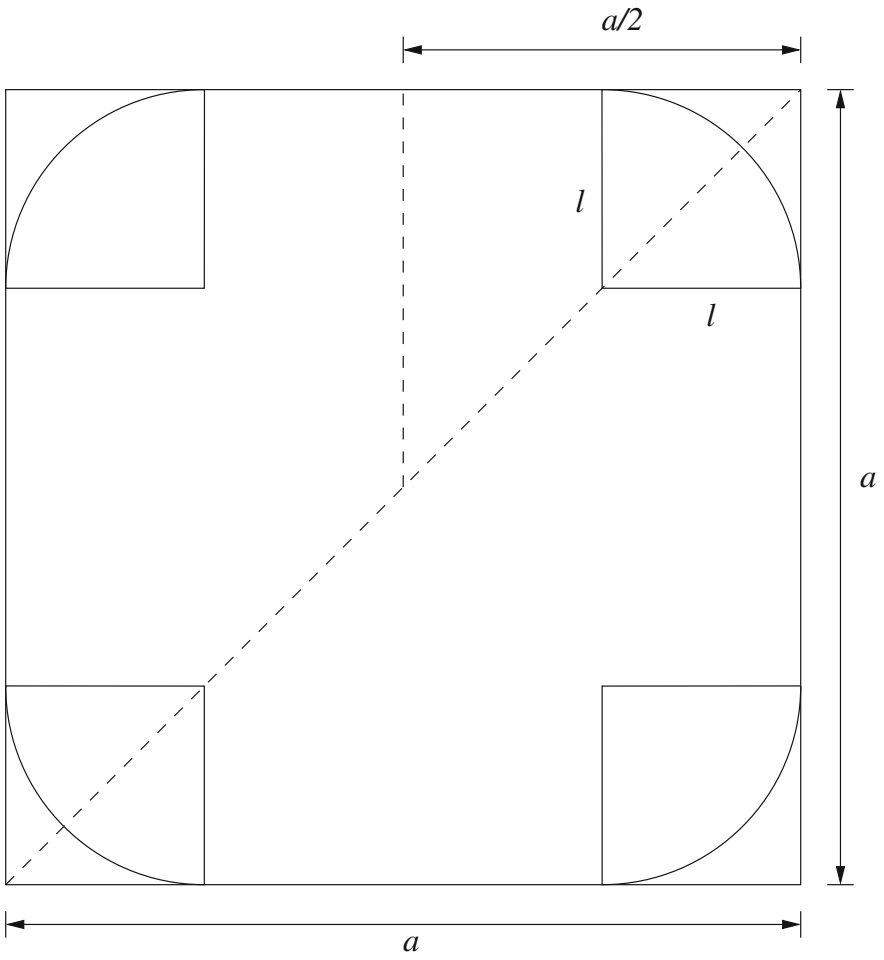

Fig. 9.2 Determining the constant M in a pipe of square cross-section

The domain Ω is defined by the square. According to Lemma 2, the boundary Γ_1 of its sub-domain Ω_1, which furnishes M, must consist of four straight lines and four circular arcs, each of which is a quarter circle. Now, choose a sub-domain Ω' with four straight edges of length $(a - 2l)$ each, and four quarter circles of radius l each. The problem is to find l so that the ratio

$$\frac{A(\Omega')}{P(\Omega')} \tag{9.1.14}$$

is a maximum. Writing the area and the perimeter in terms of l, one finds that

$$A(l) = a^2 + (\pi - 4)l^2, \quad P(l) = 4a + 2(\pi - 4)l, \quad 0 \leq l \leq a/2. \tag{9.1.15}$$

Thus, one has to maximise the ratio $A(l)/P(l)$. Solving the simple equation

$$\frac{d}{dl}\left(\frac{A(l)}{P(l)}\right) = 0 \tag{9.1.16}$$

requires finding l^* so that $A(l^*) = P(l^*)l^*$, which provides the critical value:

$$l^* = \frac{2-\sqrt{\pi}}{4-\pi}a = \frac{a}{2+\sqrt{\pi}}. \tag{9.1.17}$$

Thus, the optimum values are:

$$A(l^*) = \frac{2a^2\sqrt{\pi}}{2+\sqrt{\pi}}, \quad P(l^*) = 2a\sqrt{\pi}, \quad M = \frac{a}{2+\sqrt{\pi}}, \quad G_c = M\tau_y. \tag{9.1.18}$$

Now that the shape of the sub-domain Ω_1 has been found, the Proposition of Mosolov and Miasnikov says that the stagnant zones of the Bingham fluid lie in the four corners of the square pipe, outside Ω_1. It is important to see that M is greater than the ratio of the area of the square to its perimeter, which is $a^2/4a = a/4$. Obviously,

$$M = \frac{a}{2+\sqrt{\pi}} > \frac{a}{4}. \tag{9.1.19}$$

In the work cited [3], one can find the values of M for the following symmetric cross-sections.

1. For a pipe of circular cross-section of radius R, if the disk is itself the optimum domain, the optimal value is given by

$$M = \frac{\pi R^2}{2\pi R} = \frac{R}{2}. \tag{9.1.20}$$

   If the disk of radius R is not the optimum domain, it will contain an optimal sub-domain such that part of its boundary will consist of that of the circle with the remaining forming circular arcs inside it. See Fig. 9.3 for an example of such a domain. This clover-leaf shaped region will have an area less than that of the disk, while its perimeter is larger than that of the disk. So, the ratio of its area to the perimeter will be less than $R/2$. As the number of such intersecting circular arcs, which may be of different radii, increases, the ratio of the enclosed area to its perimeter will approach $R/2$.
   In fact, the critical pressure drop to initiate the flow in a pipe of circular cross-section has been shown earlier in (5.4.1) to be $G_c = 2\tau_y/R$, which means that one should obtain $M = R/2$ again through the Mosolov-Miasnikov Lemmas. Obviously, this has now been demonstrated.
2. In a similar manner, one can prove that for an annular region bounded by two concentric circles of radii R_1 and $R_2 > R_1$, the value of $M = (R_2 - R_1)/2$, $G_c = M\tau_y$. This value was derived earlier in (5.5.7) through a different argument.

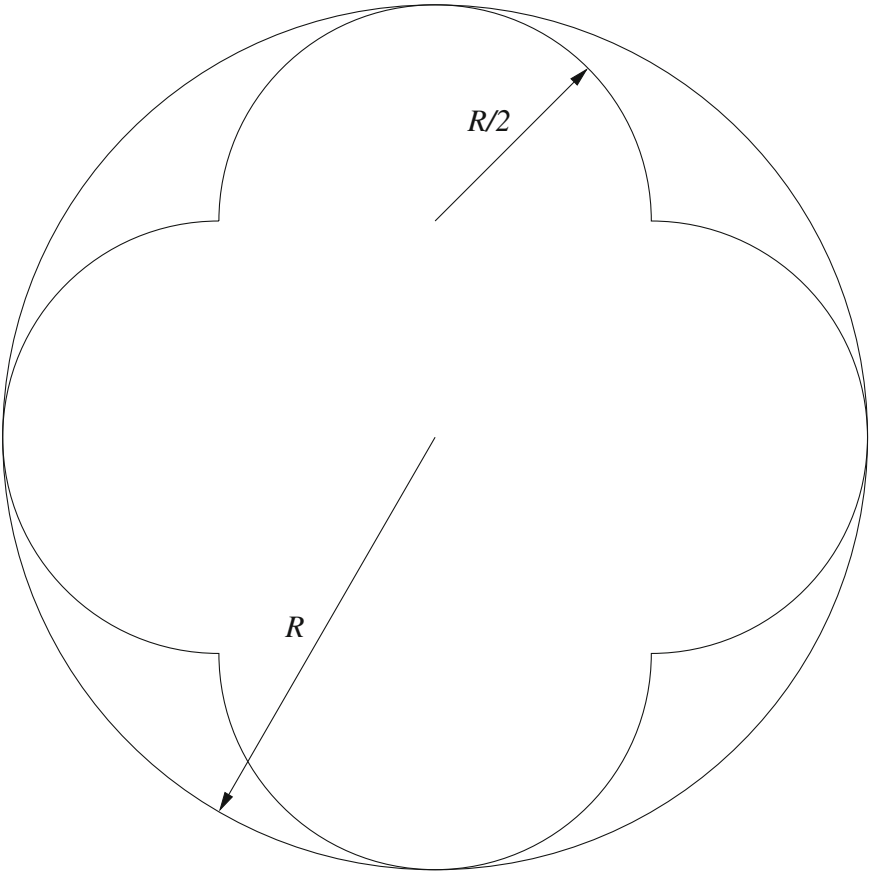

Fig. 9.3 Determining the constant M in a pipe of circular cross-section

3. For a rectangular cross-section of sides a and $b < a$,

$$M = \frac{ab}{a + b + \sqrt{(a-b)^2 + \pi ab}}, \quad G_c = M\tau_y. \tag{9.1.21}$$

See Fig. 9.4. Clearly, letting $a = b$, one can recover (9.1.19) from (9.1.21).

4. For an equilateral triangle of side a each,

$$M = \frac{\sqrt{3}}{2\left[3 + \sqrt{\pi\sqrt{3}}\right]} a \approx 0.162a, \quad G_c = M\tau_y. \tag{9.1.22}$$

See Fig. 9.5.

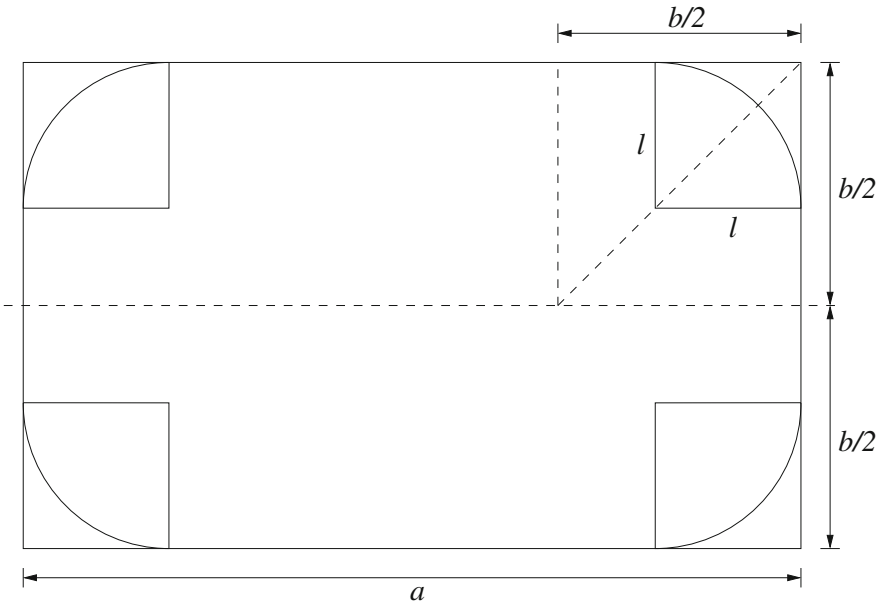

Fig. 9.4 Determining the constant M in a pipe of rectangular cross-section

5. For an $L-$shaped cross-section of arms of length L and of width b,

$$M = \frac{4L - \left[16l^2 - 20(2lb - b^2)(1 - (\pi/4))\right]^{1/2}}{10(1 - (\pi/4))}, \quad G_c = M\tau_y. \qquad (9.1.23)$$

   See Fig. 9.6. This formula holds for $0 < b < L/2$ only. See the Table below as well for a list of the optimal values of l^*/L for a given ratio of b/L (Table 9.1).
6. The cross-section of the runner in an experimental injection moulding machine has an igloo shaped cross-section; see Fig. 9.7. Since the cross-section is symmetrical about the z-axis, only the right side is depicted. Note that there is a circular arc at the top with D as its centre and two straight lines joining B to A and O to A. The coordinates of the relevant points, suitably scaled, are given in the following (Table 9.2).
   The constant M for this shape is found by locating the optimal position of G which lies on the bisector of $\angle OAB$, and forms the centre of a circular arc of radius l joining E to F. The optimal value has been found [4] to be $M = 2.02$. Note that the line AD does not play a role in the determination of M; rather, it is relevant in calculating the area of the original cross-section.

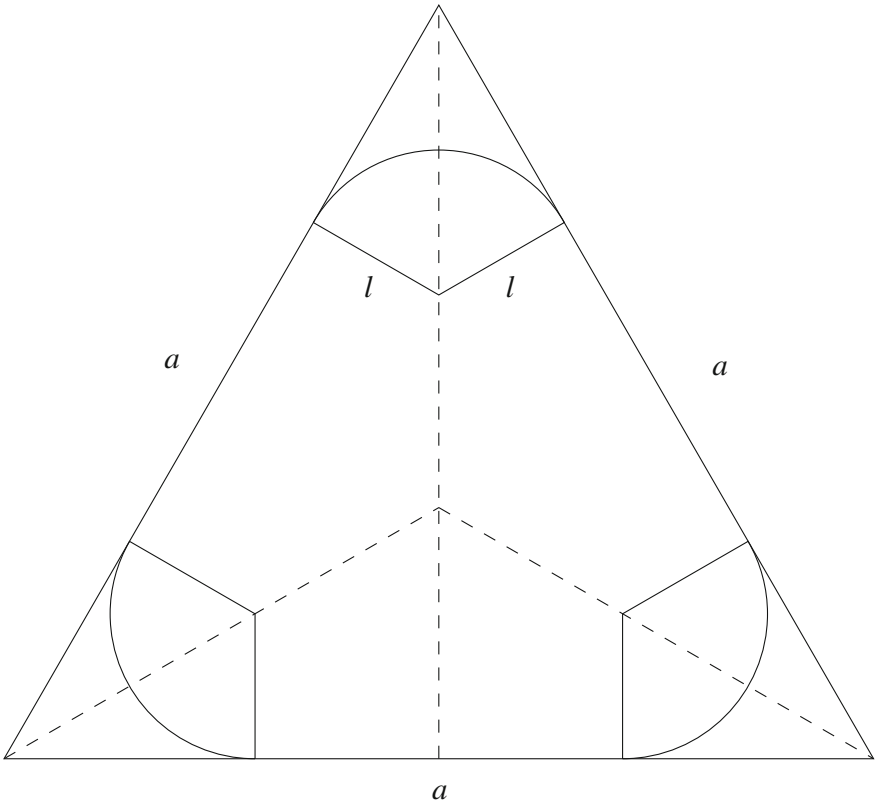

Fig. 9.5 Determining the constant M in a pipe of an equilateral triangular cross-section

9.1.2 Existence of Stagnant Zones

Suppose that the cross-section of a pipe is neither circular nor a concentric annulus. Assuming that a steady flow occurs, can one be certain that stagnant zones exist at the corners, say, in a pipe which has a simply connected cross-section? To answer this, consider the following argument. If there are no stagnant zones, then on the boundary Γ of the pipe, not only is the velocity $w = 0$, the magnitude of the shear stress on it is less than or equal to the yield stress. Hence,

$$G \times A(\Omega) \geq \tau_y \times P(\Omega), \quad \text{or} \quad G \geq \tau_y \left(\frac{A(\Omega)}{P(\Omega} \right)^{-1}. \tag{9.1.24}$$

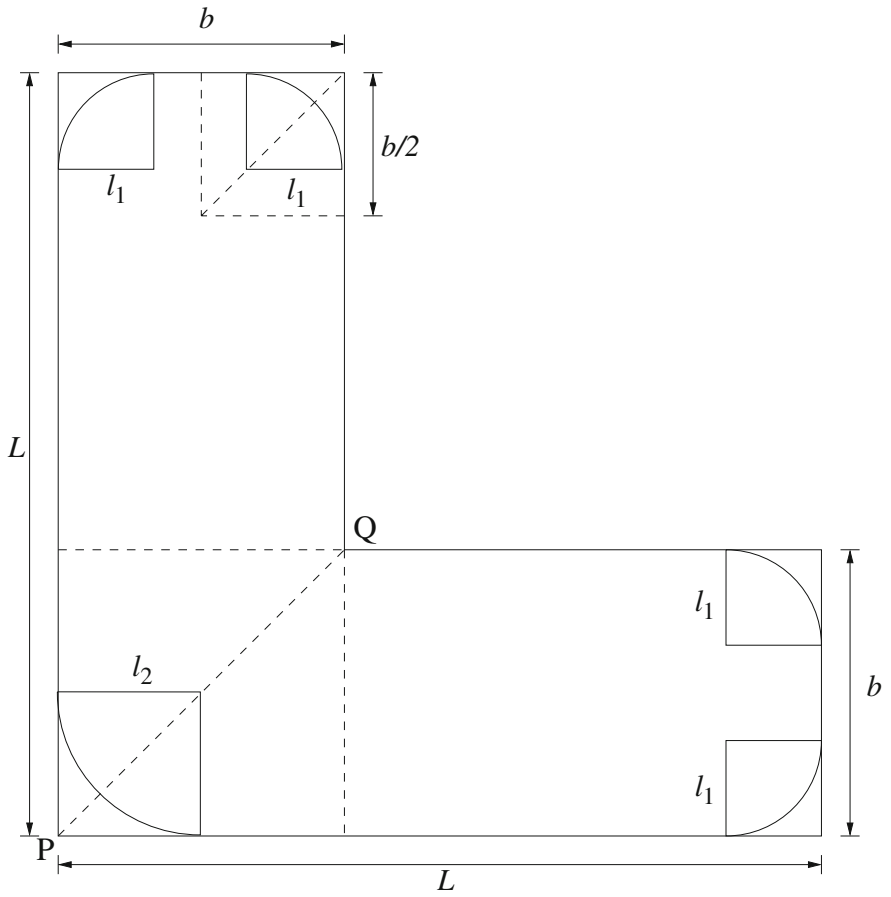

Fig. 9.6 Determining the constant M in a pipe of an L-shaped cross-section

Table 9.1 Optimal values

b/L	l^*/L
0.1	0.048
0.2	0.092
0.3	0.132
0.4	0.168
0.5	0.198

Thus, a stagnant zone will exist in such a pipe provided

$$\tau_y \left(\frac{A(\Omega)}{P(\Omega} \right)^{-1} > G. \tag{9.1.25}$$

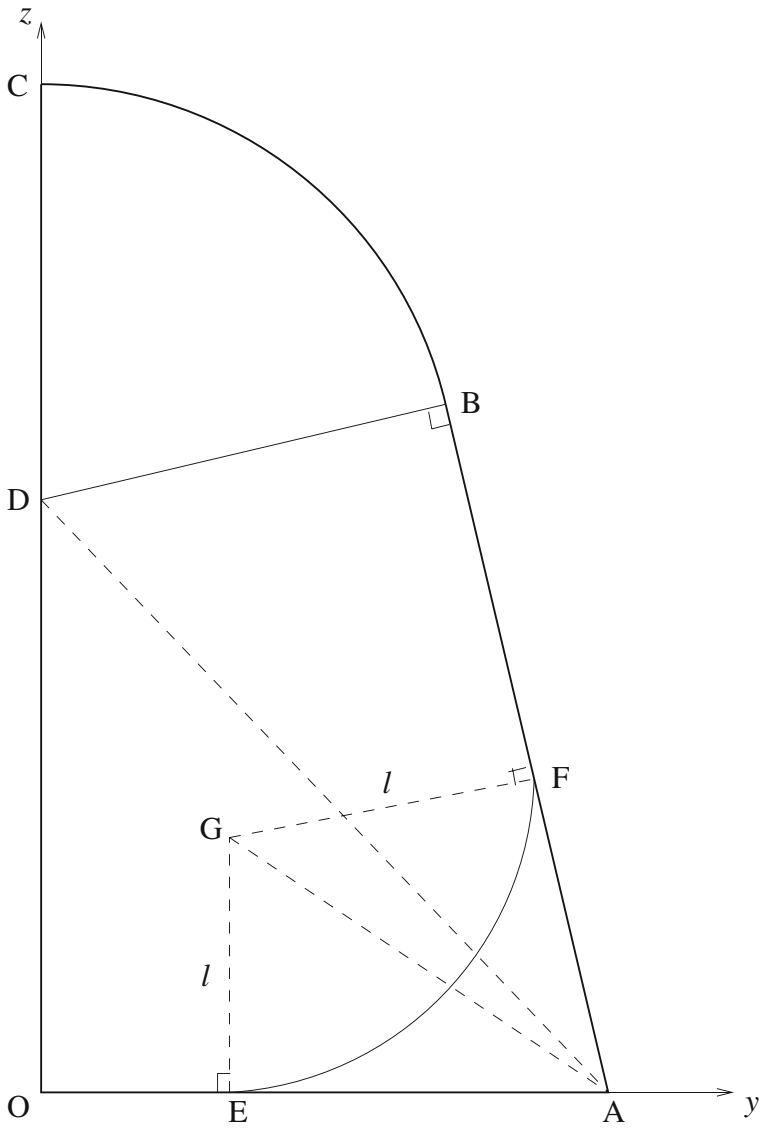

Fig. 9.7 Determining the constant M for an igloo shaped cross-section

Recall that the inequality (9.1.13) provides a lower bound to G. Thus, for example, stagnant zones exist in a pipe of square cross-section provided

$$\tau_y\left(\frac{a}{4}\right)^{-1} > G > \tau_y\left(\frac{a}{2+\sqrt{\pi}}\right)^{-1}. \tag{9.1.26}$$

This is the content of Theorem 2 in [2].

Table 9.2 Igloo shaped cross-section

Point	y-coordinate	z-coordinate
O	0	0
A	4.5	0
B	6.21	3.54
C	0	8
D	0	4.70

9.1.3 Bounds on the Magnitude of the Core and Its Maximum Velocity

Now suppose that the cross-section of the pipe is simply connected with a rigid core moving with the flow; on the boundary of the core, the shear stress is equal to the yield stress in magnitude. If the core has an area $A(C)$ and its perimeter is $P(C)$, the previous argument shows that

$$P(C) \leq \frac{G}{\tau_y} A(C). \tag{9.1.27}$$

The next question is to estimate the size of this core; rather, estimate the radius R of the largest circular disk which can lie wholly inside the core region. Since the magnitude of the shear stress on the boundary of the moving core is τ_y everywhere, it follows that inside the core, the shear stress σ is less than or equal to τ_y in magnitude. Thus, on a disk of radius R inside the core, the balance of forces using $\pi R^2 G \leq 2\pi R \tau_y$ shows that

$$R_2 = \frac{2\tau_y}{G} \geq R. \tag{9.1.28}$$

In Theorem 3 in [2], one finds the following lower bound to R:

$$R \geq R_1 = \frac{2\tau_y}{G}\left[1 + \left(1 - \frac{4\pi\tau_y^2}{G^2 A(\Omega)}\right)^{1/2}\right]^{-1}. \tag{9.1.29}$$

Turning to the maximum velocity w_C in the core, it is easy to see that the flow rate through a core of radius R_1 is less than or equal to the flow rate Q through the pipe. Thus,

$$\pi R_1^2 w_C \leq Q = \int_\Omega w \, da. \tag{9.1.30}$$

This flow rate Q can be estimated from the inequality (9.1.9) as follows. Using Cauchy-Schwarz inequality, one has that

$$\int_\Omega |\nabla w| \, da \leq \left(\int_\Omega |\nabla w|^2 \, da\right)^{1/2} A(\Omega)^{1/2}, \tag{9.1.31}$$

where $A(\Omega)$ is the area of cross-section. Using this in (9.1.9), we find that

$$\frac{1}{2}\frac{\eta}{A(\Omega)}\left(\int_{\Omega}|\nabla w|\,da\right)^2+(\tau_y-MG)\int_{\Omega}|\nabla w|\,da\le 0, \tag{9.1.32}$$

from which it follows that

$$\int_{\Omega}|\nabla w|\,da\le\frac{2A(\Omega)}{\eta}(\tau_y-MG). \tag{9.1.33}$$

Next, employing (9.1.8), we obtain

$$Q=\int_{\Omega}w\,da\le M\int_{\Omega}|\nabla w|\,da\le 2MA(\Omega)\frac{(\tau_y-MG)}{\eta}. \tag{9.1.34}$$

Thus, one finds, through (9.1.30), the following bound on the maximum velocity w_C in the core:

$$w_C\le\frac{2MA(\Omega)}{\pi R_1^2}\frac{(\tau_y-MG)}{\eta}. \tag{9.1.35}$$

9.2 Static Bubbles in Viscoplastic Fluids

Suppose that a bubble of gas of arbitrary shape is injected into a viscoplastic fluid at rest. If one knows the volume V of the bubble, one can derive a length scale R from it by assuming that the volume is equivalent to that of a sphere of radius R. That is

$$V=\frac{4}{3}\pi R^3. \tag{9.2.1}$$

The pressure p_g in the gas, as it rises slowly, is uniform, or it is assumed to depend on time only; thus $p_g = p_g(t)$. Next, on the surface of the bubble, the velocity vector in the fluid and that of the bubble are assumed to be continuous, and there are no tangential shear stresses. The difference between the pressure in the bubble and the normal stress exerted by the fluid on the bubble is balanced by surface tension effects. Given these conditions, the aim here is understand the interplay between the buoyancy force acting on the bubble and the yield stress in the fluid. To achieve this, a variational inequality for a rising bubble is derived from (8.2.19) ignoring inertial effects. It turns out that the energy equation derived from it is violated when the Bingham number exceeds a certain value; in other words, such a flow cannot exist or the bubble cannot rise. This is how the condition for a bubble to remain at rest in a Herschel-Bulkley fluid has been obtained by Dubash and Frigaard [5].

Suppose that an incompressible viscoplastic fluid, bounded by the walls of a container, is subject to a motion created by a rising bubble. On the surface of the

bubble, the fluid exerts a normal stress t_n given by $t_n = -p_L + S_{nn}$, where p_L is the pressure in the fluid and S_{nn} is the extra stress in the normal direction. That is, the stress vector $\mathbf{t}$ along the unit normal $\mathbf{n}$ *pointing into the bubble* is $\mathbf{t} = \mathbf{Tn} = t_n\mathbf{n}$. Since the pressure in the gas must exceed this normal stress, it follows that

$$p_g - (p_L - S_{nn}) = \sigma\left(\frac{1}{R_1} + \frac{1}{R_2}\right), \tag{9.2.2}$$

where σ is the surface tension, and R_1 and R_2 are the principal radii of curvature of the surface of the bubble at a given point.

Let Ω denote a finite region bounded by the container; on its walls, the fluid is at rest. One can argue that a viscoplastic fluid far removed from the rising bubble is at rest even if the domain is infinite; in this case, one truncates the velocity field inside Ω.

Let the density of the gas be ρ_g, that of the liquid be ρ, and assume that $\rho_g \ll \rho$. The buoyancy stress on the bubble, i.e., the bouyancy force per unit area, can be taken to be $\rho g R$, where g is the acceleration due to gravity. Let the constitutive equation for the viscoplastic fluid be that of the Herschel-Bulkley type, i.e., we assume that the yield stress τ_y is a constant and that the viscosity is given by

$$\eta(\dot{\gamma}) = k_b\dot{\gamma}^{m-1}, \quad 0 < m < 1, \tag{9.2.3}$$

where k_b is the consistency index and m is the power-law index. From this, we can find the velocity scale U as follows. Since the shear stress is given by $k_b\dot{\gamma}^m$, $\dot{\gamma} = U/R$, balancing the buoyancy stress and the viscous stress, one obtains:

$$\frac{\rho R g}{k_b U^m/R^m} = 1, \tag{9.2.4}$$

leading to the velocity scale:

$$U = \left(\frac{\rho g R^{m+1}}{k_b}\right)^{1/m}. \tag{9.2.5}$$

The Bingham number Bn can now be defined as the ratio of the yield stress to the viscous stress, or equivalently as the ratio of the yield stress to the buoyancy stress which is the preferred choice. Hence,

$$\mathrm{Bn} = \frac{\tau_y R^m}{k_b U^m} = \frac{\tau_y}{\rho g R}. \tag{9.2.6}$$

The non-dimensional form of the constitutive equation can now be obtained by scaling the stress tensor with respect to the buoyancy stress. It is given by

$$\mathbf{A}(\mathbf{v}) = \mathbf{0}, \quad T(\mathbf{S}) \leq \mathrm{Bn}, \tag{9.2.7}$$

$$\mathbf{S}(\mathbf{v}) = \left(K(\mathbf{v})^{m-1} + \frac{\mathrm{Bn}}{K(\mathbf{v})}\right)\mathbf{A}(\mathbf{v}), \quad T(\mathbf{S}) > \mathrm{Bn}. \tag{9.2.8}$$

Finally, the surface tension coefficient can be put in a non-dimensional form through

$$\beta = \frac{\sigma}{\rho g R^2}. \tag{9.2.9}$$

Thus, the relevant equations are (9.2.5)–(9.2.8). Of course, the velocity field must satisfy the continuity equation $\nabla \cdot \mathbf{v} = 0$.

Let us now turn to the fundamental inequality (8.2.19). In it, assume that the solution velocity field $\mathbf{u}$ and the trial velocity field $\mathbf{v}$ vanish on the walls of the container. Omit the inertial terms and assume that the non-dimensional form of the body force is vertically downwards, i.e., $\mathbf{b} = -\mathbf{k}$. Since the volume of the bubble is small compared with that of the container, one has that

$$(\mathbf{b}, \mathbf{v} - \mathbf{u}) = -\int_{\Omega} \mathbf{k} \cdot (\mathbf{v} - \mathbf{u})\, dv. \tag{9.2.10}$$

Next, the surface bounding the fluid is in two parts: one comprises the walls and the other the surface of the bubble, $\partial\Omega_b$. Let the unit normal $\mathbf{n}$ to the surface *point into the bubble* so that it is the exterior normal to the fluid surface. Thus,

$$\int_{\partial\Omega} (\mathbf{v} - \mathbf{u}) \cdot \mathbf{T}\mathbf{n}\, dS = \int_{\partial\Omega_b} (\mathbf{v} - \mathbf{u}) \cdot \mathbf{T}\mathbf{n}\, dS. \tag{9.2.11}$$

Here, in non-dimensional form,

$$\mathbf{T}\mathbf{n} = t_n \mathbf{n}, \quad t_n = -p_L + S_{nn} == -p_g + \beta\left(\frac{1}{R_1} + \frac{1}{R_2}\right), \tag{9.2.12}$$

where the radii R_1, R_2 have been scaled with respect to R. Using the divergence theorem, it follows that p_g, which depends on t only, makes no contribution to the right side of (9.2.11). Hence,

$$\int_{\partial\Omega_b} (\mathbf{v} - \mathbf{u}) \cdot \mathbf{T}\mathbf{n}\, dS = \beta \int_{\partial\Omega_b} (\mathbf{v} - \mathbf{u}) \cdot \left(\frac{1}{R_1} + \frac{1}{R_2}\right)\mathbf{n}\, dS. \tag{9.2.13}$$

Consequently, the variational inequality (8.2.19) now becomes

$$a(K(\mathbf{u}), \mathbf{u}, \mathbf{v} - \mathbf{u}) + \mathrm{Bn}[j(\mathbf{v}) - j(\mathbf{u})] \geq L(\mathbf{v} - \mathbf{u}), \tag{9.2.14}$$

where, with $\nabla \cdot \mathbf{u} = 0$, $\nabla \cdot \mathbf{w} = 0$, the three functionals are:

$$a(K(\mathbf{u}), \mathbf{u}, \mathbf{w}) = \frac{1}{2}\int_{\Omega} K(\mathbf{u})^{m-1} \mathbf{A}(\mathbf{u}) : \mathbf{A}(\mathbf{w})\, dv, \tag{9.2.15}$$

$$j(\mathbf{w}) = \int_{\Omega} K(\mathbf{w})\, dv, \tag{9.2.16}$$

$$L(\mathbf{w}) = -\int_{\Omega} \mathbf{k}\cdot\mathbf{w}\, dv - \beta \int_{\partial\Omega_b} \left(\frac{1}{R_1}+\frac{1}{R_2}\right)\mathbf{w}\cdot\mathbf{n}\, dS. \tag{9.2.17}$$

If $\mathbf{u}$ is the solution velocity field, both $\mathbf{v} = 2\mathbf{u}$ and $\mathbf{v} = \mathbf{0}$ are permissible. Thus, appealing to (8.3.3), the energy balance equation can be derived and one obtains:

$$a(K(\mathbf{u}), \mathbf{u}, \mathbf{u}) + \mathrm{Bn} j(\mathbf{u}) = L(\mathbf{u}). \tag{9.2.18}$$

If one looks at the functional $\Phi(\mathbf{v})$ in (8.1.30) and employs (4.6.41), it is easy to see that the minimiser satisfies the equation:

$$\Phi(\mathbf{u}) = \frac{1}{m+1} a(K(\mathbf{u}), \mathbf{u}, \mathbf{u}) + \mathrm{Bn} j(\mathbf{u}) - L(\mathbf{u}). \tag{9.2.19}$$

Comparing (9.2.18) with (9.2.19), it follows that the minimum value of the functional $\Phi(\mathbf{u})$ is given by

$$\Phi(\mathbf{u}) = -\frac{m}{m+1} a(K(\mathbf{u}), \mathbf{u}, \mathbf{u}). \tag{9.2.20}$$

9.2.1 *Critical Value of the Bingham Number to Prevent Bubble Motion*

Since the viscous dissipation term $a(K(\mathbf{u}), \mathbf{u}, \mathbf{u}) \geq 0$, it follows that $j(\mathbf{u}) \leq L(\mathbf{u})$ for the solution $\mathbf{u}$. That is, for a solution to exist

$$\mathrm{Bn} \leq \frac{L(\mathbf{u})}{\int_{\Omega} K(\mathbf{u})\, dv}. \tag{9.2.21}$$

Consequently, suppose that for all non-trivial admissible velocity fields $\mathbf{v}$,

$$\mathrm{Bn} \geq \mathrm{Bn}_c = \sup_{\mathbf{v}\neq\mathbf{0}} \frac{L(\mathbf{v})}{\int_{\Omega} K(\mathbf{v}))\, dv}, \tag{9.2.22}$$

where Bn_c is a critical value. The only possible solution is that $\mathbf{u} = \mathbf{0}$ in the fluid. That is, if the Bingham number exceeds the critical value, the bubble will not move.

While this is an interesting result, it is not easy to find this number, or even a lower bound to it. For instance, suppose that the bubble is of spherical shape and $\mathbf{v}$ is any admissible velocity field. In this instance, $R_1 = R_2 = 1$, a constant, and thus

$$\int_{\partial\Omega_b} \left(\frac{1}{R_1}+\frac{1}{R_2}\right)\mathbf{v}\cdot\mathbf{n}\, dS = 2\int_{\partial\Omega_b} \mathbf{v}\cdot\mathbf{n}\, dS = 0. \tag{9.2.23}$$

This simplification is not enough, for it is difficult to find an admissible velocity field which is divergence free and vanishes on the boundary of a given container. Thus, a different approach is required and this will be discussed next.

9.2.2 Critical Value from Stress Maximisation

In order to obtain a second lower bound for the critical Bingham number, one turns to the maximum principle in Sect. 8.1.3. Using the stress potential (4.6.42) for a Herschel-Bulkley fluid and (8.1.27) and non-dimensionlisation, one can prove that the true stress field maximises the functional:

$$\Psi(\mathbf{S}^*) = -\frac{m}{(m+1)2^{(m+1)/m}} \int_{\Omega} \Big(|T(\mathbf{S}^*) - \mathrm{Bn}| + T(\mathbf{S}^*) - \mathrm{Bn} \Big)^{(m+1)/m} dv. \tag{9.2.24}$$

Note that the walls of the container form the velocity boundary, $\partial\Omega_u$, and on this part $\mathbf{U} = \mathbf{0}$. Next, the admissible stress field is defined to be $\mathbf{T}^* = -p^*\mathbf{1} + \mathbf{S}^*$, if the following conditions are satisfied:

$$-\nabla p^* + \nabla \cdot \mathbf{S}^* - \mathbf{k} = \mathbf{0} \quad \text{in } \Omega, \tag{9.2.25}$$

$$(\mathbf{S}^*\mathbf{n}) \cdot \mathbf{t} = 0 \quad \text{on } \partial\Omega, \tag{9.2.26}$$

$$-p^* + (\mathbf{S}^*\mathbf{n}) \cdot \mathbf{n} = -p_g + \beta\left(\frac{1}{R_1} + \frac{1}{R_2}\right) \quad \text{on } \partial\Omega. \tag{9.2.27}$$

Here, $\mathbf{n}$ points into the bubble and $\mathbf{t}$ is any unit vector tangential to the surface of the bubble.

Now, for any admissible stress field, let the maximum of the stress invariant $T(\mathbf{S}^*)$ over the flow domain Ω be given by

$$\tilde{T}(\mathbf{S}^*) = \sup_{\mathbf{x}\in\Omega} T(\mathbf{S}^*(\mathbf{x})). \tag{9.2.28}$$

Now, suppose that $\mathrm{Bn} \geq \tilde{T}(\mathbf{S}^*)$. In this situation, (9.2.24) proves that the functional $\Psi(\mathbf{S}^*) = 0$ for all admissible stress fields, including the true stress field $\mathbf{S}$. However, from Sect. 8.1.4, is it known that the maximum value of the functional $\Psi(\mathbf{S}^*)$ is the same as the minimum value of the functional $\Phi(\mathbf{v})$. Hence, it follows from (9.2.20) that

$$\Psi(\mathbf{S}) = -\frac{m}{m+1} a(K(\mathbf{u}), \mathbf{u}, \mathbf{u}) = 0. \tag{9.2.29}$$

Since the viscous dissipation integral is non-negative, this leads to the result that $\mathbf{u} = \mathbf{0}$ in Ω.

For a spherical bubble, there exists one admissible stress field which satisfies the equations of motion (9.2.25) and the boundary conditions (9.2.26) and (9.2.27). To understand this, consider the stream function for the flow outside the bubble:

$$\psi(r,\theta,\phi) = Cr\sin^2\theta, \quad 1 \le r < \infty,\ 0 \le \theta \le \pi,\ 0 \le \phi \le 2\pi. \tag{9.2.30}$$

The velocity fields in the radial (u) and meridional directions (v) are given by:

$$u = -\frac{1}{r^2\sin\theta}\frac{\partial\psi}{\partial\theta} = -\frac{2C}{r}\cos\theta, \tag{9.2.31}$$

$$v = \frac{1}{r\sin\theta}\frac{\partial\psi}{\partial r} = \frac{C}{r}\sin\theta. \tag{9.2.32}$$

There are no shear stresses and the normal stresses, with a unit value for the viscosity, are:

$$S^*_{rr} = \frac{4C}{r^2}\cos\theta, \quad S^*_{\theta\theta} = S^*_{\phi\phi} = -\frac{2C}{r^2}\cos\theta. \tag{9.2.33}$$

The equations of motion are satisfied with the pressure field:

$$p(r,\theta) = -\frac{2C}{r^2}\cos\theta - r\cos\theta + p_0, \tag{9.2.34}$$

where p_0 is a constant. Now, on the surface of the sphere, $r = 1$, and (9.2.27) results in:

$$[2C + 1 + 4C]\cos\theta + p_0 = p_g - 2\beta, \tag{9.2.35}$$

since $R_1 = R_2 = 1$ as well. The right side is a constant and thus, $C = -1/6$. Using this value,

$$2T^2(\mathbf{S}^*) = {S^*_{rr}}^2 + {S^*_{\theta\theta}}^2 + {S^*_{\phi\phi}}^2 = \frac{2}{3r^4}\cos^2\theta, \quad r \ge 1, \tag{9.2.36}$$

whence the maximum value of $T(\mathbf{S}^*) = 1/\sqrt{3}$ when $r = 1$. This result shows that the critical Bingham number $\mathrm{Bn}_c \ge 1/\sqrt{3}$ and that a spherical bubble will not rise if the Bingham number exceeds the critical value [5].

A second method to determine the critical value is to assume that the bubble is axisymmetric and that its shape lies vertically between $0 < z_1 < z_2 < L$, where L is the height of a cylindrical column. In this case, it can be shown that [5]

$$-\int_\Omega \mathbf{k}\cdot\mathbf{v}\,dv \le \frac{1}{2\sqrt{2}}\int_\Omega K(\mathbf{v})\,dv. \tag{9.2.37}$$

In particular, for a bubble of spherical shape, the integral involving β in (9.2.17) vanishes because $R_1 = R_2 = 1$ and the velocity field $\mathbf{v}$ has zero divergence. Finally,

$z_+ - z_- = 2$, which means that

$$\mathrm{Bn}_c = \frac{1}{\sqrt{2}} \approx 0.71. \tag{9.2.38}$$

That is, the bubble is entrapped if the Bingham number exceeds this value.

A third approach to obtaining the critical value is to assume that the bubble is spherical, consisting of an incompressible viscous fluid with a viscosity $\overline{\eta}$. In this case, the constant C is given by the Hadamard-Rybczynski formula. From Eqs. (4.9.9) and (4.9.28) in [6], we find that

$$C = \frac{2\eta + 3\overline{\eta}}{4(\eta + \overline{\eta})}. \tag{9.2.39}$$

Assuming that the density $\overline{\rho}$ and the viscosity $\overline{\eta}$ of the gas in the bubble are exceedingly small, or letting $\overline{\rho}/\rho \to 0, \overline{\eta}/\eta \to 0$, one finds that $C = 1/2$. Thus, by redefining the class of admissible stress tensor fields, one finds the critical Bingham number to be $\sqrt{3}$.

However, numerical modelling [7], using the Papanastasiou model, leads to the conclusion that the critical Bingham number is 0.143. Thus, the theoretical bounds obtains from (9.2.36) and (9.2.37) are too small, while that derived from the Hadamard-Rybczynski formula is too large.

For non-spherical, axisymmetric bubbles or long cylindrical bubbles, bounds on the critical Bingham numbers have been derived; see [5]. These have been compared with experiments on bubbles resembling inverted tear drops [8]. The critical Bingham number has been found to lie in the range 0.01–0.15. While the upper limit falls close to the value 0.143 mentioned earlier, there is still a great deal of difference between bounds obtained from variational principles, numerical modelling and experiments. As far as experiments are concerned, the internal stresses in the viscoplastic fluid arising from its structural origin and the flow history, play a major role in bubble formation and propagation [9] meaning that in order to diminish the discrepancy between theory, modelling and experiment, a great deal of additional research is required.

9.2.3 A Condition for a Bubble to Move: An Upper Bound for the Bingham Number

So far, lower bounds for the critical Bingham number have been derived; these bounds tell us when the bubble is not going to move. If the bubble does rise, can one obtain an upper bound for the Bingham number? The answer can be found by considering the velocity field $\mathbf{u}_N$ in a Newtonian fluid due to a rising bubble, when there is no surface tension. The compelling reason to assume that the surface tension coefficient $\beta = 0$ in a viscoplastic fluid is that it does not affect the result from the maximisation of the stress functional; see (9.2.24).

Thus, for the sake of simplicity, consider a Bingham fluid and a Newtonian fluid with the same viscosity η, with the two true velocity fields given by $\mathbf{u}$ and $\mathbf{u}_N$ respectively. The minimiser $\mathbf{u}$ satisfies (9.2.19) with $m = 1$ and one redefines $a(\mathbf{u}, \mathbf{u}) \equiv a(1, \mathbf{u}, \mathbf{u})$. Thus,

$$\Phi(\mathbf{u}) = \frac{1}{2}a(\mathbf{u}, \mathbf{u}) + \mathrm{Bn}j(\mathbf{u}) - L(\mathbf{u}). \tag{9.2.40}$$

The velocity field $\mathbf{u}_N$ is also the minimiser of its own functional and meets:

$$\Phi_N(\mathbf{u_N}) = \frac{1}{2}a(\mathbf{u_N}, \mathbf{u_N}) - L(\mathbf{u_N}). \tag{9.2.41}$$

Now, in the absence of surface tension, a bubble will always rise in a Newtonian fluid and the balance of energy equation leads to the following:

$$a(\mathbf{u}_N, \mathbf{u}_N) = L(\mathbf{u}_N) > 0. \tag{9.2.42}$$

Thus, taking due care, one obtains:

$$\Phi_N(u_N) + \mathrm{Bn}j(\mathbf{u}_N) = \Phi(\mathbf{u}_N) \geq \Phi(\mathbf{u}), \tag{9.2.43}$$

since $\mathbf{u}_N$ is any admissible velocity field as far as the functional $\Phi(\cdot)$ is concerned.

Now, from (9.2.20), we know that the minimum values of the two functionals are:

$$\Phi(\mathbf{u}) = -\frac{1}{2}a(\mathbf{u}, \mathbf{u}), \quad \Phi_N(\mathbf{u}_N) = -\frac{1}{2}a(\mathbf{u}_N, \mathbf{u}_N). \tag{9.2.44}$$

Thus, (9.2.40) and (9.2.41) lead to the following result:

$$\Phi_N(\mathbf{u}_N) + \mathrm{Bn}j(\mathbf{u}_N) = -\frac{1}{2}a(\mathbf{u}_N, \mathbf{u}_N) + \mathrm{Bn}j(\mathbf{u}_N) \geq -\frac{1}{2}a(\mathbf{u}, \mathbf{u}). \tag{9.2.45}$$

Consequently,

$$a(\mathbf{u}, \mathbf{u}) \geq a(\mathbf{u}_N, \mathbf{u}_N) - 2\mathrm{Bn}j(\mathbf{u}_N). \tag{9.2.46}$$

By the Cauchy-Schwarz inequality,

$$j(\mathbf{u}_N) \leq V(\Omega)^{1/2}a(\mathbf{u}_N, \mathbf{u}_N), \tag{9.2.47}$$

where $V(\Omega)$ is the volume of the region Ω. Thus, (9.2.46) delivers the following inequality:

$$a(\mathbf{u}, \mathbf{u}) \geq a(\mathbf{u}_N, \mathbf{u}_N)^{1/2}[a(\mathbf{u}_N, \mathbf{u}_N)^{1/2} - 2\mathrm{Bn}V(\Omega)^{1/2}]. \tag{9.2.48}$$

Now, whenever there is a flow in a Bingham fluid due to a rising bubble, the viscous dissipation $a(\mathbf{u}, \mathbf{u}) > 0$. Since a bubble will always rise in a Newtonian fluid with a

velocity field $\mathbf{u}_N$ whenever there is no surface tension, the bubble will also rise in a Bingham fluid provided

$$\mathrm{Bn} < \frac{a(\mathbf{u}_N, \mathbf{u}_N)^{1/2}}{2V(\Omega)^{1/2}}. \tag{9.2.49}$$

While this result is elegant, it implies that a bubble will rise in a Bingham fluid if the Bingham number is small. Indeed, one can make this as small as one pleases by increasing the volume of the container, or by marginalising the yield stress.

In conclusion, there is a need to obtain better values for lower and upper bounds on the Bingham number Bn for a bubble to remain static or to move.

9.3 Motions of Rigid Bodies in Viscoplastic Fluids

The motion of a rigid body in a fluid leads two types of problems: the first one, termed *the resistance problem*, is to prescribe the translational and angular velocities of the body and to seek the subsequent forces and torques acting on the body. The second one, *the mobility problem*, is to define the force and torque acting on the body and obtain the translation and rotation of the body. The resistance problem has received much attention, beginning with the work of Stokes (c. 1851) on the drag experienced by a sphere moving with a constant speed V_N in an unbounded sea of Newtonian fluid. Stokes showed that in a creeping flow, the drag D_N experienced by a sphere of radius R is given by $D_N = 6\pi\eta V_N R$, where η is the viscosity of the Newtonian fluid. For non-Newtonian fluids, such as Bingham or second-order fluids, the drag may be significantly different from D_N.

For instance, in a viscoplastic fluid, the drag increases with the yield stress, ultimately approaching infinity and forcing the sphere to stay put. This is the conclusion reached by Beris et al. [10] that in a Bingham fluid, there is a limiting value for a yield-stress parameter beyond which the sphere cannot move or is entrapped.

To be specific, consider a solid sphere of radius R moving with a constant speed U due to the force of gravity in an unbounded domain of a Bingham fluid. This is now a resistance problem. If the density of the sphere is ρ_s and that of the fluid is $\rho(< \rho_s)$, the drag experienced by the sphere is the same as the nett force acting on it, given by

$$F = \frac{4}{3}\pi R^3(\rho_s - \rho)g = \frac{4}{3}\pi R^3\rho_s(1 - \rho_r)g, \quad \rho_r = \rho/\rho_s < 1, \tag{9.3.1}$$

where g is the acceleration due to gravity. In [10], the number N_B and the Stokes drag coefficient C_s are defined respectively as follows:

$$N_B = \frac{2\tau_y R}{\eta U}, \quad C_s = \frac{F}{6\pi\eta UR}. \tag{9.3.2}$$

The ratio of the yield stress contribution to the external force can be defined through the yield-stress parameter Y_g:

$$Y_g = \frac{2\tau_y \pi R^2}{F}, \tag{9.3.3}$$

leading to $N_B = 6C_s Y_g$, with $Y_g = 0$ corresponding to a Newtonian fluid. The relation between the Bingham number $\mathrm{Bn} = \tau_y/\rho_s Rg$ and Y_g can be established and one finds that

$$Y_g = \frac{3}{2(1-\rho_r)}\mathrm{Bn}. \tag{9.3.4}$$

Hence, as $\rho_r \to 0$, it will be seen that $Y_g \to 3/2$ Bn.

Since it is not possible to find an analytical solution to the problem of a solid sphere moving through a Bingham fluid with a constant speed under gravity, numerical methods have to be employed. The first attempt is due to Beris et al. [10] based on the finite element method using the Papanastasiou model, and assuming that solid regions exist at the front and back of the settling sphere because of stagnation points in the flow within a large domain. Note that the assumption of the flow being stagnant far away from the sphere is consistent with the existence of a yield stress.

The important result from the modelling is that the sphere will fall if $Y_g < 0.143$. That is, the resistance becomes infinitely large as this limit is approached from below. The number 0.143 is intriguing for it appears as the limiting value for the entrapment of both the solid sphere [10] and the spherical bubble in a Bingham fluid [7]; in the case of a spherical solid, numerical modelling suggests that $Y_g = 0.143 = (3/2(1-\rho_r))\,\mathrm{Bn}_c$, while the corresponding result for a spherical bubble is $\mathrm{Bn}_c = 0.143$. Thus, the former critical Bingham number is not 2/3 times the latter unless $\rho_r \ll 1$. Nevertheless, it is clear that the no-slip condition on a solid sphere requires a smaller amount of yield stress to entrap it when compared with that required to prevent a spherical bubble from rising; the latter is based on the assumption that the bubble surface is free of shear stresses [7].

This number 3/2 appears again when one considers the correlation between the rising velocity V_b of a bubble and the settling velocity V_s of a solid sphere through the Hadamard-Rybczynski solution [6] and the result due to Stokes. The former shows that the drag experienced by a spherical bubble of vanishing density and viscosity is given by $D = 4\pi\eta V_b R$, while the drag on a solid sphere is given by $D = 6\pi\eta V_s R$. That is, $V_b = (3/2)V_s$.

The second conclusion from the numerical modelling [10] is that the Newtonian limit of zero yield stress is singular in the sense that for a small value of Y_g, there is a region of flow away from the sphere where both the yield stress and the Newtonian viscous contributions are equally important. However, the calculations for the approach of the flow field to Stokes' result are in good agreement with scalings derived from the matched asymptotic expansion valid in the limit.

In sum, the modelling of the flow of a Bingham fluid around a falling sphere is not an easy task, with extensions to other bodies being even more difficult. Nevertheless, one can derive a variational inequality for such problems which can be solved numerically; see Putz and Frigaard [11]. These matters are discussed below.

Let the density of the rigid body be ρ_s and that of the Bingham fluid be ρ, with $\rho_s > \rho$. Choosing a length scale L based on the dimension of the particle, the characteristic velocity U is defined to be

$$U = \rho_s \frac{(1-\rho_r)gL}{\eta}, \quad \rho_r = \frac{\rho}{\rho_s} < 1, \tag{9.3.5}$$

where η is the viscosity of the fluid. The Bingham number, as usual, is defined by $\mathrm{Bn} = \tau_y L/\eta U$. Assuming that the finite domain Ω occupied by the fluid is exceedingly large and that the fluid is at rest far away from the rigid body, one can assume that the velocity field is zero on its boundary, i.e.,

$$\mathbf{u} = \mathbf{0}, \quad \text{on } \Gamma. \tag{9.3.6}$$

In the *resistance problem* [R], the motion of the particle is specified. Thus, if the particle occupies a region P with a boundary ∂P, it follows that

$$\mathbf{u} = \mathbf{U}_0 + \omega \times \mathbf{x}, \quad \text{on } \partial P. \tag{9.3.7}$$

The force $\mathbf{F}$ and the moment $\mathbf{M}$ exerted on the particle by the fluid are given by

$$\mathbf{F} = \int_{\partial P} \mathbf{T}\mathbf{n}\, da, \tag{9.3.8}$$

$$\mathbf{M} = \int_{\partial P} \mathbf{x} \times \mathbf{T}\mathbf{n}\, da, \tag{9.3.9}$$

where $\mathbf{n}$ is the unit normal to ∂P pointing into the fluid.

In order for a particle to be in steady motion, it is necessary that $\mathbf{F}$ and $\mathbf{M}$ must balance the nett rate of linear momentum and the buoyancy momentum $\mathbf{M}_b$ respectively; note that $\mathbf{M}_b$ vanishes under symmetry conditions on the particle. Hence, for a steady motion to occur, the following equations must be satisfied for a particle with a volume V_P:

$$\mathbf{F} - \rho_s V_P \mathbf{g} = \mathbf{0}, \tag{9.3.10}$$

$$\mathbf{M} - \mathbf{M}_b = 0. \tag{9.3.11}$$

However, for a specified $\mathbf{U}_0$ and ω, there is no guarantee that (9.3.10) and (9.3.11) are met, i.e., the assumption that the flow is steady may prove to be incorrect.

In the *mobility problem* [M], one prescribes a force $\mathbf{F}_0$ and a moment $\mathbf{M}_0$ such that (9.3.10) and (9.3.11) are satisfied with $\mathbf{F} = \mathbf{F}_0$, $\mathbf{M} = \mathbf{M}_0$. These conditions are to be used to determine the velocity field in the fluid along with the rigid body motion, $\mathbf{U}_0$ and ω. In such a situation, as the problem evolves in time, the particle may change its orientation with respect to $\mathbf{g}$ so that the flow may not be steady.

In order to simplify matters, only the mobility problem [M] will be considered for axisymmetric bodies here. In addition, it is assumed that the external moment $\mathbf{M}_0 = 0$. This is not unduly restrictive, for it is difficult to impose an external moment on the body unless one considers electro-rheological materials.

Scaling all stresses through the viscous scale $\eta U/L$, or equivalently through the buoyancy scale $\rho_s(1-\rho_r)gL$, one arrives at the following set of equations:

$$-\nabla p + \nabla \cdot \mathbf{S} + \frac{\rho_r}{1-\rho_r}\mathbf{e}_g = \mathbf{0}, \quad \text{in } \Omega \setminus \overline{P}, \tag{9.3.12}$$

$$\nabla \cdot \mathbf{u} = 0, \tag{9.3.13}$$

$$\mathbf{u} = \mathbf{0} \text{ on } \Gamma, \tag{9.3.14}$$

with the following constitutive relation for the Bingham fluid:

$$\mathbf{A}(\mathbf{v}) = \mathbf{0}, \quad T(\mathbf{S}) \le \mathrm{Bn}, \tag{9.3.15}$$

$$\mathbf{S}(\mathbf{v}) = \left(1 + \frac{\mathrm{Bn}}{K(\mathbf{v})}\right)\mathbf{A}(\mathbf{v}), \quad T(\mathbf{S}) > \mathrm{Bn}. \tag{9.3.16}$$

Further, $\mathbf{e}_g$ denotes the unit vector in the direction of gravity, i.e., $\mathbf{e}_g = -\mathbf{k}$. In addition, one recalls that the domain Ω is bounded and large enough so that the Bingham fluid is at rest on its boundary Γ.

Now, the imposed force $\mathbf{F}_0$ on the body is essentially due to gravity, i.e.,

$$\mathbf{F}_0 = V_P \frac{1}{1-\rho_r}\mathbf{e}_g, \tag{9.3.17}$$

where V_P is the scaled particle volume.

Let V_M be the subspace of $H^1(\Omega \setminus \overline{P})]^d, d \in [2,3]$, consisting of divergence free vector fields satisfying the far-field condition (9.3.14). Employing the various scaling factors listed above, the fundamental inequality (8.2.19) leads to the following variational inequality satisfied by the solution vector $\mathbf{u}$ and all trial velocity fields $\mathbf{v}$:

$$a(\mathbf{u}, \mathbf{v}-\mathbf{u}) + \mathrm{Bn}[j(\mathbf{v}) - j(\mathbf{u})] \ge L_M(\mathbf{v}-\mathbf{u}), \tag{9.3.18}$$

where

$$a(\mathbf{u}, \mathbf{w}) = \int_{\Omega\setminus\overline{P}} \mathbf{A}(\mathbf{u}) : \mathbf{A}(\mathbf{w})\, dv, \quad \mathbf{u} \in V_m, \ \forall \mathbf{w} \in V_M, \tag{9.3.19}$$

$$j(\mathbf{w}) = \int_{\Omega\setminus\overline{P}} K(\mathbf{A}(\mathbf{w}))\, dv, \tag{9.3.20}$$

$$L_M(\mathbf{w}) = \frac{\rho_r}{1-\rho_r}\int_{\Omega\setminus\overline{P}} \mathbf{e}_g \cdot \mathbf{w}\, dv + \int_{\partial P} \mathbf{U}_0 \cdot \mathbf{T}\mathbf{n}\, dS, \tag{9.3.21}$$

where the unit vector $\mathbf{n}$ points into the solid, since the rigid bod is exerting a force on the fluid. Now $\mathbf{U}_0$ is a constant vector means that

$$\int_{\partial P} \mathbf{U}_0 \cdot \mathbf{T}\mathbf{n}\, dS = \mathbf{U}_0 \cdot \mathbf{F}_0 = \frac{V_P}{1-\rho_r}\mathbf{U}_0 \cdot \mathbf{e}_g. \tag{9.3.22}$$

As shown above in Sect. 8.6.5, the solution of the inequality (9.3.18) is the same as the minimisation of the functional $\Phi(\mathbf{v})$ over V_M, where

$$\Phi(\mathbf{v}) = \frac{1}{2}a(\mathbf{v},\mathbf{v}) + \mathrm{Bn}j(\mathbf{v}) - L_M(\mathbf{v}), \quad \mathbf{v} \in V_M. \tag{9.3.23}$$

In order to employ the stress maximisation principle, one notes that on the velocity boundary $\partial\Omega_u = \Gamma$, the velocity is zero. Thus, the true stress tensor $\mathbf{S}$ field maximises the functional (cf. (4.6.37) and (8.1.39)):

$$\Psi(\mathbf{T}^*) = -\frac{1}{8}\int_{\Omega\setminus P}\left[|T(\mathbf{S}^*) - \mathrm{Bn}| + T(\mathbf{S}^*) - \mathrm{Bn}\right]^2 dv, \tag{9.3.24}$$

where each admissible stress tensor field $\mathbf{S}^*$ satisfies the equation of motion (9.3.12) and the force condition (9.3.17). Equivalently, the true stress tensor minimises

$$\int_{\Omega\setminus P}\left[|T(\mathbf{S}^*) - \mathrm{Bn}| + T(\mathbf{S}^*) - \mathrm{Bn}\right]^2 dv. \tag{9.3.25}$$

Suppose that the Newtonian fluid problem has a solution $\mathbf{u}_N$, with an admissible stress tensor $\mathbf{S}_N$. Define a critical number $B_{N,c}$ through the maximum of $T(\mathbf{S}_N)$ or its L^∞ norm:

$$B_{N,c} = ||T(\mathbf{S}_N)||_{L^\infty(\Omega\setminus P)}. \tag{9.3.26}$$

Once again, if $\mathrm{Bn} \geq B_{N,c}$, the integral (9.3.25) is zero and thus, the velocity field $\mathbf{u} = \mathbf{0}$ in a Bingham fluid. This result is similar to that obtained earlier in connection with the motion of a rising bubble; see Sect. 9.2.2.

Now, is there a critical value Bn_c for a Bingham fluid below which the Bingham fluid will flow? To answer this, assume that $\mathbf{u}_1$ and $\mathbf{u}_2$ are the solutions of (9.3.18) for the Bingham numbers Bn_1 and $\mathrm{Bn}_2 (> \mathrm{Bn}_1)$ respectively. Since each velocity field is a test function for the other, one can insert them into (9.3.18) and sum the two resulting inequalities leading to:

$$[\mathrm{Bn}_1 - \mathrm{Bn}_2][j(\mathbf{u}_2) - j(\mathbf{u}_1)] \geq a(\mathbf{u}_2 - \mathbf{u}_1, \mathbf{u}_2 - \mathbf{u}_1)] \geq 0, \tag{9.3.27}$$

where one uses the fact that the viscous dissipation integral is non-negative. This inequality may be used, as in Chap. VI, Sect. 5 in [12], to prove that the solution

$\mathbf{u}$ approaches continuously the Newtonian solution $\mathbf{u}_N$ as the Bingham number $\mathrm{Bn} \to 0$. Since $\mathbf{u}_N$ is non-zero, there must be a minimal Bingham number below which the yield stress fluid will begin to flow. Let this number be Bn_c, so that there is a flow if $\mathrm{Bn} < \mathrm{Bn}_c$ and none if $\mathrm{Bn} \geq \mathrm{Bn}_c$.

In (9.3.27), let $\mathrm{Bn}_2 > \mathrm{Bn}_1$. Thus, in order that this inequality to hold, increasing the Bingham number Bn must result in decreasing the functional $j(\cdot)$, or the critical Bingham number Bn_c is unique. To see this, we know that $j(\mathbf{u}) = 0$ at this critical number Bn_c and that $j(\mathbf{u}) = 0$ for all $\mathrm{Bn} > \mathrm{Bn}_c$.

Next, suppose that $\mathrm{Bn}_2 = \mathrm{Bn}_c$. Consider the limit as $B = \mathrm{Bn}_1 \to \mathrm{Bn}_c^-$. Since $j(\mathbf{u}_2) = 0$, it follows that

$$[\mathrm{Bn}_c - B]j(\mathbf{u}) \geq a(\mathbf{u}, \mathbf{u}) \geq 0, \tag{9.3.28}$$

where $j(\mathbf{u})$ is associated to the number B. Since $j(\mathbf{u}) \leq C[a(\mathbf{u}, \mathbf{u})]$ from the Cauchy-Schwarz inequality, with C depending on the domain $\Omega \setminus P$ only, one finds that as $B \to \mathrm{Bn}_c^-$, the following relations hold:

$$a(\mathbf{u}, \mathbf{u}) = O(|\mathrm{Bn}_c - B]^2), \tag{9.3.29}$$

$$j(\mathbf{u}) = O(\mathrm{Bn}_c - B), \tag{9.3.30}$$

$$j(\mathbf{u}) \geq a(\mathbf{u}, \mathbf{u})/[\mathrm{Bn}_c - B] \geq 0. \tag{9.3.31}$$

Finally, the balance of energy equation given by

$$a(\mathbf{u}, \mathbf{u}) + \mathrm{Bn} j(\mathbf{u}) = L_M(\mathbf{u}) \tag{9.3.32}$$

shows that as $B \to \mathrm{Bn}_c^-$, the viscous functional goes to zero faster than the yield stress term. Thus,

$$Bj(\mathbf{u}) \sim L_M(\mathbf{u}). \tag{9.3.33}$$

Once again, one can obtain a value for the critical Bingham number from the energy equation (9.3.32). Rewrite the latter as:

$$a(\mathbf{u}, \mathbf{u}) = j(\mathbf{u})\left[\frac{L_M(\mathbf{u})}{j(\mathbf{u})} - B\right], \tag{9.3.34}$$

$$\leq j(\mathbf{u})\Big[\mathrm{Bn}_c - B\Big], \tag{9.3.35}$$

where

$$\mathrm{Bn}_c = \sup_{\mathbf{v} \in V_M, \mathbf{v} \neq \mathbf{0}} \frac{L_M(\mathbf{v})}{j(\mathbf{v})}. \tag{9.3.36}$$

If $B > \mathrm{Bn}_c$, one must have $a(\mathbf{u}, \mathbf{u}) = 0$, for this functional cannot be negative.

Finally, turning to numerical modelling, the velocity field $\mathbf{u}$ can be found by minimising the functional $\Phi(\mathbf{v})$ in (9.3.23) based on the augmented Lagrangian method or by the fictitious domain method; see Sect. 10.2 for a discussion of these matters.

9.4 Initiation and Cessation of Unsteady Shearing Flows

9.4.1 The Approach to the Steady State

Suppose that the constant pressure drop per unit length $G > 0$ is sufficient to overcome the yield stress effect in a Bingham fluid. Further, under this pressure drop, let the fluid attain a steady velocity field $w_\infty = w_\infty(x, y)$ in a pipe of arbitrary cross-section, defined by Ω in the $x - y$ plane. Further, let us assume that for every initial value $w_0 = w_0(x, y)$, the unsteady pipe flow with the same, constant pressure drop per unit length $G > 0$, has a unique solution $w(t) = w(x, y, t)$.

In a start-up problem, we are interested in how the L^2 norm of the difference $||w_\infty - w(t)||$ tends to zero as $t \to \infty$. That is, if $v(t) = w_\infty - w(t)$ is the unique solution to the time-dependent flow problem with an initial value $v(0) = w_\infty - w(0)$, the problem that has to be investigated is the rate of decay of $||v(t)||$ as $t \to \infty$ under a zero pressure drop. If the fluid were Newtonian, it can be shown that $v(t) \to 0$ as $t \to \infty$; for example, see pp. 193–195 in [6]. Note that this is a result concerning the pointwise convergence of $v(t)$ to zero from which its norm limit tending to zero can be proved trivially.

Here, we recall the variational inequality for the unsteady flow, viz., (8.8.11) simplified for the case of the Bingham fluid. That is

$$\rho\left(\frac{\partial w}{\partial t}, v - w\right) + \eta a(w, v - w) + \tau_y[j(v) - j(w)] \geq (G, v - w), \tag{9.4.1}$$

where v is any trial velocity field, and the three functionals are given by

$$a(u, v) = \int_\Omega \nabla u \cdot \nabla v \, da, \quad j(u) = \int_\Omega |\nabla u| \, da, \quad (G, u) = \int_\Omega Gu \, da. \tag{9.4.2}$$

To proceed further, let us non-dimensionalise the problem. Choose a length scale L, a velocity scale U so that $x = L\hat{x}$, $y = L\hat{y}$, $w = U\hat{w}$. Further, let the cross-section be scaled so that $\Omega = L^2\hat{\Omega}$. After this has been accomplished, one drops the hat notation and considers the eigenvalue problem over the modified cross-section:

$$\frac{\partial^2 w}{\partial x^2} + \frac{\partial^2 w}{\partial y^2} + \lambda w = 0, \quad w_{|\partial\Omega} = 0. \tag{9.4.3}$$

Note that each eigenvalue is dimensionless and positive. Indeed, if $\lambda_1 > 0$ is the least eigenvalue, it is known that $\lambda_1 \geq J_{0,1}^2$, where $J_{0,1} = 2.4048\ldots$ is the first zero of the Bessel function $J_0(x)$ of order zero, with the equality holding if and only if the pipe has a circular cross-section of unit radius.

Using the maximum-minimum principle for finding the eigenvalues [13], one can prove that the viscous dissipation term obeys the coercive inequality:

$$a(w_\infty - w(t), w_\infty - w(t)) \geq \lambda_1 ||w_\infty - w(t)||^2. \tag{9.4.4}$$

The proof of the inequality (9.4.4) is not given here, for it is nothing but a statement about the variational characterisation of the least eigenvalue of the Laplacian; for example, see [13], or Theorem 4.2 in [14].

In the inequality (9.4.1), scale the pressure drop through $G = \eta U L^{-2}\hat{G}$, choose the time scale $T = \rho U^2/\eta\lambda_1$ and the Bingham number $\mathrm{Bn} = \tau_y L/\eta U$. Finally, divide through by ηU^2 and obtain the non-dimensional form of the inequality:

$$\lambda_1\left(\frac{\partial w}{\partial t}, v - w\right) + a(w, v - w) + \mathrm{Bn}[j(v) - j(w)] \geq (G, v - w). \tag{9.4.5}$$

This will be employed next to prove an energy inequality.

9.4.2 The Proof of the Energy Inequality

First of all, if we put $v = w_\infty$ in (9.4.5), we find that

$$\lambda_1\left(\frac{\partial w(t)}{\partial t}, w_\infty - w(t)\right) + a(w(t), w_\infty - w(t)) + \mathrm{Bn}[j(w_\infty) - \tau_y j(w(t))] \geq (G, w_\infty - w(t)). \tag{9.4.6}$$

When the flow is steady with the velocity field given by w_∞, the inequality has the form

$$a(w_\infty, v - w_\infty) + \mathrm{Bn}[j(v) - j(w_\infty)] \geq (G, v - w_\infty), \tag{9.4.7}$$

where, once again, v is any trial velocity field. Thus, if we put $v = w(t)$ in (9.4.7), we obtain

$$a(w_\infty, w(t) - w_\infty) + \mathrm{Bn}[j(w(t)) - j(w_\infty)] \geq (G, w(t) - w_\infty). \tag{9.4.8}$$

Since w_∞ is independent of time t, it follows that

$$-\left(\frac{\partial(w_\infty - w(t))}{\partial t}, w_\infty - w(t)\right) = \left(\frac{\partial w(t)}{\partial t}, w_\infty - w(t)\right). \tag{9.4.9}$$

Employing (9.4.9) in (9.4.6), adding (9.4.8) to the latter and taking care of the negative quantities, one obtains:

$$\lambda_1\left(\frac{\partial(w_\infty - w(t))}{\partial t}, w_\infty - w(t)\right) + a(w_\infty - w(t), w_\infty - w(t)) \leq 0. \tag{9.4.10}$$

In (9.4.10), one can use (9.4.4) and eliminate the eigenvalue λ_1 and obtain the *energy inequality*:

$$\left(\frac{\partial(w_\infty - w(t))}{\partial t}, w_\infty - w(t)\right) + ||w_\infty - w(t)||^2 \leq 0. \tag{9.4.11}$$

Next, it is obvious that

$$\left(\frac{\partial(w_\infty - w(t))}{\partial t}, w_\infty - w(t)\right) = \frac{1}{2}\frac{d}{dt}||w_\infty - w(t)||^2$$
$$= ||w_\infty - w(t)||\frac{d}{dt}||w_\infty - w(t)||. \qquad (9.4.12)$$

Thus, the inequality (9.4.11) now becomes

$$\frac{d}{dt}||w_\infty - w(t)|| + ||w_\infty - w(t)|| \le 0. \qquad (9.4.13)$$

This proves that

$$||w_\infty - w(t)|| \le ||w_\infty - w(0)||e^{-t}, \qquad (9.4.14)$$

which shows the way the norm $||v(t)||$ of the difference $v(t)$ approaches zero as $t \to \infty$. This result appears in [15] and in [16], with a detailed proof given in [17]. The version given here is to be preferred for it is succinct.

While the inequality (9.4.14) is not ideal for it does not depend on the yield stress, it is an important application of the variational inequality for the flow of a Bingham fluid in a pipe of arbitrary cross-section. These results have been generalised to viscoplastic fluids with a shear rate dependent viscosity in [18].

9.4.3 Cessation of the Steady Flow in a Channel

Consider the steady flow of a Bingham fluid in a channel of width H. Orient the axes so that the flow occurs in the x-direction and the channel walls lie at $y = 0$ and $y = H$. Let the velocity field be described through $u = u(y)$, with $u(0) = u(H) = 0$. Non-dimensionalise the problem using H as the length scale, U as the velocity scale and let the pressure drop per unit length $G = \tau_y \hat{G}/H$, with the Bingham number $\mathrm{Bn} = \tau_y H/\eta U$. Thus, after dropping the hat notation, the energy equation (1.10.10) turns into the following:

$$\frac{1}{\mathrm{Bn}}a(u,u) + j(u) = (G,u), \quad u(0) = u(1) = 0. \qquad (9.4.15)$$

Here,

$$a(u,u) = \int_0^1 \left(\frac{du}{dy}\right)^2 dy, \quad j(u) = \int_0^1 \left|\frac{du}{dy}\right| dy, \quad (G,u) = \int_0^1 Gu\, dy. \qquad (9.4.16)$$

Next, define a non-dimensional constant β through

$$\beta = \min_{v \ne 0} \frac{\int_0^1 |dv/dy|\, dy}{||v||}, \quad ||v|| = \left(\int_0^1 v^2\, dy\right)^{1/2}, \; v(0) = v(1) = 0. \qquad (9.4.17)$$

The constant $\beta > 0$. If it were zero, then $v \neq 0$ leads to $dv/dy = 0$; however, the boundary conditions would force $v(y) = 0$, which contradicts the assumption that $v \neq 0$.

The constant β appeared for the first time in the cessation of the steady flow of a Bingham fluid in a pipe of arbitrary cross-section and led to the proof that the flow comes to a halt in *a finite amount of time*, if the pressure drop per unit length G drops below the critical value G_c, a result due to Glowinski [19]; since $G_c > 0$, one can set $G = 0$, for example. It is well known that the flow takes an infinite amount of time to come to a halt in a Newtonian fluid when the pressure gradient is set to zero. Thus, the foregoing result is remarkable for it delineates one of the fundamental differences between a Newtonian fluid and a Bingham fluid.

Returning to the channel flow, one can see that (9.4.17) implies that

$$\beta||u|| \leq j(u). \tag{9.4.18}$$

Moreover,

$$(G, u) \leq ||G|| \cdot ||u||, \tag{9.4.19}$$

where the constancy of $G > 0$ means that

$$||G|| = \left(\int_0^1 G^2 \, dy \right)^{1/2} = G. \tag{9.4.20}$$

Hence the energy equation (9.4.15) becomes the inequality:

$$\frac{1}{\text{Bn}} a(u, u) + (\beta - G)||u|| \leq 0. \tag{9.4.21}$$

If the constant β is such that $\beta - G \geq 0$, it follows that $a(u, u) \leq 0$ which, together with the boundary conditions $u(0) = u(1) = 0$, means that the steady flow cannot exist in the channel. Thus, the minimum value of β must be such that $\beta - G < 0$. Now for the flow to exist, the pressure drop per unit length G must exceed G_c, where G_c is the critical value. Hence, $\beta = G_c$. In the channel flow, it can be shown quite easily through balancing the pressure and shearing forces that $G_c = 2$; for an earlier demonstration, see Sect. 1.3. Thus, $\beta = 2$. This result will be used next to examine the cessation of the steady flow in a channel when the applied pressure drop per unit length $G < \beta$.

The energy equation for the unsteady flow in a channel is given by (1.10.13). It can be put in a non-dimensional form as follows. Let H be length scale, U be the velocity scale; set $G = \tau_y \hat{c} GH$, and the time scale $T = \rho U^2/\eta\pi^2$. Note that the least eigenvalue for the non-dimensional form of the flow in a channel is obtained from the following differential equation:

$$\frac{d^2 w}{dy^2} + \lambda w = 0, \quad w(0) = w(1) = 0. \tag{9.4.22}$$

Obviously, the least eigenvalue is $\lambda_1 = \pi^2$, which explains the choice of the time scale. The final result is the following energy inequality:

$$\frac{d||u||}{dt} + ||u|| \leq \frac{\mathrm{Bn}}{\pi^2}(G-2), \quad G < 2. \tag{9.4.23}$$

Let us define a non-dimensional number H_b, called the *halting number* [18], through

$$H_b = \frac{1}{\pi^2}(2-G), \quad G < 2, \tag{9.4.24}$$

where H_b has been defined as an entity on its own, for it depends upon the geometry of the region. The inequality in (9.4.23) can now be integrated and one obtains:

$$||u(t)|| + H_b\mathrm{Bn} \leq \Big[||u(0)|| + H_b\mathrm{Bn}\Big]e^{-t}, \tag{9.4.25}$$

where $||u(0)||$ is the norm of the steady velocity field in the channel. Clearly, both sides of the inequality (9.4.25) are non-negative; however, the right side decreases rapidly because of its exponential dependence on time. At a certain instant, say $t = T_f$, it will be found that

$$H_b\mathrm{Bn} = \Big[||u(0)|| + H_b\mathrm{Bn}\Big]e^{-T_f}, \tag{9.4.26}$$

which means that $||u(T_f)|| = 0$. That is, the fluid has come to rest in the channel. It is impossible to re-start the flow, for the pressure drop per unit length G has fallen below the critical value. Thus, it has been proved that T_f provides an upper bound to the extinction time, or the time when a steady flow in the channel comes to rest due to the sudden lowering of the pressure drop per unit length below its critical value. As mentioned earlier, this is a major point of difference between a Newtonian fluid and a Bingham fluid, for the former will take an infinite amount of time to come to rest in a channel when the pressure gradient vanishes.

It is easy to obtain a formula for T_f from (9.4.26):

$$T_f = \ln\left[1 + \frac{||u(0)||}{H_b\mathrm{Bn}}\right]. \tag{9.4.27}$$

9.4.4 Cessation of Steady Simple Shear Flow

Here, assume that a steady simple shear flow, defined through $u^s(y) = \dot{\gamma}y$, $0 \leq y \leq H$, $\dot{\gamma} > 0$, comes to rest if the upper plate is brought to rest suddenly and held stationary for all $t \geq 0$. It is easy to show that the energy inequality is given by (9.4.23), except that the pressure gradient $G = 0$. Using the fact that $H_b = 2/\pi^2$ in

this situation, one finds that

$$T_f = \ln\left[1 + \frac{\pi^2 ||u(0)||}{2\mathrm{Bn}}\right]. \tag{9.4.28}$$

9.4.5 Cessation of Steady Flow in a Pipe

Suppose that a steady flow of a Bingham fluid exists along the axis of a pipe of arbitrary cross-section due to an applied pressure drop per unit length $G > 0$. Let the velocity field be defined through $\mathbf{u} = w(x, y)\mathbf{k}$, where the z-axis lies along the direction of the flow.

Suppose that at time $t = 0^+$, the pressure gradient falls below the critical value G_c. The flow will now become unsteady and employing the non-dimensionalising procedure in Sect. 9.4.1, it can be shown that the energy equation (8.8.12) leads to the following:

$$\frac{d||w||}{dt} + ||w|| \leq \frac{\mathrm{Bn}}{\lambda_1}(G - \beta), \quad G < G_c. \tag{9.4.29}$$

Here, $\lambda_1 > 0$ is the least eigenvalue of the problem (9.4.3), and

$$||v|| = \left(\int_\Omega v^2 \, da\right)^{1/2}, \quad \mathrm{Bn} = \frac{\tau_y L}{\eta U}, \tag{9.4.30}$$

$$\beta = \min_{v \neq 0} \frac{\int_\Omega |\nabla v| \, da}{||v||}, \quad v_{|\partial\Omega} = 0. \tag{9.4.31}$$

In this formulation, the number H_b is given by (cf. (9.4.24)):

$$H_b = \frac{1}{\lambda_1}(\beta - G), \quad G < \beta. \tag{9.4.32}$$

The differential inequality (9.4.29) can be integrated and one obtains a result very similar to that in (9.4.25) above. That is, the flow will come to a halt in a finite amount of time with an upper bound T_f, given by

$$T_f = \ln\left[1 + \frac{||w(0)||}{H_b \mathrm{Bn}}\right]. \tag{9.4.33}$$

It is simple to verify that

$$\int_\Omega v \, da \leq A(\Omega)^{1/2} ||v||, \tag{9.4.34}$$

where $A(\Omega)$ is the area of the cross-section of the pipe. Thus,

$$\beta \leq \frac{\int_\Omega |\nabla v|\, da}{||v||} \leq A(\Omega)^{1/2} \frac{\int_\Omega |\nabla v|\, da}{\int_\Omega v\, da}. \tag{9.4.35}$$

From the definition of M in (9.1.8), it follows that

$$1 \leq M \frac{\int_\Omega |\nabla v|\, da}{\int_\Omega v\, da}. \tag{9.4.36}$$

Hence [3],

$$\beta \leq MA(\Omega)^{1/2} \left(\frac{\int_\Omega |\nabla v|\, da}{\int_\Omega v\, da} \right)^2, \tag{9.4.37}$$

for all $v = v(x, y)$ such that it is sufficiently smooth and $v = 0$ on the boundary of the pipe. Thus, one can obtain a bound on β, if M is known. In practice, however, M is not easy to find in all instances and thus the task of estimating β is not trivial. Nevertheless, the finite extinction time property of the Bingham fluid is a remarkable discovery.

If one considers more general viscoplastic fluids with a constant yield stress, it has been shown that [18] steady flows in a pipe come to rest in a manner mimicking the Bingham fluid if the pressure gradient falls below the critical value.

9.4.6 Cessation of Steady Couette Flow

In Sect. 5.6, the steady, Couette flow of a Bingham fluid between two concentric circular cylinders of radii R_1 and R_2, where $R_1 < R_2$, has been discussed. Of interest here is the case when the outer cylinder is at rest and the inner cylinder rotates with a constant angular velocity Ω. Assuming that the steady angular velocity field is given by $\omega^s = \omega^s(r)$, $R_1 \leq r \leq R_2$, one can consider a fluid mass lying between these two cylindrical surfaces of unit height in the z-direction. The stress power is given by

$$\frac{1}{2} \operatorname{tr} \mathbf{S}\mathbf{A}_1 = \eta r^2 \left(\frac{d\omega^s}{dr} \right)^2 + \tau_y r \left| \frac{d\omega^s}{dr} \right|. \tag{9.4.38}$$

If the external moment per unit height is given by M, the energy equation has the simple form [20]:

$$\eta a(\omega^s, \omega^s) + \tau_y j(\omega^s) = \Omega M, \quad M > 2\pi R_1^2 \tau_y, \tag{9.4.39}$$

where

$$a(\omega^s, \omega^s) = \int_{R_1}^{R_2} 2\pi r^3 \left(\frac{d\omega^s}{dr} \right)^2 dr, \quad j(\omega^s) = \int_{R_1}^{R_2} 2\pi r^2 \left| \frac{d\omega^s}{dr} \right| dr. \tag{9.4.40}$$

Now, suppose that at $t = 0^+$, the inner cylinder is brought to rest and remains at rest subsequently. The power input to the fluid vanishes and the corresponding energy equation for the unsteady Couette flow, $\mathbf{u} = r\omega(r, t)\mathbf{e}_\theta$, is given by:

$$\rho\left(\frac{\partial \omega}{\partial t}, \omega\right) + \eta a(\omega, \omega) + \tau_y j(\omega) = 0, \tag{9.4.41}$$

where $\omega(R_1) = \omega(R_2) = 0$, and

$$\left(\frac{\partial \omega}{\partial t}, \omega\right) = \int_{R_1}^{R_2} 2\pi r^3 \frac{\partial \omega}{\partial t}\omega \, dr. \tag{9.4.42}$$

Of course, $a(\omega, \omega)$ and $j(\omega)$ are obtained from (9.4.40) simply by replacing $d\omega^s/dr$ with $\partial\omega/\partial r$.

The Eq. (9.4.41) can be put into a non-dimensional form easily. Set $r = R(1+x)$, where $R = (R_1 + R_2)/2$ is the mean radius and $R_1 = R(1-\alpha)$, $R_2 = R(1+\alpha)$. Next, scale the angular velocity so that $\omega = \Omega\hat{\omega}$, and set the time $t = T\hat{t}$, where the time scale T has to be determined. Introduce these into (9.4.41), drop the hat notation and divide through by $2\pi\Omega$. One obtains:

$$\int_{-\alpha}^{\alpha} (1+x)^3 \frac{\partial \omega}{\partial t}\omega \, dx + \frac{\eta T}{\rho R^2}\int_{-\alpha}^{\alpha} (1+x)^3 \left(\frac{\partial \omega}{\partial x}\right)^2 dx + \frac{\tau_y T}{\rho \Omega R^2}\int_{-\alpha}^{\alpha} (1+x)^2 \left|\frac{\partial \omega}{\partial x}\right| dx = 0. \tag{9.4.43}$$

Next, consider the eigenvalue problem

$$\frac{d^2 y}{dx^2} + \lambda y = 0, \quad y(-\alpha) = y(\alpha) = 0. \tag{9.4.44}$$

The least eigenvalue is given by $\lambda_1 = \pi^2/4\alpha^2$. Thus, the coercive inequality implies that

$$\int_{-\alpha}^{\alpha} \left(\frac{\partial \omega}{\partial x}\right)^2 dx \geq \frac{\pi^2}{4\alpha^2}\int_{-\alpha}^{\alpha} \omega^2 \, dx. \tag{9.4.45}$$

A simple calculation shows that

$$\int_{-\alpha}^{\alpha} (1+x)^3 \left(\frac{\partial \omega}{\partial x}\right)^2 dx \geq (1-\alpha)^3 \int_{-\alpha}^{\alpha} \left(\frac{\partial \omega}{\partial x}\right)^2 dx \geq \frac{\pi^2 (1-\alpha)^3}{4\alpha^2 (1+\alpha)^3}\int_{-\alpha}^{\alpha} (1+x)^3 \omega^2 \, dx. \tag{9.4.46}$$

From this inequality one can infer that the norm of $\omega = \omega(x)$ should be defined through

$$||\omega|| = \left(\int_{-\alpha}^{\alpha} (1+x)^3 \omega^2 \, dx \right)^{1/2}. \tag{9.4.47}$$

Hence, one finds that

$$\int_{-\alpha}^{\alpha} (1+x)^3 \frac{\partial \omega}{\partial t} \omega \, dx = \frac{d||\omega||}{dt} ||\omega||. \tag{9.4.48}$$

Finally, define the constant β through:

$$\beta = \min_{\omega \neq 0} \frac{\int_{-\alpha}^{\alpha} (1+x)^2 |d\omega/dx| \, dx}{||\omega||}, \tag{9.4.49}$$

where $\omega(-\alpha) = \omega(\alpha) = 0$. Once again, the constant $\beta > 0$.

Consequently, after cancelling $||\omega||$, the energy equation (9.4.43) is turned into the inequality:

$$\frac{d||\omega||}{dt} + \frac{\eta T \pi^2 (1-\alpha)^3}{4\rho R^2 \alpha^2 (1+\alpha)^3} ||\omega|| + \frac{\beta \tau_y T}{\rho \Omega R^2} \leq 0. \tag{9.4.50}$$

The time factor T and the halting number H_b can now be chosen as follows:

$$T = \frac{4\rho R^2 \alpha^2 (1+\alpha)^3}{\eta \pi^2 (1-\alpha)^3}, \quad H_b = \frac{4\beta \alpha^2 (1+\alpha)^3}{\pi^2 (1-\alpha)^3}. \tag{9.4.51}$$

The inequality (9.4.50) takes on the simple form:

$$\frac{d||\omega||}{dt} + ||\omega|| \leq -\mathrm{Bn} H_b, \tag{9.4.52}$$

where the Bingham number $\mathrm{Bn} = \tau_y / \eta \Omega$. Integrating the above differential inequality, it follows that the flow in the Couette viscometer comes to rest in a finite time with the following upper bound for the extinction time:

$$T_f = \ln \left[1 + \frac{||\omega(0)||}{\mathrm{Bn} H_b} \right]. \tag{9.4.53}$$

From (9.4.51), it can be seen that the constant β is essential to determine H_b. Just as in the case of the flow in a pipe of arbitrary cross-section, it is not possible to find β. However, by choosing $\omega(x) = (\alpha^2 - x^2)$ in (9.4.49), it can be shown that [20]

$$\beta \leq \frac{(2+\alpha^2)\sqrt{105}}{4 + \sqrt{7\alpha + 3\alpha^3}}. \tag{9.4.54}$$

If the viscometer has a very narrow gap, i.e., α is very small, one can deduce that

$$\beta \leq \sqrt{\frac{15}{4\alpha}}. \tag{9.4.55}$$

9.4.7 *Effects of Wall Slip*

The previous examples demonstrate that one may derive bounds on the cessation times provided the fluid adheres to the bounding walls, such as in a channel or a pipe. Using the channel flow as an example, suppose that the Bingham fluid slips along its walls under steady flow conditions with yielded/unyielded zones across the channel under a constant pressure drop per unit length G; it is further assumed that the critical yield stress number $S_c = 0$. At time $t = 0^+$, let this pressure drop G be reduced to zero suddenly. Because the shear stress at the wall is now less than before, the slip velocity will decrease and the fluid will adhere to the wall at some time $t = t_c$, and continue to decelerate till it comes to stop across the channel with the cessation spreading inwards from the walls.

The energy inequality (9.4.23) has to modified and is given by

$$\frac{d||u||}{dt} + ||u|| \leq -2\frac{\mathrm{Bn}}{\pi^2}, \quad t > t_c. \tag{9.4.56}$$

The halting number $H_b = 2/\pi^2$ and integrating the inequality above, one obtains (cf. (9.4.25)):

$$||u(t)|| + H_b\mathrm{Bn} \leq \left[||u(t_c)|| + H_b\mathrm{Bn}\right]e^{(t-t_c)}, \quad t \geq t_c. \tag{9.4.57}$$

While this leads once again to an upper bound T_f to the cessation time as in (9.4.26) and (9.4.27), one cannot determine T_f explicitly. The main reason is that one does not know when the steady velocity field $u(y)$ in the channel becomes unsteady and adheres to the pipe at $t = t_c$; that is, the velocity field $u(y, t_c)$, which acts as the initial condition to the subsequent retardation of the flow, is also unknown.

However, if the original steady flow be uniform across the whole channel while slipping along its walls, one can determine the extinction time explicitly. To derive this result, one begins by noting that $(1.11.3)_2$ is replaced by

$$\sigma_w = S_n u_w^s. \tag{9.4.58}$$

Suppose that at time $t = 0^+$, the pressure drop G is reduced to zero suddenly. Except for an infinitesimally narrow gap near the walls, one may assume that the fluid velocity is time dependent and uniform. Thus the rate of change of the linear momentum per unit length of the channel, across its gap of two units, is due to the

shear stresses σ_w acting on the two walls. One obtains [21]:

$$\frac{du_w}{dt} = -\sigma_w = -S_n u_w^s, \quad t > 0. \tag{9.4.59}$$

If $s = 1$, one finds that the extinction time is infinite:

$$u_w(t) = u_w(0)e^{-S_n t}. \tag{9.4.60}$$

If $s \neq 1$,

$$u_w(t) = \left[u_w(0) - (1-s)S_n t\right]^{1/(1-s)}. \tag{9.4.61}$$

Hence, it is easy to see that $u_w(t) \to \infty$ as $t \to \infty$, when $s > 1$.

Finally, if $0 \leq s < 1$, one obtains that the cessation time t_f is finite and given by

$$t_f = \frac{u_w(0)}{(1-s)S_n}. \tag{9.4.62}$$

In the case when the Bingham fluid experiences a uniform flow in a pipe of circular cross-section and slips along the wall, it is easy to show that [21]

$$\frac{du_w}{dt} = -2\sigma_w = -2S_n u_w^s. \tag{9.4.63}$$

This equation leads to predictions similar to those in (9.4.60)–(9.4.61).

9.5 Nonlinear Stability Analysis

Nonlinear stability analysis depends on proving that the mean kinetic energy $E(t)$ of an arbitrary perturbation to a basic flow goes to zero as $t \to \infty$. This idea originated in the work of Reynolds (c.1895) and was developed further by Orr (c. 1907) in investigating the stability of the flows of Newtonian fluids. Hence, once the base flow has been selected, one derives the Reynolds-Orr energy equation satisfied by $E(t)$.

To be specific, consider the steady flow of a Bingham fluid in a channel or in a pipe of circular cross-section. Let the components of this velocity field $\mathbf{U}$ be denoted by $(0, 0, W)$. Following the work of Nouar and Frigaard [22], consider the flow in a channel of width $2H$. Let U_0 be the mean axial velocity in the z-direction with the velocity field given by $W = W(y)$. The Reynolds number is given by $\mathrm{Re} = \rho U_0 H/\mu$ and the Bingham number $\mathrm{Bn} = \tau_y H/\eta U_0$. Let y^* be the solution of the Buckingham equation (1.8.3). The magnitude of the pressure gradient dp/dz is related to this root through

$$y^* = \frac{\mathrm{Bn}}{\mathrm{Re}|dp/dz|}. \tag{9.5.1}$$

Scaling the velocity with U_0, the velocity field is given by

$$W(y) = \begin{cases} \frac{\mathrm{Bn}}{2y^*}(1-y^*)^2, & 0 \le |y| \le y^*, \\ \frac{\mathrm{Bn}}{2y^*}[(1-y^*)^2 - (|y|-y^*)^2], & y^* \le |y| \le 1, \end{cases} \tag{9.5.2}$$

and the scaling with respect to the mean velocity requires that

$$\int_0^1 W(y)\, dy = 1. \tag{9.5.3}$$

The velocity field in (9.5.2) is written in a slightly unorthodox form in order to employ the asymptotic relations in (1.8.12) as $\mathrm{Bn} \to \infty$.

Now, let the perturbation velocity field $\mathbf{u}$ be three dimensional with the components (u, v, w) and the mean kinetic energy of the perturbation be given by Joseph [23]

$$E(t) = \frac{1}{|\Omega|}\int_{\Omega} \frac{|\mathbf{u}|^2}{2}\, dv = \frac{1}{|\Omega|}\int_{\Omega} \frac{u^2+v^2+w^2}{2}\, dv. \tag{9.5.4}$$

The averaging operation of integrating over the domain Ω and dividing by its volume $|\Omega|$ is denoted by the symbol $\langle\cdot\rangle$, so that $E(t) \equiv \langle|\mathbf{u}|^2\rangle/2$. For the plane channel flow, the Reynolds-Orr energy equation is given by Joseph [23]

$$\frac{d}{dt}E(t) = -\left\langle vw\frac{dW}{dy}\right\rangle - \frac{1}{\mathrm{Re}}\left\langle \frac{1}{2}\left[\mathbf{S}(\mathbf{U}+\mathbf{u}) - \mathbf{S}(\mathbf{U})\right] : \mathbf{A}(\mathbf{u})\right\rangle, \tag{9.5.5}$$

where the constitutive equation for the Bingham fluid is in its standard format:

$$\mathbf{A}(\mathbf{v}) = \mathbf{0}, \quad T(\mathbf{S}) \le \mathrm{Bn}, \tag{9.5.6}$$

$$\mathbf{S}(\mathbf{v}) = \left[1 + \frac{\mathrm{Bn}}{K(\mathbf{v})}\right]\mathbf{A}(\mathbf{v}), \quad T(\mathbf{S}) > \mathrm{Bn}. \tag{9.5.7}$$

It is assumed that the region Ω is large enough in any direction in which the channel is infinite, i.e., in the x and z directions. Any perturbation velocity $\mathbf{v}$ belongs to the set V_0 if it satisfies the following conditions:

- The velocity field is divergence free, i.e., $\nabla \cdot \mathbf{v} = 0$ in Ω, and $\mathbf{v} = \mathbf{0}$ on $\partial\Omega$.
- Borrowing the ideas from Newtonian fluid mechanics [23], $\mathbf{v}$ has compact support in the y-direction because $1 \le y \le 1$; it is almost periodic (AP) in the x- and z-directions. For such functions, the integrals (9.5.4)–(9.5.5) exist as $|\Omega| \to \infty$.
- $\mathbf{v} \in C^{\infty}(\Omega)$.
- Finally (cf. (8.6.24)):

$$\overline{V}_0 = \text{closure of } V_0 \text{ with respect to the norm } ||\cdot||_{H^1(\Omega)} : ||\mathbf{v}|| = \left\langle \mathbf{v_i}\mathbf{v_i} + \mathbf{v_{i,j}}\mathbf{v_{i,j}}\right\rangle. \tag{9.5.8}$$

Since $v_{i,i} = 0$, it follows that

$$K^2(\mathbf{A}(\mathbf{v})) = \frac{1}{2}[v_{i,j} + v_{i,j})(v_{i,j} + v_{i,j}] = v_{i,j}v_{i,j} + v_{i,j}v_{j,i} = v_{i,j}v_{i,j} + (v_{i,j}v_j)_{,i}. \quad (9.5.9)$$

If $\mathbf{v} \in V_0$, integrating the above expression over Ω, using the boundary condition on $\partial\Omega$ and the divergence theorem, it will be found that

$$\langle K^2(\mathbf{A}(\mathbf{v}))\rangle = \langle v_{i,j}v_{i,j}\rangle. \quad (9.5.10)$$

Thus, it is assumed that for all $\mathbf{v} \in \overline{V}_0$,

$$\langle K^2(\mathbf{A}(\mathbf{v}))\rangle = \langle v_{i,j}v_{i,j}\rangle, \quad (9.5.11)$$

taking the limit as $|\Omega| \to \infty$, to eliminate the boundary integral remainders for almost periodic conditions.

9.5.1 Dissipation Terms

The dissipation term in (9.5.5) is rewritten as:

$$\langle I(\mathbf{U}, \mathbf{u})\rangle = -\left\langle \frac{1}{2}\Big[\mathbf{S}(\mathbf{U} + \mathbf{u}) - \mathbf{S}(\mathbf{U})\Big] : \mathbf{A}(\mathbf{u})\right\rangle. \quad (9.5.12)$$

Bounds on the integrand $I(\mathbf{U}, \mathbf{u})$ have to be obtained in four distinct regions of flow into which, at any fixed time, the domain Ω can be subdivided. These four sub-regions need not be simply connected and are:

- Region A, where both the basic and perturbed flows are unyielded, i.e., $T(\mathbf{S}(\mathbf{U})) \leq$ Bn and $T(\mathbf{S}(\mathbf{U} + \mathbf{u})) \leq$ Bn.
- Region B, where the basic flow is unyielded, while the perturbed flow has yielded, i.e., $T(\mathbf{S}(\mathbf{U})) \leq$ Bn and $T(\mathbf{S}(\mathbf{U} + \mathbf{u})) >$ Bn.
- Region C, where the basic flow is yielded, while the perturbed flow is unyielded, i.e., $T(\mathbf{S}(\mathbf{U})) >$ Bn and $T(\mathbf{S}(\mathbf{U} + \mathbf{u})) \leq$ Bn.
- Region D, where both the basic flow and the perturbed flows have yielded, i.e., $T(\mathbf{S}(\mathbf{U})) >$ Bn and $T(\mathbf{S}(\mathbf{U} + \mathbf{u})) >$ Bn.

The following results can be proved:

1. In region A, $\mathbf{A}(\mathbf{u}) = \mathbf{0}$. Hence, $I(\mathbf{U}, \mathbf{u}) = 0$ and this is the same as

$$I(\mathbf{U}, \mathbf{u}) \leq -K^2(\mathbf{u}) = 0, \quad (9.5.13)$$

where, for the sake of simplicity, one puts $K(\mathbf{u}) \equiv K(\mathbf{A}(\mathbf{u}))$.

2. In region B, we have $\mathbf{A}(\mathbf{U}) = \mathbf{0}$. Hence, by the linearity property of the first Rivlin-Ericksen tensor, it follows that $\mathbf{A}(\mathbf{U}+\mathbf{u}) = \mathbf{A}(\mathbf{u})$. Thus,

$$I(\mathbf{U},\mathbf{u}) = -\left[1+\frac{\mathrm{Bn}}{K(\mathbf{U}+\mathbf{u})}\right]\frac{1}{2}\mathbf{A}(\mathbf{U}+\mathbf{u}):\mathbf{A}(\mathbf{u})) + S(\mathbf{U}):A(\mathbf{u})$$
$$\leq -\left[1+\frac{\mathrm{Bn}}{K(\mathbf{u})}\right]\frac{1}{2}\mathbf{A}(\mathbf{u}):\mathbf{A}(\mathbf{u})) + \mathrm{Bn}K(\mathbf{u}) = -K^2(\mathbf{u}). \quad (9.5.14)$$

Note that we have used $2K^2 = \mathbf{A}:\mathbf{A}$ and the Cauchy-Schwarz inequality to replace $\mathbf{S}(\mathbf{U}):A(\mathbf{u})$ by Bn $K(\mathbf{u})$.

3. In a similar fashion, one can show that in both of the sub-regions C and D, $I(\mathbf{U},\mathbf{u}) \leq -K^2(\mathbf{u})$.

Thus, appealing to (9.5.11), it follows that

$$\langle I(\mathbf{U},\mathbf{u})\rangle \leq \langle K^2(\mathbf{u})\rangle = \langle u_{i,j}u_{i,j}\rangle. \quad (9.5.15)$$

9.5.2 Global Stability Bounds

The next step is to obtain bounds on the inertial terms in (9.5.5). From the solution (9.5.2), it follows that

$$-\int_{\Omega}\frac{dW}{dy}vw\,dv = \frac{\mathrm{Bn}}{y^*}\int_{\Omega(y^*)}\mathrm{sgn}(y)(|y|-y^*)vw\,dv$$
$$\leq \frac{(1-y^*)\mathrm{Bn}}{2y^*}\int_{\Omega(y^*)}(v^2+w^2)\,dv, \quad (9.5.16)$$

where sgn$(\cdot)$ stands for the signum function, $\Omega(y^*)$ denotes the region $|y| > y^*$, and one uses the simple fact that $v^2+w^2 \geq 2vw$.

Consider when $y > y^*$. Here, one observes that

$$v^2 = \left[\int_1^y \frac{\partial v}{\partial s}(x,s,z,t)\,ds\right]^2 \leq (1-y^*)^2\int_{y^*}^1\left[\frac{\partial v}{\partial s}(x,s,z,t)\right]^2 ds \quad (9.5.17)$$

by the Cauchy Schwarz inequality. Similar bounds can be derived for v^2 in $y < -y^*$ as well as those for w^2. Finally, one obtains

$$\int_{\Omega(y^*)}[v^2+w^2]\,dv \leq (1-y^*)^2\int_{\omega}u_{i,j}u_{i,j}\,dv. \quad (9.5.18)$$

Combining this with the bound for dissipative terms, the energy equation (9.5.5) becomes

$$\frac{d}{dt}E(t) \leq -\left[\frac{1}{\mathrm{Re}} - \frac{\mathrm{Bn}(1-y^*)^3}{2y^*}\right]\langle u_{i,j}u_{i,j}\rangle. \tag{9.5.19}$$

Let $\mathrm{Re}_{\mathrm{GB}}$ stand for the global bound:

$$\mathrm{Re}_{\mathrm{GB}} = \frac{2y^*}{\mathrm{Bn}(1-y^*)^3}. \tag{9.5.20}$$

The result in (9.5.17) proves that an arbitrary initial perturbation decreases monotonically to zero provided

$$\mathrm{Re} < \mathrm{Re}_{\mathrm{GB}}. \tag{9.5.21}$$

Now, the global bound is not very sharp as $\mathrm{Bn} \to 0$. In fact, from (1.8.10), one finds that in this limit, $\mathrm{Re}_{GB} = 2/3$. However, as $\mathrm{Bn} \to \infty$, one finds from (1.8.12) that

$$\mathrm{Re}_{\mathrm{GB}} \sim (\mathrm{Bn}/2)^{1/2}. \tag{9.5.22}$$

That is, for a sufficiently large value of the Bingham number Bn, the flow in a channel of a Bingham fluid will be more stable than the corresponding flow of a Newtonian fluid, obtained by putting $\mathrm{Bn} = 0$. This result in [22] supports the common experimental observation of the difference between Bingham and Newtonian fluids.

In [22], one can find the bounds obtained for the stability of the Poiseuille flow of a Bingham fluid in a pipe of circular cross-section as well. The global bound is given by

$$\mathrm{Re}_{\mathrm{GB}} = \frac{4(r^*)^2}{\mathrm{Bn}(1-r^*)^3(1+r^*)}, \tag{9.5.23}$$

where r^* is the root of the Buckingham equation (5.4.21). The asymptotic value of r^* as $\mathrm{Bn} \to 0$ in (5.4.25) proves that $\mathrm{Re}_{\mathrm{GB}} \to 0$; as $\mathrm{Bn} \to \infty$, the global bound behaves as in (9.5.22).

9.5.3 Conditional Stability

In order to improve the bound obtained as $\mathrm{Bn} \to \infty$, it is essential to restrict the size of admissible perturbations. Note that such an assumption is necessary in developing a linear theory of stability. The bound considered in [22] is:

$$|S_{ij}(\mathbf{U}+\mathbf{u}) - S_{ij}(\mathbf{U})| \leq a, \tag{9.5.24}$$

where a has to be found. The basic idea behind obtaining such a value for a is to require that there is an unyielded region of fluid in the perturbed flow. This matter will be discussed next.

First of all, in the base flow, there are only two non-zero shear stresses, viz., $S_{23} = S_{32} = Gy$, where $G > 0$ is the non-dimensional pressure drop per unit length. Hence,

$$|S_{ij}(\mathbf{U}+\mathbf{u})| \le a, \quad ij \ne 23, 32. \tag{9.5.25}$$

Next, using the simple geometric inequality $|\alpha| = |\alpha - \beta + \beta| \le |\alpha - \beta| + |\beta|$, one can see that

$$|S_{ij}(\mathbf{U}+\mathbf{u})| \le |S_{ij}(\mathbf{U}+\mathbf{u}) - S_{ij}(\mathbf{U})| + |S_{ij}(\mathbf{U})| \le a + G|y|, \quad ij = 23, 32. \tag{9.5.26}$$

Hence,

$$T(\mathbf{S}(\mathbf{U}+\mathbf{u})) = \left[\frac{1}{2}\sum_{i,j=1}^{3} S_{ij}^2(\mathbf{U}+\mathbf{u})\right]^{1/2} \le \left[(G|y|+a)^2 + \frac{7}{2}a^2\right]^{1/2}. \tag{9.5.27}$$

Now, one selects a and y so that $T(\mathbf{S}(\mathbf{U}+\mathbf{u})) < \mathrm{Bn}$, i.e.,

$$(G|y|+a)^2 + \frac{7}{2}a^2 < \mathrm{Bn}^2 = (Gy^*)^2. \tag{9.5.28}$$

Defining $\beta = a/G$, the disturbed flow must be unyielded provided $|y| < y_2$, which is the larger root of

$$(G|y|+a)^2 + \frac{7}{2}a^2 < \mathrm{Bn}^2 - (Gy^*)^2 = 0. \tag{9.5.29}$$

It is easy to derive that

$$y_2 = -\beta + \sqrt{(y^*)^2 - \frac{7}{2}\beta^2}. \tag{9.5.30}$$

Since one requires the discriminant above to be positive and $y_2 > 0$, the following must hold:

$$y^* > \frac{3}{\sqrt{2}}\beta \Leftrightarrow a < (2/9)^{1/2}\mathrm{Bn}. \tag{9.5.31}$$

Thus, we have found a criterion for the disturbed flow to be unyielded. Now, define a layer thickness h through

$$h = y^* - y_2. \tag{9.5.32}$$

In sum, it has been established that

$$T(\mathbf{S}(\mathbf{U}+\mathbf{u})) \le \mathrm{Bn}, \quad |y| \le y^* - h, \tag{9.5.33}$$

$$T(\mathbf{S}(\mathbf{U}+\mathbf{u})) > \mathrm{Bn}, \quad |y| > y^* + h. \tag{9.5.34}$$

Using this, after much effort, it is shown in [22] that perturbations of size

$$|S_{ij}(\mathbf{U}+\mathbf{u}) - S_{ij}(\mathbf{U})| \le a \le (2/9)^{1/2}\frac{\mathrm{Bn}(1-y^*)}{\mathrm{Re_B}} \tag{9.5.35}$$

will decay monotonically provided the Reynolds number $\mathrm{Re} < \mathrm{Re}_{\mathrm{B}}$, where the conditional bound is given by

$$\mathrm{Re}_{\mathrm{CB}} = \frac{2y^*\mathrm{Re}_{\mathrm{B}}/\mathrm{Bn}(1-y^*)}{f\left(y^*, \mathrm{Re}_{\mathrm{B}}\right)}, \tag{9.5.36}$$

and $\mathrm{Re}_{\mathrm{B}} = 99.207$ is the constant obtained first by Busse [24] in his derivation of an energy stability criterion for the channel flow of a Newtonian fluid. Moreover,

$$f\left(y^*, \mathrm{Re}_{\mathrm{B}}\right) = [1 + (2/9)^{1/2}(y^*/\mathrm{Re}_{\mathrm{B}})]^2[1 + (2/9)^{1/2}y^* + (2/9)^{1/2}(y^*/\mathrm{Re}_{\mathrm{B}})]. \tag{9.5.37}$$

As $\mathrm{Bn} \to \infty$, the conditional bound behaves as follows:

$$\mathrm{Re}_{CB} \sim \frac{(\mathrm{Bn}/2)^{1/2}\mathrm{Re}_{\mathrm{B}}}{[1 + (2/9)^{1/2}\mathrm{Re}_{\mathrm{B}}]^2[1 + (2/9)^{1/2} + (2/9)^{1/2}\mathrm{Re}_{\mathrm{B}}]}. \tag{9.5.38}$$

These theoretical results for the conditional bound are conservative, for one order of magnitude separates them from actual transition. Several remarks concerned with the choice of the norm $||\mathbf{u}||$ of the perturbation and the bounds for the flow in a pipe of circular cross-section, along with comparison with phenomenological criteria are discussed at length in [22]. From the latter, it is found that no phenomenological prediction shows a rate of increase in the critical Reynolds number less than $\mathrm{Bn}^{1/2}$ as $\mathrm{Bn} \to \infty$.

Finally, questions of transition and and flow instability are perfectly well defined theoretically. However, both the linear theory discussed in Sect. 7.4 and the nonlinear theory covered here do not provide deep insight into the actual instability mechanisms. In addition, the dissipation terms in (9.5.15) do not depend on the Bingham number Bn, similar to that found in the initiation and approach to the steady state of the flow in a pipe of arbitrary cross-section of a Bingham fluid, discussed above in Sect. 9.4. At present, there is no known method which includes an explicit contribution of the yield stress to these flow problems.

References

1. Mosolov PP, Miasnikov VP (1965) Variational methods in the theory of fluidity of a viscous-plastic medium. J Appl Math Mech (PMM) 31:545–577
2. Mosolov PP, Miasnikov VP (1967) On qualitative singularities in the flow of a viscoplastic medium in pipes. J Appl Math Mech (PMM) 33:609–613
3. Huilgol RR (2006) A systematic procedure to determine the minimum pressure gradient required for the flow of viscoplastic fluids in pipes of symmetric cross-section. J Non-Newton Fluid Mech 136:140–146
4. Huilgol RR, You Z (2007) Determination of the minimum pressure gradient for the flow of viscoplastic fluids in the runner system. Report to Moldflow Pty. Ltd., School of Informatics and Engineering, Flinders University

5. Dubash N, Frigaard I (2004) Conditions for static bubbles in viscoplastic fluids. Phys Fluids 16:4319–4330
6. Batchelor GK (1967) An introduction to fluid dynamics. Cambridge University Press, Cambridge
7. Tsamopoulos J, Dimakopoulos Y, Chatzidai N, Karapetsas G, Pavlidis M (2008) Steady bubble rise and deformation in Newtonian and viscoplastic fluids and conditions for bubble entrapment. J Fluid Mech 601:123–164
8. Dubash N, Frigaard IA (2007) Propagation and stopping of air bubbles in carbopol solutions. J Non-Newton Fluid Mech 142:123–134
9. Mougin N, Magnin A, Piau J-M (2012) The significant influence of internal stresses on the dynamics of bubbles in a yield stress fluid. J Non-Newton Fluid Mech 171–172:42–55
10. Beris AN, Tsamopoulos JA, Armstrong RC, Brown RA (1985) Creeping motion of a sphere through Bingham plastic. J Fluid Mech 158:219–244
11. Putz A, Frigaard IA (2010) Creeping flow around particles in a Bingham fluid. J Non-Newton Fluid Mech 165:263–280
12. Duvaut G, Lions JL (1976) Inequalities in mechanics and physics. Springer, New York
13. Courant R, Hilbert D (1953) Methods of mathematical physics, vol 1. Interscience, New York
14. Friedman B (1956) Principles and techniques of applied mathematics. Wiley, New York
15. Glowinski R, Lions J-L, Trèmoliéres R (1981) Numerical analysis of variational inequalities. North-Holland, Amsterdam
16. Glowinski R (1984) Numerical methods for nonlinear variational problems. Springer, New York
17. Huilgol RR, Mena B (2000) On the time estimate for start-up of pipe flows in a Bingham fluid—a proof of the result due to Glowinski, Lions and Trèmoliéres. J Non-Newton Fluid Mech 94:113–118
18. Huilgol RR (2002) Variational inequalities in the flows of yield stress fluids including inertia: theory and applications. Phys Fluids 14:1269–1283
19. Glowinski R (1974) Sur l'ecoulement d'un fluide de Bingham dans une conduite cylindrique. J de Mécanique 13:601–621
20. Huilgol RR, Mena B, Piau JM (2002) Finite stopping times and rheometry of Bingham fluids. J Non-Newton Fluid Mech 102:97–107
21. Damianou Y, Philippou M, Koullas G, Georgiou GC (2014) Cessation of viscoplastic flow with wall slip. J Non-Newton Fluid Mech 203:24–37
22. Nouar C, Frigaard IA (2001) Nonlinear stability of Poiseuille flow of a Bingham fluid: theoretical results and comparison with phenomenological criteria. J Non-Newton Fluid Mech 100:127–149
23. Joseph DD (1976) Stability of fluid motions, vol 1. Springer, Berlin
24. Busse FH (1969) Bounds on transport of mass and momentum by turbulent flow between parallel plates. Z Angew Math Phys 20:1–14

Chapter 10
Numerical Modelling

In this chapter, we shall summarise and apply two powerful techniques for the solution of flow problems in Bingham and other viscoplastic fluids. The first one is known as the augmented Lagrangian method and the second is the operator-splitting method. Much of the material in this chapter is sourced from the publications of Glowinski and his collaborators. In particular, one may refer to [1] for an early treatment of the numerical methods for Bingham fluids, followed by the theoretical underpinnings of the augmented Lagrangian and operator-splitting methods [2]. Moreover, there is an encyclopaedic volume on numerical methods for fluid mechanics [3] and more recently, there is a very long article on numerical methods for viscoplastic fluids [4]. Obviously, this chapter has to be seen as providing the barest summary of the material developed at length and breadth in the books and articles just mentioned.

Numerical modelling of the steady flows of a Bingham fluid in pipes of arbitrary cross-section can be traced back to Cea and Glowinski [5] in 1972 where the viscoplasticity constraint tensor was used in computations. Subsequent research over the last 40 years has shown that there are two powerful, robust numerical methods for Bingham fluids. Given a steady flow, the first is one based on defining an augmented Lagrangian for the flow and solving it through the saddle point method, originally developed by Arrow et al. [6] to problems arising in linear and non-linear programming.[1] Subsequently, this algorithm has been adapted to solve problems in viscoplasticity and other materials [2]; see [3, 4] as well.

In this chapter, a brief description of the use of the Lagrangian and the saddle point method to solve a constrained minimisation problem in $\mathbb{R}^n$ is presented first in Sect. 10.1. The second procedure to solve the same problem is the quadratic penalty method and, since it suffers from some drawbacks, the original Lagrangian and the penalty function are combined to obtain an augmented Lagrangian functional with improved convergence properties. In turn, this leads to the solution of the flows of Bingham fluids in various geometries and a summary of this is given in Sect. 10.2.

[1] Uzawa's papers deal with finding the maximum of concave functions subject to constraints; see Chaps. 3, 5, 7 and 10 in [6]. The algorithm for solving the saddle point problem appears in Chap. 10.

R.R. Huilgol, *Fluid Mechanics of Viscoplasticity*, DOI 10.1007/978-3-662-45617-0_10

The second powerful technique is the operator-splitting method and its use is described in full in Sect. 10.3, which deals with the thermally driven cavity flow of an incompressible Bingham fluid. In Sect. 10.4, numerical methods for compressible viscoplastic are described and as an application, the lid driven cavity flow of a weakly compressible viscoplastic fluid is studied in Sect. 10.5. The last application has to be seen as a *numerical experiment* for reasons which are made explicit below. Finally, some comments are offered in Sect. 10.6 on the use of regularised models in numerical computations.

10.1 Augmented Lagrangian Methods: Finite Dimensional Case

To understand the augmented Lagrangian method, it is essential to recall the solution to the minimisation of a function of several variables, subject to equality constraints, commonly known as the *constrained problem*.[2] First of all, consider the following minimisation problem in $\mathbb{R}^n$:

$$f(\mathbf{x}) \leq f(\mathbf{y}), \quad \forall \mathbf{y} \in H = \{\mathbf{y} | \mathbf{g}(\mathbf{y}) = \mathbf{0}\}, \tag{10.1.1}$$

where H is the set of constraints in $\mathbb{R}^m$, such that $m < n$.

The classical method to solve the problem above is originally due to Lagrange (c. 1804–1806) and is known as the *Lagrange multiplier* method. Here, one defines a Lagrangian functional dependent on a vector $\boldsymbol{\lambda}$:

$$\mathscr{L}(\mathbf{x}, \boldsymbol{\lambda}) = f(\mathbf{x}) + \boldsymbol{\lambda} \cdot \mathbf{g}(\mathbf{x}), \tag{10.1.2}$$

and finds the extrema of the above functional regarding it as an *unconstrained problem.* In practice, one obtains a system of $(n + m)$ equations by finding the partial derivatives of the Lagrangian functional with respect to x_i, $i = 1, \ldots, n$, and λ_j, $j = 1, \ldots m$, and setting these to zero. That is:

$$\frac{\partial \mathscr{L}}{\partial x_i} = \frac{\partial f}{\partial x_i} + \sum_{j=1}^{m} \frac{\partial g_j}{\partial x_i} \lambda_j = 0, \quad i = 1, \ldots n, \tag{10.1.3}$$

$$\frac{\partial \mathscr{L}}{\partial \lambda_j} = g_j(x_1, \ldots, x_n) = 0, \quad j = 1, \ldots, m. \tag{10.1.4}$$

The basic question now is the following: do the multipliers exist at the extremal point $\mathbf{x}^*$ of $f(\mathbf{x})$? These multipliers exist provided the m gradient vectors of g are linearly independent. For a comprehensive proof of this, see Theorem 13.12 in Apostol [8].

[2] A very readable introduction to these ideas is contained in Nocedal and Wright [7]. See Chaps. 12 and 17 for the quoted results.

Consider the following example. This is a two-variable problem with a single equality constraint:

$$\min f(x_1, x_2) = x_1 + x_2, \quad \text{such that} \quad g(x_1, x_2) = x_1^2 + x_2^2 - 2 = 0. \tag{10.1.5}$$

There are two extrema. One is the minimiser given by $\mathbf{x}^* = (-1, -1)$, with $\lambda = 1/2$; the maximum occurs when $\mathbf{x}^* = (1, 1)$ and $\lambda = -1/2$. Note that at each extremal point, $\nabla g = (\pm 2, \pm 2)$, or the gradient vector is linearly independent from the zero vector.

The modern approach to solve the problem in (10.1.1) relies on the saddle point method. To describe this, suppose that $\mathbf{f}$ and $\mathbf{g}$ are C^k, $k \geq 0$, and that $(\mathbf{x}^*, \boldsymbol{\lambda}^*)$ is a saddle point of $\mathscr{L}$ over $\mathbb{R}^n \times \mathbb{R}^m$. Then, one can prove that $\mathbf{x}^*$ is a solution of the minimum problem (10.1.1) as follows. First of all, by the definition of a saddle point from the calculus of the function of several variables, one finds that[3]:

$$\mathscr{L}(\mathbf{x}^*, \boldsymbol{\mu}) \leq \mathscr{L}(\mathbf{x}^*, \boldsymbol{\lambda}^*) \leq \mathscr{L}(\mathbf{y}, \boldsymbol{\lambda}^*), \quad \forall \{\mathbf{y}, \boldsymbol{\mu}\} \in \mathbb{R}^n \times \mathbb{R}^m. \tag{10.1.6}$$

Inserting the Lagrangian in (10.1.2) into the left inequality above, one obtains:

$$\boldsymbol{\mu} \cdot \mathbf{g}(\mathbf{x}^*) \leq \boldsymbol{\lambda} \cdot \mathbf{g}(\mathbf{x}^*), \quad \forall \boldsymbol{\mu} \in \mathbb{R}^m, \tag{10.1.7}$$

which implies that the maximum of the left side is less than or equal to that of the right side, i.e.,

$$\sup_{\boldsymbol{\mu} \in \mathbb{R}^m} \boldsymbol{\mu} \cdot \mathbf{g}(\mathbf{x}^*) \leq \boldsymbol{\lambda} \cdot \mathbf{g}(\mathbf{x}^*). \tag{10.1.8}$$

Now, the supremum of the left side is $+\infty$, if $\mathbf{g}(\mathbf{x}^*) \neq \mathbf{0}$. Thus, the inequality in (10.1.8) can only be satisfied provided

$$\mathbf{g}(\mathbf{x}^*) = \mathbf{0}, \tag{10.1.9}$$

or the vector $\mathbf{x}^*$ satisfies the constraint conditions, i.e., $\mathbf{x}^* \in H$. Using this result on the right side of (10.1.6) and noting that $\mathbf{g}(\mathbf{y}) = \mathbf{0}$, one finds that

$$\mathscr{L}(\mathbf{x}^*, \boldsymbol{\lambda}^*) = f(\mathbf{x}^*) \leq f(\mathbf{y}), \quad \forall \mathbf{y} \in H. \tag{10.1.10}$$

That is, $\mathbf{x}^*$ is a solution of the problem (10.1.1).

The converse, namely that the solution $\mathbf{x}^*$ of (10.1.1) satisfies the saddle point condition (10.1.6) requires that f be *convex, lower semi-continuous and proper*, emphasising once again the importance of these conditions (cf. (8.6.32)). The proof of this converse is once again easy if f is differentiable and g is *affine*, i.e.,

$$\mathbf{g}(\mathbf{x}) = \mathbf{A}\mathbf{x} + \mathbf{b}, \tag{10.1.11}$$

[3] The proof given here follows that in Chap. 4, Sect. 19 in [3].

where $\mathbf{A}$ is an $m \times n$ matrix and $\mathbf{b} \in \mathbb{R}^m$ is a vector. Note that the affine function is convex, for it satisfies the convexity condition in (8.6.30). Since $\mathbf{x}^*$ satisfies (10.1.1), it is obvious from (10.1.2) that

$$\mathscr{L}(\mathbf{x}^*, \boldsymbol{\mu}) = f(\mathbf{x}^*) = \mathscr{L}(\mathbf{x}^*, \boldsymbol{\lambda}^*). \tag{10.1.12}$$

The functional

$$\mathscr{L}(\mathbf{y}, \boldsymbol{\lambda}^*) = f(\mathbf{y}) + \boldsymbol{\lambda}^* \cdot \mathbf{g}(\mathbf{y}) \tag{10.1.13}$$

is continuously differentiable and convex over $\mathbb{R}^n$, since f is assumed to be convex. Now,

$$\nabla_{\mathbf{y}} \mathscr{L}(\mathbf{y}, \boldsymbol{\lambda}^*) = \nabla f(\mathbf{y}) + \nabla \mathbf{g}(\mathbf{y})^T \boldsymbol{\lambda}^*, \tag{10.1.14}$$

and (10.1.3) can be written as $\nabla_{\mathbf{y}} \mathscr{L}(\mathbf{x}^*, \boldsymbol{\lambda}^*) = \mathbf{0}$. Since the functional in (10.1.13) is convex,

$$\mathscr{L}(\mathbf{x}^*, \boldsymbol{\lambda}^*) \leq \mathscr{L}(\mathbf{y}, \boldsymbol{\lambda}^*), \quad \forall \mathbf{y} \in \mathbb{R}^n. \tag{10.1.15}$$

This inequality and (10.1.12) establish the required result, viz., $(\mathbf{x}^*, \boldsymbol{\lambda}^*)$ is a saddle point of $\mathscr{L}$ over $\mathbb{R}^n \times \mathbb{R}^m$.

A different method to solve the minimisation problem is the *quadratic penalty* method [7]. Here, we replace the Lagrangian functional with a quadratic penalty function:

$$Q(\mathbf{x}, r) = f(\mathbf{x}) + \frac{r}{2} \sum_{i=1}^{m} g_i^2(\mathbf{x}), \tag{10.1.16}$$

where $r > 0$ is the penalty parameter. The basic idea is that any vector $\mathbf{x}$ which violates a constraint has a positive penalty added to the function f. By letting the parameter $r \to \infty$, the constraint violation can be penalised severely. Thus, one may consider a sequence $\{r_k\}$ with $r_k \to \infty$ as $k \to \infty$, and seek the approximate minimiser $\mathbf{x}_k$ of $Q(\mathbf{x}, r_k)$ for each k. Since the function f as well as the penalty terms in (10.1.16) are continuously differentiable, one is now faced with seeking the minimum of an *unconstrained problem*.

In practice, there are two hurdles which have to be overcome. The first one is the initial choice of r_k in the sequence, as demonstrated by the following example.

$$\min f(x_1, x_2) = -5x_1^2 + x_2^2, \quad \text{such that} \quad g(x_1, x_2) = x_1 - 1 = 0. \tag{10.1.17}$$

The penalty function is given by

$$Q(\mathbf{x}, r) = \left(\frac{r}{2} - 5\right) x_1^2 + x_2^2 - r x_1 + \frac{r}{2}, \tag{10.1.18}$$

whose minimum is unbounded for $r < 10$, while the solution of (10.1.17) is given by $\mathbf{x}^* = (1, 0)$. Thus, quadratic penalty functions suffer from some deficiency quite often.

Secondly, the approximate minimisers $\mathbf{x}_k$ of $Q(\mathbf{x}, r_k)$ are unlikely to satisfy the constraints $\mathbf{g}(\mathbf{x}) = 0$. However, if $(\mathbf{x}^*, \boldsymbol{\lambda}^*)$ exist and satisfy the Karush-Kuhn-Tucker conditions, it can be proved that [7]

$$g_i(\mathbf{x}_k) \approx \lambda_i^*/r_k. \tag{10.1.19}$$

That is, $g_i(\mathbf{x}_k) \to 0$ as $r_k \to \infty$. The drawback here is that as $r_k \to \infty$, the Hessian of the quadratic penalty function Q becomes ill-conditioned. Thus, it would be desirable to alter the function $Q(\mathbf{x}, r)$ so that the approximate minimisers satisfy the constraint equations more nearly than before, even for moderate values of r_k. This leads us to the augmented Lagrangian functional where an explicit estimate of the multipliers is made using (10.1.19).

Thus, consider the following *augmented Lagrangian functional*, which is a combination of the Lagrangian functional and the quadratic penalty function:

$$\mathscr{L}(\mathbf{x}, \boldsymbol{\lambda}, r) = f(\mathbf{x}) + \boldsymbol{\lambda} \cdot \mathbf{g}(\mathbf{x}) + \frac{r}{2} \sum_{i=1}^{m} g_i^2(\mathbf{x}). \tag{10.1.20}$$

Suppose that $\mathbf{x}_k$ are the approximate minimiser of $\mathscr{L}(\mathbf{x}, \boldsymbol{\lambda}^k, r_k)$, from which it follows that

$$\nabla f(\mathbf{x}_k) + \sum_{i=1}^{m} [\lambda_i^k + r_k g_i(\mathbf{x}_k)] \nabla g_i(\mathbf{x}_k) \approx 0. \tag{10.1.21}$$

Thus,

$$\lambda_i^* \approx \lambda_i^k + r_k g_i(\mathbf{x}_k), \tag{10.1.22}$$

or

$$g_i(\mathbf{x}_k) \approx \frac{1}{r_k}(\lambda_i^* - \lambda_i^k). \tag{10.1.23}$$

Thus, whenever $\boldsymbol{\lambda}^k$ is close to the optimal vector $\boldsymbol{\lambda}^*$, the constraint equations $\mathbf{g}(\mathbf{x}_k) = \mathbf{0}$ are more nearly satisfied when compared with the earlier estimate (10.1.19). Employing (10.1.22), we can choose the next value of the multiplier as follows:

$$\lambda_i^{k+1} = \lambda_i^k + r_k g_i(\mathbf{x}_k), \tag{10.1.24}$$

and pick $r_{k+1} \geq r_k$. Using the updated $(\lambda_i^{k+1}, r_{k+1})$, one finds the new approximate minimiser $\mathbf{x}_{k+1}$, and iterations continue till the desired tolerance is achieved. Naturally, if it so happens that for a given value of r_k, the constraint equations $\mathbf{g}(\mathbf{x}_k) \approx \mathbf{0}$ to within the desired level of tolerance, there is no pointing in increasing the penalty parameter further. Thus, it is enough that r be sufficiently large [7].

Having introduced the saddle point property of the Lagrangian and the augmented Lagrangian functional, we turn to the application of these ideas in solving the flow problems in viscoplastic fluids.

10.2 Augmented Lagrangian Methods for Bingham Fluids

In this section, we recall that in a steady flow of a viscoplastic fluid where inertia is ignored, the solution of the variational inequality and that obtained from minimising the relevant functional are identical; see Sect. 8.6.5. This equivalence leads to the augmented Lagrangian method to be discussed next.

To begin, consider the steady flow of a Bingham fluid in a pipe of arbitrary cross-section. The solution w of the variational inequality problem satisfies:

$$\eta a(w, v-w) + \tau_y[j(v) - j(w)] \geq (G, v-w), \quad \forall v, w \in H_0^1(\Omega), \tag{10.2.1}$$

where, for convenience, the three functionals in (10.2.1) are repeated from (8.6.47)–(8.6.49):

$$\begin{aligned} a(w, v-w) &= \int_\Omega \nabla w \cdot \nabla(v-w)\, da, \\ j(v) &= \int_\Omega |\nabla v|\, da, \\ (G, v-w) &= \int_\Omega G(v-w)\, da, \quad \forall v, w \in H_0^1(\Omega), \end{aligned} \tag{10.2.2}$$

Here, Ω is the domain defining the cross-section of the pipe and $G > G_c > 0$ is the pressure drop per unit length.

The classical method to solve the problem (10.2.1) and (10.2.2) is based on the Uzawa type algorithm due to Cea and Glowinski [5]; see pp. 529–531 in [4] as well. It reduces the solution to solving a sequence of linear Dirichlet problems for the Laplacian $-\eta\nabla^2$ and a simple projection operator for the viscoplasticity constraint tensor $\boldsymbol{\Lambda}$:

$$-\eta\nabla^2 w - \tau_y \nabla \cdot \boldsymbol{\Lambda} = G \text{ in } \Omega, \quad \boldsymbol{\Lambda} \cdot \nabla w = |\nabla w| \tag{10.2.3}$$

for all $\boldsymbol{\Lambda} \in \mathscr{M}$, where $\mathscr{M} = \{\boldsymbol{\mu} | \boldsymbol{\mu} = (\mu_{ij})_{1\leq i,j\leq 2} \in (L^2(\Omega))^2, ||\boldsymbol{\mu}|| \leq 1 \text{ a.e. on } \Omega\}$. Define the projection operator $P_{\mathscr{M}}$ through

$$P_{\mathscr{M}}(\mathbf{q}) = \frac{\mathbf{q}}{\max(1, |\mathbf{q}|)}, \quad \text{a.e. in } \Omega, \quad \forall \mathbf{q} \in (L^2(\Omega))^2. \tag{10.2.4}$$

Thus, let $\boldsymbol{\Lambda}^0$ be given, say it is $\mathbf{0}$. If $\boldsymbol{\Lambda}^n$ is known, compute w^n and $\boldsymbol{\Lambda}^{n+1}$ by the following iterative procedure. Firstly, solve in $H_0^1(\Omega)$:

$$-\eta\nabla^2 w^n = \tau_y \nabla \cdot \boldsymbol{\Lambda}^n + G, \quad w^n = 0 \text{ on } \partial\Omega, \tag{10.2.5}$$

and use the projection:

$$\boldsymbol{\Lambda}^{n+1} = P_{\mathscr{M}}\left(\boldsymbol{\Lambda}^n + r\tau_y \nabla w^n\right). \tag{10.2.6}$$

Successive iterations are performed till convergence is achieved to the desired level of accuracy. Note that the yield surface is the boundary between $||\boldsymbol{\Lambda}|| < 1$ and $||\boldsymbol{\Lambda}|| = 1$. Hence, the solution of the boundary value problem delivers in the limit both the velocity field as well as the shape and location of the yield surface. For an application of this method to the flow in an eccentric annulus and an L-shaped region of a Bingham fluid, see [9]; for the solution of the steady flows of Casson and Herschel-Bulkley fluids in pipes of circular and square cross-sections, see [10].

A second method to solve the flow problem arises from the fact that in a Bingham fluid, the velocity field $w = w(x, y) \in H_0^1(\Omega)$ is also the minimiser of the functional $\Phi(v)$ defined through:

$$\Phi(v) = \frac{1}{2}\eta \int_{\Omega} (\nabla v \cdot \nabla v)\, da + \tau_y \int_{\Omega} |\nabla v|\, da - \int_{\Omega} Gv\, da, \quad \forall v \in H_0^1(\Omega). \quad (10.2.7)$$

That is, $\Phi(w) \leq \Phi(v)$. This equivalence between the two methods has been established earlier in Sect. 8.6.5. Obviously, one can introduce a suitable augmented Lagrangian functional for the solution of (10.2.7), as in Sect. 10.1 above. This is described next.

The basic idea is to decouple the nonlinearity and the gradients. This is done by treating ∇w as an independent variable $\mathbf{q}$ and then forcing the relation $\nabla w - \mathbf{q} = \mathbf{0}$ by quadratic penalisation and the use of a Lagrange multiplier. The procedure, reproduced here from pp. 541–543 in [4], is as follows:

1. Let
$$\mathbf{Q} = \{\mathbf{q} \mid \mathbf{q} \in (L^2(\Omega))^2\}. \quad (10.2.8)$$

2. Define $\mathbf{W}$ and $F(\cdot, \cdot)$ through
$$\mathbf{W} = \{\{v, \mathbf{q}\} \mid v \in H_0^1(\Omega), \quad \mathbf{q} \in \mathbf{Q}, \quad \nabla v - \mathbf{q} = \mathbf{0}\}, \quad (10.2.9)$$
and
$$F(v, \mathbf{q}) = \frac{1}{2} \int_{\Omega} \eta |\nabla v|^2\, da + \tau_y \int_{\Omega} |\mathbf{q}|\, da - \int_{\Omega} Gv\, da. \quad (10.2.10)$$

3. Note that if w is the solution and $\mathbf{p}$ is its gradient vector, it is obvious that $\{w, \mathbf{p}\} \in \mathbf{W}$. Thus, the minimisation problem is the same as solving:
$$F(w, \mathbf{p}) \leq F(v, \mathbf{q}), \quad \forall \{v, \mathbf{q}\} \in \mathbf{W}. \quad (10.2.11)$$

4. This suggests the introduction of an *augmented Lagrangian functional* over $(H_0^1(\Omega) \times \mathbf{Q}) \times \mathbf{Q}$ with $r > 0$:
$$\mathscr{L}_r(\{v, \mathbf{q}\}, \boldsymbol{\mu}) = F(v, \mathbf{q}) + \frac{1}{2} r \int_{\Omega} |\nabla v - \mathbf{q}|^2\, da + \int_{\Omega} \boldsymbol{\mu} \cdot (\nabla v - \mathbf{q})\, da. \quad (10.2.12)$$

If $\{\{w, \mathbf{p}\}, \boldsymbol{\lambda}\}$ is a saddle point of $\mathscr{L}_r$, that is it satisfies (cf. (10.1.6)):

$$\mathscr{L}_r(\{w, \mathbf{p}\}, \boldsymbol{\mu}) \leq \mathscr{L}_r(\{w, \mathbf{p}\}, \boldsymbol{\lambda}) \leq \mathscr{L}_r(\{v, \mathbf{q}\}, \boldsymbol{\lambda}) \tag{10.2.13}$$

for all $\{\{v, \mathbf{q}\}, \boldsymbol{\mu}\} \in (H_0^1(\Omega) \times \mathbf{Q}) \times \mathbf{Q}$, then the pair $\{w, \mathbf{p}\}$ is a solution of the minimisation problem, and conversely.

Now, the task is to find a sequence $\{\{w^n, \mathbf{p}^n\}, \boldsymbol{\lambda}^n\}$ to solve the saddle point problem (10.2.13). The following Uzawa type algorithm is recommended in [4] for this purpose. Essentially, it assumes a given value w^{n-1} and $\boldsymbol{\lambda}^n$ for $n \geq 0$, and seeks the gradient $\mathbf{p}^n$ through the solution of the minimisation problem:

$$\mathscr{L}_r(\{w^{n-1}, \mathbf{p}^n\}, \boldsymbol{\lambda}^n) \leq \mathscr{L}_r(\{w^{n-1}, \mathbf{q}\}, \boldsymbol{\lambda}^n), \quad \forall \mathbf{q} \in L^2(\Omega))^2. \tag{10.2.14}$$

The second step is to solve for w^n through

$$\mathscr{L}_r(\{w^n, \mathbf{p}^n\}, \boldsymbol{\lambda}^n) \leq \mathscr{L}_r(\{v, \mathbf{p}^n\}, \boldsymbol{\lambda}^n), \quad \forall v \in H_0^1(\Omega). \tag{10.2.15}$$

The third step is to update $\boldsymbol{\lambda}^n$:

$$\boldsymbol{\lambda}^{n+1} = \boldsymbol{\lambda}^n + r(\nabla w^n - \mathbf{p}^n). \tag{10.2.16}$$

For the iterations to converge to the desired solution $\{w, \nabla w\}$, the choice of r is very critical as shown by the example in (10.1.17) and (10.1.18). For a discussion of this matter, see pp. 182–183 in [1] and pp. 102 in [2] where it is demonstrated that $r = 1$ is a suitable value.

Here, one may seek an answer to the following question: what is the relation between the solution $\{w, \mathbf{p}\}$ of the saddle point problem and that which follows from the equations of motion and the constitutive relation for the Bingham fluid? The answer lies in examining the properties of the augmented Lagrangian functional at these *optimal conditions*. First of all, the Gateaux derivatives of this functional exist in the *direction* h for all $h \in H_0^1(\Omega)$ at w, and in the *direction* $\boldsymbol{\xi}$ for all $\boldsymbol{\xi} \in \mathbf{Q}$ at $\boldsymbol{\lambda}$. Note that this functional is not differentiable with respect to $\mathbf{q}$ at $\mathbf{q} = \mathbf{0}$. These matters are discussed next.

10.2.1 Optimality Conditions of the Augmented Lagrangian Functional

To find the Gateaux derivative of the functional in (10.2.12) at $\{\{w, \mathbf{p}\}, \boldsymbol{\lambda}\}$ in the *direction* $h \in H_0^1(\Omega)$, replace v by $(w + \varepsilon h)$ while keeping the other two vectors fixed. Then, find the derivative of the resulting functional with respect to ε at $\varepsilon = 0$. This results in four functionals, which are:

$$\frac{1}{2}\eta \int_\Omega \nabla w \cdot \nabla h \, da, \quad -\int_\Omega Gh \, da, \quad r \int_\Omega \nabla h \cdot (\nabla w - \mathbf{p}) \, da, \quad \int_\Omega \boldsymbol{\lambda} \cdot \nabla h \, da. \tag{10.2.17}$$

Here, the first and the last two integrals involve the dot product of ∇h with another vector, say $\mathbf{m}$. In each case, it is obvious that

$$\begin{aligned}\int_{\Omega} \nabla h \cdot \mathbf{m}\, da &= \int_{\Omega} \nabla \cdot (h\mathbf{m})\, da - \int_{\Omega} h \nabla \cdot \mathbf{m}\, da \\ &= \int_{\partial\Omega} h\, \mathbf{m} \cdot \mathbf{n}\, ds - \int_{\Omega} h\, \nabla \cdot \mathbf{m}\, da \\ &= -\int_{\Omega} h\, \nabla \cdot \mathbf{m}\, da, \end{aligned} \tag{10.2.18}$$

where $\mathbf{n}$ is the external unit normal to the boundary and, since $h \in H_0^1(\Omega)$, this function h vanishes on the boundary of the flow domain. Hence, the Gateaux derivative leads to:

$$\left\langle \frac{\partial}{\partial v} \mathscr{L}_r(\{w, \mathbf{p}\}, \boldsymbol{\lambda}), h \right\rangle = \int_{\Omega} \Big[-(\eta + r)\nabla^2 w - G + \nabla \cdot (\boldsymbol{\lambda} - r\mathbf{p}) \Big] h\, da = 0. \tag{10.2.19}$$

This is essentially the variational form of the equation of motion.

The condition $\mathscr{L}_r(\{w, \mathbf{p}\}, \boldsymbol{\lambda}) \leq \mathscr{L}_r(\{w, \mathbf{q}\}, \boldsymbol{\lambda})$ leads to the following inequality:

$$\begin{aligned} &\tau_y \int_{\Omega} |\mathbf{q}|\, da - \int_{\Omega} \boldsymbol{\lambda} \cdot \mathbf{q}\, da + \frac{r}{2} \int_{\Omega} |\nabla w - \mathbf{q}|^2\, da \\ &\quad \geq \tau_y \int_{\Omega} |\mathbf{p}|\, da - \int_{\Omega} \boldsymbol{\lambda} \cdot \mathbf{p}\, da + \frac{r}{2} \int_{\Omega} |\nabla w - \mathbf{p}|^2\, da, \quad \forall \mathbf{q} \in \mathbf{Q}. \end{aligned} \tag{10.2.20}$$

This is equivalent to

$$\begin{aligned} &\frac{r}{2} \int_{\Omega} \mathbf{q} \cdot \mathbf{q}\, da + \tau_y \int_{\Omega} |\mathbf{q}|\, da - \int_{\Omega} (\boldsymbol{\lambda} + r\nabla w) \cdot \mathbf{q}\, da \\ &\quad \geq \frac{r}{2} \int_{\Omega} \mathbf{p} \cdot \mathbf{p}\, da + \tau_y \int_{\Omega} |\mathbf{p}|\, da - \int_{\Omega} (\boldsymbol{\lambda} + r\nabla w) \cdot \mathbf{p}\, da \quad \forall \mathbf{q} \in \mathbf{Q}. \end{aligned} \tag{10.2.21}$$

We now use the fact that, for any fixed $\mathbf{p} \in \mathbf{Q}$ and $\forall \mathbf{q} \in \mathbf{Q}$, the inequality $\mathbf{q} \cdot \mathbf{q} - \mathbf{p} \cdot \mathbf{p} \geq 0$ is equivalent to $2(\mathbf{q} - \mathbf{p}) \cdot \mathbf{p} \geq 0$. Hence, the following implies (10.2.21) and vice versa:

$$\begin{aligned} &r \int_{\Omega} (\mathbf{q} - \mathbf{p}) \cdot \mathbf{p}\, da + \tau_y \int_{\Omega} |\mathbf{q}|\, da - \tau_y \int_{\Omega} |\mathbf{p}|\, da \\ &\quad - \int_{\Omega} (\boldsymbol{\lambda} + r\nabla w) \cdot (\mathbf{q} - \mathbf{p})\, da \geq 0, \quad \forall \mathbf{q} \in \mathbf{Q}. \end{aligned} \tag{10.2.22}$$

The solution of this variational inequality is given by

$$\mathbf{p} = \begin{cases} \frac{1}{r}\left(1 - \frac{\tau_y}{|\boldsymbol{\lambda}+r\nabla w|}\right)(\boldsymbol{\lambda} + r\nabla w), & \text{if} \quad |\boldsymbol{\lambda} + r\nabla w| > \tau_y \\ 0, & \text{if} \quad |\boldsymbol{\lambda} + r\nabla w| \le \tau_y. \end{cases} \tag{10.2.23}$$

This is equivalent to the constitutive equation of the Bingham fluid in terms of the Lagrange multiplier.

One can make the solution (10.2.23) more transparent when one derives an *equation of energy balance* associated to the inequality (10.2.22). The procedure is similar to that in deriving (8.3.3) and consists of setting $\mathbf{q} = 2\mathbf{p}$ and $\mathbf{q} = \mathbf{0}$. This results in the equation:

$$r\int_{\Omega} \mathbf{p}\cdot\mathbf{p}\, da + \tau_y \int_{\Omega} |\mathbf{p}|\, da - \int_{\Omega} (\boldsymbol{\lambda} + r\nabla w)\cdot\mathbf{p}\, da = 0. \tag{10.2.24}$$

Since $\mathbf{p}\cdot\mathbf{p} \ge 0$, it is obvious that the solution of this energy equation is given by (10.2.23).

Finally, using the method in deriving (10.2.19), we find that

$$\left\langle \frac{\partial}{\partial \boldsymbol{\mu}} \mathscr{L}_r(\{w, \mathbf{p}\}, \boldsymbol{\lambda}), \boldsymbol{\xi} \right\rangle = \int_{\Omega} (\nabla w - \mathbf{p})\cdot\boldsymbol{\xi}\, da = 0, \tag{10.2.25}$$

which is the variational form of the equation of constraint.

10.2.2 More General Problems

In the steady flow of a Bingham fluid in a pipe of arbitrary cross-section, there is no acceleration and the pressure field is known. However, in a majority of problems, inertia is present and the pressure field has to be found. As a typical example, consider the following problem:

$$\nabla\cdot\mathbf{u} = 0 \quad \text{in } \Omega, \tag{10.2.26}$$

$$\rho\frac{\partial \mathbf{u}}{\partial t} + \nabla\cdot\mathbf{S} - \nabla p = \mathbf{f}, \quad \text{in } \Omega, \tag{10.2.27}$$

$$\mathbf{u} = \mathbf{g} \text{ on } \partial\Omega \times (0, T), \tag{10.2.28}$$

$$\text{with} \int_{\partial\Omega} \mathbf{g}(t)\cdot\mathbf{n} = 0, \text{ a.e. on } (0, T) \tag{10.2.29}$$

$$\mathbf{u}_{|t=0} = \mathbf{u}_0, \quad \nabla\cdot\mathbf{u}_0 = 0, \tag{10.2.30}$$

with the usual constitutive equation for the Bingham fluid. Note that the body force, if any, is included in $\mathbf{f}$. The variational inequality formulation of the problem now

becomes (cf. (8.4.6)):

$$\rho \int_{\Omega} \frac{\partial \mathbf{u}}{\partial t} \cdot (\mathbf{v} - \mathbf{u})\, dv + \rho \int_{\Omega} (\mathbf{u} \cdot \nabla)\mathbf{u} \cdot (\mathbf{v} - \mathbf{u})\, dv + \frac{1}{2}\eta \int_{\Omega} \mathbf{A}(\mathbf{u}) : \mathbf{A}(\mathbf{v} - \mathbf{u})\, dv + \tau_y[j(\mathbf{v}) - j(\mathbf{u})] - \int_{\Omega} p\nabla \cdot \mathbf{v}\, dv \geq \int_{\Omega} \mathbf{f} \cdot (\mathbf{v} - \mathbf{u})\, dv, \quad \forall \mathbf{v} \in (H^1(\Omega))^d, \tag{10.2.31}$$

with $\mathbf{v} = \mathbf{g}$ on $\partial\Omega$. We have to find $\{\mathbf{u}, p\} \in (H^1(\Omega))^d \times L^2(\Omega)$, with $\nabla \cdot \mathbf{u} = 0$. If we assume further that the velocity field $\mathbf{v}$ also satisfies $\nabla \cdot \mathbf{v} = 0$, the pressure term drops out of the above inequality. This means that p has to be reintroduced as a Lagrange multiplier as in Sect. 4.1. And, a new symmetric tensor $\mathbf{q}$ has to be introduced to satisfy the constraint $\mathbf{A}(\mathbf{v}) - \mathbf{q} = \mathbf{0}$. The augmented Lagrangian is derived at length in Chap. 3, Sect. 20 in [4] and the procedure to solve the saddle point problem is also listed therein.

Essentially, the augmented Lagrangian functional has to be such that at the optimality conditions it delivers the following set of equations:

- The equations of motion, similar to (10.2.19).
- The continuity equation; for an example, see (10.3.25) below. As mentioned earlier, this did not arise in the steady flow of the Bingham fluid in a pipe of arbitrary cross-section.
- The constitutive equation in terms of the Lagrange multiplier, similar to (10.2.23).
- The equation of constraint similar to (10.2.25).

For another example of these equations, see the simulation of the non-isothermal flows of viscoplastic waxy crude oils in [11].

In order to solve other problems such as the settling motion of a rigid body in a Bingham fluid, one can either use the augmented Lagrangian method [12] or the fictitious domain method employed in [13]. The latter method has been combined with an operator-splitting scheme in [4] to solve the sedimentation problem. It is to the operator-splitting method to which we turn next.

10.3 Operator-Splitting Method for Thermally Driven Flows

In this section, the operator-splitting method is explained and applied to the flow of a Bingham fluid in a square cavity with two vertical walls at different temperatures. To begin, as is well known, the isothermal fluid flow of an incompressible Newtonian fluid is governed by the Navier-Stokes equations, which need to be solved together with appropriate boundary conditions to find the flow quantities, i.e., the velocity

field $\mathbf{u}$ and the pressure field p. Since the convected acceleration terms $(\mathbf{u} \cdot \nabla)\mathbf{u}$ are nonlinear, an efficient way of solution is to split the original problem into two sub-problems which are much easier to deal with. The first sub-problem is of the Stokes type, where the pressure field p and the velocity field $\mathbf{u}$ are determined by omitting the nonlinear convection terms $(\mathbf{u} \cdot \nabla)\mathbf{u}$, while retaining the incompressibility condition $\nabla \cdot \mathbf{u} = 0$. The second sub-problem incorporates the nonlinear convected acceleration terms $(\mathbf{u} \cdot \nabla)\mathbf{u}$ to determine $\mathbf{u}$, using the velocity field derived from the first sub-problem as an initial condition. The solution $\mathbf{u}$ from the second sub-problem now forms the initial value for the first one, along with the previously determined p in the next iteration. This is the spirit of the operator-splitting method applied to Navier-Stokes equations; see Li [14] and Glowinski and Pironneau [15].

To incorporate the yield stress into the numerical scheme, the viscoplastic fluid can be thought of as the sum of a viscous and a viscoplastic constraint part[4] as in Sect. 8.9. Having solved the viscous flow problem in two sub-routines as mentioned above, one determines the viscoplastic constraint tensor field $\boldsymbol{\Lambda}$ from the updated velocity field. This method has been applied to the lid driven cavity flow of a Bingham fluid by Sanchez [17] as well as by Dean and Glowinski [18], and in the study of particle sedimentation in Bingham fluids by Yu and Wachs [13].

When the temperature Θ is taken into account, the energy equation for the non-isothermal flow has to be included in the governing equations. In this case, the flow quantities $\mathbf{u}, p$ and Θ give rise to two sets of governing equations (10.3.5) and (10.3.6), and an iterative, operator-splitting scheme is the natural choice for their solution. Using the two sub-problems for the isothermal flow as a basis, the temperature of the non-isothermal flow in the current step can be found from the energy equation using the velocity field in the previous step. Next the viscoplasticity tensor is also determined from the velocity field as in the isothermal case. Iteration proceeds till convergence to the desired accuracy of the solution is attained. Note that the constitutive model employed in this section is the viscoplasticity constraint tensor as described above in Sect. 8.9.

Turning to the examples in the literature regarding non-isothermal flows of yield stress fluids, we are aware of the existence and uniqueness theorems by Duvaut and Lions [19] for a Bingham fluid with a temperature dependent viscosity and a constant yield stress; those of Kato [20] for a yield stress fluid with a power-law viscosity and a yield stress, both of which are temperature dependent. In the problem discussed here, both the viscosity and yield stress are assumed to be constant.

10.3.1 The Flow Problem and Mathematical Formulation

The natural convection flow of a Bingham fluid is supposed to take place in an upright square cavity with an edge of length of L. The horizontal walls are insulated, and the

[4] In viscoelastic fluid mechanics, splitting the constitutive equation into a viscous and an elastic part was conceived and applied to Oldroyd-B fluids in 1977; see [16].

vertical left and right walls are at temperatures Θ_h and $\Theta_c < \Theta_h$, respectively. The flow velocity is zero on the walls. The gravity vector $\mathbf{g} = -g\mathbf{e}_2$ is directed in the negative y-coordinate direction, with $\mathbf{e}_2$ the relevant unit vector. Following the conventional Boussinesq approximation [21], we consider small temperature variations only, i.e., the relative change in temperature $\delta\Theta/\Theta \ll 1$. The density ρ, thermal conductivity k, the heat capacity c_p and viscosity η are set to be constants here.

Employing the equations of motion (8.9.6) involving the constraint tensor Λ, the relevant equations are

$$\nabla \cdot \mathbf{u} = 0, \tag{10.3.1}$$

$$\rho\mathbf{a} + \nabla p - \eta\nabla \cdot \mathbf{A}(\mathbf{u}) - \sqrt{2}\tau_y \nabla \cdot \boldsymbol{\Lambda} = \rho\mathbf{b}, \tag{10.3.2}$$

where the body force $\mathbf{b}$ is the sum of that due to gravity and the buoyancy effects. Thus, using the average temperature $\Theta_r = (\Theta_h + \Theta_c)/2$ as the reference temperature and β as the coefficient of thermal expansion, we obtain:

$$\mathbf{b} = [1 + \beta(\Theta_r - \Theta)]\mathbf{g}, \quad \mathbf{g} = -g\mathbf{e}_2. \tag{10.3.3}$$

Now, let the pressure p be written as the sum $p = p_s + p_d$, with the static part p_s accounting for gravity, and p_d is the dynamic part. That is:

$$\nabla p_s = \rho\mathbf{g}, \tag{10.3.4}$$

so that $p_s = -\rho g y$. Hence, the momentum equation incorporates the dynamic part only, and is of the form

$$\rho\left[\frac{\partial \mathbf{u}}{\partial t} + (\mathbf{u} \cdot \nabla)\mathbf{u}\right] + \nabla p_d - \eta\nabla \cdot \mathbf{A}(\mathbf{u}) + \sqrt{2}\tau_y \nabla \cdot \boldsymbol{\Lambda} = \rho\beta(\Theta_r - \Theta)\mathbf{g}, \tag{10.3.5}$$

where $\mathbf{u}$ is the unknown velocity field. Next, the energy equation is given by

$$\rho c_p\left[\frac{\partial \Theta}{\partial t} + (\mathbf{u} \cdot \nabla)\Theta\right] - k\nabla^2\Theta = 0, \tag{10.3.6}$$

where ∇^2 is the two-dimensional Laplacian.

Note that the right hand side of Eq. (10.3.5) accounts for the buoyancy effect under the Boussinesq approximation, in which temperature deviations from the reference temperature have to be small.

10.3.2 Non-dimensionalisation

Letting L be the length scale, the average temperature Θ_r be the temperature scale, and $\delta\Theta = \Theta_h - \Theta_c$, we define the buoyancy velocity scale $U = \sqrt{gL\beta\delta\Theta}$, and the

Bingham (Bn), the Rayleigh (Ra) and the Prandtl (Pr) numbers as follows:

$$\mathrm{Bn} = \frac{\sqrt{2}\tau_y L}{\eta U}, \quad \mathrm{Ra} = \frac{g\beta\rho L^3 \delta\Theta}{\alpha\eta}, \quad \mathrm{Pr} = \frac{\eta c_p}{k}, \tag{10.3.7}$$

where $\alpha = k/\rho c_p$ is the thermal diffusivity. Next, set

$$\mathbf{u} = U\mathbf{u}^*, \ \mathbf{x} = L\mathbf{x}^*, \ t = \frac{L}{U}t^*, \ p_d = \frac{\eta U}{L}p^*, \ \Theta = \Theta_r + \delta\Theta \cdot \Theta^*. \tag{10.3.8}$$

Finally, we define the local Nusselt number Nu and the averaged Nusselt number Nu_{avg} through

$$\mathrm{Nu} = -\frac{d\Theta}{dx}_{|x=0}, \quad \mathrm{Nu}_{avg} = \int_0^1 \mathrm{Nu}\, dy. \tag{10.3.9}$$

The following non-dimensional governing equations, where the asterisks have been omitted for convenience, are easily derived:

$$\nabla \cdot \mathbf{u} = 0, \tag{10.3.10}$$

$$\sqrt{\frac{\mathrm{Ra}}{\mathrm{Pr}}}\left[\frac{\partial \mathbf{u}}{\partial t} + (\mathbf{u}\cdot\nabla)\mathbf{u}\right] - \nabla\cdot\mathbf{A}(\mathbf{u}) + \nabla p - \mathrm{Bn}\,\nabla\cdot\boldsymbol{\Lambda} = \sqrt{\frac{\mathrm{Ra}}{\mathrm{Pr}}}\,\Theta\mathbf{e}_2, \tag{10.3.11}$$

$$\frac{\partial\Theta}{\partial t} + (\mathbf{u}\cdot\nabla)\Theta - \frac{1}{\sqrt{\mathrm{RaPr}}}\nabla^2\Theta = 0. \tag{10.3.12}$$

Now, let the flow domain $\Omega = (0,1)\times(0,1)$, and the boundary $\Gamma = \partial\Omega$, with a subset $\Gamma_1 = \{\mathbf{x}|\mathbf{x} = \{x, y\}, 0 \le x \le 1, y = 0 \text{ or } 1\}$. The boundary condition for the velocity is straightforward: $\mathbf{u}|_\Gamma = 0$. The thermal boundary conditions are

$$\Theta(0,y,t) = \frac{1}{2}, \quad \Theta(1,y,t) = -\frac{1}{2}, \quad \left.\frac{\partial\Theta}{\partial y}\right|_{\Gamma_1} = 0, \ t \ge 0. \tag{10.3.13}$$

The initial conditions are of the form:

$$\mathbf{u}(x,y,0) = \mathbf{0}, \quad \Theta(x,y,0) = \frac{1}{2} - x, \quad (x,y) \in \overline{\Omega}. \tag{10.3.14}$$

First of all, it is worth noting that if the Bingham number $\mathrm{Bn} = 0$, one recovers the Newtonian fluid model. Thus, there is no need to find the viscoplastic constraint tensor $\boldsymbol{\Lambda}$. It can be put to zero everywhere in the numerical scheme developed for the Bingham fluid which means that there is no need to produce a separate routine for the Newtonian fluid.

Next, as mentioned earlier, the relation (8.9.3) between the tensor $\boldsymbol{\Lambda}$ and the solution vector $\mathbf{u}$ was proved by Duvaut and Lions [22, 23] for isothermal flows with zero boundary conditions on the velocity field. Subsequently, they proved that [19] the tensor $\boldsymbol{\Lambda}$ exists in non-isothermal flows provided the velocity field vanishes on the boundary and it meets (8.9.3) once again. Thus, the operator-splitting method can be used in the buoyancy driven flow in a square cavity with confidence.

Now, we turn to the determination of the constraint tensor $\boldsymbol{\Lambda}$. It is based on the classical Uzawa type algorithm [5] as mentioned earlier. In this method, $\boldsymbol{\Lambda}$ can be obtained from a simple projection operation as follows [3, 13, 24]:

$$\boldsymbol{\Lambda} = P_{\mathscr{M}}\Big(\boldsymbol{\Lambda} + r\tau_y \mathbf{A}(\mathbf{v})\Big), \quad \forall r > 0, \tag{10.3.15}$$

where $\mathscr{M} = \big\{\boldsymbol{\mu} = \boldsymbol{\mu}^T | \boldsymbol{\mu} = (\mu_{ij})_{1\le i,j\le 2} \in (L^2(\Omega))^4, ||\boldsymbol{\mu}|| \le 1 \text{ a.e. on } \Omega\big\}$ and

$$P_{\mathscr{M}} : (L^2(\Omega))^4 \to \mathscr{M} \tag{10.3.16}$$

is the projection operator defined so that $P_{\mathscr{M}}(\boldsymbol{\mu}) = \boldsymbol{\mu}$, if $||\boldsymbol{\mu}|| < 1$, and $P_{\mathscr{M}}(\boldsymbol{\mu}) = \boldsymbol{\mu}/||\boldsymbol{\mu}||$ otherwise. Note that in the context of Eq. (10.3.15), the tensor $\boldsymbol{\mu} = \boldsymbol{\Lambda} + r\tau_y \mathbf{A}(\mathbf{v})$ and it is symmetric. Further, the tensor $\boldsymbol{\mu}$ and $r\tau_y \mathbf{A}(\mathbf{v})$ must both be dimensionless for $\boldsymbol{\Lambda}$ is also dimensionless. The exact form taken by the product $r\tau_y \mathbf{A}(\mathbf{v})$ can be determined as follows.

Since $\mathbf{A}(\mathbf{v})$ is of dimension $U/L = T^{-1}$, where T denotes time, one can find quite easily that r has the dimension $M^{-1}LT^{-3}$. The question is how one can define this constant r. Recalling Eq. (10.3.7), it is easy to show that

$$\mathrm{Bn} \cdot \mathrm{Pr} = \frac{c_p}{k} \cdot \frac{\sqrt{2}\tau_y L}{U}. \tag{10.3.17}$$

Obviously,

$$\frac{k}{c_p} \cdot \frac{\mathrm{Bn} \cdot \mathrm{Pr}}{\sqrt{2}} \cdot \frac{U^2}{L^2} = \tau_y \frac{U}{L}. \tag{10.3.18}$$

Since $U = \sqrt{gL\beta\delta\Theta}$, we find that $r\tau_y(U/L)$ is dimensionless if

$$r = \frac{\sqrt{2}c_p}{k} \cdot \frac{L^2}{U^2} = \frac{\sqrt{2}c_p}{k} \cdot \frac{L}{g\beta\delta\Theta}. \tag{10.3.19}$$

When we want to replace τ_y by Bn, and $\mathbf{A}(\mathbf{v})$ by its non-dimensional version, we begin with $\nabla_{\mathbf{x}}\mathbf{v}$ and obtain that it is equal to $(U/L)\nabla_{\mathbf{x}^*}\mathbf{v}^*$, where the latter gradient is of zero dimension.

Thus,

$$r\tau_y \mathbf{A}(\mathbf{u}) = r\tau_y (U/L)\mathbf{A}^*(\mathbf{u}^*) = r^* \mathrm{Bn} \mathbf{A}^*(\mathbf{u}^*), \tag{10.3.20}$$

from which it follows that

$$r^* = \frac{\eta U^2}{\sqrt{2}L^2} r = \frac{\eta U^2}{\sqrt{2}L^2} \cdot \frac{\sqrt{2}c_p}{k} \cdot \frac{L}{g\beta\delta\Theta} = \frac{\eta c_p}{k} = \mathrm{Pr}. \tag{10.3.21}$$

That is, the constant r^* is the Prandtl number.

There is one final question to answer, viz., does the finite element numerical scheme converge? Currently, there are no restrictions on the value of r^*. However, in the isothermal, lid driven cavity flow problem, one finds a sufficient condition for the parameter r in (10.3.15) in Eq. (17.58) [4]:

$$0 < r < \frac{\eta}{2\tau_y^2}. \tag{10.3.22}$$

Since $r\tau_y \mathbf{A}(\mathbf{u})$ is dimensionless and $\mathbf{A}(\mathbf{u}) \sim U/L$, one sees that the condition above is equivalent to $||r\tau_y \mathbf{A}(\mathbf{u})|| < 1/(2\,\mathrm{Bn})$. This bound can be improved; see Eq. (17.64) in [4].

10.3.3 Numerical Procedure

In this subsection, we shall explain the numerical scheme employed in [25] to solve the thermally driven cavity flow problem, basing it on the operator-splitting method developed for isothermal problems [13, 14, 21, 24]. This new scheme has been designed to examine the non-isothermal viscoplastic problem, and the algorithm is written in a variational form in order to facilitate its finite element implementation.

Let Δt be the time step and f^n denote the value of function $f(t)$ at time $t = t^n$. As usual, $t^{n+\gamma} = (n+\gamma)\Delta t$. Assuming that $\mathbf{u}^n, p^n, \Theta^n, \Lambda^n$ are known, the numerical scheme works in the following iterative manner:

1. **The temperature problem**:

   Solve the energy equation together with the boundary conditions for Θ^{n+1}:

$$\frac{1}{\Delta t}\int_\Omega (\Theta^{n+1} - \Theta^n)\varphi \, da + \int_\Omega (\mathbf{u}^n \cdot \nabla)\Theta^{n+1}\varphi \, da + \chi \int_\Omega \nabla\Theta^{n+1} \cdot \nabla\varphi \, da = 0, \quad \forall \varphi \in H_0^1(\Omega). \tag{10.3.23}$$

2. **The generalised Stokes problem**:

   Find $\left\{\mathbf{u}^{n+1/3}, p^{n+1}\right\} \in (H_0^1)^2 \times L^2$ such that

$$\frac{\alpha}{\Delta t}\int_{\Omega}(\mathbf{u}^{n+1/3}-\mathbf{u}^{n})\cdot\mathbf{v}\,da+\frac{1}{3}\int_{\Omega}\nabla\mathbf{u}^{n+1/3}:\nabla\mathbf{v}\,da-\int_{\Omega}p^{n+1}\nabla\cdot\mathbf{v}\,da$$

$$=\alpha\int_{\Omega}\frac{\Theta^{n+1}+\Theta^{n}}{2}\mathbf{e}_2\cdot\mathbf{v}\,da,\quad\forall\mathbf{v}\in(H_0^1(\Omega))^2,\tag{10.3.24}$$

$$\int_{\Omega}\nabla\cdot\mathbf{u}^{n+1/3}q=0\,da,\quad\forall q\in L^2(\Omega).\tag{10.3.25}$$

3. **The convected derivative problem**:

   Solve for $\mathbf{u}^{n+2/3}\in(H_0^1)^2$:

$$\frac{\alpha}{\Delta t}\int_{\Omega}(\mathbf{u}^{n+2/3}-\mathbf{u}^{n+1/3})\cdot\mathbf{v}\,da+\alpha\int_{\Omega}(\mathbf{u}^{n+1/3}\cdot\nabla)\mathbf{u}^{n+2/3}\cdot\mathbf{v}\,da$$
$$+\frac{1}{3}\int_{\Omega}\nabla\mathbf{u}^{n+2/3}:\nabla\mathbf{v}\,da=0,\quad\forall\mathbf{v}\in(H_0^1(\Omega))^2.\tag{10.3.26}$$

   Note that in Eq. (10.3.26), $(\mathbf{u}^{n+1/3}\cdot\nabla)\mathbf{u}^{n+2/3}$ is the linearised form of the original nonlinear term $(\mathbf{u}^{n+2/3}\cdot\nabla)\mathbf{u}^{n+2/3}$. By this simplification, we can take advantage of saving the computational cost without losing any accuracy [3].

4. **The viscoplasticity constraint tensor problem**:

   Given $\mathbf{u}^{n+2/3}$, solve for $\left\{\mathbf{u}^{n+1},\boldsymbol{\Lambda}^{n+1}\right\}\in(H_0^1)^2\times\mathscr{M}$:

$$\frac{\alpha}{\Delta t}\int_{\Omega}(\mathbf{u}^{n+1}-\mathbf{u}^{n+2/3})\cdot\mathbf{v}\,da+\frac{1}{3}\int_{\Omega}\nabla\mathbf{u}^{n+1}:\nabla\mathbf{v}\,da$$
$$+\mathrm{Bn}\int_{\Omega}\boldsymbol{\Lambda}^{n+1}:\nabla\mathbf{v}\,da=0,\quad\forall\mathbf{v}\in(H_0^1(\Omega))^2,\tag{10.3.27}$$

$$\boldsymbol{\Lambda}^{n+1}=P_{\mathscr{M}}\left(\boldsymbol{\Lambda}^{n}+\mathrm{Pr}\cdot\mathrm{Bn}\mathbf{A}(\mathbf{u}^{n+2/3})\right).\tag{10.3.28}$$

One should note that we have taken $\alpha=\sqrt{\mathrm{Ra}/\mathrm{Pr}}$ in Eqs. (10.3.24), (10.3.26) and (10.3.27), and $\chi=1/\sqrt{\mathrm{Ra}\cdot\mathrm{Pr}}$ in Eq. (10.3.23) for convenience.

As mentioned below Eq. (10.3.16), the new value of $\boldsymbol{\Lambda}^{n+1}$ depends on the magnitude of $\boldsymbol{\Lambda}^{n}+\mathrm{Pr}\cdot\mathrm{Bn}\mathbf{A}(\mathbf{u}^{n+2/3})$. That is, we use $P_{\mathscr{M}}(\boldsymbol{\mu})=\boldsymbol{\mu}$, if $||\boldsymbol{\mu}||<1$, and $P_{\mathscr{M}}(\boldsymbol{\mu})=\boldsymbol{\mu}/||\boldsymbol{\mu}||$ otherwise, to find the new value of $\boldsymbol{\Lambda}^{n+1}$.

Again, recall that if the Bingham number $\mathrm{Bn}=0$, then one can put $\boldsymbol{\Lambda}^{n}=\mathbf{0}$ in Eq. (10.3.28). Then, it follows that $\boldsymbol{\Lambda}^{n+1}=\mathbf{0}$ automatically and in Eq. (10.3.27), we can omit the integral involving this tensor. Thus, Eq. (10.3.27) becomes a sub-problem for finding $\mathbf{u}^{n+1}$ only.

It is clear that the original complicated problem has been split into four subproblems in each time step and solved by the iterative algorithm. In Step 1, the new updated temperature Θ^{n+1} is calculated from the values of Θ^n and $\mathbf{u}^n$ obtained in the previous time step. Then the pressure p^{n+1} in the new time step is updated and the intermediate velocity $\mathbf{u}^{n+1/3}$ is solved in Step 2. Step 3 gives the intermediate velocity $\mathbf{u}^{n+2/3}$ and, finally, the velocity in the new time step $\mathbf{u}^{n+1}$ together with $\boldsymbol{\Lambda}^{n+1}$ is updated in Step 4. The stopping criterion for the iteration is $\left\|\mathbf{u}^{n+1}-\mathbf{u}^n\right\|_{L^2}+\left\|\Theta^{n+1}-\Theta^n\right\|_{L^2}<\varepsilon$, in which ε is a convergence parameter.

10.3.4 Discussion of the Results

The description of the results follows closely that in [25] with some minor changes. Overall, the convection problem has been investigated at different Rayleigh numbers, $\mathrm{Ra}=10^3-10^5$, Prandtl numbers, $\mathrm{Pr}=0.1-10$ and the Bingham numbers between 1 and 27. The operator-splitting method based on FEM has been utilised to perform the numerical simulations. A uniform triangulation mesh has been applied to the problem with the maximum length of the edges fixed at $h=0.01$. Moreover, the time step is selected to be $\triangle t=0.001$, and the convergence parameter is $\varepsilon=10^{-6}$. To check the accuracy of the results, the present code has been validated for a Newtonian fluid with published studies on natural convection in a cavity.

Figure 10.1 illustrates the isotherms, the streamlines and the yielded/unyielded zones for different Rayleigh numbers at Bn = 3 and Pr = 0.1. At $\mathrm{Ra}=10^3$, the temperature contours are parallel to the wall which demonstrates that conduction is dominant in the enclosure. As the Rayleigh number increases, the movements of the isotherms between the cold and hot walls change significantly and they become progressively curved. Moreover, the gradient of temperature on the hot wall rises with the rise of Rayleigh number, for the thermal boundary layer thickness on the side walls decreases with increasing Rayleigh number. The streamlines show that the convection process has been enhanced by the growth of Rayleigh numbers as the core of the streamline changes from the circular shape to an elliptical one gradually and the streamlines traverse further into the cavity. The last column displays the yielded (White) and unyielded (Black) regions for the studied Rayleigh numbers at Bn = 3. It is clear that the proportion of the yielded sections in the enclosure has been enhanced markedly with the increase of the Rayleigh number. Therefore, for constant Bingham and Prandtl numbers, the increase in the Rayleigh number causes the unyielded zones to decline.

Figure 10.2 shows the temperature across the cavity, the vertical velocity along the horizontal mid-plane of the cavity and the local Nusselt number on the hot wall for different Rayleigh numbers when $\mathrm{Bn}=3$ and $\mathrm{Pr}=0.1$. When $\mathrm{Ra}=10^3$, the distribution of the temperature is nearly linear and the vertical velocity component is essentially negligible due to a very weak flow, as the buoyancy forces are dominated by viscous effects. In this situation, the heat transfer takes place entirely by conduction across

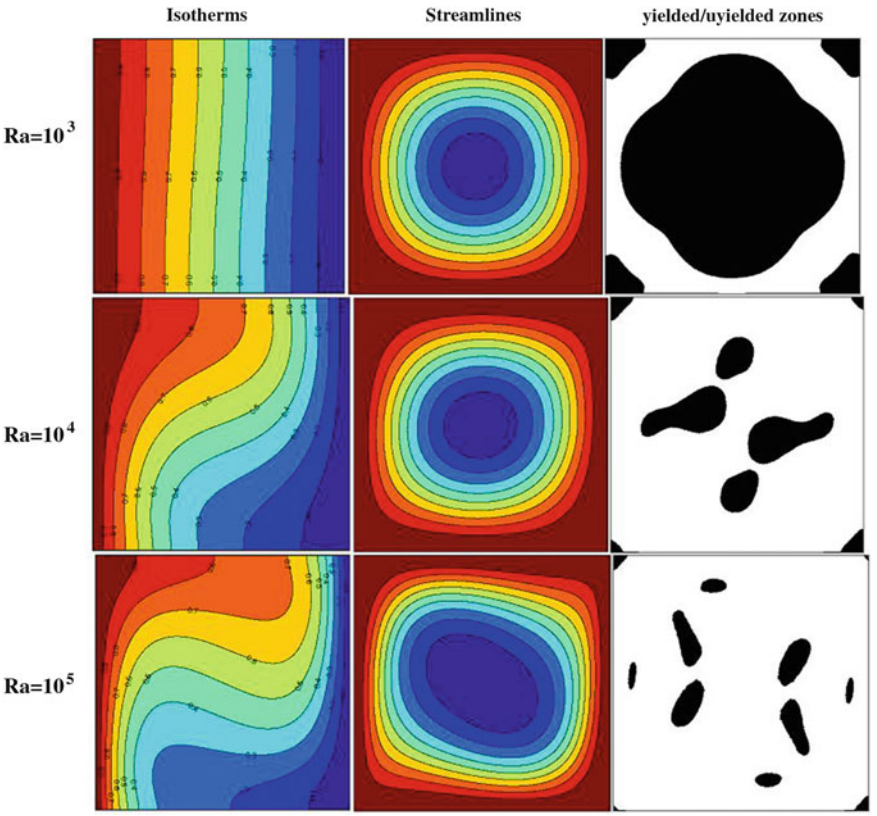

Fig. 10.1 Comparison of the isotherms, streamlines and yielded/unyielded zones for various Rayleigh numbers at Bn = 3 and Pr = 0.1. *Black* unyielded zone and *white* yielded zone

the enclosure. While the vertical velocity does indeed augment with an increase of the Rayleigh number, the temperature profile becomes increasingly non-linear with the strengthening of convective transport for higher values of the Rayleigh number. The local Nusselt number on the hot wall for $Ra = 10^3$ is roughly equal to one which demonstrates that the heat transfer takes place due to conduction being dominant, in agreement with the comments about the Nusselt number in Sect. 5.9.1. Moreover, the effects of buoyancy forces strengthen in comparison with the viscous effects, as the Rayleigh numbers increase. Therefore, as the Rayleigh number rises, the magnitude of the local Nusselt number is enhanced.

The influence of the rise in the Bingham number on the isotherms, streamlines and the proportion of the yielded/unyielded regions has been depicted in Fig. 10.3 for $Ra = 10^5$ and Pr = 0.1. It shows that the curved shapes of the isotherms decline with the rise of the Bingham number. This process causes the gradient of the temperature on the hot wall to drop and therefore heat transfer decreases with the rise of Bingham numbers. The streamlines demonstrate this decrease in the convection process with

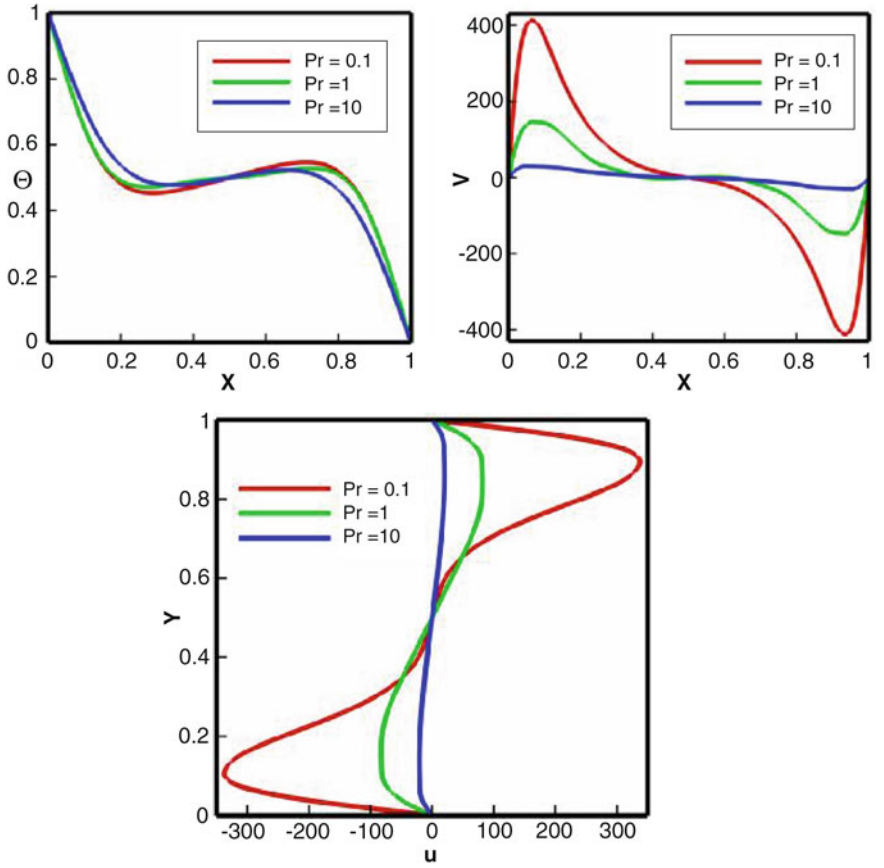

Fig. 10.2 Temperatures and vertical velocities in the middle of the cavity and local Nusselt number on the hot wall for different Rayleigh numbers at Bn = 3 and Pr = 0.1

the growth of the Bingham number, for the inclined elliptical form in the core of the cavity alters to a circular shape. In addition, the maximum strength of the streamlines $|\psi_{\max}|$ or the vortex intensity [26], the maximum horizontal and vertical velocities all decrease as the Bingham number is increased. As a result, the convection process decreases with the enhancement of Bingham number. The unyielded sections occupy more spaces in the cavity as the Bingham number augments and the rise of the Bingham number causes the yielded regions to disappear gradually. In other words, there is a critical Bingham number Bn_c above which the fluid is completely unyielded. An empirical relationship between the critical value of the Bingham number and the Prandtl and Rayleigh numbers can be derived:

$$\mathrm{Bn}_c = 0.152\mathrm{Ra}^{0.37}\mathrm{Pr}^{-0.39}. \tag{10.3.29}$$

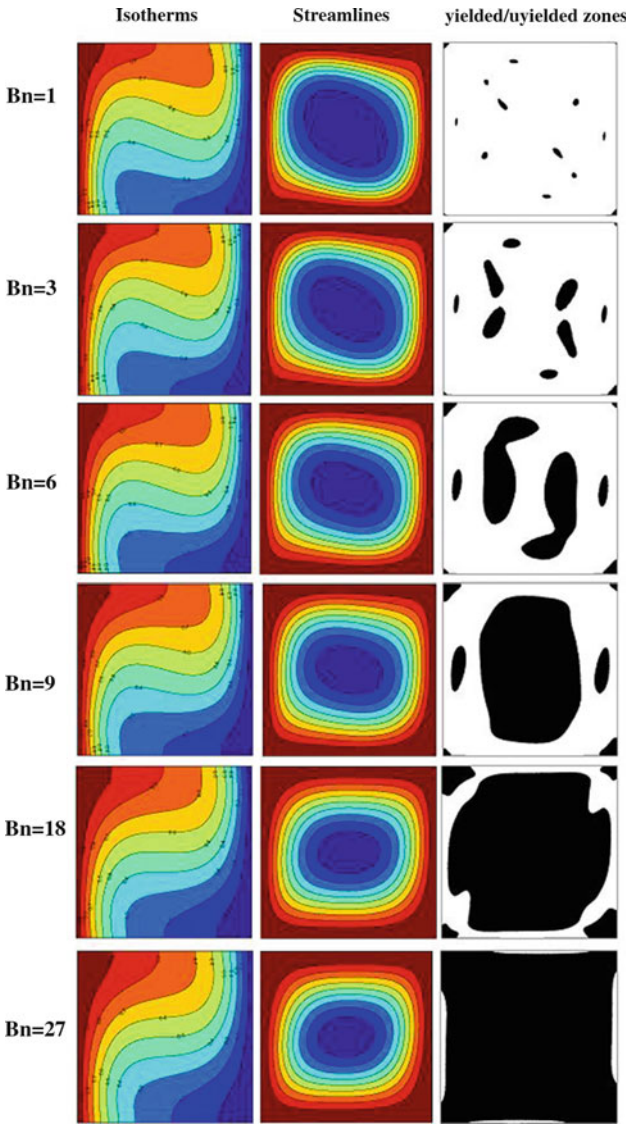

Fig. 10.3 Comparison of the isotherms, streamlines and yielded/unyielded zones for various Bingham numbers at Pr = 0.1 and Ra = 10^5. *Black* unyielded zone and *white* yielded zone

Thus, the critical Bingham number increases with the Rayleigh number for a fixed Prandtl number, while it decreases with the Prandtl number for a fixed Rayleigh number in line with the definitions of these numbers in (10.3.7).

Next, in Fig. 10.4, the temperature and vertical velocity along the horizontal midplane of the cavity and the local Nusselt number are shown for different Bingham numbers between 1 and 27, when Ra = 10^5 and Pr = 0.1. The temperature profile

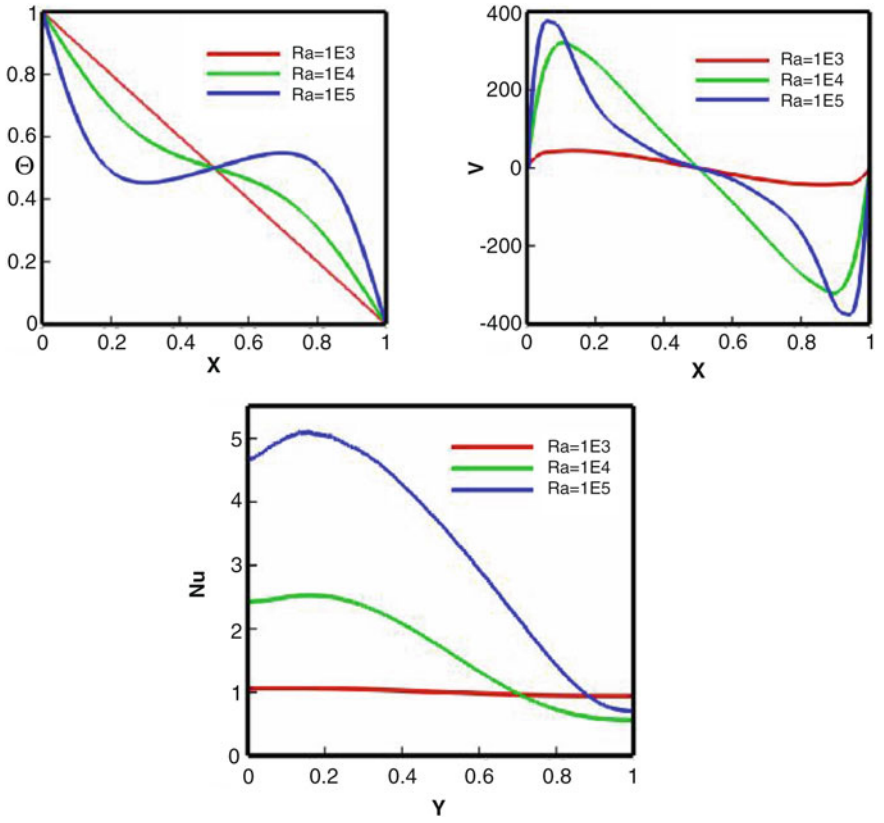

Fig. 10.4 Temperatures and vertical velocities in the middle of the cavity and local Nusselt number on the hot wall for different Bingham numbers at Pr = 0.1 and Ra = 10^5

becomes linear when the Bingham number increases which clarifies the Bingham number effect, for the convection process decreases. This pattern is also mirrored by the vertical velocity in the middle of the cavity where its magnitude drops significantly with the increase in the Bingham number. The local Nusselt number also decreases with the enhancement of the Bingham number. In fact, for high values of the Bingham number, the yield stress effects overcome the buoyancy force and as a result of this, no significant flow is induced within the enclosure which is to be expected. The mode of heat transfer and the relationship between the Bingham and Nusselt numbers observed here are also in accord with the observations made earlier in Sect. 5.9.1.

Figure 10.5 shows the isotherms, the streamlines and the yielded/unyielded zones for various Prandtl numbers when Bn = 1 and Ra = 10^5. It can be seen that the gradient of the isotherms on the hot wall decreases as the Prandtl number increases. This trend can been confirmed by examining the streamlines of the core which demonstrate that the convection process decreases with the rise of the Prandtl number. Further, it can be seen that the unyielded section for the chosen Bingham and Rayleigh

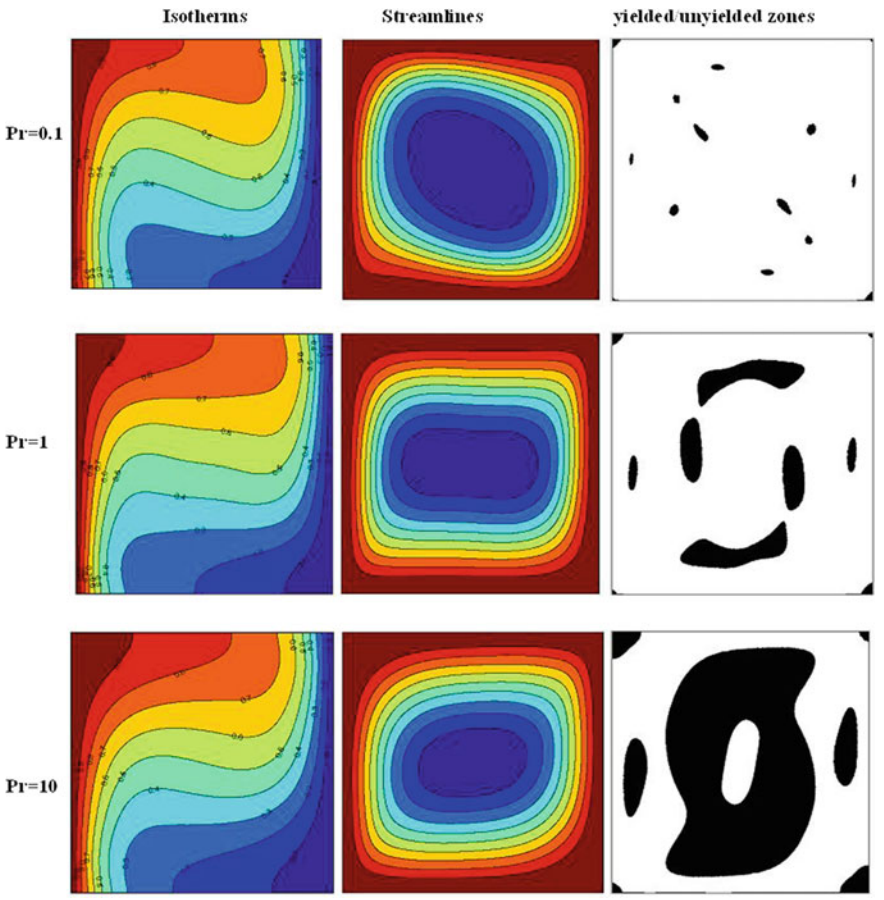

Fig. 10.5 Comparison of the isotherms, streamlines and yielded/unyielded zones for various Prandtl numbers at Bn = 1 and Ra = 10^5. *Black* unyielded zone and *white* yielded zone

numbers increases with the augmentation of the Prandtl number. In fact, the increase of the unyielded sections at higher Prandtl numbers causes the heat transfer to drop (cf. (10.3.29)).

The influence of altering the Prandtl number can be observed on the temperature, the vertical and horizontal velocities in the middle of the cavity in Fig. 10.6. It is evident that the effect of the Prandtl number on the temperature is marginal, although the increase in this number declines the curved shape of the temperature slightly and therefore reduces the convection process. The vertical and horizontal velocity distributions in the middle of the cavity indicate that the growth of the Prandtl number decreases the velocity in the cavity drastically. The results demonstrate that the development of the unyielded sections, which increases at higher Prandtl numbers, causes the velocities to drop markedly.

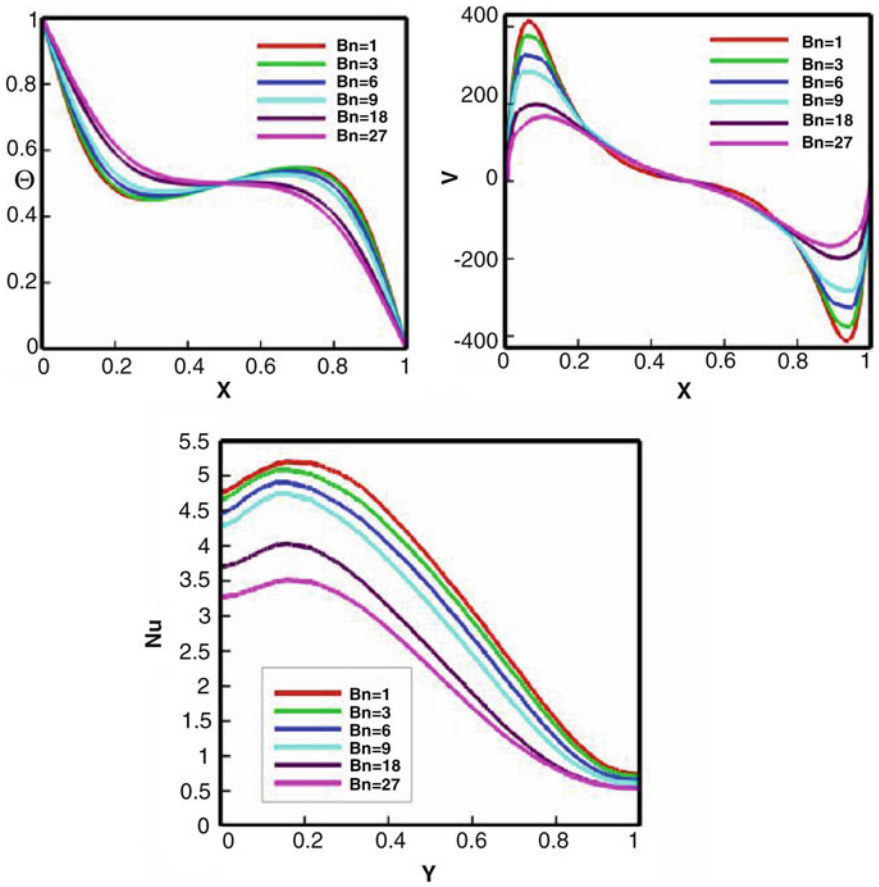

Fig. 10.6 Temperatures, vertical and horizontal velocities in the middle of the cavity for different Prandtl numbers at Bn = 1 and Ra = 10^5

Overall, it is found that the rise of the Rayleigh number increases the heat transfer for it causes the unyielded zones to decline for various Bingham and Prandtl numbers. The increase in the Bingham number decreases the heat transfer as it augments the unyielded sections. The unyielded regions are also enhanced with the augmentation of the Prandtl number for certain Rayleigh and Bingham numbers. These results are qualitatively similar to those in Figs. 10.7, 10.8 and 10.9 in [26], derived by using the augmented Lagrangian method. To be specific, the streamline patterns in Fig. 10.3 and those in Fig. 10.7 [26] are similar for increasing values of the Bingham number; the temperature variation along the horizontal axis and the vertical velocity distribution at the middle of the cavity in Fig. 10.8 [26] mirror those in Fig. 10.2; and, finally, in Fig. 10.9 [26], one can see that the average Nusselt number and the vortex intensity decline with an increase in the yield stress, similar to that found here and depicted in Fig. 10.2.

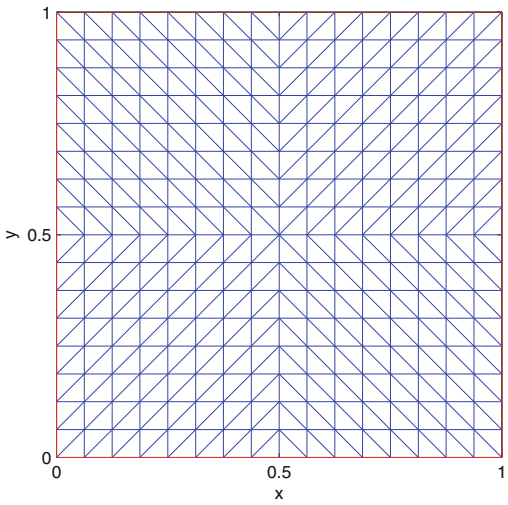

Fig. 10.7 Square cavity and mesh system

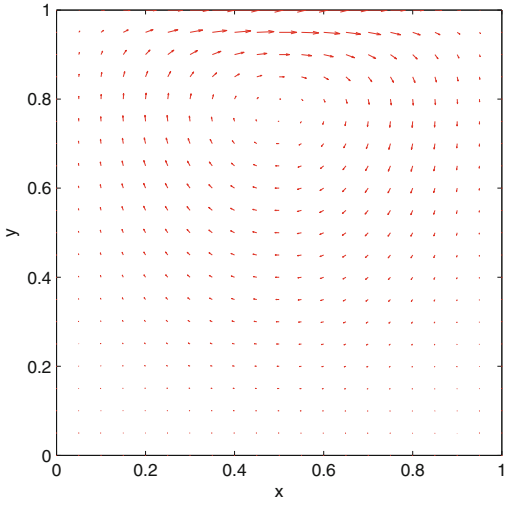

Fig. 10.8 Flow pattern in the cavity for an incompressible Bingham fluid

Putting these comparisons aside, it is not possible at present to discern which of the two methods, viz., the augmented Lagrangian method or the operator-splitting one is superior; in fact, Glowinski and Wachs [4] make the following remark on p. 504 of their review article: "The computational methods derived from either the *augmented Lagrangian method* or *orthogonal projection* approaches are fairly *modular*, making them relatively easy to implement." The italics are in the original. Note that the operator-splitting method is derived from the *orthogonal projection* approach; see Eq. (10.3.28) above. Clearly, more comparative studies are called for to decide which one of the two methods is preferable.

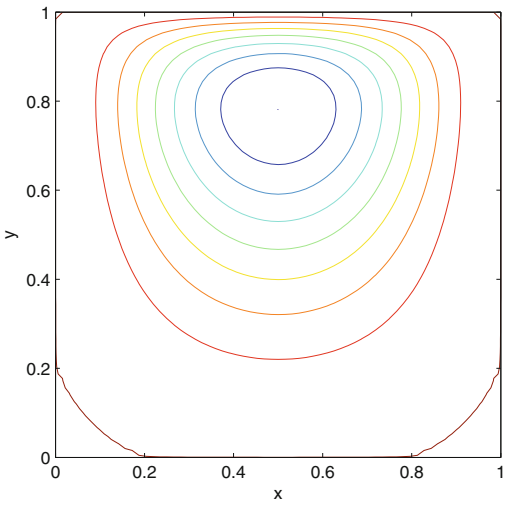

Fig. 10.9 Streamlines corresponding to the flow pattern

10.4 Compressibility Effects: Numerical Experiments

Much of the material in this section is derived from [24] with some modifications and a summary is offered here.

10.4.1 Operator-Splitting Methods: Compressible Viscous Fluids

As a prelude to discussing viscoplastic fluids, we shall follow the treatment in [24] and begin with compressible Newtonian fluids. As is well known, numerical simulation of the flows of compressible viscous fluids is not as advanced as it is for incompressible fluids. A couple of schemes exist for isentropic flows and low Mach number flows and we shall discuss them next.

The constitutive equation for a viscous fluid is taken to be the compressible Newtonian fluid, viz.,

$$\mathbf{S} = -p\mathbf{1} + \lambda(\nabla \cdot \mathbf{u})\mathbf{1} + \eta\mathbf{A}, \tag{10.4.1}$$

where p is the thermodynamic pressure which depends on the density ρ and the temperature Θ. The material properties λ and η are the Lamé viscosity coefficients, which depend on ρ, Θ and the invariants of $\mathbf{A}(\mathbf{u})$ as well. No numerical schemes are available for solving flow problems at this level of generality. So, we shall look at two special cases.

1. **The isentropic case**

   Here, we assume that the flow is isothermal and ignore the energy equation. Next, we assume that Stokes' relation holds, i.e., $3\lambda + 2\eta = 0$. Also, we demand that

η is a constant and that $\rho - \rho_0 = \varepsilon p$, where $\rho_0 > 0$ and ε is a "small" parameter. Assuming that Ω is a bounded domain, conservation of mass implies that

$$\int_{\Omega} p(\mathbf{x}, t)\, dv = 0. \tag{10.4.2}$$

The equations of motion are:

$$\rho\left[\frac{\partial \mathbf{u}}{\partial t} + (\mathbf{u}\cdot\nabla)\mathbf{u}\right] - \nabla\cdot\eta[\mathbf{A}(\mathbf{u}) - \frac{2}{3}(\nabla\cdot\mathbf{u})\mathbf{1}]$$
$$+ \frac{1}{\varepsilon}\nabla\rho = \rho\mathbf{b}, \tag{10.4.3}$$

where we have replaced ∇p by $\nabla\rho/\varepsilon$. This form of the equations of motion have been studied by Lions [27, 28]. Turning to the numerical scheme [3], the solution is sought as a perturbation in ε, i.e.,

$$\mathbf{u} = \mathbf{u}_0 + \sum_{k=1}^{\infty} \varepsilon^k \mathbf{u}_k, \tag{10.4.4}$$

$$\rho = \rho_0 + \sum_{k=1}^{\infty} \varepsilon^k \rho_k, \tag{10.4.5}$$

$$p = p_0 + \sum_{k=1}^{\infty} \varepsilon^k p_k. \tag{10.4.6}$$

Then, for $k = 0, 1, 2, \ldots$, one can derive a sequence of Navier-Stokes equations, applicable to incompressible fluids, and these can be solved. For the case when $k = 0, 1, 2$, see Glowinski [3].
When the perturbation method is applied to viscoplastic fluids, the Rivlin-Ericksen tensor has the following expansion:

$$\mathbf{A}(\mathbf{u}) = \mathbf{A}(\mathbf{u}_0) + \sum_{k=1}^{\infty} \varepsilon^k \mathbf{A}(\mathbf{u}_k). \tag{10.4.7}$$

At a given point in the flow, it is possible that the flow is rigid up to a certain order in ε, and may not be so at the next order of perturbation. That is, the perturbation of the velocity field may change the location and shape of the yielded/unyielded regions. To keep track of these changes in developing a numerical scheme is cumbersome and would appear to be insurmountable. Indeed, the difficulties associated with solving problems using a perturbation method have been highlighted in discussing the flow in a wavy channel and the linearised stability of the flow in a channel; see Sects. 7.2 and 7.4 respectively. From the foregoing, it would appear

that the above method of solution for a viscoplastic isentropic flow is not viable. We shall now turn to a discussion of low Mach number flows.

2. **Low Mach number flows**

Low Mach number flows are of interest in modelling the flows of viscoplastic fluids in the start-up of the flow in a pipe of circular cross-section of a weakly compressible Bingham fluid; for example, see [4, 29, 30]. For a discussion of the scaling procedures needed to derive the relevant Navier-Stokes equations for compressible fluids, see p. 11 of [27].
To begin, we need a definition of the Mach number M, given by [27]

$$\mathrm{M} = \frac{|\mathbf{u}|}{c}, \quad c = \sqrt{p'(\rho)}. \tag{10.4.8}$$

Next, it is known that if the Mach number is small, the continuity equation

$$\frac{d\rho}{dt} + \rho \nabla \cdot \mathbf{u} = \frac{\partial \rho}{\partial t} + \nabla \cdot (\rho \mathbf{u}) = 0 \tag{10.4.9}$$

and the momentum equations lead to acoustic waves. That is, these disturbances propagate at the speed of sound c and contaminate the solution $\mathbf{u}$.
In examining low Mach number flows, Lions [27] has shown that the pressure term p should be of the form

$$p(\mathbf{x}, t) = P(t) + \varepsilon P_1(t) + \varepsilon^2 p_d(\mathbf{x}, t). \tag{10.4.10}$$

Here, $P(t)$, which is the thermodynamic pressure, and P_1 are independent of $\mathbf{x}$. However, the numerical schemes which have been developed depend on the following decomposition of the pressure p:

$$p(\mathbf{x}, t) = p_T(t) + p_d(\mathbf{x}, t), \tag{10.4.11}$$

where p_T is the thermodynamic pressure and the dynamic pressure $p_d << p_T$. It has been shown by Horibata [31] that in this case, acoustic waves do not exist. To proceed further, we shall follow Li and Glowinski [21] and assume that the total pressure obeys the equation of state

$$p = R\rho\Theta, \tag{10.4.12}$$

where R is a constant and Θ is the absolute temperature. From this, it is obvious that

$$\frac{1}{\rho}\frac{d\rho}{dt} = \frac{1}{p}\frac{dp}{dt} - \frac{1}{\Theta}\frac{d\Theta}{dt}. \tag{10.4.13}$$

From the continuity equation, we see that $d\rho/dt = -\rho \nabla \cdot \mathbf{u}$. Thus, the above equation can be written as

$$\frac{dp}{dt} + p \nabla \cdot \mathbf{u} = R\rho \frac{d\Theta}{dt}. \tag{10.4.14}$$

Since $p(\mathbf{x}, t) = p_T(t) + p_d(\mathbf{x}, t)$, $p_d << p_T$, we now put $p_T = R\rho\Theta$ and replace dp/dt by dp_T/dt in Eq. (10.4.14) and integrate over the flow domain Ω. This results in an ordinary differential equation for p_T:

$$|\Omega|\frac{dp_T}{dt} + \left(\int_\Omega \nabla\cdot\mathbf{u}\,dv\right)p_T = R\int_\Omega \rho\left(\frac{\partial\Theta}{\partial t} + \mathbf{u}\cdot\nabla\Theta\right)dv, \tag{10.4.15}$$

where $|\Omega|$ is the volume of Ω. Note that we have used the assumption that $p_T = p_T(t)$ above. In addition to this equation, we collect below the remaining Navier-Stokes equations for compressible fluids in the non-isothermal case. They are:

$$\frac{\partial\rho}{\partial t} + \nabla\cdot(\rho\mathbf{u}) = 0, \tag{10.4.16}$$

$$\rho\left[\frac{\partial\mathbf{u}}{\partial t} + (\mathbf{u}\cdot\nabla)\mathbf{u}\right] - \nabla\cdot\eta[\mathbf{A}(\mathbf{u}) - \frac{2}{3}(\nabla\cdot\mathbf{u})\mathbf{1}] + \nabla p_d = \rho\mathbf{b}, \tag{10.4.17}$$

$$\rho C_p\left(\frac{\partial\Theta}{\partial t} + \mathbf{u}\cdot\nabla\Theta\right) - \nabla\cdot k\nabla\Theta = \frac{dp_T}{dt} + Q, \tag{10.4.18}$$

$$p_T = R\rho\Theta. \tag{10.4.19}$$

Note that the viscosity η and the thermal conductivity coefficient k are functions of the temperature Θ. And, $Q = (1/2)S_{ij}A_{ij}$ is the volumetric heat source due to dissipation. As well, we have assumed that the Lamé coefficients λ and η obey $3\lambda + 2\eta = 0$.

Before proceeding further, let us make the following changes to the continuity equation and the equation of state respectively:

$$\nabla\cdot\mathbf{u} = W(Z, \mathbf{u}) = -\left(\frac{\partial Z}{\partial t} + \mathbf{u}\cdot\nabla Z\right), \quad Z = \ln\rho, \tag{10.4.20}$$

$$\rho = \rho(p_T, \Theta). \tag{10.4.21}$$

Next, define a new dynamic pressure term through

$$p_d^* = p_d + \frac{2}{3}\eta\nabla\cdot\mathbf{u}. \tag{10.4.22}$$

Having defined p_d^*, we drop the asterisk in what follows.

Assuming that ρ^n, Θ^n, η^n, k^n, p_T^n, Z^n, $\mathbf{u}^n$, p_d^n are known, the method of solution works as follows:

1. Solve for Θ^{n+1} the heat equation:

$$\rho^n C_p\left(\frac{\partial\Theta}{\partial t} + \mathbf{u}^n\cdot\nabla\Theta\right) - \nabla\cdot k^n\nabla\Theta = Q + \frac{p_T^n - p_T^{n-1}}{\triangle t}. \tag{10.4.23}$$

2. Compute $\eta^{n+1} = \eta(\Theta^{n+1})$ and $k^{n+1} = k(\Theta^{n+1})$.
3. Solve the ordinary differential equation for p_T^{n+1}:

$$|\Omega|\frac{p_T^{n+1} - p_T^n}{\triangle t} + \left(\int_\Omega \nabla \cdot \mathbf{u}^n \, dv\right) p_T^{n+1} = R\int_\Omega \rho^n \left(\frac{\Theta^{n+1} - \Theta^n}{\triangle t} + \mathbf{u}^n \cdot \nabla\Theta^{n+1}\right) dv. \tag{10.4.24}$$

4. Compute $\rho^{n+1} = \rho(p_T^{n+1}, \Theta^{n+1})$ and $Z^{n+1} = \ln \rho^{n+1}$.
5. Next, obtain $\rho^{n+1/2} = (\rho^{n+1} + \rho^n)/2$ and $Z^{n+1/2} = \ln \rho^{n+1/2}$.
6. Solve the following Navier-Stokes equations for $\mathbf{u}^{n+1}$ and p_d^{n+1}:

$$\rho^{n+1/2}\left[\frac{\partial \mathbf{u}^{n+1}}{\partial t} + (\mathbf{u}^n \cdot \nabla)\mathbf{u}^{n+1}\right] - \nabla \cdot \eta^{n+1}\mathbf{A}(\mathbf{u}^{n+1}) + \nabla p_d^{n+1} = \rho^{n+1/2}\mathbf{b}, \tag{10.4.25}$$

$$\nabla \cdot \mathbf{u}^{n+1} = W(Z^{n+1/2}, \mathbf{u}^n), \tag{10.4.26}$$

where

$$W(Z^{n+1/2}, \mathbf{u}^n) = -\left(\frac{Z^{n+1} - Z^n}{\triangle t} + \mathbf{u}^n \cdot \nabla Z^{n+1/2}\right). \tag{10.4.27}$$

Finally, as observed by Li and Glowinski [21], the discrete solution p_T^{n+1} of step 3 above does not, in general, preserve global conservation of mass exactly, although the deviation is usually small. So, one has to apply a correction to p_T^{n+1} to ensure global mass conservation. Denoting the discrete solution p_T^{n+1} of step 3 above by p_T^* and noting that p_T^* is spatially uniform, the correction can be accomplished through the following steps:

(i) Calculate the initial mass:

$$M^0 = \int_\Omega \rho^0 \, dv.$$

(ii) Compute the new density and the new mass:

$$\rho^* = \rho(p_T^*, \Theta), \quad M^* = \int_\Omega \rho^* \, dv.$$

(iii) Compute the correction $\triangle p$ through:

$$\triangle p = \frac{M^0 - M^*}{M^*} p_T^*.$$

(iv) Reset $p_T^{n+1} = p_T^* + \triangle p$.

10.4.2 Compressible Viscoplastic Fluids: Isothermal Case

Clearly, one can replace the constitutive equations for the compressible Newtonian fluid with equations relevant to compressible viscoplastic fluids from Sect. 4.5. Instead of pursuing this in detail, let us consider a more modest isothermal flow problem for a viscoplastic fluid with a variable density, viscosity and yield stress assumed to depend on $(\mathbf{x}, t)$ only. That is, while the viscosity depends on the pressure, the three invariants of $\mathbf{A}$ as well as the absolute temperature, and the yield stress is a function of the pressure and the absolute temperature only, we simplify this by assuming that these material properties depend on $(\mathbf{x}, t)$, borrowing an idea from [3, 21] where a similar assumption has been made regarding the viscosity of a compressible Newtonian fluid. The relevant equations, with a viscoplastic constraint tensor (4.5.10), are:

$$\rho\left(\frac{\partial u_i}{\partial t} + u_{i,j}u_j\right) - (\eta A_{ij}(\mathbf{u}))_{,j} - \sqrt{2}(\tau_y \Lambda_{ij})_{,j} + p_{,i} = \rho b_i. \tag{10.4.28}$$

Since we will be considering weakly compressible fluids in the sequel, the continuity Eq. (10.4.20) is modified so that

$$\nabla \cdot \mathbf{u} = W(\mathbf{u}). \tag{10.4.29}$$

This has the effect of simplifying the viscous term in (10.4.28) as we shall see next. Clearly,

$$(\eta u_{i,j})_{,j} v_i = (\eta u_{i,j} v_i)_{,j} - \eta u_{i,j} v_{i,j}. \tag{10.4.30}$$

Hence, using the divergence theorem,

$$\begin{aligned}\int_\Omega (\eta u_{i,j})_{,j} v_i \, dv &= \int_\Gamma \eta u_{i,j} n_j v_i \, dS - \int_\Omega \eta u_{i,j} v_{i,j} \, dv \\ &= \int_{\partial\Omega} \eta \frac{\partial \mathbf{u}}{\partial \mathbf{n}} \cdot \mathbf{v} \, dS - \int_\Omega \eta \nabla \mathbf{u} : \nabla \mathbf{v} \, dv. \end{aligned} \tag{10.4.31}$$

Next

$$\begin{aligned}(\eta u_{j,i})_{,j} v_i &= \eta_{,j} u_{j,i} v_i + \eta u_{j,ji} v_i \\ &= \nabla\eta \cdot (\mathbf{v} \cdot \nabla)\mathbf{u} + \eta(\mathbf{v} \cdot \nabla) W(\mathbf{u}),\end{aligned} \tag{10.4.32}$$

where we have used $u_{j,ij} = u_{j,ji}$. Thus,

$$\int_{\Omega} (\eta u_{j,i})_{,j} v_i \, dv = \int_{\Omega} \Big(\nabla\eta \cdot (\mathbf{v} \cdot \nabla)\mathbf{u} + \eta(\mathbf{v} \cdot \nabla) W(\mathbf{u}) \Big) \, dv. \tag{10.4.33}$$

Next,

$$\begin{aligned}\int_{\Omega} (\tau_y \Lambda_{ij})_{,j} v_i \, dv &= \int_{\Omega} (\tau_y \Lambda_{ij} v_i)_{,j} \, dv - \int_{\Omega} \tau_y \Lambda_{ij} v_{i,j} \, dv \\ &= \int_{\partial\Omega} \tau_y \mathbf{v} \cdot \boldsymbol{\Lambda}\mathbf{n} \, dS - \frac{1}{2} \int_{\Omega} \tau_y \boldsymbol{\Lambda} : \mathbf{A}(\mathbf{v}) \, dv.\end{aligned} \tag{10.4.34}$$

Finally, noting that $\mathbf{v} \cdot \mathbf{n} = \mathbf{n} \cdot \mathbf{v}$, one obtains

$$\begin{aligned}\int_{\Omega} p_{,i} v_i \, dv &= \int_{\Omega} \Big[(p v_i)_{,i} - p v_{i,i} \Big] dv \\ &= \int_{\partial\Omega} p\mathbf{n} \cdot \mathbf{v} \, dS - \int_{\Omega} p \nabla \cdot \mathbf{v} \, dv.\end{aligned} \tag{10.4.35}$$

Thus, the equivalent variational problem of solving Eqs. (10.4.28) and (10.4.29) is the following:

$$\begin{aligned}&\int_{\Omega} \rho \frac{\partial \mathbf{u}}{\partial t} \cdot \mathbf{v} \, dv + \int_{\Omega} \eta \nabla\mathbf{u} : \nabla\mathbf{v} \, dv + \int_{\Omega} \rho(\mathbf{u} \cdot \nabla)\mathbf{u} \cdot \mathbf{v} \, dv \\ &\quad - \int_{\Omega} p \nabla \cdot \mathbf{v} \, dv + \frac{1}{\sqrt{2}} \int_{\Omega} \tau_y \boldsymbol{\Lambda} : \mathbf{A}(\mathbf{v}) \, dv \\ &= \int_{\Omega} (\nabla\eta) \cdot (\mathbf{v} \cdot \nabla)\mathbf{u} \, dv + \int_{\Omega} \eta(\mathbf{v} \cdot \nabla) W(\mathbf{u}) \, dv \\ &\quad + \int_{\Omega} \rho \mathbf{b} \cdot \mathbf{v} \, dv + \int_{\partial\Omega} \eta \frac{\partial \mathbf{u}}{\partial \mathbf{n}} \cdot \mathbf{v} \, dS \\ &\quad + \sqrt{2} \int_{\partial\Omega} \tau_y \mathbf{v} \cdot \boldsymbol{\Lambda}\mathbf{n} \, dS - \int_{\partial\Omega} p\mathbf{n} \cdot \mathbf{v} \, dS,\end{aligned} \tag{10.4.36}$$

for all admissible trial velocity fields $\mathbf{v}$. To the above, we add:

$$\int_{\Omega} (\nabla \cdot \mathbf{u}) q \, dv = \int_{\Omega} W(\mathbf{u}) q \, dv, \tag{10.4.37}$$

for all $q \in L^2(\Omega)$. Two types of boundary conditions which have been considered by Li and Glowinski [21] are:

1. The enclosed flow (BC1):

$$\mathbf{u} = \mathbf{0} \text{ on } \partial\Omega, \quad \int_{\Omega} q \, dv = 0. \tag{10.4.38}$$

   Thus, all of the boundary terms in equation (10.4.36) vanish because $\mathbf{v} = \mathbf{0}$ on $\partial\Omega$.
2. Open or partly open flow (BC2), where the velocity is prescribed on one part and the normal stress on the other part of the boundary:

$$\mathbf{u} = \mathbf{g} \text{ on } \partial\Omega_0, \quad -p\mathbf{n} + \eta \frac{\partial \mathbf{u}}{\partial \mathbf{n}} = \mathbf{g}_1 \text{ on } \partial\Omega_1, \tag{10.4.39}$$

   where $\partial\Omega_0 \cup \partial\Omega_1 = \partial\Omega$, $\partial\Omega_0 \cap \partial\Omega_1 = \emptyset$. The second condition is imposed because the term $\eta(\partial \mathbf{u}/\partial \mathbf{n}) - p\mathbf{n}$ appears in (10.4.36).

Note that in the case of BC2, if $\partial\Omega_1 = \emptyset$, one lets $\mathbf{v} = \mathbf{g}$ on $\partial\Omega$. If $\partial\Omega_1 \neq \emptyset$, one lets $\mathbf{v} = \mathbf{0}$ on $\partial\Omega_0$. Assuming the latter,

$$\int_{\partial\Omega} \left[\eta \frac{\partial \mathbf{u}}{\partial \mathbf{n}} - p\mathbf{n} \right] \cdot \mathbf{v} \, dS = \int_{\partial\Omega_1} \mathbf{g}_1 \cdot \mathbf{v} \, dS. \tag{10.4.40}$$

Let us now obtain the final set of equations for BC2:

$$\begin{aligned} \int_{\Omega} \rho \frac{\partial \mathbf{u}}{\partial t} \cdot \mathbf{v} \, dv + \int_{\Omega} \eta \nabla \mathbf{u} : \nabla \mathbf{v} \, dv + \int_{\Omega} \rho (\mathbf{u} \cdot \nabla) \mathbf{u} \cdot \mathbf{v} \, dv \\ - \int_{\Omega} p \nabla \cdot \mathbf{v} \, dv + \frac{1}{\sqrt{2}} \int_{\Omega} \tau_y \boldsymbol{\Lambda} : \mathbf{A}(\mathbf{v}) \, dv \\ = \int_{\Omega} (\nabla \eta) \cdot (\mathbf{v} \cdot \nabla) \mathbf{u} \, dv + \int_{\Omega} \eta (\mathbf{v} \cdot \nabla) W(\mathbf{u}) \, dv \\ + \int_{\Omega} \rho \mathbf{b} \cdot \mathbf{v} \, dv + \int_{\partial\Omega_1} \mathbf{g}_1 \cdot \mathbf{v} \, dS + \sqrt{2} \int_{\partial\Omega_1} \tau_y \mathbf{v} \cdot \boldsymbol{\Lambda} \mathbf{n} \, dS, \end{aligned} \tag{10.4.41}$$

$$\int_{\Omega} (\nabla \cdot \mathbf{u}) q \, dv = \int_{\Omega} W(\mathbf{u}) q \, dv. \tag{10.4.42}$$

We note that in the case of BC1 or when $\partial\Omega_1 = \emptyset$ in BC2, one has:

$$\begin{aligned}\int_\Omega (\eta A_{ij}(\mathbf{u}))_{,j} v_i \, dv &= \int_\Omega (\eta A_{ij}(\mathbf{u}) v_i)_{,j} \, dv - \int_\Omega \eta A_{ij}(\mathbf{u}) v_{i,j} \, dv \\ &= \int_{\partial\Omega} \eta A_{ij}(\mathbf{u}) v_i n_j \, dS - \frac{1}{2} \int_\Omega \eta A_{ij}(\mathbf{u}) A_{ij}(\mathbf{v}) \, dv \\ &= -\frac{1}{2} \int_\Omega \eta A_{ij}(\mathbf{u}) A_{ij}(\mathbf{v}) \, dv, \end{aligned} \tag{10.4.43}$$

because $\mathbf{v} = \mathbf{0}$ on $\partial\Omega$. Thus, instead of Eq. (10.4.41), we get

$$\begin{aligned}&\int_\Omega \rho \frac{\partial \mathbf{u}}{\partial t} \cdot \mathbf{v} \, dv + \frac{1}{2} \int_\Omega \eta \mathbf{A}(\mathbf{u}) : \mathbf{A}(\mathbf{v}) \, dv + \int_\Omega \rho (\mathbf{u} \cdot \nabla)\mathbf{u} \cdot \mathbf{v} \, dv \\ &\quad - \int_\Omega p \nabla \cdot \mathbf{v} \, dv + \frac{1}{\sqrt{2}} \int_\Omega \tau_y \boldsymbol{\Lambda} : \mathbf{A}(\mathbf{v}) \, dv \\ &= \int_\Omega \rho \mathbf{b} \cdot \mathbf{v} \, dv. \end{aligned} \tag{10.4.44}$$

10.4.3 Operator-Splitting Method

We are now in a position to describe an operator-splitting method to solve the problems in Eqs. (10.4.41) and (10.4.42). This method is similar to that used above in Sect. 10.3, except that there are no thermal effects. Thus, it consists of three steps only and they are:

1. **The generalised Stokes problem**:

   Given $\mathbf{u}^n$, p^n for $n \geq 0$, find $\mathbf{u}^{n+1/3}$, p^{n+1} through

$$\begin{aligned}&\int_\Omega \rho \frac{\mathbf{u}^{n+1/3}}{\triangle t} \cdot \mathbf{v} \, dv + \frac{1}{3} \int_\Omega \eta \nabla \mathbf{u}^{n+1/3} : \nabla \mathbf{v} \, dv \\ &\quad - \int_\Omega p^{n+1} \nabla \cdot \mathbf{v} \, dv = \int_\Omega \rho \mathbf{f}^n \cdot \mathbf{v} \, dv + \int_{\partial\Omega_1} \mathbf{g}_1^n \cdot \mathbf{v} \, dS, \end{aligned} \tag{10.4.45}$$

$$\int_\Omega (\nabla \cdot \mathbf{u}^{n+1/3}) q \, dv = \int_\Omega W(\mathbf{u}^n) q \, dv. \tag{10.4.46}$$

Here, for all $n \geq 0$,

$$\mathbf{f}^n = \mathbf{b} + \frac{\mathbf{u}^n}{\triangle t} \quad \text{in } \Omega, \quad \mathbf{g}_1^n = \mathbf{g}_1 \quad \text{on } \partial\Omega_1. \tag{10.4.47}$$

2. **The convected derivative problem**:

Ignoring the yield stress terms and using the previously determined $\mathbf{u}^{n+1/3}$, find $\mathbf{u}^{n+2/3}$ through

$$\begin{aligned} &\int_\Omega \rho \frac{\mathbf{u}^{n+2/3} - \mathbf{u}^{n+1/3}}{\triangle t} \cdot \mathbf{v}\, dv + \frac{1}{3}\int_\Omega \eta \nabla \mathbf{u}^{n+2/3} : \nabla \mathbf{v}\, dv \\ &\quad + \int_\Omega \rho(\mathbf{u}^{n+1/3} \cdot \nabla)\mathbf{u}^{n+2/3} \cdot \mathbf{v}\, dv = \int_\Omega (\nabla \eta) \cdot (\mathbf{v} \cdot \nabla)\mathbf{u}^{n+1/3}\, dv \\ &\quad + \int_\Omega \eta(\mathbf{v} \cdot \nabla) W(\mathbf{u}^{n+1/3})\, dv. \end{aligned} \tag{10.4.48}$$

Once again, note that we have used the linearised form $(\mathbf{u}^{n+1/3} \cdot \nabla)\mathbf{u}^{n+2/3}$ instead of the nonlinear term $(\mathbf{u}^{n+2/3} \cdot \nabla)\mathbf{u}^{n+2/3}$; this simplification has been used earlier in (10.3.26) as well.

3. **The viscoplasticity constraint tensor problem**:

Ignoring the convected acceleration and pressure terms, find $\mathbf{u}^{n+1}$ and the multiplier $\boldsymbol{\Lambda}^{n+1}$ through

$$\begin{aligned} &\int_\Omega \rho \frac{\mathbf{u}^{n+1} - \mathbf{u}^{n+2/3}}{\triangle t} \cdot \mathbf{v}\, dv + \frac{1}{3}\int_\Omega \eta \nabla \mathbf{u}^{n+1} : \nabla \mathbf{v}\, dv \\ &+ \frac{1}{\sqrt{2}} \int_\Omega \tau_y \boldsymbol{\Lambda}^{n+1} : \mathbf{A}(\mathbf{v})\, dv = \sqrt{2} \int_{\partial\Omega_1} \tau_y \mathbf{v} \cdot \boldsymbol{\Lambda}^n \mathbf{n}\, dS, \end{aligned} \tag{10.4.49}$$

$$\boldsymbol{\Lambda}^{n+1} = P_{\mathscr{M}}(\boldsymbol{\Lambda}^n + \sqrt{2} r \tau_y \mathbf{A}(\mathbf{u}^{n+2/3})). \tag{10.4.50}$$

At this point, one notes that there is no proof that the viscoplasticity constraint tensor $\boldsymbol{\Lambda}$ in a compressible viscoplastic fluid satisfies (8.9.3) and that it can be obtained through the projection operation as in (10.3.15) and (10.3.16). This explains the reason behind labelling the results of numerical simulation presented next in Sect. 10.5 as performing *numerical experiments*; for instructive cases, see Chap. X of [3]. Clearly, the development of numerical codes for compressible viscoplastic fluids presents a serious challenge and a golden opportunity for fundamental and innovative research.

10.5 Flow in a Cavity: Weakly Compressible Fluid

The flow of a weakly compressible Bingham fluid that we study takes place in a lid driven, square cavity. Assume that the flow domain $\Omega = (0, 1) \times (0, 1)$, and the boundary $\Gamma = \partial\Omega$. To make a comparison with the available results, we have applied the regularised boundary conditions used in [3] and [18], which are slightly different from the standard boundary conditions in the cavity problem. Letting $\Gamma_N = \{\mathbf{x}|\mathbf{x} = \{x, y\}, 0 < x < 1, y = 1\}$, we impose the following boundary conditions:

$$\mathbf{u}_\Gamma(\mathbf{x}) = \begin{cases} \mathbf{0} & \text{if} \quad \mathbf{x} \in \Gamma \backslash \Gamma_N, \\ 16\left\{x^2(1-x)^2, 0\right\} & \text{if} \quad \mathbf{x} \in \Gamma_N. \end{cases} \tag{10.5.51}$$

For the slightly compressible Bingham fluid, we suppose that the density ρ is a function of the pressure p only. The viscosity η and the yield stress τ_y are constants. The set of parameters used in the computation are:

$$\alpha = \frac{1}{\triangle t}, \quad \beta = \frac{\mathrm{Bn}}{\mathrm{Re}}, \quad \nu = \frac{1}{3\mathrm{Re}}. \tag{10.5.52}$$

The density ρ is defined in terms of the pressure difference $p - p_0$, where p_0 is a reference pressure, and a reference density ρ_0. Now, let us consider the following two models:

Model 1: Linear Model

In the linear model, the density and pressure variations are proportional to one another as follows:

$$\rho - \rho_0 = c_1(p - p_0), \tag{10.5.53}$$

where c_1 is a constant, p_0 is a reference pressure, and ρ_0 is the value of density corresponding to p_0. Without losing generality, we set $p_0 = 0$, then obtain a simple form of Eq. (10.5.53) by dividing throughout by ρ_0:

$$\rho^* = 1 + c_1^* p^*. \tag{10.5.54}$$

The asterisks are dropped hereafter for simplicity and we get the final form

$$\rho = 1 + c_1 p. \tag{10.5.55}$$

Model 2: Exponential Model

In the exponential model, the density ρ is related to the density variation as follows:

$$\rho = \rho_0 \exp\left[c_2(p - p_0)\right], \tag{10.5.56}$$

where c_2 is another constant. Once again, we divide by ρ_0 and get

$$\rho^* = \exp\left(c_2^* p^*\right). \tag{10.5.57}$$

Dropping the asterisks, we have

$$\rho = \exp\left(c_2 p\right). \tag{10.5.58}$$

In what follows, we choose $c_1 = c_2 = 10^{-3}$, which correspond to weakly compressible fluids. Using the operator-splitting method discussed above in Sect. 10.4.3, we perform numerical simulations for the flows of these two weakly compressible fluids. The standard P2–P1 finite element method is employed for the space discretisation. The following discrete spaces are introduced:

$$P_h = \left\{q_h | q_h \in C^0\left(\overline{\Omega}\right), q_h|_T \in P_1, \forall T \in \mathscr{T}_h\right\}, \tag{10.5.59}$$

$$V_h = \left\{\mathbf{v}_h | \mathbf{v}_h \in \left(C^0\left(\overline{\Omega}\right)\right)^2, \mathbf{v}_h|_T \in \left(P_2\right)^2, \forall T \in \mathscr{T}_h\right\}, \tag{10.5.60}$$

$$V_{0h} = \left\{\mathbf{v}_h | \mathbf{v}_h \in V_h, \mathbf{v}_h = \mathbf{0} \text{ on } \Gamma\right\}, \tag{10.5.61}$$

$$V_{gh} = \left\{\mathbf{v}_h | \mathbf{v}_h \in V_h, \mathbf{v}_h = \mathbf{u}_\Gamma \text{ on } \Gamma\right\}. \tag{10.5.62}$$

After appropriate discretisation in finite element spaces, the variational forms of the three sub-problems are obtained:

1. **The generalised Stokes problem**:

$$\begin{aligned}
&\mathbf{u}_h \in V_{gh},\ p_h \in P_h,\\
&\alpha \int_\Omega \rho\left(p_h\right)\mathbf{u}_h \cdot \mathbf{v}_h\, da + \nu \int_\Omega \nabla \mathbf{u}_h : \nabla \mathbf{v}_h\, da - \int_\Omega p_h \nabla \cdot \mathbf{v}_h\, da\\
&\quad = \int_\Omega \mathbf{f}_h \cdot \mathbf{v}_h\, da, \quad \forall \mathbf{v}_h \in V_{0h},\\
&\int_\Omega \nabla \cdot \mathbf{u}_h q_h\, da = \int_\Omega W\left(\mathbf{u}_h\right) q_h\, da, \quad \forall q_h \in P_h.
\end{aligned} \tag{10.5.63}$$

Here, we have $W\left(\mathbf{u}_h\right) = -\mathbf{u}_h \cdot \nabla \ln \rho\left(p_h\right)$.

2. **The convected derivative problem**:

$$\begin{aligned}
&\mathbf{u}_h \in V_{gh},\\
&\alpha \int_{\Omega} \rho\left(p_h\right) \mathbf{u}_h \cdot \mathbf{v}_h \, da + \nu \int_{\Omega} \nabla \mathbf{u}_h : \nabla \mathbf{v}_h \, da \\
&\quad + \int_{\Omega} \rho\left(p_h\right) \left(\mathbf{u}_h \cdot \nabla\right) \mathbf{u}_h \cdot \mathbf{v}_h \, da = \int_{\Omega} \mathbf{f}_h \cdot \mathbf{v}_h \, da, \quad \forall \mathbf{v}_h \in V_{0h}.
\end{aligned} \tag{10.5.64}$$

3. **The viscoplasticity constraint tensor problem**:

$$\begin{aligned}
&\mathbf{u}_h \in V_{gh}, \ \boldsymbol{\Lambda}_h \in L_h,\\
&\alpha \int_{\Omega} \rho\left(p_h\right) \mathbf{u}_h \cdot \mathbf{v}_h \, da + \nu \int_{\Omega} \nabla \mathbf{u}_h : \nabla \mathbf{v}_h \, da + \beta \int_{\Omega} \lambda_h : \nabla \mathbf{v}_h \, da \\
&\quad = \int_{\Omega} \mathbf{f}_h \cdot \mathbf{v}_h \, da, \quad \forall \mathbf{v}_h \in V_{0h},\\
&\boldsymbol{\Lambda}_h = \mathscr{P}_{\mathscr{M}}\left(\boldsymbol{\Lambda}_h + r\beta \mathbf{A}\left(\mathbf{u}_h\right)\right),
\end{aligned} \tag{10.5.65}$$

where $L_h = \left\{ \mathbf{q}_h = \mathbf{q_h}^T | \mathbf{q}_h \in \left(L^2\left(\Omega\right)\right)^4, \mathbf{q}_h|_T \in \mathbb{R}^4, \forall T \in \mathscr{T}_h \right\}$. Naturally, we apply the standard Uzawa algorithm to solve the problem (10.5.65) [3, 17, 18].

We have taken $\Delta t = 10^{-3}$, the same as in [3] and [18]. The non-dimensional numbers are Re = 0.53 and Bn = 0.1, corresponding to $U = 1, \mu = 1, g = 0.1$ in [3] and [18], with a mesh of size 128×128. Since a coarser mesh of size 32×32 has been used here (see Fig. 10.7), the lid driven cavity flow has been modelled for the incompressible Bingham fluid first using the relevant sub-problems. Details are to be found in [24].

The flow pattern is visualised in Fig. 10.8 and the streamlines of the computed solution are given in Fig. 10.9, which is identical to Fig. 6.2b in [18] and Fig. 50.2b in [3]. In Fig. 10.10, the yielded and unyielded regions can be clearly found. The fluid is considered unyielded at the bottom left and right hand corners as well as in the core near the top (black zone). Elsewhere the fluid has yielded (white zone). Figure 6.2c in [18] and Fig. 50.2c in [3] show the same result. It is assumed that the yielded region corresponds to $||\boldsymbol{\Lambda}|| = 1$, while $||\boldsymbol{\Lambda}|| < 1$ in the unyielded region. The distribution of the norm of $\boldsymbol{\Lambda}$ can be seen in Fig. 10.11, or 6.2d in [18] and Fig. 50.2d in [3], alternatively. Comparison of the three sets of results shows a good agreement between them to proceed to the problem for the compressible fluid.

For the compressible fluid, the problems (10.5.63)–(10.5.65) combined with the models (10.5.55) and (10.5.58) respectively are solved in the cavity domain numerically using the schemes mentioned above. It is also worth remarking that in the compressible fluid, the zero trace property of the tensor $\boldsymbol{\Lambda}$ is not conserved, as

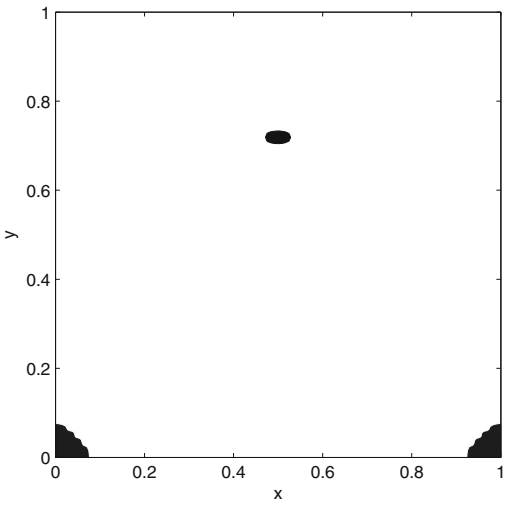

Fig. 10.10 Yielded (*white*) and unyielded (*black*) regions in the incompressible fluid

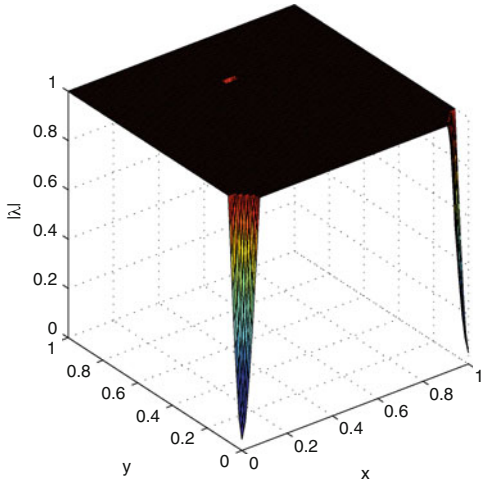

Fig. 10.11 Norm of the viscoplastic constraint tensor for the incompressible fluid

in the incompressible case, since the trace of $\mathbf{A}(\mathbf{u})$ is not always zero in all flows of a compressible fluid. Nevertheless, the trace of $\boldsymbol{\Lambda}$ plays no part in the numerical simulation, just like that in incompressible fluids [18]. This permits one to begin by setting the initial value of $\boldsymbol{\Lambda}$ to be zero in the iterations.

The distribution of the density ρ using Model 1 is shown in Fig. 10.12 and the yielded and unyielded regions obtained using Model 1 are shown in Fig. 10.13. With Model 2, we find the profile of ρ in Fig. 10.14, and the yielded/unyielded regions in Fig. 10.15. Comparing Figs. 10.13 and 10.15 with Fig. 10.10, we find that the location of the rigid core near the top is unchanged. However, Model 1 leads to a larger core area than the incompressible model does, and Model 2 even larger. The effects of the

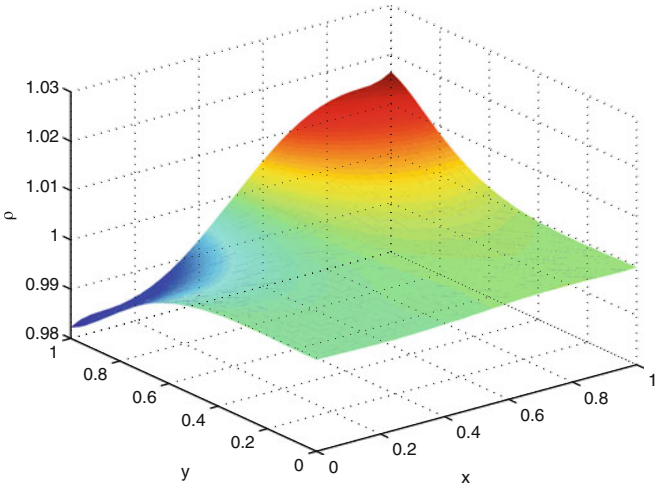

Fig. 10.12 Distribution of density in Model 1 across the cavity

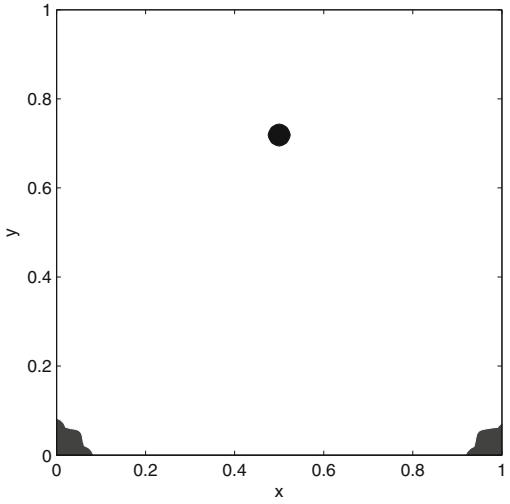

Fig. 10.13 Yielded (*white*) and unyielded (*black*) regions using Model 1

two compressible models on the bottom rigid corners are not remarkable. As to the distribution of the density, it can be seen in Figs. 10.12 and 10.14 that the magnitude of the density reaches its minimum at the top left corner and reaches its maximum at the top right corner. This is reasonable because the top lid of the cavity moves from left to right and the pressure is smaller at the top left corner and larger at the top right corner. Figure 10.16 provides a comparison of the densities between Model 1 and Model 2 along the top lid, where $0 \leq x \leq 1, y = 1$. It is seen that with the

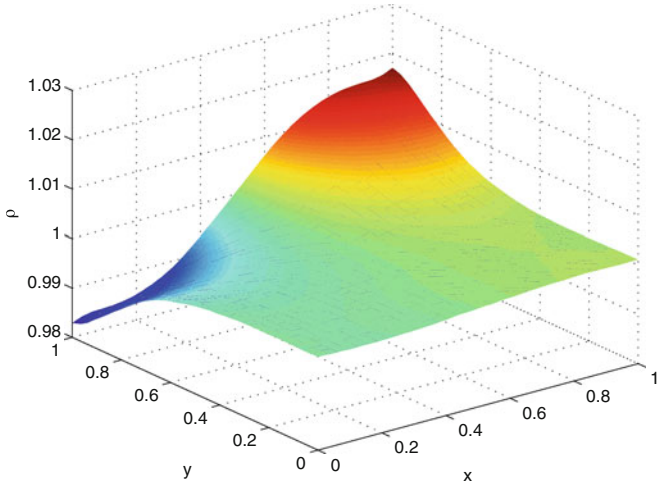

Fig. 10.14 Distribution of density in Model 2 across the cavity

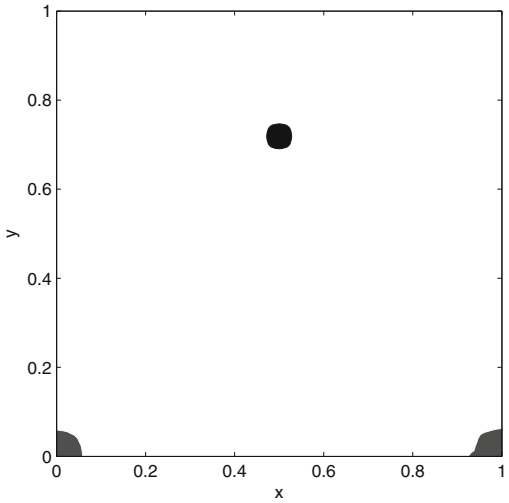

Fig. 10.15 Yielded (*white*) and unyielded (*black*) regions using Model 2

similar trends of variation, the values of ρ obtained from Model 1 are smaller than those from Model 2.

Turning to the velocity, we have compared the profiles of the two components u and v in Figs. 10.17 and 10.18 respectively. Figure 10.17 gives the u profile along the vertical centre line, where $x = 0.5$, $0 \leq y \leq 1$. Except at the top, bottom boundaries and the core centre, the values of u of the incompressible fluid are smaller than those of the compressible fluids, in which Model 2 predicts a greater effect than

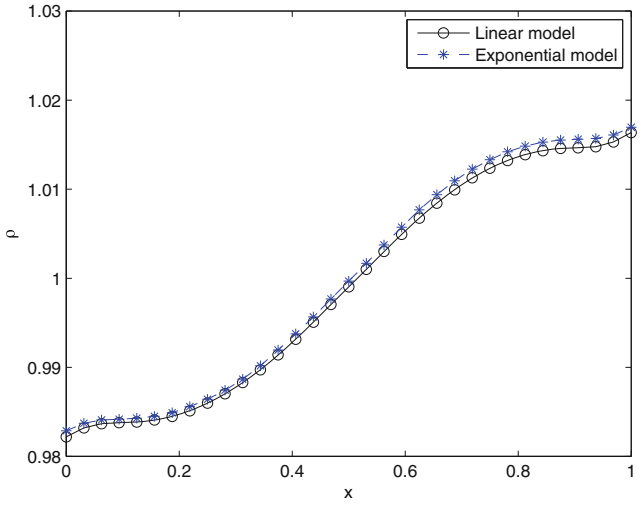

Fig. 10.16 Comparison of densities along the top lid

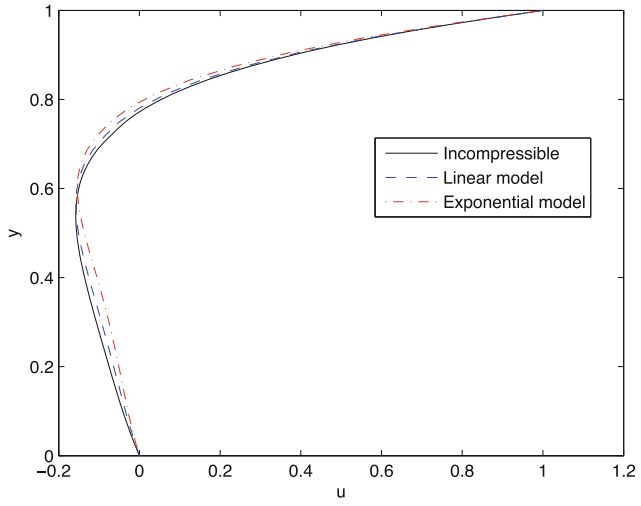

Fig. 10.17 Velocity u along the vertical line at $x = 0.5$.

Model 1. Figure 10.18 shows the v profile along the horizontal centre line, where $0 \leq x \leq 1, y = 0.5$. The fluctuation of v of the incompressible fluid is larger than that of the compressible fluids, with Model 2 showing a weaker effect than Model 1. All the models lead to the same value $v = 0$ at the left and the right boundaries and the core centre. Comparison of the pressure along the top lid shows that the incompressible fluid has the largest value of p while Model 1 has the least.

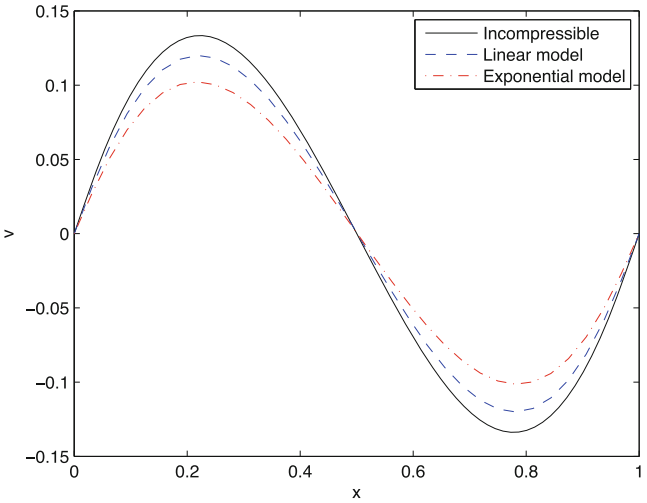

Fig. 10.18 Velocity v along the horizontal line at $y = 0.5$.

As mentioned earlier, while the numerical iterations converge and seem to agree with one another, it has to be emphasised that results are in the nature of *numerical experiments* because there is no proof that the viscoplasticity constraint tensor $\boldsymbol{\Lambda}$ exists in the flow of a compressible viscoplastic fluid under Dirichlet boundary conditions.

10.6 Regularised Models

There are numerous examples of modelling the flows of Bingham fluids using either the bi-viscosity model or the Papanastasiou model. The regularised models have been employed to overcome the numerical modelling difficulties associated with the non-differentiable yield stress dissipation functional (cf. (8.2.15)):

$$j(\mathbf{v}) = \int_{\Omega} K(\mathbf{v})\, dv, \tag{10.6.66}$$

at $K(\mathbf{v}) = 0$. Since the latter value determines the region and its boundary where the viscoplastic fluid is unyielded, the regularised models *smooth out* this singularity either by assuming that the fluid has a very high viscosity when the shear rate is very small as in the bi-viscosity model, or by a nonlinear viscosity function in the case of the Papanastasiou model. Given that there now exist two robust numerical methods, viz., the augmented Lagrangian method and the operator-splitting method, to solve the flow problems using the exact visoplastic fluid models, such as the Bingham fluid, it can be argued that the use the non-exact models needs a re-evaluation.

Indeed, there are other compelling reasons arising from a comprehensive review of the convergence of the regularised solutions to those corresponding to exact models [32], which points out many of the shortcomings of using inexact constitutive relations. As an illustration, consider a two-dimensional flow in a bounded domain Ω, driven by a body force $\mathbf{b}$ and Dirichlet boundary conditions. If $\mathbf{u}_\varepsilon$ is the solution of the problem using a regularised model and $\mathbf{u}$ is that produced by employing the Bingham fluid, it can be shown that norm convergence in the following sense occurs:

$$||\mathbf{u} - \mathbf{u}_\varepsilon||_{H^1(\Omega)} \leq \frac{2\mathrm{Bn}|\Omega|}{C_\Omega}\varepsilon^{1/2}, \tag{10.6.67}$$

where $|\Omega|$ is the area of Ω, and C_Ω is a constant that depends on the domain.

As an example of such norm convergence, suppose that the flow of a Bingham fluid in a channel is steady under an applied pressure drop G per unit length. Further, at time $t = 0^+$, let this be reduced so that $G < \beta$, where $\beta = 2$ is the constant which appears in Sect. 9.4.3. In this situation, it has been proved earlier that the flow of the Bingham fluid comes to rest in a finite amount of time, with its upper bound given by T_f in Eq. (9.4.27). When the Papanastasiou model is used to model this initial/boundary value problem [33], it is found that the flow never comes to rest; indeed, in the Papanastasiou model, a steady velocity profile persists corresponding to a small but non-zero volumetric flow rate. That is, while norm convergence occurs, the regularised model does not reproduce the finite extinction time property of the Bingham fluid.

In [32], it is also shown that the regularised models generate maximum errors in lubrication and thin-film flows; that stability characteristics are incorrectly predicted for a large class of problems. In addition, on p. 944 of his encyclopaedic article [3], Glowinski has pointed out that when $K(\mathbf{u})$ is small,

$$||j''(\mathbf{u}_\varepsilon)|| \approx 1/\varepsilon. \tag{10.6.68}$$

That is, for $\mathbf{u}_\varepsilon$ to be good approximation to $\mathbf{u}$, the parameter ε has to be small; on the other hand, an initial/boundary value problem is badly conditioned for those situations where the set Ω_0, on which $\mathbf{A}(\mathbf{x}, t) = \mathbf{0}$, is large. This has been confirmed by the numerical simulation of a steady bubble rise in Herschel-Bulkley fluids using the augmented Lagrangian method and comparing the results with that using the Papanastasiou model [34]. These computations show that as the Bingham number increases and the size of the unyielded region becomes bigger, much larger values of the parameter m in the Papanastasiou model are needed; indeed, m can exceed 10^4.

Of course, a great deal of insight has been obtained into the flows of viscoplastic fluids so far by the use of the regularised models. Here, one may mention the solutions to creeping flow problems [35–38], entry flows [39], extrudate swell [40], fountain flow effects [41], finite extinction results [33, 42], rising bubbles [43] and thermally driven cavity flows [44]. While a couple of results using the regularised models have been mentioned in this monograph, the existence of robust numerical schemes for the exact models has overcome the need to provide a detailed exposition.

References

1. Glowinski R (1984) Numerical methods for nonlinear variational problems. Springer, New York
2. Glowinski R, Le Tallec P (1989) Augmented Lagrangian and operator-splitting methods in nonlinear mechanics. SIAM, Philadelphia
3. Glowinski R (2003) Finite element methods for incompressible viscous flow. In: Ciarlet PG, Lions J-L (eds) Handbook of numerical analysis, vol IX. North-Holland, Amsterdam, pp 3–1176
4. Glowinski R, Wachs A (2011) On the numerical simulation of viscoplastic fluid flow. In: Handbook of numerical analysis, vol XVI. Ciarlet PG (General Ed), Glowinski R, Xu J (Guest eds.) North-Holland, Amsterdam, pp 483–717
5. Cea J, Glowinski R (1972) Methodes numeriques pour l'ecoulement laminaire d'un fluide rigide viscoplastique incompressible. Int J Comp Math Sec B 3:225–255
6. Arrow KJ, Hurwicz L, Uzawa H (1958) Studies in linear and nonlinear programming. Stanford University Press, Stanford
7. Nocedal J, Wright SJ (2006) Numerical optimization, 2nd edn. Springer, New York
8. Apostol TM (1974) Mathematical analysis, 2nd edn. Addison-Wesley, Reading
9. Huilgol RR, Panizza MP (1995) On the determination of the plug flow region in Bingham fluids through the application of variational inequalities. J Non-Newton Fluid Mech 58:207–217
10. Huilgol RR, You Z (2005) Application of the augmented Lagrangian method to steady pipe flows of Bingham, Casson and Herschel-Bulkley fluids. J Non-Newton Fluid Mech 128:126–143
11. Vinay G, Wachs A, Agassant J-F (2005) Numerical simulation of non-isothermal viscoplastic waxy crude oil flows. J Non-Newton Fluid Mech 128:144–162
12. Putz A, Frigaard IA (2010) Creeping flow around particles in a Bingham fluid. J Non-Newton Fluid Mech 165:263–280
13. Yu Z, Wachs A (2007) A fictitious domain method for dynamic simulation of particle sedimentation in Bingham fluids. J Non-Newton Fluid Mech 145:78–91
14. Li CH (1991) Numerical solution of Navier-Stokes equations by operator splitting. In: Proceedings sixth international conference in Australia on finite element methods, vol 1. pp 205–214
15. Glowinski R, Pironneau O (1992) Finite element methods for Navier-Stokes equations. Ann Rev Fluid Mech 24:167–204
16. Perera MGN, Walters K (1977) Long-range memory effects in flows involving abrupt changes in geometry. Part I : flows associated with L-shaped and T-shaped geometries. J Non-Newton Fluid Mech 2:49–81
17. Sánchez FJ (1998) Application of a first-order operator splitting method to Bingham fluid flow simulation. Comp Math Appl 36:71–86
18. Dean EJ, Glowinski R (2002) Operator-splitting methods for the simulation of Bingham viscoplastic flow. Chin Ann Math 23B:187–204
19. Duvaut G, Lions JL (1972) Transfert de chaleur dans un fluide de Bingham dont la viscosité dépend de la température. J Funct Anal 11:93–110
20. Kato Y (1992) On a Bingham fluid whose viscosity and yield limit depend on the temperature. Nagoya Math J 128:1–14
21. Li C-H, Glowinski R (1996) Modelling and numerical simulation of low-mach-number compressible flows. Int J Numer Methods Fluids 23:77–103
22. Duvaut G, Lions JL (1972) Les Inéquations en Physique et en Mécanique. Dunod, Paris
23. Duvaut G, Lions JL (1976) Inequalities in mechanics and physics. Springer, New York
24. Huilgol RR, You Z (2009) Prolegomena to variational inequalities and numerical schemes for compressible viscoplastic fluids. J Non-Newton Fluid Mech 158:113–126
25. Huilgol RR, Kefayati GHR (2014) Natural convection problem in a Bingham fluid using the operator-splitting method. J Non-Newton Fluid Mech. doi:10.1016/j.jnnfm.2014.06.005

26. Vola D, Boscardin L, Latché JC (2003) Laminar unsteady flows of Bingham fluids: a numerical strategy and some benchmark results. J Comp Phys 187:441–456
27. Lions P-L (1996) Mathematical topics in fluid mechanics, vol 1. Incompressible models, Clarendon Press, Oxford
28. Lions P-L (1998) Mathematical topics in fluid mechanics, vol 2. Compressible models, Clarendon Press, Oxford
29. Vinay G, Wachs A, Agassant J-F (2006) Numerical simulation of weakly compressible Bingham flows: the restart of pipeline flows of waxy crude oils. J Non-Newton Fluid Mech 136:93–105
30. Frigaard I, Vinay G, Wachs A (2007) Compressible displacement of waxy crude oils in long pipeline startup flows. J Non-Newton Fluid Mech 147:45–64
31. Horibata Y (1992) Numerical simulation of low-Mach-number flow with a large temperature variation. Comp Fluids 21:185–200
32. Frigaard IA, Nouar C (2005) On the usage of viscosity regularisation methods for visco-plastic fluid flow computation. J Non-Newton Fluid Mech 127:1–26
33. Chatzimina M, Georgiou GC, Argyropaidas I, Mitsoulis E, Huilgol RR (2005) Cessation of Couette and Poiseuille flows of a Bingham plastic and finite stopping times. J Non-Newton Fluid Mech 129:117–127
34. Dimakopoulos Y, Pavlidis M, Tsamopoulos J (2013) Steady bubble rise in Herschel-Bulkley fluids and comparison of predictions via the Augmented Lagrangian Method with those via the Papanastasiou model. J Non-Newton Fluid Mech 200:34–51
35. Beris AN, Tsamopoulos JA, Armstrong RC, Brown RA (1985) Creeping motion of a sphere through Bingham plastic. J Fluid Mech 158:219–244
36. Blackery J, Mitsoulis E (1997) Creeping motion of a sphere in tubes filled with a Bingham plastic material. J Non-Newton Fluid Mech 70:59–77
37. Beaulne M, Mitsoulis E (1997) Creeping motion of a sphere in tubes filled with Herschel-Bulkley fluids. J Non-Newton Fluid Mech 72:55–71
38. Patel SA, Chhabra RP (2014) Steady flow of Bingham plastic fluids past an elliptical cylinder. J Non-Newton Fluid Mech 202:32–53
39. Mitsoulis E, Huilgol RR (2004) Entry flows of Bingham plastics in expansions. J Non-Newton Fluid Mech 122:45–54
40. Mitsoulis E (2007) Annular extrudate swell of pseudoplastic and viscoplastic fluids. J Non-Newton Fluid Mech 141:138–147
41. Mitsoulis E (2010) Fountain flow of pseudoplastic and viscoplastic fluids. J Non-Newton Fluid Mech 165:45–55
42. Chatzimina M, Xenopohontos C, Georgiou G, Argyropaidas A, Mitsoulis E (2007) Cessation of annular Poiseuille flows of Bingham plastics. J Non-Newton Fluid Mech 142:135–142
43. Tsamopoulos J, Dimakopoulos Y, Chatzidai N, Karapetsas G, Pavlidis M (2008) Steady bubble rise and deformation in Newtonian and viscoplastic fluids and conditions for bubble entrapment. J Fluid Mech 601:123–164
44. Turan O, Chakraborty N, Poole RJ (2010) Laminar natural convection of Bingham fluids in a square enclosure with differentially heated side walls. J Non-Newton Fluid Mech 165:901–913

Index

A
Acceleration
convected, 25
local, 25
material/Lagrangian description, 24
spatial/Eulerian description, 25
wave, 103
Augmented Lagrangian, viii, ix
functional, 229, 231, 232, 235
method, 20, 47, 206, 225, 226, 235, 248, 249, 267, 268

B
Banach space, 162
Bi-viscosity model, 56, 267
Bingham
fluid, vii, viii, 1, 3, 7, 10, 14, 16, 18, 20, 30, 32, 48, 51, 53, 56, 60, 63, 65, 66, 68, 72, 81–83, 85, 87, 91, 99, 100, 103, 106, 107, 110, 114, 116, 117, 124, 128, 132, 136, 142, 149, 150, 156, 158, 162, 163, 165–167, 170, 174, 175, 181–183, 186, 200, 201, 205, 207, 210–213, 216–218, 221, 223, 225, 226, 230–232, 234–236, 238, 262, 267, 268
weakly compressible, 252, 260
number, vii, 8–10, 71, 75, 85, 90, 114, 117, 118, 125, 132, 136, 193, 194, 196, 198, 199, 201, 202, 206, 208, 209, 215, 217, 221, 223, 237, 238, 241, 243, 244, 248, 268
Bingham fluid
drag, 201
entrapment
sphere, 202
spherical bubble, 202
extinction time, 16
rising bubble, 201
Bingham, E. C., 18
Boundary condition
enclosed flow, 257
open or partially open, 257
Boussinesq approximation, 237
Bubble
critical Bingham number, 196, 198, 199, 201
static, 193
Buckingham equation, vii, 9, 71, 118, 217, 221

C
Casson fluid, 48, 83, 109, 124, 128, 142, 150, 163, 165, 231
Cauchy
first law of motion, 38, 134
second law of motion, 40
stress principle, 38, 69, 72, 78
Cauchy-Schwarz inequality, 142, 150, 151, 154, 175, 177, 192, 200, 206, 220
Cavity flow
lid driven, 236, 262, 264
thermally driven, viii, 235, 240
Compressible fluid
exponential model, 260
linear model, 260
weak, 261
Conservation of mass, 26, 36, 42, 174, 251, 254
correction, 254
Constitutive equation, vii, 3, 5, 20, 48, 50, 54–56
Bingham fluid, 53, 60, 63

R.R. Huilgol, *Fluid Mechanics of Viscoplasticity*, DOI 10.1007/978-3-662-45617-0

Casson fluid, 61, 64
compressible viscoplastic fluid, 58, 177
Herschel-Bulkley fluid, 60, 63
weakly compressible viscoplastic fluid, 255
Continuity equation, 36, 252, 253, 255
Continuum mechanics, 24, 26, 27, 35–38, 43, 48, 49, 51, 140
Control surface, 43
Control volume, 43
Convected derivative problem, 241, 259, 261
Convex analysis, viii, 139, 158
Convex set, 163
Critical
pressure drop per unit length, 1, 3, 68, 73, 88
Reynolds number, 136, 137
shear rate, 56
value for plug break, 121
value of shear stress, 157
yield stress number, 17
Cubic equation, 9, 80, 115
Curl of a vector
physical components, 32
Cartesian coordinates, 33
cylindrical coordinates, 33
spherical coordinates, 33

D

Deformation gradient, 26
Direct method, 159–161
Dirichlet
boundary condition, 56, 139, 161, 164, 171, 175, 176, 230, 267
principle, 159
Dirichlet, P. G. L., 159
Discriminant, 10, 71, 81, 222
Divergence of a vector
physical components, 32
Cartesian coordinates, 32
cylindrical coordinates, 33
spherical coordinates, 33

E

Energy balance equation, 42
Equation of state, 252
Equations of motion
Cartesian coordinates, 45
cylindrical coordinates, 45
spherical coordinates, 46
Equivalence
variational inequality and equations of motion, 168
variational inequality and variational principle, 166, 230, 231
variational inequality and viscoplasticity constraint tensor, 176
Euler
turbomachine equation, 44
Extinction time
channel flow, 211
Couette flow, 215
pipe flow, 212
simple shear, 212
wall slip, 216

F

Fictitious domain method, 206, 235
Finite element method, 86, 161, 168, 202, 240, 261
Finite extinction time, 213, 268
First Rivlin-Ericksen tensor, 29
Flow
approach to steady state, 209
Couette, 32
helical/spiral, 32
in a channel, 31, 268
in a wavy channel, 116
in an annulus, 31
inclined plane, 66
Poiseuille, 31
simple shear, 30
steady
in a pipe, 149
Flow in a cavity
lid driven, 260
Flow rate, 115, 118, 192, 268
Fluidity function
Bingham fluid, 124
Casson fluid, 124
Hershel-Bulkley fluid, 124
Papanastasiou model, 125
Fourth order equation, 71
Free surface problem, 66, 91, 171, 174
Function space, 158, 161, 163
Functional
bilinear, 153
convex, 164
kinematically admissible, 143, 145, 148, 150, 158
presence of wall slip, 157
minimiser, 166
proper, 164

statically admissible, 144, 146, 148
presence of wall slip, 157
strictly convex, 164
trilinear, 153, 173
Fundamental inequality
compressible fluid, 59, 178
incompressible fluid, 139, 150, 152, 157, 172, 176, 195, 204

G
Galerkin, B. G., 161
Gateaux derivative, 166, 232
Gateaux differential, 166
General energy balance equation, 139, 155
Green, H., 18

H
Hadamard
Lemma, 104, 105, 109
propagating singular surfaces, viii, 97, 100
Hadamard-Rybczynski formula, 199, 202
Halting number, 211, 215, 216
Heat transfer, 83
across a cavity, 242
circular tube, 85
parallel walls, 65, 85
Hele-Shaw flow, 81, 114, 122, 126, 128, 131, 132
average velocity field
asymmetric case, 130
Bingham fluid, 128
power law fluid, 127
symmetric case, 126
viscous fluid, 127
Herschel-Bulkley fluid, 48, 53, 83, 109, 124, 128, 142–144, 150, 165, 194, 231
Hilbert space, 162

I
Incompressibility, 44, 47, 50, 51, 54, 87, 103

J
Jerk wave, 103, 106–109

K
Karush-Kuhn-Tucker condition, 229
Kinematic invariant, 42, 63
Kolodner
functional equation, 91, 95
method, 90, 99

L
L.s.c, 160, 161
convex functional, 166
functional, 167
proper and convex, 164
Lagrange multiplier, 50, 229, 231
method, 226
Lagrange, J-L., 226
Lagrangian mechanics, 37, 48, 51
Lamé coefficients, 253
Lambert W function, 125
Laplace transform, 98
Laplace's equation, 128, 159
Laplacian, 230, 237
Lebesgue, H., 160
Lid driven flow, viii, 171, 226, 240, 266
Low Mach number
flow, 250, 252
Lower semi-continuity, 160
Lubrication approximation, 114, 116
Lubrication paradox, 114, 116, 119

M
Mach number, 252
Material derivative, 25
Maximum principle
parabolic equations, 98
Mixed boundary condition, 161

N
Navier, C - L., 16
Navier-Stokes equation
compressible fluid, 252, 254
incompressible fluid, 113, 168, 235, 251
Navier-Stokes equations
compressible fluid, 253
Neumann
boundary condition, 161
Newton
heat transfer coefficient, 84
second law, 35
Newtonian fluid, 136, 174
compressible, 250, 255
drag, 201
rising bubble, 199
No slip boundary condition, 134
Non-isothermal flow, 235, 236, 239, 240, 253

Non-Newtonian
fluid, 18, 19, 56, 81, 85, 174, 201
fluid mechanics, 168
viscosity, 56, 84
Numerical experiments, 166, 176, 226
Nusselt number, 65, 83–85
averaged, 238, 248
local, 238, 245

O
Obstacle problem, 12, 14
Operator-splitting, viii, ix, 249
method, 20, 56, 139, 225, 235, 236, 239, 242, 261, 267
methods, 176
scheme, 47
Operator-splitting method
compressible fluid, 258
Orr, W. M., 217
Orr-Sommerfeld energy equation, 132, 181
Orthogonal projection method, 249

P
Papanastasiou model, 56, 109, 124, 128, 199, 202, 267, 268
parameter, 58, 268
Perturbation
first order, 118, 120
isentropic case, 251
kinetic energy, 217
long wavelength, 114, 121
modal, 136
non-modal, 136
one dimensional, 135
periodic, 134
regular, 10, 71
span wise, 136
stream wise, 136
three dimensional, 136
two dimensional, 135
velocity field, 218, 221, 222
Plug
annular, 73
central, 69
flow, 67
pseudo, 118–120
rigid, 68
semi-width, 5
solid, 3
true, 120
velocity, 4
Polar decomposition theorem, 28
Prandtl number, 238, 245
Pressure
definition, 51
field, 1, 51, 66, 79, 82, 128, 168, 198, 234, 236
scaling, 132
Pressure drop per unit length, 80, 88, 132, 135, 149, 171
critical, 181, 182, 184
circular pipe, 186
equilateral triangular pipe, 187
igloo shape, 188
in an annulus, 186
L-shaped cross-section, 188
rectangular pipe, 187
square pipe, 186
Projection operator, 230, 239, 259

R
Rate of deformation/stretching tensor, 29
Rayleigh number, 238, 242
Regularised models, viii, 20, 47, 56, 226, 267, 268
Reynolds
number, 8, 117, 223
critical, 114, 132, 223
transport theorem, 24, 36
Reynolds'
transport theorem, 35–37
Reynolds, O., 217
Reynolds-Orr energy equation, 217, 218
Riemann, B., 159
Rigid body motion
mobility problem, 201
resistance problem, 201
Rigid motion, 27
Ritz, W., 161
Rivlin-Ericksen tensor, 23, 29, 30, 33, 42, 47, 52, 54, 182, 251
physical components, 33
Rivlin-Ericksen tensors, 30

S
Saddle point, 228, 229, 232
method, 225, 227
problem, 235
Second invariant, 63
kinematic, 42, 152, 165
stress, 52
Shear rate, 4, 6, 8, 19, 43, 53, 56, 58, 60, 63, 81, 83, 99, 100, 122–124, 142, 165, 209, 267

Shear stress, 1–3, 5, 8, 19, 55, 58, 60, 63, 65, 73, 83, 87, 102, 123
bi-viscosity model, 56
Casson fluid, 53
channel flow, viii, 66
Couette flow, 77
flow in an annulus, 72
helical/spiral flow, 80
Herschel-Bulkley fluid, 53
inclined plane, 67
non-Newtonian, 165
Papanastasiou model, 58, 124
parallel plate flow, 83
Poiseuille flow, 69
scaling, 117
simple shear, 66
unsteady channel flow, 88
unsteady flow in a half-space, 100, 101
vector, 122, 126
Size of core
pipe flow, 192
Sobolev space, 161
Spectral element method, 161
Sphere
critical Bingham number, 206
Spin tensor, 29
physical components, 34
Stability
conditional bound
channel flow, 223
global bound
channel flow, 221
Poiseuille flow, 221
linearised
channel flow, 132, 136, 251
helical flow, 136
nonlinear, 181, 217, 221
Stagnant zone, 183
existence, 190
Stefan problem, vii, 11, 12
Stick-slip model, 18, 157
Stokes problem, 240, 258, 261
Stokes' law
drag, 201, 202
Stokes' relation, 250
Stream function, 128, 135, 198
Stress field
in shear, 68, 100
scaling, 132
statically admissible, 140
with slip, 157
Stress potential, 62
Bingham fluid, 60, 63
Casson fluid, 61, 64
Herschel-Bulkley fluid, 61, 64
Stress power difference
non-zero, 173
zero, 170
Stress tensor
extra, 45, 47–49
total, 47–50
Stress vector, 37
Surface of constraint, 50
Surface tension, 194, 195

T
Thermodynamic pressure, 250
Trace of a function, 162

U
Unsteady flow
Bingham fluid
channel flow, 87
Couette flow, 99
in a half-space, 100
Poiseuille flow, 99
Rayleigh problem, 107, 109
Uzawa algorithm, 230, 239, 262
Uzawa, H., 225

V
Variational inequal0ity, vii, 12, 14, 15, 18, 113, 150, 158, 165–170, 172, 176, 193, 204, 209, 230, 234
falling sphere, 202
static bubble, 195
steady flow in a pipe, 230
unsteady flow in a pipe, 172, 207
Variational principle, viii, ix, 16, 18, 20, 59, 139, 140, 149, 154, 158, 181, 199
steady flow in a pipe, 150, 231
Velocity
Eulerian description, 23, 25
gradient, 25
Lagrangian description, 23
material/Lagrangian description, 24
maximum in a core, 193
steady, 23
Velocity field
kinematically admissible, 140
steady, 25
unsteady, 25
Velocity potential, 62
Bingham fluid, 60, 63

Casson fluid, 61, 64
Herschel-Bulkley fluid, 61, 63
Virtual power
principle, viii, 140, 145, 147, 148
Viscometric fluidity function, 81, 114, 123, 124
Viscoplastic fluid
compressible, 255
Viscoplasticity constraint tensor, vii, 47, 55, 59, 139, 225, 230, 236, 259
Viscoplasticity constraint tensor problem, 241, 259, 262
Viscosity
Bingham fluid, 53
Casson fluid, 53
Herschel-Bulkley fluid, 53
power law, 53, 124, 128
shear rate dependent, 52
Viscous
dissipation rate integral, 152, 163, 178
Vortex sheet, 103
Vorticity vector, 30

W
Wall shear stress, 6, 17, 18, 68, 132, 156
critical, 17
Wall slip, 18, 139, 156, 157
Weierstrass, K., 159

Y
Yield stress, 1, 3, 7, 17, 52–54, 56, 58, 65, 68, 73, 84, 86, 100, 102, 105, 106, 127, 142
dissipation, 136, 137, 151
dissipation rate integral, 153, 163, 178
shear rate dependent, 149
Yield stress fluid, 119, 122
Yield surface, viii, 5, 6, 14, 16, 55, 77, 78, 82, 87, 90, 91, 93, 95, 97, 99–103, 105–110, 114, 118, 120, 134, 136, 231
perturbed, 134
pseudo, 118, 119